

UNIVERSITE PARIS XIII (PARIS NORD)
LABORATOIRE DES SCIENCES DES PROCÉDES ET DES
MATERIAUX (LSPM)

IFP ENERGIES NOUVELLES

THESE

Pour obtenir le titre de :

DOCTEUR DE L'UNIVERSITE PARIS XIII

Discipline : Génie des Procédés

Présentée et soutenue publiquement par :

TRINH Thi Kim Hoang

Le 25 Septembre 2015

**PREDICTION OF PHASE EQUILIBRIA
ASSOCIATED WITH HYDROTREATING
PROCESS OF BIOMASS BY GC-PPC-SAFT
EQUATION OF STATE**

Directeur de thèse : M. Jean-Philippe Passarello

Promoteur IFPEN : M. Jean-Charles de Hemptinne

Co-Promoteur IFPEN : M. Rafael Lugo

Jury:

M. Jean-Philippe Passarello Directeur de thèse

M. Jean-Charles De Hemptinne Encadrant

M. Joachim Gross Rapporteur

M. Patrice Paricaud Rapporteur

M. Erich Muller Examineur

M. Dominique Vrel Examineur



UNIVERSITÉ PARIS 13



REMERCIEMENTS/ACKNOWLEDGEMENTS

Ces travaux ont été réalisés à IFP Energies Nouvelles au sein du département Thermodynamique et Modélisation Moléculaire ainsi qu'au Laboratoire de Sciences des Procédés et des Matériaux (LSPM), sous la direction de Mr. Jean-Philippe Passarello, Professeur à l'Université Paris 13, Mr. Jean-Charles de Hemptinne, Professeur de l'IFP School, et Mr. Rafael Lugo, Chef de projet d'IFP Energies Nouvelles.

Dans un premier temps, je voudrais remercier Véronique Ruffier-Meray, Directrice de la Direction Chimie et Physico Chimie Appliquées et Pascal Mougín, Chef du Département de Thermodynamique et Modélisation Moléculaire, pour m'avoir donné l'opportunité de réaliser cette thèse à IFP Energies Nouvelles. J'aimerais également adresser mes remerciements à la Fondation TUCK qui a participé au financement de cette thèse. Aussi, un grand merci au GENCI (Grand Equipement National de Calcul Intensif) qui m'a donnée accès aux moyens de calcul du CINES au travers de l'allocation de ressources 2013-X2013096349 et 2014-X2014096349.

Je tiens à remercier également mon directeur de thèse, Jean-Philippe Passarello, Professeur de l'Université Paris 13, qui a fait preuve d'une grande disponibilité et a été une source constante de conseils et de réflexions en particulier sur l'équation d'état GC-PPC-SAFT. Merci à toi Jean-Philippe, pour ton humour et ton soutien !

J'adresse mes plus vifs remerciements à Jean-Charles de Hemptinne, Professeur d'IFP School, pour m'avoir proposé ce sujet de thèse et pour son encadrement. Je lui suis très reconnaissant de sa contribution au développement de ces travaux et de m'avoir fait profiter de ses connaissances et de sa grande expérience en thermodynamique. Jean-Charles, c'est un grand plaisir de travailler avec toi. Merci pour ta patience et ta disponibilité !

Je suis reconnaissante à Rafael Lugo, Chef de projet de l'IFP Energies Nouvelles, pour son encadrement et ses conseils concernant surtout en modélisation moléculaire, qu'il m'a apportés. Rafael, je te remercie beaucoup de ton humour et ton encouragement !

Patrice Paricaud et Joachim Gross ont accepté d'être les rapporteurs de cette thèse, et je les en remercie, de même que pour leur participation au Jury.

Erich Muller et Dominique Vrel m'ont fait l'honneur de participer au Jury de soutenance; je le en remercie profondément.

Tous mes remerciements vont aussi à Nicolas Ferrando et Véronique Lachet, Ingénieurs de Département de Thermodynamique et Modélisation Moléculaire, qui m'ont formée aux méthodes dans la simulation moléculaire Monte Carlo. Je voudrais vous remercier Nicolas, Véronique, pour votre disponibilité et aussi votre bonne humeur.

Mes très sincères remerciements à Angela Di Lella, Armelle Nigon, Catherine Lefebvre, Isabelle Brunella, Aurélie Wender. Merci de votre soutien et votre amitié pendant ces trois ans de thèse. C'est avec vous que j'ai passé trois ans en partageant des moments inoubliables que j'emmènerai avec moi pour moi pour toute ma vie ! Aussi, les grands remerciements à mes chers amis : Le Vi, Trang, Thuy An, Ha Giang, Phuong Linh, Tuan Tu, Thanh Dat, Kinh Hoc, Nguyet Anh, Thanh Nghi, Cam Hoang, Van Long. Merci de votre soutien, votre amitié et les moments avec pleine de sourires. Je vous aime !

De plus, je voudrais adresser de très chaleureux et sincères remerciements à toute l'équipe de Thermo qui m'a donné la chance de partager avec eux le travail et aussi la bonne ambiance, bonne humeur pendant trois ans. Merci à Annabelle, Isabelle, Auriane, Xavier, Thanh Binh, Johan, Damelys, Denis, Stéphane, Christophe, Théo, Carlos, Benoit, Brigitte, Michel.

Une dédicace spéciale à tous les gens que j'ai eu le plaisir de côtoyer durant ces quelques années à IFP Energies Nouvelles : Mai Quyen, Marine, Marie, Camillo, Christian, Christiane et aussi à Villeteuseuse : Hang Nga, Philippe, Patrick, Bernard, Mamadou, Rachid.

Enfin, ces remerciements ne seraient pas complets sans mentionner ma famille. Merci à mes parents, ma chère sœur, mon petit frère qui sont toujours à côté de moi, leur soutien et leur amour sans conditions pour tous les moments de ma vie malgré douze milles kilomètre de séparation. Je vous aime du fond de mon cœur. Un dernier mot, un grand souvenir à ma chère grand-mère. Même si tu n'es plus ici, je sais que tu veilles sur moi toujours. Je t'aime !

SOMMAIRE

REMERCIEMENTS

SOMMAIRE

GENERAL INTRODUCTION.....	9
CHAPTER I.....	15
BACKGROUND AND LITERATURE REVIEW.....	15
I.1 INTRODUCTION.....	15
I.2 PREDICTIVE MODELS FOR BIOMASS HYDROTREATMENT	15
I.2.1 PHASE EQUILIBRIUM CALCULATION	15
I.2.2 OVERVIEW OF THE EXPRESSIONS OF HENRY'S CONSTANT	20
I.2.3 ACTIVITY MODELS	22
I.2.4 EQUATION OF STATE	25
I.2.5 SUMMARY OF THE REFERENCES DEALING WITH HYDROGEN SOLUBILITY	40
I.2.6 OUR CHOICE: GC-PPC-SAFT	42
I.3 EXPERIMENTAL DATA AND THEIR CONSISTENCY	43
I.3.1 PROBLEM STATEMENT	43
I.3.2 EXPERIMENTAL TECHNIQUES.....	44
I.3.3 CONSISTENCY ANALYSIS	49
I.4 MOLECULAR SIMULATION	50
I.4.1 GENERALITIES OF MOLECULAR SIMULATION	51
I.4.2 MOLECULAR MODEL	53
I.4.3 FORCE FIELDS FOR HYDROGEN	54
I.4.4 INTERMOLECULAR POTENTIAL OF OXYGENATED COMPOUNDS	54
I.4.5 COMPUTATION OF STRUCTURAL OR MACROSCOPIC PROPERTIES	56
I.5 CONCLUSION.....	59
CHAPTER II.....	63

<u>HYDROGEN SOLUBILITY IN OXYGENATED COMPOUNDS</u>	63
II.1 INTRODUCTION	64
II.2 DATA INVENTORY.....	65
II.2.1 DATA SOURCES	65
II.2.2 DATA EVALUATION	72
II.3 CONSISTENCY ANALYSIS	75
II.3.1 ALKANES	78
II.3.2 ALCOHOLS	79
II.3.3 OTHER OXYGENATES.....	84
II.3.4 WATER.....	86
II.4 MONTE CARLO MOLECULAR SIMULATION	87
II.4.1 INTERMOLECULAR POTENTIAL OF HYDROGEN	88
II.4.2 INTERMOLECULAR POTENTIAL OF OXYGENATED COMPOUNDS.....	88
II.4.3 CALCULATION OF HENRY’S CONSTANT FROM MONTE CARLO SIMULATIONS	89
II.4.4 VALIDATION OF MONTE CARLO SIMULATION (INSERTION TEST)	91
II.4.5 COMPLETING THE DATABASE USING MONTE CARLO MOLECULAR SIMULATION RESULTS	95
II.5 FINAL DISCUSSION : COMPARISON OF HYDROGEN HENRY’S CONSTANT IN DIFFERENT ORGANIC FAMILIES	100
II.6 CONCLUSIONS.....	102
APPENDIX II-A: CONVERSION INTO HENRY’S CONSTANT	102
APPENDIX II-B: MOLECULAR SIMULATION RESULTS	104
<u>CHAPTER III</u>	112
<u>DEVELOPMENT OF A NON ADDITIVE HOMONUCLEAR SQUARE WELL CHAINS EQUATION OF STATE VALIDATED AGAINST MONTE CARLO SIMULATION</u>	112
III.1 INTRODUCTION.....	112
III.2 DEVELOPMENT OF NON-ADDITIVE SQUARE WELL CHAIN EQUATION OF STATE.....	114
III.2.1 GENERAL EXPRESSION OF THE EQUATION OF STATE.....	114
III.2.2 COMPUTATION OF THE PERTURBED CONTRIBUTION OF THE HELMHOLTZ FREE ENERGY	116
III.2.3 DETERMINATION OF INTER SEGMENT DISTRIBUTION FUNCTION $g_{ijSWC}(r)$	119
III.3 MONTE CARLO SIMULATION DATA	123
III.3.1 PURE CHAINS OF SQUARE WELLS	124
III.3.2 MIXTURES OF CHAINS OF SQUARE WELLS	125
III.4 VALIDATION OF SQUARE WELLS CHAINS EOS AGAINST MONTE CARLO SIMULATION RESULTS	131
III.4.1 VALIDATION OF INTER-SEGMENT DISTRIBUTION FUNCTION.....	131
III.4.2 VALIDATION OF COMPRESSIBILITY FACTOR.....	133
III.5 CONCLUSIONS	135
APPENDIX III-A: THE VALUES OF A_{PQ} AND B_{PQ} IN EQUATION (3.26) AND (3.27) AT CONTACT AND AT $\lambda = 1.5$	136
APPENDIX III-B: THE INTER-SEGMENT DISTRIBUTION FUNCTIONS OF PURE CHAINS OF SQUARE WELLS.	138

CHAPTER IV	144
<u>USE OF A NON ADDITIVE GC-PPC-SAFT EQUATION OF STATE TO MODEL HYDROGEN SOLUBILITY IN OXYGENATED ORGANIC COMPOUNDS</u>	
IV.1 INTRODUCTION.....	145
IV.2 GC-PPC-SAFT EQUATION OF STATE	146
IV.2.1 MODEL DESCRIPTION	146
IV.2.2 GROUP CONTRIBUTION PARAMETERIZATION OF THE PPC-SAFT MODEL	151
IV.3 PREDICTIVE USE OF GC-PPC-SAFT ON HYDROGEN + OXYGENATED MIXTURES.....	153
IV.4 EXTENSION OF GC-PPC-SAFT TO NON-ADDITIVE SQUARE WELLS CHAINS	159
IV.5 RESULTS OF THE PREDICTION AND CORRELATION OF HYDROGEN SOLUBILITY IN OXYGENATED SOLVENTS.....	163
IV.5.1 DETERMINATION THE PSEUDO-IONIZATION ENERGY OF OXYGENATED GROUPS.....	163
IV.5.2 PREDICTIVE METHOD OF NON-ADDITIVE PARAMETER L_{ij}	166
IV.6 CONCLUSIONS	172
APPENDIX IV-A PARAMETERS FOR THE USE OF GC-PCC-SAFT	172
APPENDIX IV-B EXPERIMENTAL DATA IN THE LITERATURE	176
APPENDIX IV-C: DERIVATIVES OF THE FREE ENERGY OF NON-ADDITIVE TERM	182
CHAPTER V	196
<u>SOLUBILITY OF THE OTHER GASES IN OXYGENATED SOLVENTS</u>	
V.1 INTRODUCTION.....	196
V.2 GENERAL STRATEGY FOR MODELING SOLUBILITY OF CO, H ₂ S AND NH ₃ IN POLAR SOLVENTS	198
V.2.1 REPRESENTATION OF PURE COMPONENTS WITH PPC-SAFT	198
V.2.2 MIXTURES	199
V.3 SOLUBILITY OF CARBON MONOXIDE (CO) IN OXYGENATES	201
V.3.1 DATABASE AND CONSISTENCY TESTS	201
V.3.2 PREDICTION OF PHASE EQUILIBRIUM AND THE SOLUBILITY OF CARBON MONOXIDE IN OXYGENATED SOLVENT.....	208
V.4 SOLUBILITY OF HYDROGEN SULFIDE (H ₂ S) IN OXYGENATES	209
V.4.1 DATABASE AND CONSISTENCY ANALYSIS.....	209
V.4.2 PREDICTION OF PHASE EQUILIBRIUM AND THE SOLUBILITY OF HYDROGEN SULFIDE IN OXYGENATED SOLVENTS.....	212
V.5 SOLUBILITY OF AMMONIA (NH ₃) IN OXYGENATES.....	215
V.5.1 DATABASE AND CONSISTENCY ANALYSIS.....	215
V.5.2 PREDICTION AND CORRELATION OF PHASE EQUILIBRIUM AND THE SOLUBILITY OF AMMONIA IN OXYGENATED SOLVENTS	218
V.6 CONCLUSION	223

<u>GENERAL CONCLUSIONS</u>	<u>226</u>
<u>PERSPECTIVES</u>	<u>228</u>
<u>PUBLICATION LIST</u>	<u>229</u>
<u>REFERENCES</u>	<u>230</u>

GENERAL INTRODUCTION

To reduce the emissions of carbon dioxide and meet the worldwide energy demand, biomass is considered as a new friendly resource for fuels production. First generation biofuels are today in increasing use. Their feedstock originated from agriculture make them competitors of food production, thus limiting their further development. Second generation biofuels, on the opposite, use waste or lignocellulosic material (wood products) as a feedstock. However these products are much more difficult to transform into fuels, which is why a large number of research and development projects focus on this problem¹.

In 2020, the estimated energy demand in the world is about 180 billion liters of ethanol and 60 billion liters of biodiesel while production of the world will be about 160 billion liters for ethanol and 50 billion liters for biodiesel.² With the current technology, the production cannot meet the demand of biofuel market. It is therefore necessary to develop new technologies to increase the efficiency of biorefineries.

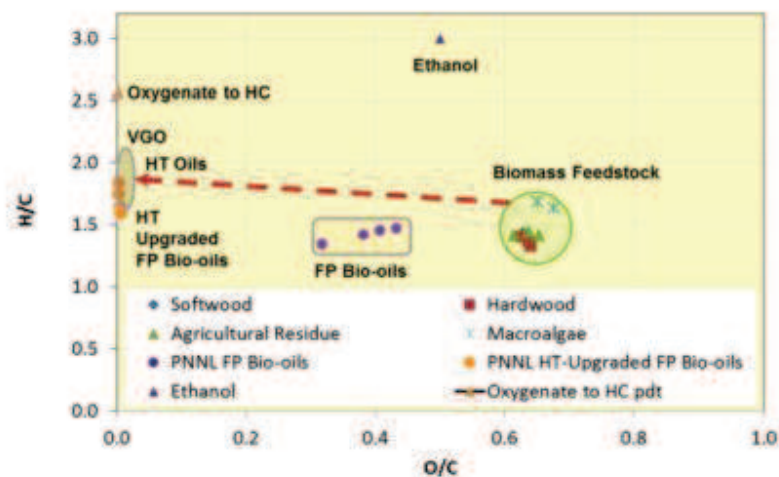


Figure 1: Van Krevelen diagram for comparison between biomass feed- stock with vacuum gas oil (VGO). H/C = hydrogen – carbon atom ration, O/C = oxygen – carbon atom ration, HC = hydrocarbons, FP = fast pyrolysis, HT = hydrotreated³

Figure 1 shows one of the major differences that are observed between conventional fuel and their feedstock (crude oil) and biomass feedstocks. The conventional products contain almost no oxygen, which makes them stable and highly energy intensive. The feeds from biomass however generally contain oxygenated groups such as alcohol (OH), aldehyde (CHO), ester (COO-) and carboxylic acid (COOH) : the presence of oxygen results in a larger reactivity and lower calorific values (the oxygen present in the material replaces that which is naturally brought by air in the combustion). In order to improve the biofuel quality to reach that of crude oil, it is necessary to raise the ratio H/C from 1.5 to 2 and in parallel the ratio O/C should become approximate zero.

In biorefineries, there are three industrial processes to produce the biofuel from biomass. At first, biomass must be pretreated, dried and crushed into powder. This step allows injecting biomass under pressure via a fluidization system. The first process that we would like to mention here is the gasification at high temperature (between 1200°C to 1600°C) with the presence of oxygen. The important product of this process is synthesis gas. The second process is the fermentation by using enzymes. This process produces an important quantity of bio-ethanol for the production of biofuel. Finally, the pyrolysis or hydrothermal treatment that represent a direct thermal decomposition method for the production of a liquid product from biomass in the absence of oxygen.

The Fast Pyrolysis bio-oil, shown on Figure 1, is the liquid obtained after a first treatment of biomass. In order to remove oxygen, the well-known hydrotreatment process can be used. The operation principle of this process is similar to that of hydrodesulfurization (HDS) in conventional refineries (catalytic reaction of hydrogen). Here, it allows eliminating the oxygen from the bio-oil at extreme conditions : high temperature (300°C – 400°C) and high pressure (7MPa – 10MPa). In this process, hydrogen is dissolved in the liquid and the reaction products such as H₂O, H₂S, NH₃, CO, CO₂ ... are distributed between the fluid phases. In order to design and optimize the HDO (HydroDeOxygenation) process, it is necessary to understand the partitioning of hydrogen as well as the reaction products in oxygenated solvents.

Currently, some thermodynamic models exist to model the hydrogen/hydrocarbons

equilibria encountered in conventional hydrotreating processes. We can mention for example the method of Grayson Streed⁴ (GS), which is very often used in the petroleum industry, or the cubic equations of state such as Soave - Redlich - Kwong⁵ (SRK) and Peng Robinson⁶ (PR), which must be parameterized based on experimental data. These models cannot be sufficient considering the large number of systems and the limited number of data. Today, no predictive thermodynamic model exists to this end. IFP Energies Nouvelles has been working for many years in collaboration with the Laboratory of Processes and Materials Science (LSPM) on the development of the Statistical Associating Fluid Theory (SAFT) coupled with a group contribution method. This SAFT equation of state has proved to have a good predictive capacity for oxygenated mixtures. The first version of SAFT was introduced by Chapman and al^{7,8}. It is developed on the basis of the theory of Wertheim⁹⁻¹². For the last twenty years, several versions of SAFT have been proposed in the literature and used to model the behavior of complex fluids. Due to its strong theoretical foundation, it extrapolates well. PC-SAFT (Perturbed Chain - Statistical Associating Fluid Theory) is a specific version that was designed based on hydrocarbons behavior, and that therefore has had an important success in the engineering community. In recent years, several theories have focused on the extension of the PC-SAFT¹³ equation of state first in order to add a group contribution method¹⁴ (Group Contribution - PC-SAFT) and then to extend it to polar compounds¹⁵ thus yielding the GC-PPC-SAFT equation, the additional P referring to 'Polar'. The predictive quality was assessed by Nguyen Huynh.¹⁵ Both Thi¹⁶ and NguyenHuynh¹⁷ proposed predictive approaches more specifically for H₂/hydrocarbon systems. The internship of M. Kadri¹⁸ has identified some limitations of the model for mixtures of H₂/oxygen-bearing solvents as will be discussed later.

Thesis objectives

The main objective of this thesis is to develop a predictive tool to compute the vapor-liquid equilibria (VLE) associated with hydrotreating operation of biomass feeds. For this purpose, we will work on the complementarities between data, molecular simulation and equations of state:

- Data are the final referee for the quality of any computational approach, this is why they are essential for any model development. In addition, since most modeling tools require regressing a number of empirical parameters, they are needed in the parameterization procedure. Yet, considering the scarcity of the data, they must be complemented, whenever possible using, true experimental tools. An adequate analysis of the existing data may help identifying the most crucial data.
- When true experimental measurements are not feasible, they can be complemented using theoretical tools. This is one of the interests of Molecular Simulation which we have used in this work.
- Molecular simulation also helps understanding the phenomena at hand, and therefore it contributes to the development of new equations of state that have sufficient physical foundation to support predictive approaches. This was also the principle that has led us in the development of an additional contribution to the existing SAFT Equation of State.

This thesis consists of 5 chapters, each of which, except the first, is constructed so that it can be published as a separate paper :

In the first chapter, we present the state of the art of thermodynamic models that allow predicting the phase equilibrium of small molecules in the oxygenated solvents (or the solubility of these molecules in oxygenated solvents). In this thesis, the thermodynamic property that we study is mainly Henry's constant because the solubility of small gases especially hydrogen in solvents, is very low i.e. near conditions of as an infinite dilution state. After that, the data analysis methods have been described. Otherwise, the molecular simulation is used in this work as an efficient tool to produce pseudo-experimental data and validate the model development.

The Chapter II focuses on the construction of a database of binary systems containing hydrogen and oxygenated solvents. The next step is the analysis of experimental data by internal and external analysis methods. This helps evaluating the consistency of available data and so we can obtain a good database for the prediction using a thermodynamic model. In this chapter, the production of pseudo data of Henry's constant by Monte Carlo simulation

has been done.

The regressions using GC-PPC-SAFT on Henry's constant of hydrogen needs non-zero k_{ij} that are negative k_{ij} . This is in principle not physically acceptable. We therefore suggest to consider a correction on the repulsive contribution and therefore develop a new contribution in GC-PPC-SAFT called non-additive term. The introduction of this new term is presented in two subsequent chapters. Chapter III presents the development of this term applied for square well chains. This development is validated by Monte Carlo simulation.

The next chapter (Chapter IV) is devoted to the application of this development on the GC-PPC-SAFT EoS and for systems of hydrogen and oxygenated compounds. A predictive method for this non-additive parameter based on a group contribution approach is proposed.

Chapter V describes the application of the GC-PPC-SAFT model to mixtures containing product gases of the hydrotreating process like hydrogen sulfide, ammonia and carbon monoxide. Optimized parameters for computing the solubility of these gases in oxygenated components are proposed.

Finally, we finish this manuscript with a general conclusion that summarizes this work and discusses its perspectives.

CHAPTER I

BACKGROUND AND LITERATURE REVIEW

I.1 Introduction

In this introductory chapter, we shall review the state of the art of the main tools used during the thesis. The chapter starts with generalities about phase equilibrium calculations in process simulation; it is followed by a presentation of the main models available for industrial use. Some comments are proposed for data evaluation, and finally important concepts concerning the use of molecular simulation are introduced.

I.2 Predictive models for biomass hydrotreatment

The objective of this work is the development of a predictive tool for the solubility of gases, in particular hydrogen, in oxygenated compounds. This tool should eventually be made available for use in industrial process simulation software. There are two approaches for this type of calculations. The first is called the homogeneous or $\varphi - \varphi$ approach and uses a single equation of state (EoS) for all the phases. The cubic EoS Peng-Robinson or Soave-Redlich-Kwong are the most well-known. The second approach is the heterogeneous or $\gamma - \varphi$ approach and is based on both activity coefficient models and equations of state. The typical examples of such activity coefficient models are UNIQUAC or its predictive version called UNIFAC. In this paragraph, we try to give a brief summary about these thermodynamic models and their applications.

I.2.1 Phase equilibrium calculation

For a two phase system, at the given temperature and pressure, thermodynamically, equilibrium is obtained when the chemical potentials of all components in the two phases are

equal:

$$\mu_i^\alpha = \mu_i^\beta \quad (1.1)$$

One may rewrite this equality by introducing fugacity. The fugacity is a thermodynamic property that has dimensions of pressure and that is related to the chemical potential through the definition:

$$\mu_i = \mu_i^\circ + RT \ln \left(\frac{f_i}{P^\circ} \right) \quad (1.2)$$

Where f_i is the fugacity of component i ; the superscript ‘ \circ ’ refers to the reference state of component i , as a pure ideal gas at the pressure P° . For systems involving a single liquid phase in equilibrium with its vapor phase, i.e. a vapor-liquid equilibrium (VLE) and the criterion for equilibrium is written as:

$$f_i^V = f_i^L \quad (1.3)$$

1.2.1.1 Homogeneous method

In the homogeneous approach, both phases are described using the same model, classically an equation of state (see section I.2.4). The fugacity of each compound in each phase is given by:

$$f_i = \varphi_i P z_i \quad (1.4)$$

Where φ_i is called the fugacity coefficient; z_i is the molar fraction of component i in the phase of interest and P is its pressure. The equality of fugacities (Equation 1.3) can then be written equivalently introducing fugacity coefficients for each phase as:

$$y_i \varphi_i^V = x_i \varphi_i^L \quad (1.5)$$

Where y_i is molar fraction of component i in vapor phase, x_i is molar fraction of component i in liquid phase; φ_i^V and φ_i^L are the fugacity coefficients in vapor phase and liquid phase respectively. This equation can be also rewritten introducing the distribution coefficient K_i :

$$K_i = \frac{y_i}{x_i} = \frac{\varphi_i^L}{\varphi_i^V} \quad (1.6)$$

I.2.1.2 Heterogonous methods

Heterogonous methods consist in the use of different thermodynamic models for each phase in the system. Fugacity is always the product of a reference term, a composition term and a deviation to the ideality. For the liquid phase, the non-ideality is frequently described by an activity model which is a function of the composition of the phase. The fugacity is given by :

$$f_i^L = f_i^{L*}(T, P) \gamma_i x_i \quad (1.7)$$

Where $f_i^{L*}(T, P)$ is the pure component liquid fugacity, x_i is the molar fraction of component i in liquid phase and γ_i is the activity coefficient.

The most general expression for the liquid phase fugacity is equivalent to :

$$f_i^L = f_i^{L*}(T, P_i^\sigma) \phi_i \gamma_i x_i = P_i^\sigma \varphi_i^\sigma \phi_i \gamma_i x_i \quad (1.8)$$

Where P_i^σ is the vapor pressure of component i ; $\phi_i = \exp\left(\frac{1}{RT} \int_{P_i^\sigma}^P v_i^L dP\right) \approx \exp\left(\frac{v_i^L(P-P_i^\sigma)}{RT}\right)$ is the Poynting correction that uses v_i^L , the liquid molar volume of component i and T and assumed to be independent of P , P_i^σ is the pressure of saturation of component i . This correction takes into account the pressure difference between P_i^σ to P . The Poynting correction is only of importance for pressures that are 10 bar above the vapor pressure. φ_i^σ is the fugacity coefficient of component i at saturation calculated using the vapour phase.

The activity coefficient models are developed to describe the non-ideality of mixtures (especially high when very different molecules in term of size or chemical functionality, or when interactions are involved). It is only used for the liquid phase where these interactions are significantly strong. These models are generally limited to low pressure (generally less than 1.5 MPa) because the models feature no dependence on pressure.

For the vapor phase, an equation of state is used for computing φ_i^V . The ideal gas is a special case where $\varphi_i^V = 1$. The vapor phase is also described with an equation of state and the fugacity is still given by:

$$f_i^V = \varphi_i^V P y_i \quad (1.9)$$

And the distribution coefficient is given by:

$$K_i = \frac{f_i^{L*}(T, P_i^\sigma) \phi_i \gamma_i}{\varphi_i^V P} \quad (1.10)$$

In fact, Equation (1.7) is used when the component i can be described as a pure liquid in the pressure and temperature conditions of the system. It means that the reference term is equal

to the product of the vapor pressure of the pure liquid at the specific temperature and the Poynting correction to take into account a difference of pressure between saturation conditions and the considered pressure. This framework is classically used for systems including only liquid as reference conditions and it is the symmetric convention.

For components that have no vapor pressure at the temperature of interest (supercritical gases or ionic species), an asymmetric approach (cf. Figure I-1) must be used, using the Henry constant as f_i^{L*19} . In this case, we should consider the solvent which is the major component and is described by its vapor pressure and the solute (minority components) which is described by the Henry constant. The fact that Henry's constants are rarely known makes the use of this approach more complex for gas-liquid systems.

The Figure I-1 illustrates these two conventions. In the symmetric one, the reference state of both compounds are the vapor pressure. In the asymmetric convention, the reference state of the solvent is related to its vapor pressure and the reference state of the solute is the Henry constant which is given by the following relationship :

$$H_i = \lim_{x_i \rightarrow 0} \left(\frac{f_i^L}{x_i} \right) \quad (1.11)$$

In the case of the solvent, the equilibrium constant is still given by relation (1.10) and for the solute, the equilibrium constant is given by :

$$K_i = \frac{H_i \phi_i^\infty \gamma_i^*}{\phi_i^V P} \quad (1.12)$$

Including γ_i^* is the activity coefficient in asymmetric convention and ϕ_i^∞ is the Poynting correction defined with the solute partial molar volume at infinite dilution. For a solute who has a vapor pressure at the given temperature, it is still possible to use the symmetric convention and in this case, the equilibrium constant is given by :

$$K_i = \frac{\gamma_i^\infty P_i^\sigma \phi_i}{\phi_i^V P} \quad (1.13)$$

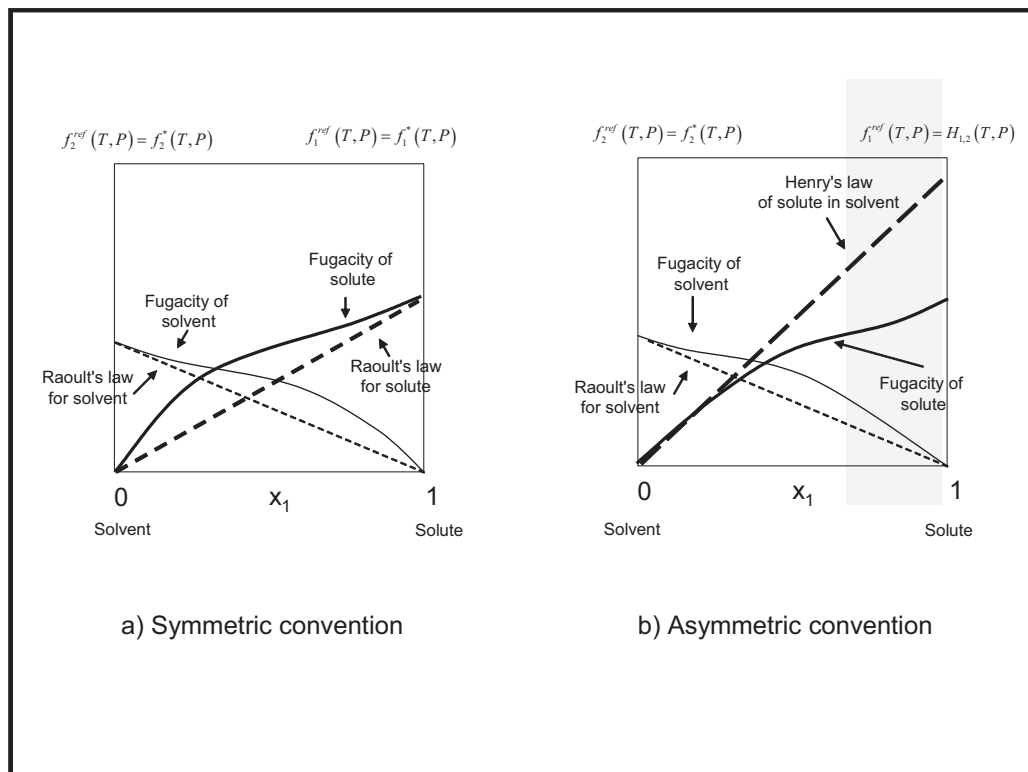


Figure I-1: Fugacities for symmetric and asymmetric conventions¹⁹

I.2.2 Overview of the expressions of Henry's constant

Henry's constants play a key role in the description of a low soluble gas in a solvent, especially when they are supercritical. Henry's constant can be obtained by different correlation methods. In their book, Fogg and Gerrard²⁰ cite some equations of correlation of solubility of hydrogen and other gases in hydrocarbons^{21,22}. These equations are generalized as:

$$\ln x_i = A + \frac{B}{T} \quad (1.14)$$

Where A and B are determined empirically and depend on the solvents, x_i is the mole fraction of gas in the liquid phase. When the pressure of system and the vapor pressure of the solvent are low, the mole fraction can be readily related to the Henry constant using the following relationship :

$$H_i = \frac{P_i}{x_i} \quad (1.15)$$

An equation that allows correlating Henry's constant is reported by Benson and Krause²³ and is discussed in the book of Prausnitz et al²⁴:

$$\ln H_i = a \left(1 - \frac{T}{T_c}\right) + b \left(1 - \frac{T}{T_c}\right)^2 + c \quad (1.16)$$

Where a, b and c are empirical constants. This equation is applied primarily on experimental data in the region 0 to 50°C.

Other authors have worked on the gas solubility using the solubility parameter^{25,26}. Recently, Harvey et al²⁷ have reported about the correlation of Henry's constant of some gases in water (including hydrogen). In their work, they showed the relationship between Henry's constant and distribution coefficient:

$$K_i = \frac{H_i}{\varphi_i^{\infty V} P_1^\sigma} \quad (1.17)$$

Where P_1^σ is the vapor pressure of the solvent. The index 1 here is used to indicate the solvent in the system.

The Henry's constant is correlated by following equation proposed by Japas and Levelt Sengers²⁸:

$$RT \ln \left(\frac{H_i}{f_1} \right) = C_1 + \frac{1}{(\rho_{c1})^2} \left(\frac{\partial P}{\partial x_i} \right)_{T,V}^{\infty,c} [\rho_1^*(1) - \rho_{c1}] \quad (1.18)$$

Where C_1 is the derivative (at constant T and V) of the residual Helmholtz energy with respect to x_i at the critical point, and ρ_{c1} is the critical density of the solvent, $\rho_1^*(1)$ is the saturated density of solvent. The derivative $\left(\frac{\partial P}{\partial x_2} \right)_{T,V}^{\infty,c}$ is known as the Krichevskii parameter, is taken at infinite dilution at the critical point of the solvent. An approximation have been used for the variation $\rho_1^*(1) - \rho_{c1}$ given by:

$$[\rho_1^*(1) - \rho_{c1}] = [T - T_{c1}]^\beta \quad (1.19)$$

Where β is the thermodynamic exponent and its value is 0.326 ± 0.002^{28} . In fact, this asymptotic value is difficult to observe, experiments typically produce an “effective” β near 0.355.

1.2.3 Activity models

Famous examples of activity coefficient models, are UNIQUAC²⁹ (UNIversal QUAsi-Chemical) Wilson. They are constructed as a sum of an enthalpic and an entropic contribution. The NRTL³⁰ model is described by an enthalpic contribution. Both the UNIQUAC and the NRTL models are adapted for the calculations of liquid-liquid equilibrium^{29,31–33}. In all cases, their parameters are fitted on experimental data: none of them is truly predictive.

Another well-known model is UNIFAC. The UNIFAC is a predictive version of the UNIQUAC equation for which parameters are obtained a the contribution group method. The

parameters of this model are associated with the volume fraction and surface fraction¹⁹. Generally, several versions of UNIFAC are proposed in process simulators. The most up-to date one is that of Dortmund that has been developed by the UNIFAC consortium. This model is used for systems containing oxygenated compounds³⁴⁻³⁶ which parameters are found in Figure II-2. However, it is not adapted to represent equilibria with supercritical gases.

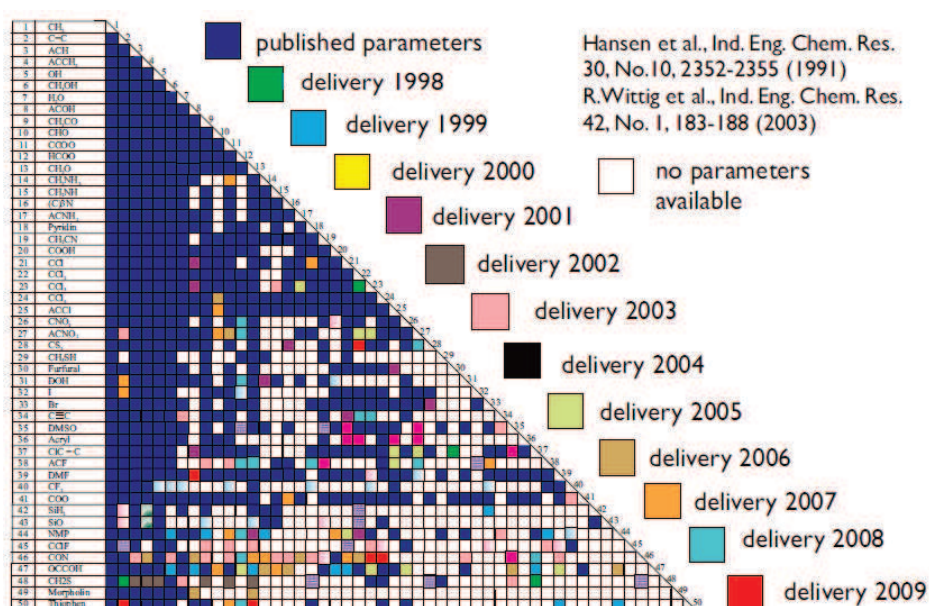


Figure II-2: UNIFAC Parameter Matrix^{37,38}

Another predictive way to compute activity coefficients for highly polar mixtures is COSMO-RS (Conduct-like Screening Model for Real Solvent). This model is based on quantum mechanical calculations: the starting point is an *ab initio* calculation on an isolated molecule surrounded by an ideal conductor.³⁹⁻⁴² This calculation allows determining the charge density distribution around the molecule, known as the σ -profile. In this model, the chemical potential is a function of the surface area of the molecule (A_i), the composition (x_i) and the σ -profile ($p_i(\sigma)$)

of each component in the system.⁴³ The model has been extended to polymers, proteins, ionic liquids,...⁴³⁻⁴⁵

In the oil industry, the most famous model for hydrogen equilibrium is the Grayson Streed method, based on a heterogeneous asymmetric approach. The distribution coefficient K_i in Equation (1.6) is rewritten as:

$$K_i = \frac{\varphi_i^{L*} \gamma_i}{\varphi_i^V} \quad (1.20)$$

Where φ_i^{L*} is the pure liquid fugacity coefficient that is calculated by using a specific method.⁴⁶

$$\varphi_i^{L*}(T_r, P_r) = \log \varphi_i^{(0)}(T_r, P_r) + \omega_i \log \varphi_i^{(1)}(T_r, P_r) \quad (1.21)$$

Where $\varphi_i^{(0)}$, $\varphi_i^{(1)}$ are universal corrections based on the principle of corresponding states. The liquid activity coefficient γ_i is calculated by using a regular solution model proposed by Scatchard et al⁴⁷:

$$\ln \gamma_i = \frac{v_i (\delta_i - \bar{\delta})^2}{RT} \quad (1.22)$$

where v_i is the molar volume of component i , δ_i is its solubility parameter and $\bar{\delta}$ is the solubility parameter for the solution⁴⁸.

The vapour phase fugacity coefficient φ_i^V is obtained from Redlich Kwong equation of state. This method is a predictive model for the solubility of hydrogen in hydrocarbons in petroleum industry. In Figure I-3, we observe that the classical Grayson-Streed (GS) method cannot reproduce correctly the change in Henry's constant with molar mass of the solvent. This is why Torres et al⁴ proposed to add a Flory contribution to the usual Scatchard equation for the

activity coefficient calculation (Augmented Grayson Streed, AGS). This way, an improvement in calculations are achieved. Unfortunately, the Grayson-Streed model has never been extended to oxygenated compounds.

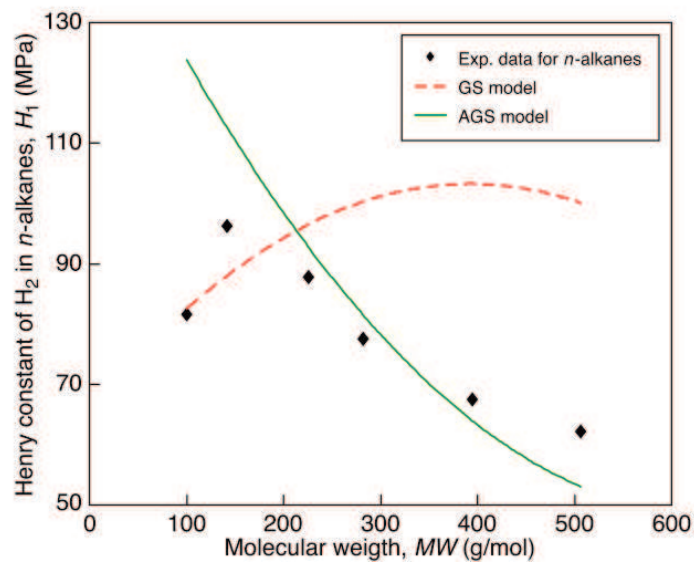


Figure I-3: Henry constant of hydrogen in n-alkanes at 423 K⁴

I.2.4 Equation of state

Equations of state (EoS) are mathematical relationships that enable calculation of the Helmholtz energy as a function of temperature, volume, and composition. Using thermodynamic relationships, other relevant properties (pressure, chemical potential, compressibility, speed of sound) can be assessed. The most important properties are pressure and chemical potentials, which are derived from:

$$P = \frac{RT}{V} - \left. \frac{\partial A^{res}(T, V, N)}{\partial V} \right|_{T, N} \quad (1.23)$$

Where $A^{res}(T, V, N)$ is the residual Helmholtz free energy of system, T is the temperature, P is the pressure, V is volume of the system and N is the number of molecules in the system. We then have :

$$RT \ln \varphi_i = \left. \frac{\partial A^{res}(T, V, N)}{\partial N_i} \right|_{T, V, N_{j \neq i}} - RT \ln \left(\frac{PV}{NRT} \right) \quad (1.24)$$

When the equation of state is expressed as a pressure explicit in volume, the fugacity coefficient can be computed equivalently using:

$$RT \ln \varphi_i = \int_{\infty}^V \left(- \left. \frac{\partial P}{\partial N_i} \right|_{T, V, N_j} + \frac{RT}{V} \right) dV - RT \ln \left(\frac{PV}{NRT} \right) \quad (1.25)$$

Where V is the molar volume, P is the pressure, T is the temperature, N_i is the number of molecules i in the system and R is the universal constant of ideal gas.

Equations of state have the following advantages:

- They are applicable to a large range of pressure and temperature. They allow taking into account the existence of critical points and represent the properties of pure components and also the mixtures in a coherent framework.
- Equations of state can describe more realistically both liquid and vapour phases in terms of structure and interactions than activity models.¹⁵

For engineering purposes, besides the virial equations, two principal types of equation of

state exist. Firstly, the cubic equations of state are mentioned because of their huge success in predictions of phase equilibrium of systems containing hydrocarbons that are of interest in the oil & gas industry. There are numerous versions of this type of model and their improvements in the literature. Secondly, the equations of state based on statistical mechanics which have a strong physical foundations capable of taking into account the physical nature of the fluids (e.g., interactions between hydrogen-bonding species, chain formation, etc).⁴⁹ We will describe briefly these equations in the next section.

1.2.3.1 Cubic equations of state

The most simple cubic equation of state is the Van der Waals equation proposed in 1873⁵⁰ which allows predicting vapor-liquid coexistence:

$$P = \frac{RT}{v - b} - \frac{a}{v^2} \quad (1.26)$$

Where T is temperature of system, v is the molar volume, P is pressure and R is the molar universal gas constant. The parameter a in this equation is a measure of attraction forces between molecules, and b is the covolume of the molecule. These two parameters a and b can be determined from the critical properties of the fluids in the system:

$$a = \Omega_a \frac{R^2 T_c^2}{P_c} \quad (1.27)$$

$$b = \Omega_b \frac{RT_c}{P_c} \quad (1.28)$$

where T_c and P_c are critical temperature and pressure; Ω_a and Ω_b are constant values which depend on the version of the equation.

As observed in equation (1.26), the Van der Waals equation consists of two terms, a hard sphere “repulsive” and another, called “attractive”. Their sum presents the interactions between molecules. Despite the fact that the description of these interactions is qualitatively correct, it is not accurate for the calculation of phase equilibrium.

All cubic EoS are modifications of this equation on either the repulsive term or on the attractive term or even both. The most famous equations of state modified from Van der Waals are Soave-Redlich-Kwong⁵ (also called SRK) and Peng-Robinson equation of state⁶ which are described in Table I-1.

Table I-1: Some cubic equation of state used mostly in oil & gas industry

Equation	Expression
Soave-Redlich-Kwong (SRK)	$P = \frac{RT}{v - b} - \frac{a(T)}{v(v + b)}$ $a(T) = a_c \alpha(T) = a_c [1 + m(1 - \sqrt{T/T_c})]^2$ <p>with $m = 0.48 + 1.574\omega - 0.176\omega^2$ ω is acentric factor. a_c and b is defined by equation (27) and (28)</p>
Peng-Robinson (PR)	$P = \frac{RT}{v - b} - \frac{a(T)}{v^2 + 2vb - b^2}$ <p>with $m = 0.37464 + 1.54226\omega - 0.26992\omega^2$.</p>

Either of these two equations of state is used widely in petroleum industry for hydrocarbons systems containing hydrogen.⁵¹⁻⁵³ Notice that for the mixtures, it is necessary to

use mixing rules for the parameters. The simple mixing rules of Van der Waals are often applied:

$$a_m = \sum_i \sum_j x_i x_j a_{ij} \quad (1.29)$$

$$b_m = \sum_i \sum_j x_i x_j b_{ij} \quad (1.30)$$

with

$$a_{ij} = (1 - k_{ij}) \sqrt{a_i a_j} \quad (1.31)$$

$$b_{ij} = (1 - l_{ij}) \frac{b_i + b_j}{2} \quad (1.32)$$

Where k_{ij} and l_{ij} are binary interaction parameters. l_{ij} is most often taken as zero.

These mixing rules are adequate for hydrogen + hydrocarbon mixtures but not or polar and associative systems. Huron and Vidal^{54,55} proposed a solution by modifying the mixing rules⁵⁶. This modification based on the equality of the excess Gibbs energy computed by the cubic EoS with that of an activity coefficient model at a reference pressure. Subsequently this method was improved by Michelsen^{57,58}, Wong and Sandler⁵⁹, Tassios^{60,61},...

In order to increase the predictive power of cubic EoS, Gmehling et al⁶² developed a version of SRK⁶³ (Soave Redlich Kwong) which is combined with the predictive activity model UNIFAC (including a group contribution). This model, named PSRK, is widely used in chemical industry. In PSRK (Predictive SRK)⁶⁴, the parameters a_m and b_m are computed by the following mixing rule:

$$a_m = b_m \left[\frac{g_0^E}{A_1} + \sum x_i \frac{a_i}{b_i} + \frac{RT}{A_1} \sum x_i \ln \left(\frac{b_m}{b_i} \right) \right] \quad (1.33)$$

$$b_m = \sum x_i b_i \quad (1.34)$$

with $A_1 = -0.64663$; g_0^E is the UNIFAC excess Gibbs energy model. The disadvantages of this model is the poor results on the excess enthalpies, activity coefficients at infinite dilution and liquid densities.⁶⁵

In order to further improve the model in term of liquid phase density representation, the VTPR (Volume Translated Peng Robinson) EoS has been developed more recently, based on the same principle. It consists of a combination of the Peng-Robinson EoS and a group contribution method.

In general, the cubic equations of state reproduce very well phase equilibrium of non-polar mixtures even containing supercritical components⁶⁶. The combination of cubic EoS with Huron-Vidal type mixing rules improve significantly their capacity for describing complex polar systems, and they have been modified so as to become fully predictive for mixtures through PSRK and VTPR. However, while they are used extensively in the chemical industry, they have not been applied for hydrotreatment conditions. Indeed, for the polar components, the cubic equations of state have some difficulties in prediction and extrapolation.

I.2.3.2 Statistical mechanics based equation of state

Basically, two large families of such equations can be identified: those based on the lattice fluid theory and those based on the perturbation theory.

a. The lattice fluid theory

The first type of equation of state is based on the lattice fluid theory. The initial theory by

Flory considered the molecules as beads or chains of beads that occupy well-identified lattice sites in the fluid. Extensions of this theory have been proposed allowing empty sites or sites with variable size. In this way, the impact of volume could be incorporated. Similarly, enthalpic interactions can also be included.

The earliest lattice model was developed for vapour-liquid equilibrium calculations of polymers in supercritical fluids⁶⁷. The most well-known model is by Sanchez⁶⁸ and Vera^{69,70}, still mostly used for polymer systems. Recently, to account for hydrogen bonding interactions, Panayiotou et al. presented the so-called Non Random Hydrogen-Bonding (NRHB) model which is an extension of the Panayiotou and Vera EoS^{71,72}. The modification with the possibility to consider the presence of proton acceptors and proton donors makes it possible to account explicitly and generally for specific interactions such as hydrogen bonding. This EoS has been shown to be a promising model for vapour-liquid, liquid-liquid, and solid-liquid equilibria (with liquid or supercritical solvents) of highly polar and hydrogen bonding molecules.⁷³⁻⁷⁶

b. Perturbation theory

Since the 1960s, there has been considerable progress in the application of statistical thermodynamics to predict thermodynamic properties of equilibrium of pure fluids at high pressures and in the condensed state.⁷⁷

These methods of statistical thermodynamics, which are collectively called perturbation methods⁷⁸, give excellent results in predicting thermodynamic properties of simple fluids. Consider a thermodynamic system with N spherical molecules and total intermolecular potential energy U at the equilibrium and at the temperature T . We can write the following relationship between the Helmholtz free energy, A , and the canonical partition function, Q , of such a system:

$$A = -k_B T \ln Q \quad \text{with} \quad Q = \frac{Z_N}{N!} \left(\frac{h^2}{2\pi m k T} \right)^{-\frac{3N}{2}} \quad (1.35)$$

In the relationships above, h is Planck's constant, k is Boltzmann's constant, m is the molecular mass and Z_N is the configurational partition function which is defined by the following expression:

$$Z_N = \int_V \dots \int \exp\left(\frac{-U}{k_B T}\right) dr_1 \dots dr_N \quad (1.36)$$

Integrations in the relationship above are performed with respect to the volume, V , of the thermodynamic system; dr_i is the contracted notation of dx_i, dy_i, dz_i , where x_i, y_i, z_i are the spatial coordinates (cartesian) of molecule i . The total intermolecular potential energy, U , includes the potential energies of all possible interactions between the molecules of the system, namely:

$$U = \sum_{j>i=1}^N u_p(r_{ij}) + \sum_{l>j>i=1}^N w(r_{ij}, r_{il}, r_{jl}) + \dots \quad (1.37)$$

Where u_p is the energy of interaction between two molecules i and j while w is the change of energy of interaction between three molecules i, j and l . In most studies, it is restricted to two-body interactions. Note that in the case $U = 0$ (ideal gas), $Z_N = V^N$.

Knowing the potential of two-body interaction, it is theoretically possible to estimate the free energy A and to deduce the pressure (equation of state):

$$P = -\left(\frac{\partial A}{\partial V}\right)_{T,n} \quad (1.38)$$

The main difficulty in developing an equation of state in fact lies in the evaluation of A that cannot be done rigorously, but only by using approximation such as perturbation techniques.

This technique requires the definition of a potential of reference term and a potential of a perturbation term.

$$\mathbf{u}(\mathbf{r}) \equiv \mathbf{u}^{ref}(\mathbf{r}) + \mathbf{u}^{pert}(\mathbf{r}) \quad (1.39)$$

Although in principle many choices are possible to split the potential into reference and perturbation terms, it was devised that a good choice (in term of convergence of the series, see Equation 1.39) would be that the reference term is essentially repulsive whereas perturbation term is essentially attractive.

These definitions allow writing a new “hypothetical” potential:

$$\mathbf{u}(\mathbf{r}, \lambda) = \mathbf{u}^{ref}(\mathbf{r}) + \lambda \mathbf{u}^{pert}(\mathbf{r}) \quad (1.40)$$

For $\lambda = 1$, we find the function of intermolecular potential of the real system. And for $\lambda = 0$, the equation above reduces in a function of the potential of the reference system. The Helmholtz free energy of the real system is obtained from a Taylor series expansion of A in the neighborhood of $\lambda = 0$:

$$A_\lambda = A_{\lambda=0}^{ref} + \sum_{n=1}^{\infty} \frac{\lambda^n}{n!} A_{\lambda,n} \quad (1.41)$$

Where A_λ^{ref} represents the free energy of the reference fluid with $\lambda = 0$. It is an arbitrary hypothetical fluid with λ -value $\hat{\lambda}$.

and $A_{\lambda,n}$ is defined by the following relation:

$$A_{\lambda,n} = \left(\frac{\partial^n A_\lambda}{\partial \lambda^n} \right)_{\lambda=0} \quad (1.42)$$

The free energy of the real fluid is obtained by performing $\lambda = 1$ in the equation (1.41):

$$A = A^{ref} + A_1 + A_2 + \dots \quad (1.43)$$

One may show the first order term is given by :

$$A_1 = \frac{N\rho}{2} \int g^{ref}(r) u^p(r) dr \quad (1.44)$$

where $g^{ref}(r)$ is the radial distribution function of the reference system; the radial distribution function is defined as the ratio of the local density $\rho(r)$ at a distance r on the reference molecule on the average density $\rho = N/V$ in the fluid; to that effect, $g(r)$ characterizes the molecular structure, it means the organization of molecules around a reference molecule.

The terms A_2, A_3, \dots are very complex. A_i becomes more complex as the order i increases. However, by appropriately selecting the reference potential and the perturbation potential, it is a priori possible to limit the development in free energy to the first two or three terms (fast convergence of the Taylor development). For this purpose, it is preferable to choose the reference term to be the repulsive part of the potential and the perturbation is then the attractive part. Notice that the expression of A_1 may be extended to homonuclear chains by :

$$\frac{A_1}{NkT} = \frac{1}{2} \rho \sum_i \sum_j x_i m_i x_j m_j \int 4\pi r^2 dr g_{ij}^{ref}(r) \beta u_{ij}^{pert}(r) \quad (1.45)$$

Where x_i, x_j are molar fractions of molecule i and j respectively; m_i, m_j are the number of

constitutive segments or the length chain of molecule i and j ; ρ is the total molecular density and

$$\beta = \frac{1}{kT}.$$

At first, we can list some equations based on this theory : Chain of rotators (COR)⁷⁹ and Boublik-Chen-Alder-Kreglewski (BACK)⁸⁰. Another successful model in this category, was developed by Ikonomou and Donohue^{81,82} and called the Associated Perturbed Anisotropic Chain Theory (APACT). This model takes into account the isotropic repulsive and attractive interactions, anisotropic interactions caused by hydrogen bonding and dipolar, quadrupolar moments of molecules. It includes five parameters representing a characteristic energy, size, shape, association enthalpy and entropy. As for all equations of state, they are obtained by fitting on experimental data such as vapor pressure and liquid density. The APACT EoS was used for systems containing water⁸³ or alcohols⁸⁴ to predict their liquid-liquid phase equilibrium. The expressions of the compressibility factor using these equations of state are summarized in Table I-2.

Table I-2: Equations of molecular thermodynamics : $Z = Z^{\text{rep}} + Z^{\text{disp}} + Z^{\text{assoc}} + Z^{\text{polaire}}$

Equation	Z^{rep}	Z^{disp}	Z^{polaire}	Z^{assoc}
Chain of rotators (COR) ⁷⁹	Prigogine ⁸⁵ , Boublik and Nezbeda ⁸⁶ $1 + \frac{4\left(\frac{\bar{v}}{\tau}\right)^2 - 2\left(\frac{\bar{v}}{\tau}\right)}{\left(\frac{\bar{v}}{\tau} - 1\right)^3} + \frac{c}{2}(\alpha - 1) \frac{3\left(\frac{\bar{v}}{\tau}\right)^2 + 3\alpha\left(\frac{\bar{v}}{\tau}\right) - (\alpha + 1)}{\left(\frac{\bar{v}}{\tau} - 1\right)^3}$	Alder et al ⁸⁷ . $\left[1 + \frac{c}{2}(B_0 + B_1/T + B_2/T)\right] \sum_{n,m} \frac{A_{n,m}}{T^n \bar{v}^m}$	-	-
Boublik-Chen-Alder-Kreglewski (BACK) ⁸⁰	Boublik ⁸⁸ $\frac{1 + (3\alpha - 2)\zeta_3 + (3\alpha^2 - 3\alpha + 1)\zeta_3^2 - \alpha^2\zeta_3^3}{(1 - \zeta_3)^3}$	Alder et al ⁸⁷ . $- \sum_i \sum_j j D_{ij} \left[\frac{u}{kT} \right]^i \left[\frac{\zeta_3}{\tau} \right]^j$	-	-
Associated PACT (APACT)	$1 + c \frac{4(\tau/\bar{v}) - 2(\tau/\bar{v})^2}{(1 - \tau/\bar{v})^3}$	$\left[Z_1^{LJ} + Z_2^{LJ} - 2Z_1^{LJ} \left(\frac{A_2^{LJ}}{A_1^{LJ}} \right) \right] / \left(1 - \frac{A_2^{LJ}}{A_1^{LJ}} \right)^2$ $Z_1^{LJ} = \frac{c}{T} \sum_i \frac{i A_{1i}}{\bar{v}^i} \quad A_1^{LJ} = \frac{c}{T} \sum_i \frac{A_{1i}}{\bar{v}^i}$ $Z_2^{LJ} = \frac{c}{T^2} \sum_i \frac{i C_{1i}}{2\bar{v}^i} + \frac{(i+1)C_{2i}}{\bar{v}^{i+1}} + \frac{(i+2)C_{3i}}{2\bar{v}^{i+2}}$ $\frac{A_2^{LJ}}{kT} = \frac{c}{T^2} \sum_i \frac{C_{1i}}{2\bar{v}^i} + \frac{C_{2i}}{\bar{v}^{i+1}} + \frac{C_{3i}}{2\bar{v}^{i+2}}$	Gubbins and Twu ⁸⁹ modified	Chemical theory of association ⁹⁰⁻⁹² $\frac{n_T}{n_0} - 1$

\bar{v} : reduced molecular volume, $\bar{v} = V\sqrt{2}/Nrd^3$

c : Prigogine factor

V : total volume of N molecules

τ : valant constant 0.7405

ζ_3 : compactity

α : non sphericity parameter

ϵ_q : parameter of molecular energy

n_0 : number of total moles without association

n_T : number of total moles of all chemical components with association

R : universal constant of ideal gas

T : Temperature

A_{nm}, B_i, D_{ij} : universal constants

c : parameter of rotation and vibration

k : Boltzmann's constant

\bar{T} : reduced temperature, $\bar{T} = ckT/\epsilon_q$

However, the most famous equation of state based on statistical mechanics is SAFT (Statistical Associating Fluid Theory), first proposed by Chapman et al^{7,8}. This equation of state considers that a molecule is a chain of segments that are covalently linked to each other. Using the Wertheim association theory^{11,93}, SAFT also takes into account explicitly the intensive interactions such as charges transfer and hydrogen bonding.

There are many versions of this equation of state which are summarized in the review papers of Wei and Sadus⁹⁴ and Colina et al⁹⁵. We can mention here some well-known versions:

- Hard-sphere SAFT^{8,96}: Molecules are viewed as chains of hard spheres with van der Waals interactions
- Square-well SAFT⁹⁷: Extended thermodynamic perturbation to include square-well chains which quantifies monomer-monomer potential
- Lennard-Jones SAFT (LJ-SAFT)^{98,99}: Includes effects from dipole interactions and modifications to the hard sphere term
- soft-SAFT¹⁰⁰: a virial-type EoS is used to map the Lennard-Jones spheres behavior to molecular simulation results
- variable-range SAFT (SAFT-VR)¹⁰¹: Addresses chain contribution with segments of variable range potentials
- perturbed-chain SAFT (PC-SAFT)¹³: The reference is the chain of segments and the dispersive contributions are fitted to the behavior of alkanes.
- Dimer SAFT (D-SAFT)¹⁰²: Inclusion of a Dimer equation for hard-sphere chain molecules SAFT- γ -Mie^{103,104}: the Mie potential, with variable exponents, is used as a basis for the description of the sphere-sphere interactions

The differences between these versions of SAFT depend on the reference term, repulsive and attractive interactions chosen. For example, in LJ-SAFT, Lennard-Jones spheres are used as a reference whereas in PC-SAFT it is the hard sphere chain. Recently, several authors have proposed a further refinement to the theory by adding a specific term for polar interactions.^{12,105,106} (dipole-dipole, dipole-quadrupole or quadrupole-quadrupole)

I.2.3.3 Hybrid equation of state

A number of authors have proposed to construct equations of state by combining terms originating from different theories. Although this approach somehow loses the physical coherence of the model, from a pragmatic point of view, they seem to work rather well. The two good examples we can mention in this category are Cubic Plus Association (CPA) EoS and Group Contribution Association (GCA) EoS.

The first one is an equation of state combining between the Soave-Redlich-Kwong EoS⁶³ with the association term from SAFT¹⁰⁷. The pressure is written by:

$$P = \frac{RT}{v-b} - \frac{a}{v(v+b)} + \frac{RT}{v} \rho \sum_A \left[\frac{1}{X^A} - \frac{1}{2} \right] \frac{\partial X^A}{\partial \rho} \quad (1.46)$$

Where ρ is the molar density and X^A is the molar fraction of the compound not bonded at site A. The CPA EoS parameters are determined by fitting experimental data of the vapor pressure and saturated liquid density. CPA describes very well the solubility of water in the esters and biodiesels¹⁰⁸, binary mixtures of fatty acids¹⁰⁹ and phase equilibrium of glycerol, alcohols with water.¹¹⁰

The second hybrid equation of state is GCA EoS proposed by Gros et al.¹¹¹ In this model, the association term from Wertheim's theory¹¹ is combined with the group contribution EoS developed by Skjold-Joergensen et al.^{112,113} There are two important parameters for each term in this EoS : volume, association energy for association contribution and surface, dispersive energy for group contribution. This state equation performs well for predicting the phase equilibrium in the binary¹¹⁴ and ternary mixtures¹¹⁵ composed of oxygenated species (such as water, alcohols in mixture with hydrocarbons).

I.2.5 Summary of the references dealing with hydrogen solubility

Table I-3 summarizes the references of authors who investigated phase equilibrium of mixtures containing hydrogen. We have noticed the equation of state used, the fitting parameters and the deviations obtained by the authors. Most of the investigation concern systems of hydrogen in hydrocarbons where the predictions using cubic equations of state give good results. Most authors regress a binary interaction parameter in the equation of state to obtain the good calculation. The prediction of systems containing oxygenated compounds sometimes gave good results but these authors have only worked on specific systems.

Table I-3: Summary of systems containing hydrogen and different types of solvents treated by different models reported in the literature

Mixtures	Authors	Equation of state	k_{ij} and/or l_{ij}	AAD %
H ₂ +alkane	Gao et al. ¹¹⁶	SRK PR	k_{ij} (Tc, Pc)	15,65%
	Ferrando et al. ¹¹⁷	PR	k_{ij}	7.2%
	Torres et al. ⁴	AGS GS		30% 55%
	Moysan et al. ¹¹⁸	SRK PR	k_{ij}	<10%
	Breman et al. ¹¹⁹	PR	k_{ij}	<98%
	Park et al. ¹²⁰	SRK PR	k_{ij}	<5%
	Gao et al. ¹²¹	SRK PR	k_{ij}	<5%
	Huang et al. ¹²²	SRK	-	<6%
	Twu et al. ¹²³	SRK	k_{ij}	-

	Valderama et al. ¹²⁴	SRK PR VC	k_{ij}	5.2% 3.4% 3.1%
	Huang et al. ¹²⁵	PR NRTL Wong-Sandler mixing rule	k_{ij}	-
	Moysan et al. ¹²⁶	SRK	k_{ij}	4%
	Laugier et al. ⁵³	SRK	k_{ij}	1.5%
	Qian et al. ⁵²	GC-PR	k_{ij}	8.14%
	Florusse et al. ¹²⁷	Soft-SAFT		1.5%
H ₂ +alkene or aromatic	Ferrando et al. ¹¹⁷	PR	k_{ij}	7.2%
	Moysan et al. ¹²⁶	SRK	k_{ij}	4%
	Xie et al. ¹²⁸	PR	k_{ij}	<8%
H ₂ + oxygenated compound	Pereira et al. ¹²⁹	GC-PPC-SAFT PSRK	k_{ij}	6% 2.7%
	Breman et al. ¹¹⁹	PR	k_{ij}	<98%
	Luehring et al. ¹³⁰	RGT SPT	-	16.7% 7.2%
	Jonasson et al. ¹³¹	CPA	PGG	NA
	Purwanto et al. ¹³²	UNIFAC UNIQUAC	-	9%
	D'Angelo et al. ¹³³	PR	-	<40%
	Xie et al. ¹²⁸	PR	k_{ij}	<8%
	Jonasson et al. ¹³⁴	SRK, PR combined UNIFAC	-	-

PR = Peng-Robinson

SAFT = statistical associating fluid theory

SRK = Soave-Redlich-Kwong

UNIFAC = UNiversal Functional Activity Coefficient

UNIQUAC = UNiversal QUasi-chemical Activity Coefficients

VC = Valderrama-Cisternas equation of state

CPA = cubic plus association

PACT = perturbed anisotropic chain theory

GC = contribution de groupe

PGG = utilisation de paramètres groupe-groupe

RGT= Regular

SPT= Space particle theory

NRTL = Non-Random Two Liquid model

GS = Grayson-Streed

AGS= Augmented Grayson-Streed

I.2.6 Our choice: GC-PPC-SAFT

As mentioned above, the heterogeneous models are generally not recommended for systems at high-pressure, which is the operating condition of the hydrotreatment process. In addition, the cubic equations of state have difficulties in representation of oxygenated compound which are associative and/or polar components. Therefore in this thesis, we have selected the GC-PPC-SAFT. It is an extension of the PPC-SAFT (Polar – Perturbed SAFT)^{13,15} combined with a group contribution method developed by Tamouza et al.¹⁴ because of its strong theoretical basis. IFPEN and LSPM have been collaborating for over ten years now on subsequent versions of this equation in order to improve its predictive capacity for mixtures containing polar and associative molecules. This equation of state has shown to perform very well for the prediction of phase equilibria of systems of aromatic oxygenated compounds with some gases¹²⁹ and with

water.^{135,136}

In recent years, several contributions have focused on the extension of the PC-SAFT equation of state (Perturbed Chain - Statistical Associating Fluid Theory), first in order to add a method of group contribution¹⁴ (Group Contribution – PC-SAFT) and then to extend it to polar¹⁵ compounds, thus renamed as GC-PPC-SAFT equation, the additional P referring to 'Polar'. The predictive quality was assessed by NguyenHuynh et al¹⁷. Le Thi et al.¹⁶ and Nguyen et al.⁴⁹ proposed predictive approaches more specifically for H₂/hydrocarbon systems. M. Kadri¹⁸ has identified the limitations of the model for the binary mixtures of H₂/oxygen-bearing solvent. We take their work as a basic to go further.

I.3 Experimental data and their consistency

Experimental data are essential for the development of thermodynamic models. They are used both for fitting and for validation. This is true both for pure component and for multi-component systems data. In this work, we used, whenever possible, the DIPPR database for pure components data. This database is the result of an in-depth analysis of all data by the Brigham Young University team which is now known worldwide. For mixtures, the data considered originate mostly from the DETHERM database which is also known worldwide for its exhaustive data availability. However, these data have not necessarily been screened for their quality, which is why a specific treatment is needed.

I.3.1 Problem statement

When data for a specific system, in a well-defined region of pressure and temperature, are searched, it may happen that (1) no data is found or (2) a large number of data exist but the scatter is such that it is difficult to evaluate what is the true physical behavior. In order to analyze these data in a coherent way so as to extract the maximum of information from the existing data and make clear recommendations for additional measurements, a number of steps are proposed:

- Firstly, we need to understand the ways that the experimental data have been obtained. Many different techniques exist in order to describe a phase diagram. Also, from the evaluation of experimental data in the literature, we can estimate the experimental uncertainty of investigated property i.e. Henry's constant.
- Generally, the raw data do not necessarily correspond to the final values as reported in the publications and/or databases: a treatment is needed that may rely on calibration and/or theoretical tools.
- The same data can be reported in many different ways: solubility, Henry constant, bubble pressure, ... Again, a conversion is often needed, which may require the use of additional fluid properties (e.g. solvent density or molecular weight).
- The difficulty in the construction of database is the data consistency. So the comparison between the different authors who worked on same systems is an indispensable way to find out. The internal and external data analysis play important role in this work.

In this thesis, the Henry's constant is considered as a main property to evaluate the solubility of hydrotreating gases (e.g. hydrogen). The lack of data and the problem of data reliability is very clearly observed.

I.3.2 Experimental techniques

The first step in data analysis is to understand the origin of the data. In this paragraph, we present the different ways (type of data) that authors use to report the solubility information. This has been described quite extensively by Dohrn et al¹³⁷.

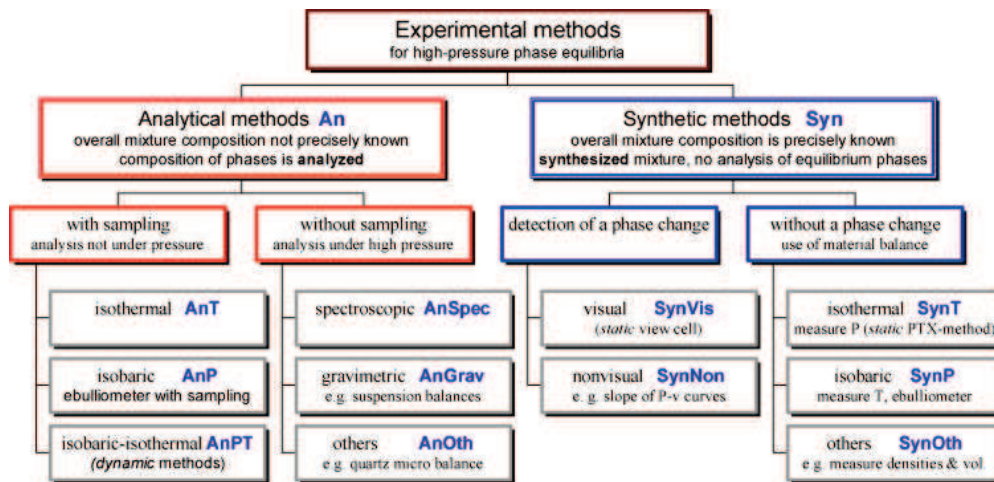


Figure I-4: Classification of experimental methods for high-pressure phase equilibria^{137,138}.

Figure I-4 attempts to provide a synthetic view of the experimental ways to obtain phase equilibrium data. The equilibrium is achieved using either a static (once the cell is loaded, the fluid does not move and equilibrium is achieved by stirring) or a dynamic technique (one component flows through the other). The determination of the phase composition can be performed in a synthetic way : the amount of each component introduced into the cell is carefully determined prior to equilibration or in an analytic way : the composition of the phases in equilibrium is measured after sampling (using gas chromatography). This last method is especially used in case of low molar fraction of solvent.

Table I-4 presents a number of examples taken from literature for hydrogen + oxygenates systems. Some use a static technique with a stirred autoclave. In order to obtain the gas solubility some authors use the synthetic approach. The initial pressure of pure solvent is performed. Injection of a well-identified quantity of hydrogen in the cell. The global cell composition is then exactly known. The analytical approach is then used to determine phase equilibrium.

More rarely, the second technique called dynamic method is used. It is achieved using a high-pressure cell containing pure solvent with a specified level. A solvent recirculation helps achieving equilibrium. This method requires liquid pumps and a valve system. To measure the

gas solubility in oxygen-bearing components, an analysis method is also requested with two methods mentioned above.

Table I-4 summarizes the experimental methods used to obtain data (by using analytical^{128,139,134,140–144} or synthetic^{132,133,143–150} methods to detect quantities of gas and solvent in the investigated systems) as well as the uncertainty of available data as reported by the authors.

Table I-4: Experimental data of hydrogen solubility with references

Type of data	Author	Apparatus and experiment type	Analysis method	Uncertainty
Henry's constant	Purwanto et al. ¹³²	Static technique with stirred autoclave	Synthetic method	1-4%
	D'Angelo et al. ¹³³	Static technique with stirred autoclave	Synthetic method	20%
	Bezanehtak et al. ¹⁴⁰	Dynamic technique	Analytical method	4.4%
	Lenoir J-Y. et al. ¹⁵¹	Dynamic technique	Analytical method	4-5%
	Liu Q. et al. ¹⁵²	Static technique with stirred autoclave	Synthetic method	12%
	Dake S. et al. ¹⁵³	Static technique with stirred autoclave	Synthetic method	2-3%
Bunsen coefficient	Maxted et al. ¹⁴⁵	Stirred autoclave (Horiuti type)	Synthetic method	2%
Ostwald coefficient	Katayama et al. ¹⁴¹	Stirred autoclave (Horiuti type)	Analytical method	2%

	Bo S. et al. ¹⁵⁴	Static technique	Synthetic method	0.1%
Equilibrium phase (VLE)	Wainwright et al. ¹⁴²	Static technique with stirred autoclave	Analytical method	3-11%
	Brunner, E. et al. ¹⁴³	Static technique with stirred autoclave	synthetic method (at low mole fraction of methanol) and analytical method (at high mole fraction of methanol)	3-7%
	Descamps, C. et al. ¹³⁹	Static technique with stirred autoclave	Analytical method	10%
	Brunner, E. et al. ¹⁴⁴	Static technique with stirred autoclave	synthetic method (at low mole fraction of ethanol) and analytical method (at high mole fraction of ethanol)	
	Kwang J. Kim et al. ¹⁴⁹	Dynamic technique	synthetic method	0.4-7%
	Lu, X. et al. ¹⁵⁰	Dynamic technique	synthetic method	1%
	Xie, Z. et al. ¹²⁸	Dynamic technique	Analytical method	5%

	Brunner, E. et al. ¹⁴⁷	Static technique with stirred autoclave	synthetic method	0.5%-20%
	Brunner, E. et al. ¹⁴⁸	Static technique with stirred autoclave	synthetic method	2%
	Jonasson, A. et al. ¹³⁴	Static technique with stirred autoclave	Analytical method	1.1%
	Leu A. et al. ¹⁵⁵	Static technique	Analytical method	2%
	Fischer K. et al. ¹⁵⁶	Static technique	synthetic method	4%
	Inomata H. et al. ¹⁵⁷	Dynamic technique	Analytical method	2.5%
	Schafer D. et al. ¹⁵⁸	Static technique	Analytical method	2%
	Zeng Z. et al. ¹⁵⁹	Static technique	Analytical method	1.2%
	Huang L. et al. ¹⁶⁰	Static technique	Analytical method	4.42%
	Wilcock R. et al. ¹⁶¹	Static technique	synthetic method	2%

As shown in Table I-4, the same type of data may be reported in different ways: vapor-liquid equilibrium data, allow plotting the entire bubble curve of a system, but either Ostwald coefficient, Bunsen coefficient, Kuenen coefficient or Henry's constants express the solubility at infinite dilution (generally at atmospheric pressure). All these quantities can be converted to a unique value which is the Henry constants. This conversion is mentioned in the IUPAC¹⁶² guide (Appendix II-A). As will be shown in Chapter II, for hydrogen – organic solvent systems, Henry's constant is sufficient for describing most of the phase diagram.

I.3.3 Consistency analysis

After determining the type of data that we will work on (in our case is Henry's constant) and converting all available data into this property, the consistency analysis is an essential step because the quality of data is the key of success of the final model. There are different methods to evaluate the coherence between different experimental data for pure components and for mixtures. Different authors discuss about this subject by using the Gibbs – Duhem relationship^{163,164} for mixtures. For pure components, Rowley et al¹⁶⁵ have checked the data accuracy of DIPPR. There are two methods that allow checking the consistency of experimental data: the internal check discussed by Frenkel et al.^{166,167}; the external check studied by Mathias et al.¹⁶⁸

I.3.3.1 Internal consistency analysis

In order to consider the data consistency of a system, there are different methods. For data validation of a pure component, especially for vapor pressure, Wilsak and Thodos¹⁶⁹ have proposed a method using a high resolution graphical representation.

For mixtures, the simplest test is to evaluate whether the bubble and dew points converge to the vapour pressure of the pure components. Another well-known test method is that of the Gibbs-Duhem criterion²⁴ to validate isothermal phase equilibrium data (both liquid and vapour composition must be provided). For liquid-liquid equilibria, Othmer et al.¹⁷⁰ proposed a graphical method.

In our case, we consider VLE of highly asymmetric systems. In order to be able to present all data on a single plot so as to be able to compare and evaluate their internal coherence, it was chosen to transform all data into Henry's constants and plot it as a function of temperature. It was then possible to evaluate how well the results reported by various authors follow the same trend.

I.3.3.2 External consistency analysis

This method of data validation is based on the comparison of the behavior of a property of different components in the same chemical family. A diagram of this property as a function of for instance number of carbon atoms are presented. The points that are out of trend are the incorrect value.. Recently, in their work, Mathias et al.¹⁶⁸ and Rozmus et al.¹⁷¹ have used this approach for evaluating the vapor pressure of families of compounds. It consists for each component investigated, a value at the same temperature for example and we can easily identify the trends.

I.4 Molecular simulation

Historically the role of the simulation for thermodynamical applications was to obtain data for systems interacting via given and well defined potential models and validate the corresponding free energy models. Whenever data are lacking or for theoretical developments, molecular simulation may also play a complementary tool. In this work, we plan to use molecular simulation for producing pseudo-experimental data of Henry's constant of gases in oxygenated compounds. We will determine the phase properties and the conditions of thermodynamic equilibrium from the calculation of molecular interactions coupled with statistical averages on a system with a few hundred molecules. Although these methods require computing time much greater than conventional models as equations of state, they experience considerable success in industrial research (Ungerer and al.¹⁷²). Indeed, these methods are reliable and compare well to classical equations of state and excess models^{117,129} or used as a method for data extrapolation.¹⁷³

Furthermore, molecular simulation is used to study the behavior of fluids and materials at the scale of atoms and establish the link between this behavior and the macroscopic properties. Nowadays, we know that the application of these approaches to hydrocarbons gives excellent results^{174,175} and we begin to see their extension to more complex molecules with particularly

oxygen-bearing groups.^{176–178}

I.4.1 Generalities of molecular simulation

Molecular simulation is a method that explicitly takes into account every single position and conformation of each molecule in the investigated system. In this method, the detailed electronic structure of each molecule is not considered as much as the molecular interactions. The concept of statistical ensemble defined in statistical thermodynamics is necessary for molecular simulation. To put it simply, a statistical ensemble is the collection of all possible states that a system can reach considering a set of constraints, such as imposed temperature, volume and number of molecules (this is the canonical ensemble). A “state” is here the set of all positions and velocities of all the particles within the system, and the system is the collection of molecules of interest in a sufficiently large number so that the averages converge to the macroscopic properties.

Considering the extremely large number of molecules (typically of the order of the Avogadro number), and therefore the extreme difficulty to have access to the full ensemble, a number of tricks must be used to make sure that the averages are representative of the true fluid behavior: in practice, both the number of molecules considered, and the collection of ensembles is far smaller than what is found in real life.

Regarding the number of molecules, we have typically worked with systems containing a hundred molecules. The extrapolation to ‘infinity’ is performed using periodic boundary conditions, so that the real fluid is modeled with an infinite number of identical boxes containing the molecules under consideration.

Even within this small box, a very large number of possible ensembles can be constructed. In order to retain only the ones that have a statistically reasonable chance of occurrence, two major approaches exist (summarized in Figure I-5). The first is through molecular dynamics, which consists in solving the equations of motion, and the second is Monte Carlo simulation, in which a statistical method is used. In both cases, a first realistic ensemble is generated at random (as an initialization). Using molecular dynamics, the next state is

constructed from the previous one using the Newton mechanics formulae: all particles move according to the velocities defined in the previous state, and they bounce on each other depending on their relative positions. The average properties (denoted by $\langle \dots \rangle$ on Figure I-5) are obtained by sampling the space of time. Using Monte Carlo simulation, each configuration is generated from the previous one by performing a Monte Carlo type of movement (e.g. conformational change of a molecule, rotation, translation, volume change,...) and is accepted or rejected according to a probability criteria based on the energy of the system. The properties are obtained by using averages in the configurational space.

Both methods allow calculating equilibrium properties like density and enthalpy but Monte Carlo simulation converges faster. The molecular dynamics are usually used for the dynamic behavior of a system, especially the transport properties (e.g. diffusion coefficients, thermal conductivity, viscosity).

Here we need to calculate the energy of the system and it is given by :

$$U_{tot} = U_{ext} + U_{int} \quad (1.47)$$

U_{ext} is external energy (or intermolecular) which is a sum of electrostatic potential energy, polarization, dispersion and repulsion. As for intramolecular energy U_{int} , it is also a sum of the energies elongation, bending, twisting and interaction between distant neighbors. In order to compute these quantities, it is essential to determine how the molecules interact via force fields. Molecular models are used to that end.

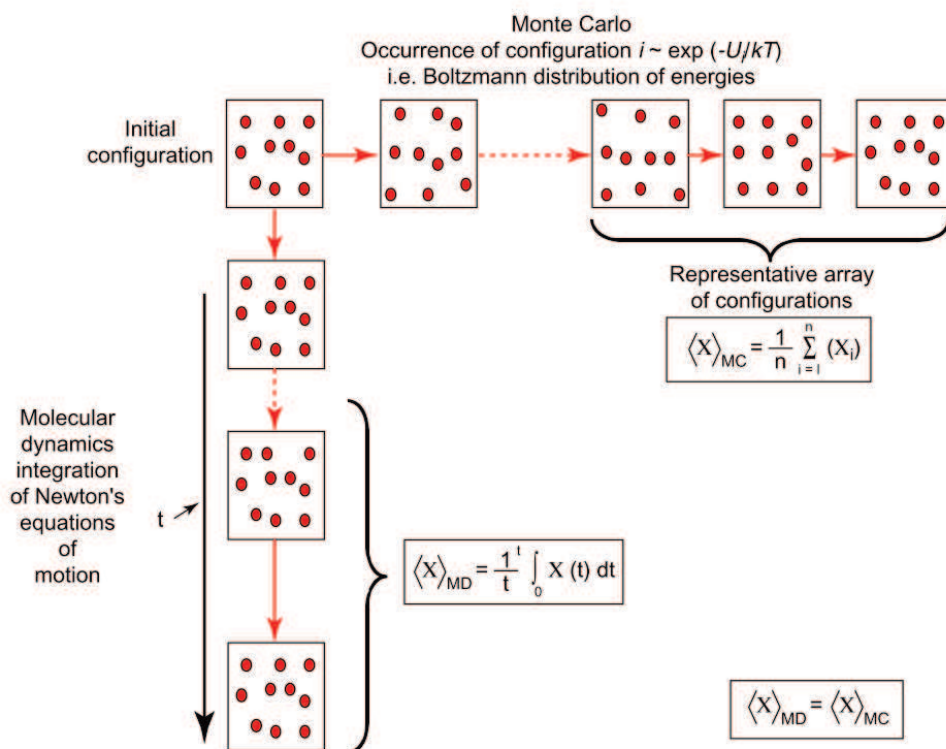


Figure I-5: The two ways of building a statistical ensemble: Molecular dynamics (MD) and Monte Carlo (MC) simulation. Average properties can be determined from time averages in MD and from ensemble averages in MC. Both averages are equivalent, as a consequence of the ergodicity theorem¹⁷⁹

I.4.2 Molecular model

Intermolecular interactions are determined by using a force field which is a set of equations and parameters to calculate the potential of interaction between and within two molecules. In reality, the interactions are determined between the force centers (atoms or groups of atoms) that compose the molecule. We can use different types of molecular simulation force fields. In some cases (for hydrogen), the molecule is represented as a single force center. When dealing with more complex molecules, it is decomposed into groups, each of which is described using a specific force center. There are three approaches that allow describing molecular groups

in terms of force centers: all atoms (AA), united atoms (UA) or anisotropic united atoms (AUA).

I.4.3 Force fields for hydrogen

Usually, the force field parameters can be regressed on vapor pressure and liquid volume data. Because hydrogen is a very light gas with a low critical temperature and for which quantum effects are considerable, the properties such as volume and vapor pressure (at very low temperature) cannot be used to adjust the molecular potential.

This is why Hirschfelder et al.¹⁸⁰ proposed to set the parameters of hydrogen by using Virial coefficient and viscosity data while considering that the hydrogen molecule behaved like a Lennard-Jones sphere. Other studies¹⁸¹⁻¹⁸⁵ on hydrogen adsorption used a simple Lennard-Jones sphere as well. In these works, it was observed that this type of model yields accurate results. Darkrim et al.¹⁸⁶ used a single Lennard-Jones sphere model with a quadrupole moment. In their study, Ferrando et al.¹¹⁷ tested different models for the hydrogen molecule in hydrogen/hydrocarbons (e.g. n-hexane, cyclohexane, benzene,...). These authors compared the calculation errors of hydrogen molar fraction using both the Darkrim model and the Hirschfelder model. From the results of their work, it appears that the best is that of Darkrim et al.¹⁸⁶.

I.4.4 Intermolecular potential of oxygenated compounds

Complex molecules are constructed using force fields representing individual groups. Any of the below choices can be used, depending on how the molecule is decomposed into groups.

a. All Atoms Approach

When a force field is assigned to each atom in the molecule, it is called an All Atoms (AA) force field¹⁷². This approach allows representing a molecule by describing all atoms

included in the molecule. For the research about the molecular structure and geometry, this method should be privileged. However, it requires a huge amount of computing time because of the number of force centers for each molecule. Otherwise, in this approach there are many types of parameters which depend also on the environment. It means that the parameters of hydrogen atoms bonded to oxygen atoms is different from those of hydrogen atoms bonded to carbon atoms. In the literature, several known models use this approach: AMBER¹⁸⁷ (Assisted Model Building with Energy Refinement), OPLS-AA¹⁸⁸ (Optimized Potentials for Liquid Simulations – All Atoms), CHARMM¹⁸⁹ (Chemistry at HARvard Macromolecular Mechanics), COMPASS¹⁹⁰ (condensed-phase optimized molecular potentials for atomistic simulation studies).

b. United Atoms Approach

If the force field is assigned to groups of atoms (force centers) such as CH₂, CH₃ or CH, it is called United Atoms force field (UA).¹⁷² In this case, the force centers in CH_x groups are located on the C atoms. In fact, the position of these force centers would decide the type of force field. We have 2 types here: United Atoms (UA) or Anisotropic United Atoms (AUA), where the force center is displaced by Δ with respect to the main atom.

Typical models which use this approach are TraPPE-UA¹⁹¹ (Transferable Potentials for Phase Equilibria), OPLS-UA¹⁹² (Optimized Potentials for Liquid Simulations – United Atoms).

c. Anisotropic United Atoms Approach

In order to consider the influence of the hydrogen atoms in a molecule, this approach suggests displacing the force center to a position between the atom center and the hydrogen atoms.^{193,194} For instance, in the case of a CH₂ group (cf. Figure I-6), the displacement occurs along the external bisector of the angle C – C – C.

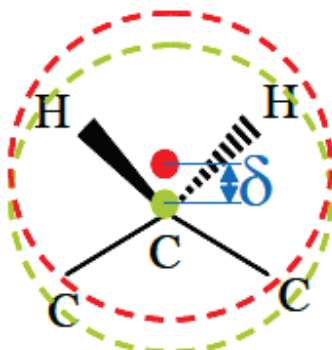


Figure I-6: Example of a position of force center in the AUA approach

This molecular model is a good compromise between simplicity and physical relevance.¹⁷⁹ In this method, the presence of hydrogen atoms is implicit compared to the UA approach. In addition, the computing time decreases considerably in comparison with the AA approach.

As an example, we can mention the AUA4 intermolecular potential initially developed by Ungerer et al¹⁹⁵. It allows using this model for hydrocarbons, and most of mono-functional oxygen-bearing compounds.^{178,196–199} This model has proven to be well adapted for phase equilibrium calculations. Typical average deviations in terms of vapor pressure and density are respectively 5% and 1.5%.¹⁹⁹

At first, it is important to validate this approach for calculation of Henry's constant of hydrogen in oxygenated fluids through molecular simulation. This validation step was performed and is described in the next section.

I.4.5 Computation of structural or macroscopic properties

Molecular simulation has been used in this work in order to compute a number of macroscopic or structural properties. This paragraph summarizes the methods used to obtain

Henry's constant, radial distribution function and compressibility factor.

I.4.5.1 Henry's constant from Monte Carlo simulations

In this thesis, Monte Carlo simulation is used to determine the Henry's constants of hydrogen in different solvents modeled with the AUA4^{178,196-199} force field. The most suitable approach for calculating Henry's constant is that of the Widom's insertion¹⁷² test. This method allows evaluating the chemical potential of a solute in a solvent. It consists of a simulation box with the imposed conditions like the pressure P , the temperature T and the number of particles N in this box. The "phantom" molecule is inserted into the simulation box in order to determine the potential energy. After that, the inserted particle is removed from the system and the procedure is repeated. The pressure of system is required to maintain higher than the pressure of saturation of the solvent as predicted by molecular simulation using the same force field (the Henry's constant is defined at this pressure, but in practice, we must make sure that the solvent is liquid).

I.4.5.2 Radial distribution function

Radial distribution function $g(r)$ describes the probability distribution that two particles are located at a distance r from each other. This allows understanding the heterogeneity in the system. This information makes it possible to evaluate the structure of a fluid. As an example, the comparison of the radial distribution function between the oxygen and hydrogen atom of the hydroxyl groups of neighbouring molecules makes it possible to evaluate the strength of hydrogen bonding as illustrated by Ferrando et al.²⁰⁰ The radial distribution function is an important feature that is used in the perturbation theory.

In Gibbs ensembles, in order to determine the $g(r)$, it is necessary to obtain the histogram that represents the number of times that a reference particle is located from another particle at a distance between $d(i)$ and $d(i+1)$. Afterwards, the radial distribution function is calculated by this

expression:

$$g(r) = \frac{h(r)}{\frac{N}{V} \times \frac{4}{3} \pi ((r + dr)^3 - r^3)} \quad (1.48)$$

Where $h(r)$ is the histogram; N is total number of particles in the system; V is the volume of the simulation box; r is the diameter of reference particle.

I.4.5.3 Compressibility factor

Among the most simple properties to be evaluated is the relationship between pressure-volume and temperature. A convenient way to express this relationship is by evaluating the non-dimensional compressibility factor, defined as :

$$Z = \frac{P}{\rho kT} \quad (1.49)$$

Where P , ρ , T are pressure, density and temperature of the system respectively, k is Boltzmann's constant.

For doing this a Gibbs ensemble at fixed NPT conditions is selected. It means that the pressure P , the number of particles N and the temperature of system are imposed T . The computation yields a density that yields directly the compressibility factor.

Otherwise, we also use some parameters such as the reduced temperature T^* ($T^* = \varepsilon/kT$ where ε is the dispersive energy), the reduced pressure P^* ($P^* = \sigma^3 P/\varepsilon$, where σ is diameter of particle). We present usually the compressibility factor Z in function of the compacity η ($\eta = \rho v_m$ with v_m is molar volume of system)

In fact, we must know about the values of T^* and P^* in order to validate our development

in molecular simulation with other authors in the literature. The density and the molar volume are the properties obtained after a post-treatment in Monte Carlo simulation.

I.5 Conclusion

In this chapter, a review of a number of important issues dealt with in the thesis is proposed:

- First, a literature review of the engineering models available for vapor – liquid calculations of hydrogen containing systems is proposed.
- A short comment is made regarding the use of experimental data.
- Finally, generalities on molecular simulation on provided since in this work we will use this tool (1) as an alternative for data generation, (2) in order to generate information regarding the microstructure of a fluid and (3) to validate the development of a new contribution to an equation of state.

A predictive model needs to be developed and validated using a consistent set of experimental data. The main purpose of the next chapter is analyzing the available data in the literature including the data collection, the consistency check of experimental data in order to produce a reference database. It is observed that there is a lack of data, especially at high temperature. Molecular simulation is therefore used as a tool to produce pseudo-experimental data for some binary systems. Therefore, in this section, some techniques and methods of data analysis are briefly described. This work has been submitted as an article in the Journal of Chemical Engineering Data.

CHAPTER II

HYDROGEN SOLUBILITY IN OXYGENATED COMPOUNDS

Thi-Kim-Hoang TRINH^{a,b}, Jean-Charles DE HEMPTINNE^{a,}, Rafael LUGO^a, Nicolas FERRANDO^a, Jean-Philippe PASSARELLO^b*

^a IFP Energies nouvelles, 1 & 4 avenue de Bois-Préau, 92852 Rueil-Malmaison Cedex, France

^b Laboratoire de Science des Procédés et des Matériaux (LSPM), Université Paris Nord, CNRS, Institut Galilée, 99 avenue Jean-Baptiste Clément, 93430 Villetaneuse, France

Keyword: hydrogen, Henry's constant, oxygenated compound, hydrotreatment

Abstract

In this work, a database of binary systems of hydrogen and 42 organic compounds including alcohols, aldehydes, carboxylic acid, esters and ethers, glycols, n-alkanes and one particular case of hydrogen/water is constructed. From different available sources, we have derived the Henry constants as a measure of the hydrogen solubility in different organic solvents. After removing inconsistent data, a correlation as a function of temperature is proposed whenever possible (many data are limited to room temperature). Its average deviation is consistent with experimental uncertainty between 5% and 10%. Further data reduction could then be performed by comparing the Henry constant behavior among solvents.

Considering the lack of data for some binary mixtures, Monte Carlo molecular simulation precisely the insertion test (called Widom test) is chosen as a method to obtain pseudo-experimental data of hydrogen solubility at high temperature in 19 oxygen-bearing compounds such as alcohols, linear ketones, ethers, esters (573.15 K to 723.15 K) within average statistical uncertainties of 8%. The trend of Henry's constant from the results of molecular simulation is similar to that of the experimental data.

The analysis of the entire database shows that the Henry constants depend on chemical family in following way:

$$H_{\text{diols}} > H_{\text{alcools}} > H_{\text{esters}} > H_{\text{aldehydes}} > H_{\text{ethers}} > H_{\text{alkanes}}$$

The trend with molecular weight is generally decreasing, even though for some families this is less clear. The Henry constants of hydrogen in all solvents decrease with temperature. The slope of $\ln H$ vs $1/T$ depends little on chemical family. At high temperature, a few experimental data confirm the observation of molecular simulation showing an increase of this slope.

II.1 Introduction

In the context of the reduction of carbon dioxide emissions and the willingness to decrease the dependency on fossil energies, the concept of biorefinery has gained an increased interest. In order to meet the requirements for producing biomass-based fuels, several major issues of biomass feeds must be overcome, such as a low LHV (lower heating value), high viscosity or chemical stability.^{201,202} These major drawbacks are caused by the presence of molecules^{203,204} containing oxygen-bearing groups such as OH, CHO, COO, COOH, ... These are the main reasons why hydrotreating processing (hydrodeoxygenation, HDO) units are used, whose operating principle is similar to hydrodesulfurization (HDS) units in classic petroleum refineries. In these units, biomass feeds are processed under a hydrogen partial pressure of about 7-20 MPa at high temperature²⁰⁵ (573.15 K to 723.15 K). To design and optimize the HDO process, it is necessary to understand and model the thermodynamic behavior (vapor - liquid equilibrium, VLE) of feedstocks in presence of gases resulting from the HDO reactions, which include mainly hydrogen but also carbon dioxide, carbon monoxide, ammonia, hydrogen sulfide and water. Considering the low solubility of these gases, specially hydrogen, in the organic solvents, Henry's constant is a good descriptor of the almost linear bubble curve of these binary systems.

An important step towards the design of classical hydroprocessing units involves the determination of mutual solubilities of these gas-liquid systems. Predictive tools are therefore

needed. These approaches are also required for preliminary process engineering calculations in order to check the technico – economic viability of biomass process technologies. Some authors have proposed specific approaches for predicting the solubility of gases in hydrocarbons, especially for hydrogen solubility. The Grayson-Streed⁴ approach is probably the most widely used method, but cubic equations of state are increasingly used^{16,117,123,118}. For oxygen-bearing compounds, there is no recognized approach for predicting the solubility of gases in these compounds. Therefore, the development of predictive methods for computing the solubility of H₂O gases in oxygen-bearing molecules is still required. As in any thermodynamic study, the first step is data inventory and analysis.

In the present work, we have made an inventory of the available VLE data for binary systems of hydrogen/oxygenated molecules and water. The data compiled include compositional VLE data (P-T-x_y), Henry's constants and other types of infinite dilution properties: Ostwald, Bunsen and Kuenen coefficients. After having converted all the data into Henry's constants, we have checked the consistency of the available data and we have also identified the major gaps in terms of chemical families and temperature range. An improved Henry constant correlation is proposed and used to this end. The molecular simulation (called Widom test) was then validated and used to generate new pseudo-experimental data when required in order to extend the trends in terms of alkyl chain and temperature.

II.2 Data inventory

II.2.1 Data sources

In order to verify the consistency of the experimental data available before using a model for the prediction, it is necessary to build a database and to analyze it. As a first step, we gathered a large number of available experimental data for binary systems containing hydrogen and an organic compounds with a special focus on oxygen-bearing components. Here we considered only the data for the solubility of hydrogen in a mono-functional organic solvents. These data are

reported in different ways: vapor-liquid equilibrium (VLE), Henry's constant, Ostwald coefficient, Bunsen coefficient and Kuenen coefficient.

Table II-1 summarizes the data that we have extracted from the literature sources that we have found. We consider here all types of solubility data of hydrogen in oxygenated solvents with the widest ranges of temperature and pressure. The data are classified by family of solvents. The temperature range of the data is also provided (often data are only available at a single temperature, which is most of time 298.15 K), as well as the pressure range (often atmospheric pressure), the number of points and the data type.

Table II-1: Database of binary mixtures of hydrogen in n-alkanes and organic components

Groups	Compounds	Temperature range (K)	Pressure range (MPa)	N _{Total pts} / N _{Accepted pts}	Type of data (with references)
1-alcohol	methanol	213.15-413.15	0.0117-110.3	75/49	PTxy ^{139,140,142,143,206-211} , H ^{133,140,212} , L ^{141,213,214} , α ²¹⁵ , H* ^{130,216}
	ethanol	213.15-508.15	4.1-33.3	49/26	Removed: H ¹³³ , PTxy ²⁰⁶ PTX ^{142,144} , L ^{141,213,214} , H ^{132,133} , α ^{145,217,218} , H* ¹³⁰
	1-propanol	213-513.6	0-10.6	35/10	Removed: H ¹³³ , α ²¹⁸ PTX ^{142,218} , L ^{141,213} , H ¹³³
	1-butanol	213-533.15	1.52-30.3975	41/31	Removed: H ¹³³ PTX ^{142,218-220} , L ^{141,213} , H ^{133,219} , H* ¹³⁰
	1-pentanol	298.15-373.15	0-9.8	6/4	Removed: H ¹³³ PTX ²¹⁸ , L ^{213,214}
	1-hexanol	298.15-373.15	0-10.24	4	Removed: L ²¹⁴
	1-heptanol	298.15	0.1	3	PTX ²¹⁸ , L ²¹³
	1-octanol	273.32-553.15	0.69-30.0	15	L ²¹³ , α ²²¹
	1-nonanol	298.15	0.1	1	PTxy ^{149,150,219} , L ²¹³ , α ²²¹
	1-decanol	298.15	0.1	1	L ²¹³
	1-undecanol	298.15	0.1	1	L ²¹³
	1-dodecanol	298.15	0.1	1	L ²¹³
	1-tetradecanol	323.15-373.15	0.98-3.923	5	L ²¹³
	1-hexadecanol	498	0.1	1	H* ²²² H ¹¹⁹

aldehyde	propanal	293.2-393.2	2.5-20.0	12	PTX ²²³ , H ²²³ PTX ²²³ PTX ²²⁴ , H ²²⁴ PTxy ¹²⁸ , H* ²²⁵ Removed: H*²²⁵
	butanal	293.15-393.15	2.53-25.3	6	
	2-methylbutanal	303.15-363.15	0.1-10.13	12	
	nonanal	313.15-333.15	0.94-6.91	5/2	
acid	acetic acid	298.15-348.15	0.27-7.45	17	PTxy ¹³¹ , L ²¹⁴ , α ¹⁴⁵
diol	1,2-ethanediol	298.15-373.15	2.53-8.97	3	PTX ¹⁴⁸ PTX ¹⁴⁸ PTX ¹⁴⁸ PTX ¹⁴⁸
	1,3-propanediol	298.15-373.15	1.877-10.32	3	
	1,4-butanediol	298.15-373.15	1.542-9.89	3	
	2,2'-oxybisethanol	298.15-373.15	1.916-9.99	3	
ether	Di methyl ether	288.15-373	0.43-8.8	4/0	PTxy ^{134,226} Removed: PTxy^{134,226} L ^{227,228} α ²²⁹
	Di ethyl ether	192.55-294.25	0.1	10	
	Di n-propyl ether	293.15-298.15	0.1	2	
ester	formic acid methyl ester	291	1.19-2.71	1	PTX ¹⁴² PTX ¹⁴² PTX ¹⁴² PTX ¹⁴² , L ²²⁷ PTxy ¹⁴² , H, L ²¹⁴ , α ¹⁴⁵ , H* ¹³⁰ PTX ¹⁴² PTX ¹⁴² , H* ¹³⁰ L ²¹⁴ PTX ¹⁴² L ²¹⁴ PTX ¹⁴² L ²¹⁴ PTX ¹⁴²
	formic acid ethyl ester	291	1.6-4.1	1	
	formic acid 2-methylpropyl ester	291	1.59-4.12	1	
	acetic acid methyl ester	194.65-313.15	1.15-3.11	8	
	acetic acid ethyl ester	273.65-312.95	1.6-4.6	11	
	acetic acid propyl ester	291	1.59-4.09	1	
	acetic acid butyl ester	291-293.2	1.42-3.1	2	
	acetic acid pentyl ester	293.15-298.15	0.1	2	
	acetic acid 1-methylethyl ester	291	1.31-3.04	4	
	acetic acid 2-methylpropyl ester	293.15-298.15	0.1	2	
	propanoic acid methyl ester	291	1.6-4.11	1	
	butanoic acid methyl ester	291	1.59-3.85	1	

ketone	2-propanone	298.15-373.15	0.082-9.96	15	PTx ¹⁴⁷ , H ¹³² , L ^{214,227} , H* ¹³⁰
	cyclopentanone	273.15-303.15	0	5	H ²³⁰
	cyclohexanone	303.15-553.2	0.689-30.0	19	PTx ^{231,232} , H ²³² , α ²²⁹
	cycloheptanone	273.15-303.15	0.1	5	H ²³⁰
n-alkane	Propane	93.15-348.15	1.0342-20.6843	38	PTx ²³³⁻²³⁷
	n-Butane	199.82-394.25	2.7783-16.876	17	PTxy ²³⁸⁻²⁴¹
	n-Pentane	273.15-453.15	0.693-27.59	20	PTxy ^{242,243} , L ²⁴⁴
	n-Hexane	213.15-377.59	0.0077-68.948	32	PTx ^{116,147,245} , L ^{141,244} , α ^{229,246} , S, H ¹¹⁶
	n-heptane	293.15-498.85	0.1-78.454	24	PTxy ²⁴⁷⁻²⁴⁹ , α ^{221,229,250,251} , S ²⁵²
	n-octane	295-533.15	0.1-13.79	32	PTx ^{147,149,249,253,254} , L ²⁴⁴ , α ^{221,250} , S ²⁵²
	n-nonane	298.15-323.65	0.1	7	L ²⁴⁴ , α ^{230,255}
	n-decane	293.15-583.45	0-30.3975	35	L ²⁴⁴ , α ^{221,250} , PTxy ^{120,147,243,256-258}
	n-undecane	298.15	0.1	1	L ²⁴⁴
	n-dodecane	298.15-410.9	0.1-13.24	4	L ²⁴⁴ , PTx ¹²¹
	n-tridecane	298.15	0.1	1	L ²⁴⁴
	n-tetradecane	298.15-473.15	0.1-30.3975	4	L ²⁴⁴ , PTx ²⁵⁷
	n-pentadecane	298.15	0.1	1	L ²⁴⁴
	n-hexadecane	293.2-664.05	0.1-30.0	26	L ²⁴⁴ , PTxy ^{256,259} , H ^{119,260-262}
	n-octadecane	303.2-353.2	0.1	6	H ²⁶¹
	eicosane	323.2-573.25	0.994-12.91	6	PTxy ^{120,122}
	octacosane	348.2-573.15	0.1-13.1	11	PTxy ^{120,122} , H ^{119,263} , H* ²⁶⁴
	water	273.15-636.1	0-101.325	269	PTxy ^{239,265-272} , H ^{132,294,295,296} , α ^{215,217,273-288} , L ^{214,228,289-292,293} , H* ^{225,297} , S ^{269,298-301}

Note: Npt: number of data points

PTx, PTxy: Equilibrium phase binary H₂/oxygen-bearing compounds

H: Henry's law constant (Pa.mol/mol)

L: Ostwald coefficient

α : Bunsen coefficient

S: Kuenen coefficient

H*: Henry constant with different units like Pa.m³/mol or Pa.m³/kg

Note that authors use many different ways (type of data) to report the solubility information and also their experimental uncertainties. Values of experimental uncertainty are given based on the measurements of vapour-liquid equilibrium (VLE)^{128,132,133,139,134,140,142–144,147–150} or solubility coefficients.^{141,145} Regarding VLE data, the uncertainty on hydrogen mole fraction in the liquid phase varies depending on the investigated solvents. After analysis of these articles, we can estimate that the data uncertainty of Henry's constant varies from 5% to 10%. Regarding the data themselves, we notice that the best documented family of organic solvents is that of alcohols, after that of n-alkanes. It is seen that for the lower alcohols such as methanol, ethanol or 1-propanol, many experimental data are available with wide temperature and pressure ranges compared to longer alcohols (from 1-hexanol, except 1-octanol), where data are mostly available at 298.15K only. In contrast, for the esters, also very abundant, experimental data exist only for one or two temperatures, usually near ambient conditions. In the case of diols, we have 3 data points corresponding to 3 different temperatures for each component. For carboxylic acids, there is only one compound for which data were found: acetic acid with 17 data points. Similarly, we found only one linear ketone (acetone with 15 data points). The other ketones are cyclic such as cyclopentanone, cyclohexanone and cycloheptanone. Only 3 ethers and 4 aldehydes have been found with data at low temperature. As a benchmark, we also have collected solubility data of hydrogen in n-alkanes (from propane to octacosane).

Figure II-1 summarizes the data found, per chemical family and as a function of temperature. Clearly, the temperature range of the data found is well below the operating temperature of the hydrotreatment processes (from 573.15 K to 723.15 K), and an extrapolation method will therefore be needed. In addition, it can be seen that for most families, only the lower molecular weight representatives have been investigated.

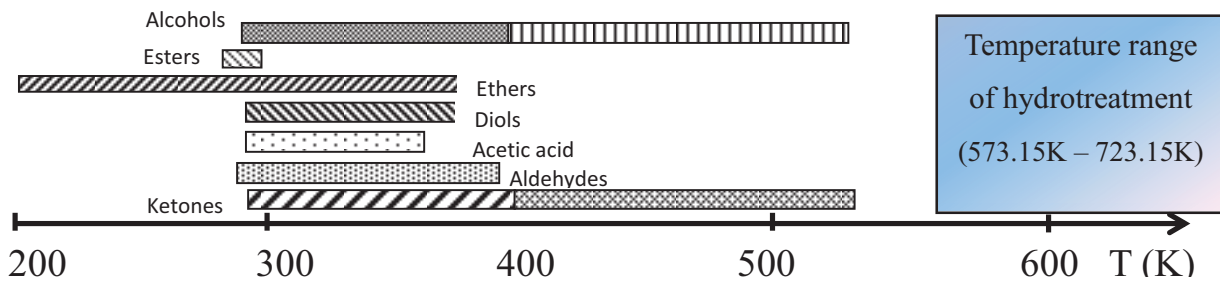




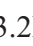






Figure II-1: Schema of database include temperature range. Alcohols (273.32K-400K; 192 points, ), Alcohols (400K-553.15K; 46 points, ), Esters (194.65K-313.15K, 35 points, ), Ethers (192.55K-373K, 16 points, ), Diols (298.15K-373.15K, 12 points, ), acetic acid (298.15K-348.15K, 17 points, ), Aldehydes (293.15K-393.2K, 35 points, ), Ketones (273-15K-400K, 36 points, ), Ketones (400K-553.2K, 8 points, )

II.2.2 Data Evaluation

In order to investigate the trends that may exist in the solubility behavior of hydrogen in various solvents, Henry's constant appears to be a relevant descriptor. Henry's law constant is widely used to describe the low solubility of light solutes (such as hydrogen) in a variety of solvents over a wide temperature range.^{24,302,303} When Henry's constant of a solute increases with temperature, it corresponds to a decrease in the solubility. In our case, the solute is hydrogen and the solvents are the molecules listed in Table II-1. The Henry's law constant of a solute in a solvent, H_i is defined by the expression:

$$H_i = \lim_{x_i \rightarrow 0} \left(\frac{f_i^L}{x_i} \right) \quad (2.1)$$

Where f_i^L is the fugacity of hydrogen in liquid phase, x_i is the mole fraction of hydrogen in the liquid phase at infinite dilution.

All the data described in Table II-1 have therefore been converted into Henry's constants. In addition to the vapor-liquid equilibrium data, we also have in our database solubility coefficients such as Ostwald coefficient, Bunsen coefficient and Kuenen coefficient. They have been converted into Henry's constant using the definitions provided in the IUPAC¹⁶² guide (see Appendix II-A)

The Henry constant is often obtained from VLE data using the simplified equation:

$$H_i = \frac{y_i P}{x_i} \quad (2.2)$$

Where P is the total pressure of the system and $y_i P$ is the partial pressure of the solute. Equation (2.2) is deduced from (2.1) using :

- (1) The iso-fugacity condition: $f_i^L = f_i^V$ where f_i^V is the fugacity of hydrogen in vapor phase
- (2) The approximation : $f_i^V = y_i P$.

This last approximation is only valid at low pressures where the vapor behaves as an ideal gas. Therefore, we know that the simplified expression (2.2) is not always correct.

According to equation (2.2), Henry's constant is equal to the slope of the (approximately linear) bubble curve. In fact, isothermal data such as PTx and PTxy data are largely available in our database. By using the equation (2.2), we can calculate Henry's constant at each temperature from isothermal VLE data. The results are shown in Table II-2 for the example of hydrogen/1-propanol.

Another approach that is more rigorous is to use an equation of state to fit experimental data and to extrapolate it to zero concentration in solute. In that case, equation (2.1) becomes:

$$H_i = P_s^\sigma \cdot \varphi_i^{L,\infty}(P_s^\sigma) \quad (2.3)$$

Where $\varphi_i^{L,\infty}$ is the fugacity coefficient of hydrogen in the liquid mixture at infinite dilution, as calculated at the vapor pressure of the solvent P_s^σ .

In order to make sure that the equation of state (EoS) describes the experimental data points correctly, an interaction parameter k_{ij} is fitted, on each isotherm. In this work, we use the Peng Robinson (PR)^{6,304} EoS with a binary interaction parameter k_{ij} . Table II-2 shows for the example of hydrogen in 1-propanol, the k_{ij} that was obtained as well as the resulting Henry's constants. The average deviation (AAD) is here defined as the average difference between the experimental and the calculated value of Henry's constants.

Table II-2: Henry's constant of hydrogen in 1-propanol calculated by equation (2.2) and calculated by equation (2.3) at different temperature. Data are taken from Brunner et al²¹⁸

Temperature (K)	Henry's constant (MPa) by eq (2.2)	Henry's constant (MPa) by eq (2.3)	AAD* (%)	k_{ij}
298.15	450	421	6%	0.0148
323.15	398	372	7%	0.0937
373.15	295	280	5%	0.2507

$$*AAD = \frac{1}{N_{pt}} \sum \left| \frac{H_i^{cal1} - H_i^{cal2}}{H_i^{exp}} \right| \times 100 \quad (\%)$$

The analysis therefore shows that if the simplified equation (2.2) provides reasonable results, which are difficult to distinguish from the more accurate analysis with an EoS, the deviation is always positive, i.e. one will always overestimate the Henry constant value. In fact, the deviation is larger at higher pressures. In this case, the difference is smaller than the experimental uncertainty, but the systematic error should be avoided if possible. In this work, all the conversions were carried out based on the rigorous equation (2.3).

II.3 Consistency analysis

Both an internal consistency analysis (i.e. confronting the existing data for a given component or solvent) as an external consistency analysis¹⁷¹ is performed here (i.e. comparing the behavior of different solvents). Both are strengthened if we have a tool (a correlation or model) that mimics as closely as possible the expected physical behavior. Regarding Henry's constants, several equations have been proposed in the literature^{305,306,23}. Since one important objective of this work is to evaluate the extrapolation of the Henry constant to high temperature (hydrotreatment conditions), it seemed of interest to use the simplified expression proposed by Harvey²⁷, which is based on the theoretical developments by Japas & Levelt-Sengers.²⁸ They suggest that the function defined as $RT \ln \frac{H_i}{f_S^\sigma}$ (where f_S^σ is the solvent fugacity at saturation) converges to the solvent critical point in a linear way as a function of the difference between solvent density and solvent critical density. Harvey modified this equation in order to make it easier to handle for engineering purposes, by (1) considering the solvent vapour pressure rather than fugacity and (2) using critical exponents to express the equation as a function of temperature rather than density. He also proposed an empirical term so that the equation be applicable at temperatures well below the solvent critical temperature. His final equation looks as follows:

$$\ln H_i = \ln P_i^\sigma + \frac{A}{T_r} + B(1 - T_r)^{0.355} + C \exp(1 - T_r) T_r^2 \quad (2.4)$$

Where $T_r = \frac{T}{T_c}$ is the solvent reduced temperature. It must be noted that in this equation, if the last term is a correction to the first three terms (which are a simplification of the Japas & Levelt-Sengers theory), then it should become zero when $T = T_c$ or when T_r becomes one. This is not the case, which means that the expression must be revised if one wants to use it in the way it should.

In order to evaluate whether we could use an expression as suggested by Harvey, we have

plotted $RT \ln \frac{H_i}{P_S^\sigma}$ as a function of T_r for a number of solvents, starting with the n-alkanes. The result is shown in Figure II-2. It shows rather linear behavior, indicating that :

$$T_r \ln \frac{H_i}{P_S^\sigma} = a + b(1 - T_r) \quad (2.5)$$

Note that in this work, all vapour pressure and critical properties originate from the DIPPR correlations.³⁰⁷

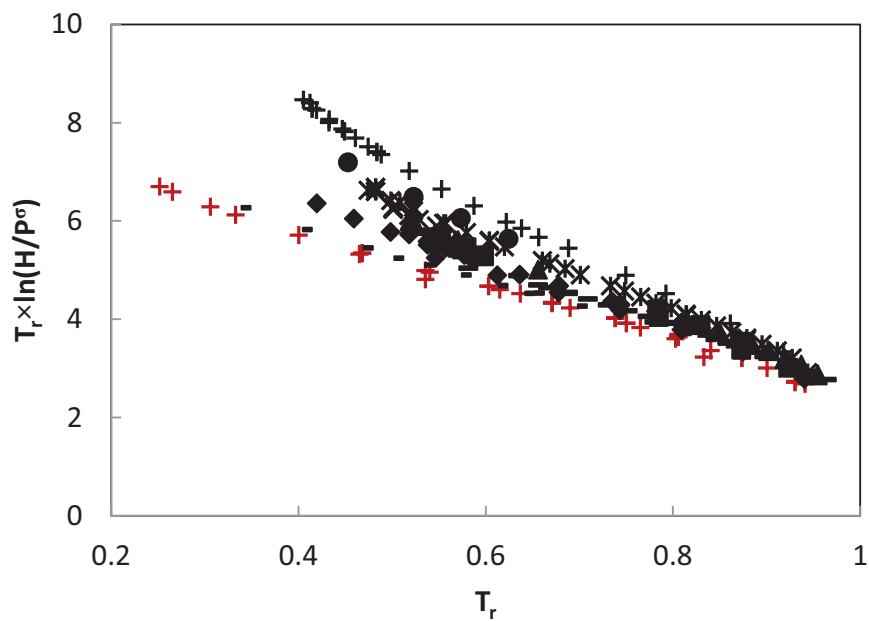


Figure II-2: Diagram of $T_r \times \ln(H/P^\sigma)$ as a function of the reduced temperature T_r for binary mixtures of hydrogen/n-alkanes: (+) propane, (-) n-butane, (—) n-pentane, (◆) n-hexane, (■) n-heptane, (▲) n-octane, (×) n-nonane, (*) n-decane, (●) n-dodecane, (+) n-hexadecane

It is worth noting that because of equation (2.3), we have $\frac{H_i}{P_S^\sigma} = \varphi_i^{L,\infty}$ which means that our equation (3.2) is identical to:

$$\ln \varphi_i^{L,\infty} = (a + b) \frac{1}{T_r} - b \quad (2.6)$$

The logarithm of the fugacity coefficient at infinite dilution is a linear function of $1/T$. Considering the scatter in the data and the small temperature ranges, it is reasonable to consider only two parameters (Harvey et al.²⁷ proposed to use maximum three). Looking at the Figure II-2, it is even possible to fix the value of $a = \ln \varphi_i^{L,\infty}(T = T_c)$ to a unique value close to 2.5.

Whenever the temperature range is larger and a better extrapolation to high temperatures is required, the Harvey equation can be rewritten as:

$$T_r \ln \frac{H_i}{P_S^\sigma} = a' + b'(1 - T_r)^{0.355} + cT_r \left(\frac{1}{T_r} - 1 \right)^{1.5} \quad (2.7)$$

This three parameter equation allows an extrapolation to the solvent critical temperature in the way suggested by Harvey³⁰³, while the third term, which is empirical, allows the inclusion of low temperature data. The use of this last expression in a predictive way was found very difficult because most data are located at low temperature, meaning that the values of a' and b' are extrapolated and contain a very large uncertainty.

Table II-3 summarizes the parameters for all regressions made during this work. We notice that naturally the deviations are much smaller for the three parameter correlation than for the two parameter correlation (except for methanol where the data scatter is very large). The experimental uncertainty being generally close to 10%, it cannot be expected to improve the correlation above what is proposed here. It can be observed that when data exist over a temperature range smaller than 200 K, the two parameter correlation is sufficient. The analysis below made it possible to eliminate unreliable data and to add data originating from molecular simulation.

II.3.1 Alkanes

Alkanes have been extensively investigated because many more data exist and they can therefore be used as a benchmark. For many alkanes, and especially those where the temperature range is large, the two parameter fit is not accurate enough. As an example, we can show n-hexadecane (cf. Figure II-3) where high temperature data are abundant. In the case of n-hexane, the fact that the AAD are large for both correlations indicates that the scatter in the data is rather large.

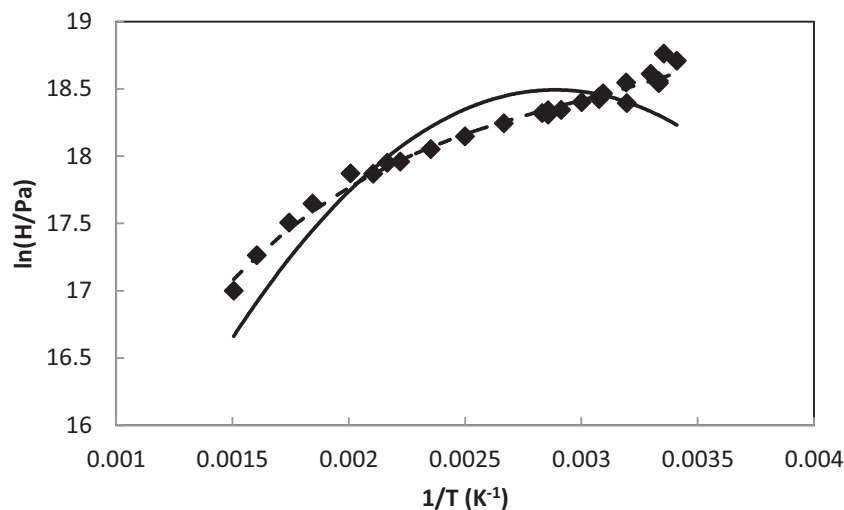


Figure II-3: Diagram of $\ln H$ as a function of $1/T$ for system of hydrogen and n-hexadecane between experimental data (\blacklozenge) and different correlations: with 2 parameters (—), with 3 parameters (---)

It may also be of interest to compare the numerical values of the parameters found. As noticed earlier, the a parameter of both correlations has the meaning of $\ln \varphi_i^{L,\infty}(T = T_c)$. From the two-parameter correlation, this value seems to depend very little on the solvent. Yet, when

applying the three-parameter correlation, no real trend can be identified any longer (Table II-3). This again is related to the fact that no data exist at close to critical temperatures.

The analysis of the parameters for n-nonane also indicates that the three parameter correlation can most probably not be extrapolated: In fact, out of the seven points, four are at almost identical temperature.

II.3.2 Alcohols

As an example, Figure II-4 represents all the values of Henry's constants of hydrogen in methanol. This diagram allows us to evaluate the behavior of the available data, including data consistency between different sources. For instance, we can observe that the data of Yorizane et al.²⁰⁶ on this diagram are not consistent with the other data. In addition, the Henry constants obtained by D'Angelo et al.¹³³ does not follow the same trend as the other data. Note that this work is the only one providing data at high temperature. However, all our attempts to reproduce their Henry's constant data from their VLE measurements failed. Therefore, these points were not considered in this work. We decided removing these data points from the database. The correlation of Henry's constant for this mixture gave a deviation about 9% (9.23% and 9.57% respectively if using 3 parameters and 2 parameters). This deviation is acceptable because it is within the experimental uncertainty (~10%)

In addition, the experimental data of Henry's constants of hydrogen (direct data without conversion), respectively with ethanol, 1-propanol (cf. Figure II-5), 1-butanol (cf. Figure II-6), are from the same article of D'Angelo et al.¹³³ and these values strongly overestimate the solubility of hydrogen in comparison with other solubility data. Therefore, these data were not considered as reliable in our study.

The same type of evaluation was performed for all other systems in the database. This is how we discarded the unreliable data of Just et al.²¹⁴ for the mixtures of hydrogen with 1-pentanol and acetone. The number of investigations is however too small for other solvents to discard any other series.

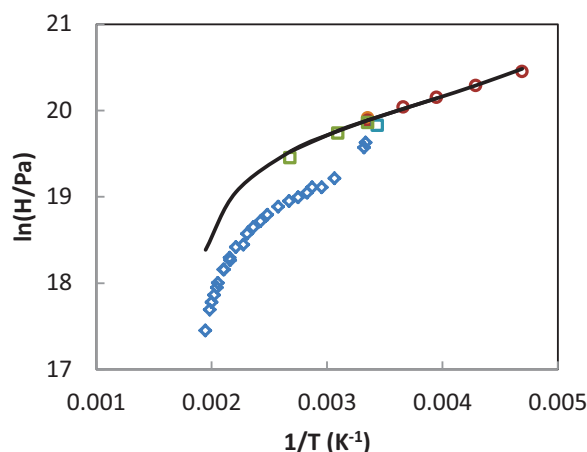
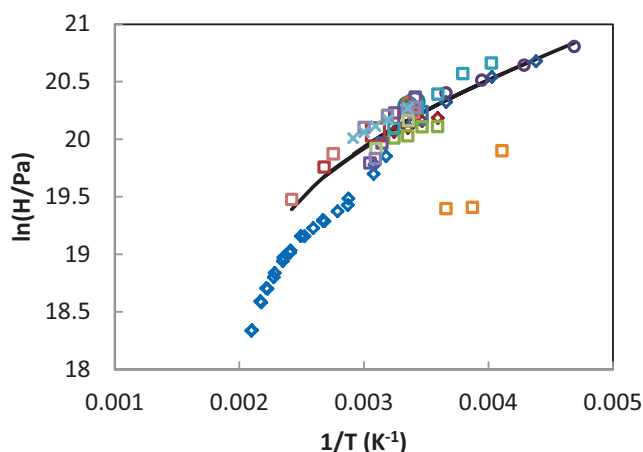


Figure II-4: Diagram of $\ln H = f(1/T)$ of binary mixture hydrogen/methanol. Experimental data are taken from Shenderei et al.²¹² (\diamond), Bezanehtak et al.¹⁴⁰ (\diamond , \square), D'Angelo et al.¹³³ (\diamond), Ipatiev et al.²¹⁵ (Δ), Katayama et al.¹⁴¹ (\circ), Just et al.²¹⁴ (\circ), Makranczy et al.²¹³ (\circ), Wainwright et al.¹⁴² (\square), Brunner et al.¹⁴⁴ (\square), Choudhary et al.²¹⁰ (\square), Descamps et al.¹³⁹ (\square), Yorizane et al.²⁰⁶ (\square), Krichevskii et al.²⁰⁷ (\square), Krichevskii et al.²⁰⁸ (\square), Michels et al.²⁰⁹ (\square), Horstmann et al.²¹¹ (\square), Radhakrishnan et al.²¹⁶ (\times), Henry's constant correlation curve (—)

Figure II-5: Diagram of $\ln H = f(1/T)$ of binary mixture hydrogen/1-propanol. Experimental data are taken from D'Angelo et al.¹³³ (\diamond), Makranczy et al.²¹³ (\circ), Katayama et al.¹⁴¹ (\circ), Wainwright et al.¹⁴² (\square), Brunner, et al.²¹⁸ (\square), Henry's constant correlation curve (—)

This preliminary work resulted in a validated database as well as a set of correlation parameters (Table II-3) that could then be used for evaluating general trends. (cf. excluding the data of D'Angelo et al.¹³³).

The absolute deviation AAD (%) between the experimental and the correlated data are also shown in Table II-3, and often vary from 1% to 10%. For n-butanol and n-octanol, the deviation is reduced from 15.4%, resp 19.2% down to 9.5% resp 10.5% from the two parameters to the three parameters correlation. A closer look at the data in Figure II-6, shows that the trend of experimental data is indeed not linear. It is however also observed that both 1-butanol and 1-

octanol data span over a wide temperature range, in particular due to the measurements made by Naumova et al²¹⁹. In fact, at high temperature, the slope of $d(\ln H)/d(1/T)$ becomes very high which explains that even the three-parameter correlation yields a large average deviation. The same observation could be made in the case of hydrogen/1-octanol.

Table II-3: Coefficients in Equation (2.5) for 2 parameters, Equation (2.7) for 3 parameters and Absolute Average Deviation (AAD %) between experimental data and correlated value of hydrogen Henry's constant in alkanes and oxygenated solvents

	Tc	Tmin	Tmax	Npts	comments	2 parameters			3 parameters			
						a	b	AAD*	a'	b'	c	AAD*
propane	369.83	93.15	348.15	38		2.4473	5.5363	11.9%	0.9458	4.5593	1.2749	5.2%
butane	425.12	144.26	394.25	17		2.6139	5.4125	7.1%	1.2958	4.0960	1.5539	2.5%
pentane	469.7	273.15	453.15	20		2.6782	5.8791	5.1%	1.4737	3.9444	2.0505	3.2%
hexane	507.6	213.15	477.59	32	scattered data	2.5833	6.3636	10.4%	1.1189	4.5518	2.1594	9.0%
heptane	540.2	293.15	498.85	24		2.6268	6.6245	5.7%	0.8788	5.2011	1.9842	5.1%
octane	568.7	295	543.15	32		2.6724	6.8149	4.8%	1.4021	4.2656	2.7311	2.7%
nonane	594.6	298.05	325.65	7		2.3795	7.7557	1.8%	6.9815	-4.4306	5.4846	1.4%
decane	617.7	293.15	583.45	35		2.6463	7.5658	6.5%	1.3046	4.5690	3.1285	3.4%
dodecane	658	298.15	410.9	4		2.1651	9.1465	4.9%	2.0273	3.5212	3.8613	1.1%
hexadecane	723	293.2	664.05	26		2.1758	10.2698	16.7%	1.3076	4.7779	4.3689	3.8%
methanol	512.5	213.15	476.6	49		2.9188	7.5392	9.57%	0.7503	6.2275	2.1136	9.23%
ethanol	514	213.15	476.5	26		2.9776	8.2325	9.6%	0.6391	6.6996	2.3668	3.9%
1-propanol	536.8	213.15	373.1500	10		2.7012	8.9619	10.6%	0.8389	6.0231	3.1903	2.2%
			513.6	16	with MS**	2.0735	10.1239	15.2%	1.4339	5.1304	3.4058	4.5%
1-butanol	563.1	213.15	533.15	31		2.1770	10.0494	15.0%	-0.0510	7.1544	3.2506	7.7%
			533.15	41	with MS**	2.2399	9.9417	15.4%	0.1052	6.9322	3.3023	9.5%
1-pentanol	588.1	293.15	373.15	4		1.5692	8.8661	5.2%	2.3324	1.6727	4.7625	3.5%
			573.15	11	with MS**	1.6856	8.6605	8.5%	0.2941	5.1656	3.3805	4.3%
1-hexanol	611.3	298.15	373.15	4		1.0657	8.9794	4.2%	0.3903	4.2448	3.6831	3.1%
			573.15	11	with MS**	1.3701	8.3835	6.1%	-0.2901	5.4924	3.1179	4.0%
1-octanol	652.3	273.32	553.15	15		1.6674	11.1338	18.9%	1.6986	3.6126	5.3189	9.8%
			573.15	22	with MS**	1.9194	10.6473	19.2%	1.6986	3.6126	5.3189	10.5%

propanal	503.6	293	473.15	12		2.7539	6.0378	5.2%	0.9880	4.8968	1.9676	5.2%
butanal	537.2	293.15	473.15	6		3.0329	4.8921	0.4%	1.3012	4.5115	1.3142	0.4%
nonanal	658.5	313.15	333.15	2		4.2068	4.2926	8.2%	5.0702	0.2182	2.2170	8.2%
acetone	508.1	191.25	373.15	14		3.0736	5.8327	6.5%	0.2452	6.7042	0.9975	5.9%
			373.15	18	with MS**	3.1096	5.7715	6.9%	0.4982	6.3338	1.0750	6.6%
ethandiol	720	298.15	373.15	3		2.6769	8.9684	1.4%	0.3600	7.2239	2.2985	0.0%
propanediol	718.2	298.15	373.15	3		2.1688	10.5954	2.1%	1.2327	5.8143	3.3637	0.3%
butanediol	723.8	298.15	373.15	3		1.3843	12.5559	2.1%	-1.1128	8.9894	3.4821	0.3%
dimethylether	400.1	288.15	373	4	inconsistent behaviour	1.2479	10.3913	10.7%	-1.6522	9.2635	-0.9845	1.0%
diethylether	466.7	192.55	294.25	10		2.7770	5.9608	5.9%	3.0466	1.7679	2.5840	3.3%
			423.15	18	with MS**	2.8381	5.8440	4.5%	1.4078	4.3913	1.8060	3.2%
methyl acetate	506.55	194.65	313.15	8		2.7345	6.7498	4.6%	1.3433	4.8118	1.9578	1.7%
			473.15	18	with MS**	2.7752	6.6275	5.8%	1.2707	4.8355	2.0232	3.6%
ethyl acetate	523.3	273.65	312.95	11		3.0135	6.3224	2.7%	0.6616	6.0503	1.5709	2.7%
			523.15	22	with MS**	2.7577	6.9045	5.6%	2.3075	2.9571	3.2570	4.7%
methyl propanoate	530.6	291	523.15		with MS**	2.6594	6.9415	9.2%	1.8003	3.6040	3.1006	4.0%
methyl butanoate	554.5	291	523.15		with MS**	2.7982	6.7000	4.6%	1.5327	4.2515	2.6275	1.4%
water	647.096	273.15	636.1	269		3.9798	5.1325	79.8%	0.3612	8.7155	-1.0836	7.79%

$$* AAD = \frac{1}{N_{pt}} \sum \left| \frac{H_i^{cal} - H_i^{exp}}{H_i^{exp}} \right| \times 100 \text{ (%)}$$

** with MS: with molecular simulation

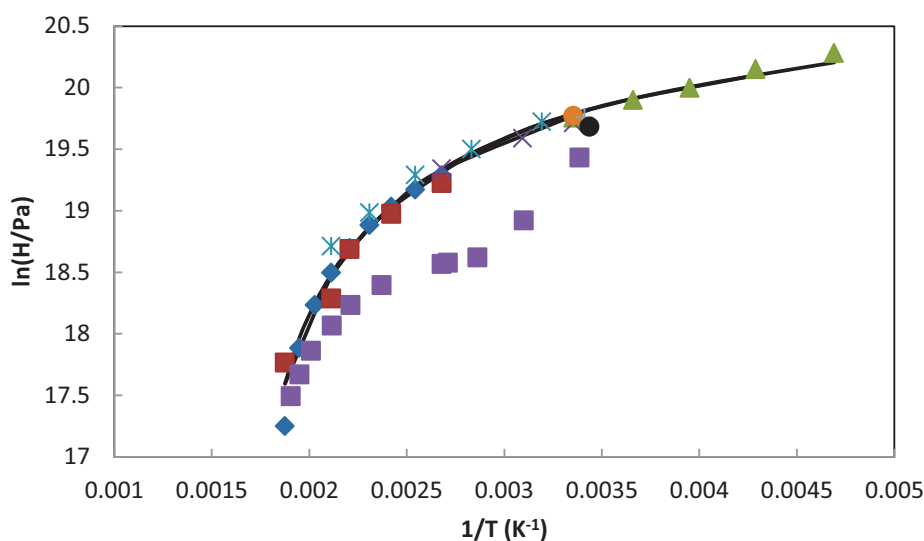


Figure II-6: Diagram of $\ln H = f(1/T)$ in case of hydrogen/1-butanol. Experimental data are taken from Naumova et al.²¹⁹ (\diamond), Katayama et al.¹⁴¹ (\blacktriangle), Makranczy et al.²¹³ (\circ), Tyvina et al.²²⁰ ($*$), Brunner et al.²¹⁸ (\times), Naumova et al.²¹⁹ (\blacksquare), Wainwright et al.¹⁴² (\bullet), D'Angelo et al.¹³³ (\blacksquare), Henry's constant correlation curve (—)

II.3.3 Other oxygenates

For mixtures containing other oxygen-bearing components and n-alkanes, the results of Henry's constant correlation with two parameters are also presented in Table II-3. Very small values of AAD for hydrogen/diols (about 1%) are observed because only three temperature points exist. Otherwise, acceptable deviations are observed for mixtures of hydrogen in propanal, acetone and diethyl ether (respectively 5.2%, 6.9% and 4.5%). For these compounds, the deviations are almost identical whether the three or the two-parameter equation is used.

In case of hydrogen/dimethyl ether, the two-parameter correlation shows an average deviation of 10.7% with an a parameter ($\ln \varphi_i^{L,\infty}(T = T_c)$) which is much smaller than those obtained for other solvents. The three-parameter correlation shows also parameter values that are unreasonable. One may note for example that, while the a parameter of this equation has the same significance as that of the two parameter equation ($a = \ln \varphi_i^{L,\infty}(T = T_c)$), its value is here very different, reaching a highly negative value. This observation leads us to consider that there

might be a problem of consistency for these data, which we will therefore not consider for future work (cf. Figure II-7).

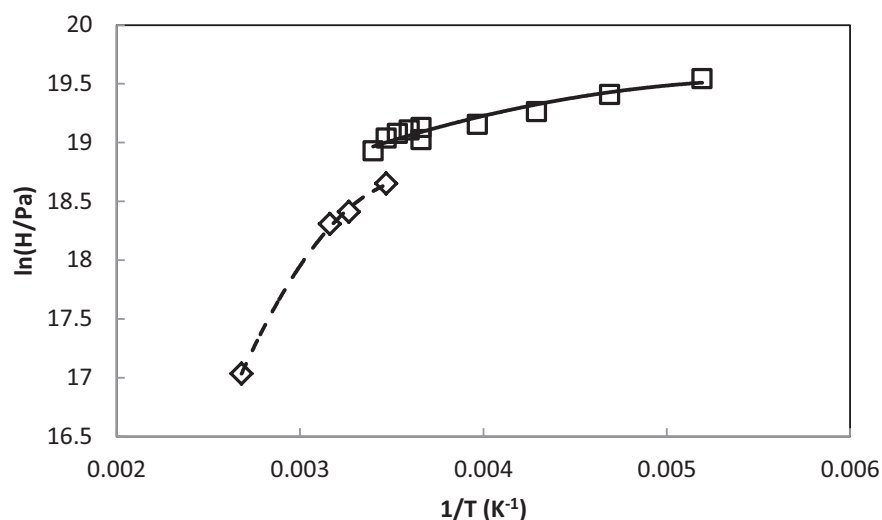


Figure II-7: Diagram of $\ln H$ as a function of $1/T$ for mixture of hydrogen/dimethyl ether: experimental data (\diamond), correlation curve (---) and hydrogen/diethyl ether: experimental data (\square), correlation curve (—)

We also questioned the results of hydrogen/nonanal. For this system, large differences are observed between the Henry constants of Xie, Z et al.¹²⁸ and those of Jauregui-Haza et al.²²⁵ (cf. Figure II-8). After having analyzed Henry's constant of hydrogen in aldehydes like propanal, butanal, we noticed that the order of Henry's constants should be: $H_{\text{propanal}} > H_{\text{butanal}} > H_{\text{nonanal}}$. In agreement with this expected behavior, we have discarded the values of Jauregui-Haza et al.²²⁵

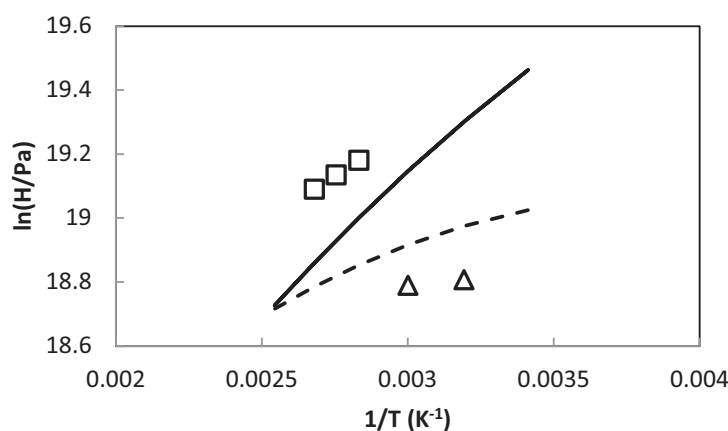


Figure II-8: Diagram of $\ln H = f(1/T)$ in case of hydrogen/aldehydes. Correlation curve: H_2 /propanal (—), H_2 /butanal (---). Experimental data of H_2 /nonanal: Jauregui-Haza et al.²²⁵ (□), Xie. Z et al.¹²⁸ (Δ)

II.3.4 Water

We considered the solubility of hydrogen in water. This is an important case because water is an important product of hydrotreatment process. The solubility of several gases, among which hydrogen, in water, has been extensively investigated by Fernandez-Prini et al.²⁷. We have considered essentially the same data.

As observed in Figure II-9, the experimental Henry's constants data are consistent with each other. Unlike other components, it is observed that Henry's constant of hydrogen in water increases at low temperature ($T < \sim 325$ K) and decreases at high temperature. A peak is observed close to 325 K. In order to describe this behavior, a three parameter correlation is essential. The average deviation is about 8% (cf. Table II-3).

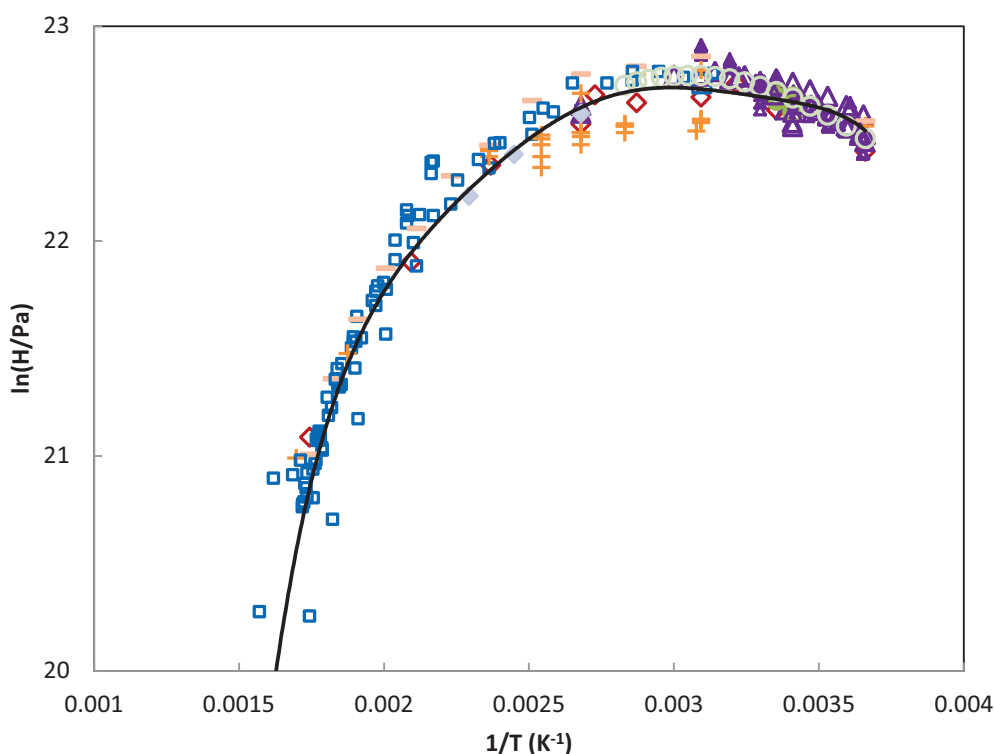


Figure II-9: Henry's constant of hydrogen in water. Experimental data are taken from database and converted from VLE data^{259,265-272} (\diamond), Bunsen coefficients^{215,217,273-288} (Δ), Ostwald coefficients^{214,228,289-292,293} (\circ), experimental Henry constant^{132,294,225,297,296,295} (\square), Kuenen coefficients^{269,298-301} ($+$), Henry's constant correlated curve (—)

II.4 Monte Carlo molecular simulation

After removing inconsistent data, it appears that there is a clear lack of high temperature data. Considering the difficulty to make experimental measurements at high temperatures with hydrogen, it was decided in the same way as Hinkle et al.¹⁷³, to evaluate the use of molecular simulation for completing the database with pseudo-experimental data.

Monte Carlo simulation has proven recently to be an appropriate tool to obtain thermodynamic data for pure oxygen-bearing components as well as for binary systems.^{178,196,198,199} The necessary input for carrying out a Monte Carlo simulation are intermolecular potentials of molecules which correspond to the potential energy arising from the

interactions between molecules in the system.

II.4.1 Intermolecular potential of hydrogen

Usually, the force field parameters can be regressed on vapor pressure and liquid volume data. Because hydrogen is a very light gas with a low critical temperature and for which quantum effects are considerable, the properties such as volume and vapor pressure (at very low temperature) cannot be used to adjust the molecular potential.

This is why Hirschfelder et al.¹⁸⁰ proposed to set the parameters of hydrogen by using Virial coefficient and viscosity data while considering that the hydrogen molecule behaved like a Lennard-Jones sphere. Other studies^{181–185} on hydrogen adsorption used a simple Lennard-Jones sphere as well. In these works, it was observed that this type of model yields accurate results. Darkrim et al.¹⁸⁶ used a single Lennard-Jones sphere model with a quadrupole moment. In their study, Ferrando et al.¹¹⁷ tested different models for the hydrogen molecule in hydrogen/hydrocarbons (e.g. n-hexane, cyclohexane, benzene,...). These authors compared the calculation errors of hydrogen molar fraction using both the Darkrim model and the Hirschfelder model. From the results of their work, it appears that the best is that of Darkrim et al.¹⁸⁶.

II.4.2 Intermolecular potential of oxygenated compounds

For phase equilibrium purposes, the United Atoms type (UA) allows reasonable prediction with a reduced computation time compared to All Atoms (AA) approaches. In UA approaches, a unique force center is placed on the carbon atoms thus implicitly taking into consideration the bonded hydrogen atoms. Widely used UA intermolecular potentials used for this purpose are the TraPPE UA¹⁹¹ and the Anisotropic United Atoms (AUA)¹⁹³ models. The AUA4 intermolecular potential initially developed by Ungerer et al.¹⁹⁵ allows using this model for hydrocarbons, and most of mono-functional oxygen-bearing compounds.^{178,196–199} This model has proven to be well adapted for phase equilibrium calculations. Typical average deviations in

terms of vapor pressure and density are respectively 5% and 1.5%.¹⁹⁹ In this work, the TIP4P/2005 was chosen for the water model³⁰⁸ with a deviation of 0.07% for liquid density.

At first, it is important to validate this approach for calculation of Henry's constant of hydrogen in oxygenated fluids through molecular simulation. This validation step was performed and is described in the next section.

II.4.3 Calculation of Henry's constant from Monte Carlo simulations

In this work, we used Monte Carlo simulation to determine the Henry's constants of hydrogen in different solvents modeled with the AUA4^{178,196–199} force field. The simulation box contained 300 particles of oxygenated solvents. The average properties are computed during a production run lasting 100 million Monte Carlo steps. Before each production run, a preliminary run of 200 million Monte Carlo steps is carried out to achieve equilibrium. In the case of Lennard-Jones interactions, a spherical cutoff equal to half of the simulation box was used while the classical tail correction was employed.³⁰⁹ For long-range electrostatic energy, the Ewald summation technique was used, with a number of reciprocal vectors k equal to 7 in all three space directions and a Gaussian width α^{red} equal to 2 in reduced units. The different Monte Carlo moves and their corresponding attempt probabilities used during the simulations are molecular translation (15%), molecular rotation (15%), regrowth with configurational bias (20%), insertion move (49.5%), and volume change (0.5%). The amplitude of translations, rigid rotations and volume changes was adjusted during the simulation to achieve an acceptance ratio of 40% for these moves. The cross Lennard-Jones interactions between H_2 and the force centers belonging to the oxygenated solvents are calculated with the classical Lorentz-Berthelot combining rules. This choice is motivated by a previous study on hydrogen + hydrocarbon systems which shown that these combining rules lead to the best predictions in term of hydrogen solubility compared to other combining rules (e.g. the Kong rules).⁴

The most suitable approach for calculating Henry's constant is that of the Widom's insertion¹⁷² test. The Widom insertion test is a way to evaluate the chemical potential of a solute in a solvent. The principle is to consider a box containing N_s solvent molecules at a given temperature T and pressure P and to add one new "phantom" solute molecule into the system.

The position of this inserted particle is chosen randomly. The potential energy of this insertion can then be determined. After that, the inserted particle is removed from the system and the procedure is repeated. In order to maintain one single liquid phase in the system, the pressure must be chosen slightly higher than the saturation pressure of the solvent as predicted by molecular simulation using the same force field (the Henry's constant is defined at this pressure, but in practice, we must make sure that the solvent is liquid). The chemical potential of the inserted particle is then obtained by the following expression (4.1)¹⁷²:

$$\hat{\mu}_i = -kT \ln \left\langle \frac{V}{(N_s + 1) \Lambda^3} \exp(-\beta \Delta U^+) \right\rangle \quad (2.8)$$

Where the angular bracket $\langle \dots \rangle$ stands for the ensemble average. ΔU^+ is the change in potential energy of the total system due to the insertion of the molecule. $\beta = \frac{1}{kT}$, k is the Boltzmann constant, and T is the specified temperature.

Λ is the de Broglie wavelength: $\Lambda = \frac{h}{\sqrt{2\pi m k T}}$

N_s is number of molecules of solvent in simulation box.

V volume of simulation box.

We use the notation $\hat{\mu}_i$ to distinguish the chemical potential used in molecular simulation (in Joule/molecule) from the classical chemical potential μ (expressed in Joule/mole). It should also be noted that the reference used here is that of a perfect gas with zero intermolecular energy ($\Delta U^+ = 0$) and with a molecular density of Λ^{-3} .

The fugacity is then written as :

$$f_i = f_i^0 \exp\left(\frac{\hat{\mu}_i - \hat{\mu}_i^0}{kT}\right) \quad (2.9)$$

Where f_i is the fugacity of component i in the imposed condition.

f_i^0 is the fugacity of component i in the reference state, which is in this case an ideal gas ($f_i^0 = P_o$ is calculated with the ideal gas equation).

$\hat{\mu}_i$ is the chemical potential of component i and $\hat{\mu}_i^0$ is its chemical potential in the reference state

(here equal to 0 by construction due to the reference conditions, see equation (2.9)). From the fugacity f_i , obtained under these conditions (infinite dilution), we can compute Henry's constant using equation (2.1) with the approximation:

$$H_i \approx \frac{f_i}{x_i} \quad (2.10)$$

Where x_i is the molar fraction of the inserted molecule, equal to $1/(N_s + 1)$.

II.4.4 Validation of Monte Carlo simulation (insertion test)

The first series of simulations was performed with hydrocarbon solvents, for which many reliable experimental data exist to compare with. Figure II-10 shows the results obtained with H₂ – n-hexane system. The simulation results are compared with experimental data of Henry's constants of hydrogen. The comparison for hydrogen/n-hexane system shows that the Henry constant is well reproduced. A very good consistency between the data and the simulation is observed, even though the simulation always lead to a slight overestimation. Average deviations are estimated at about 8%.

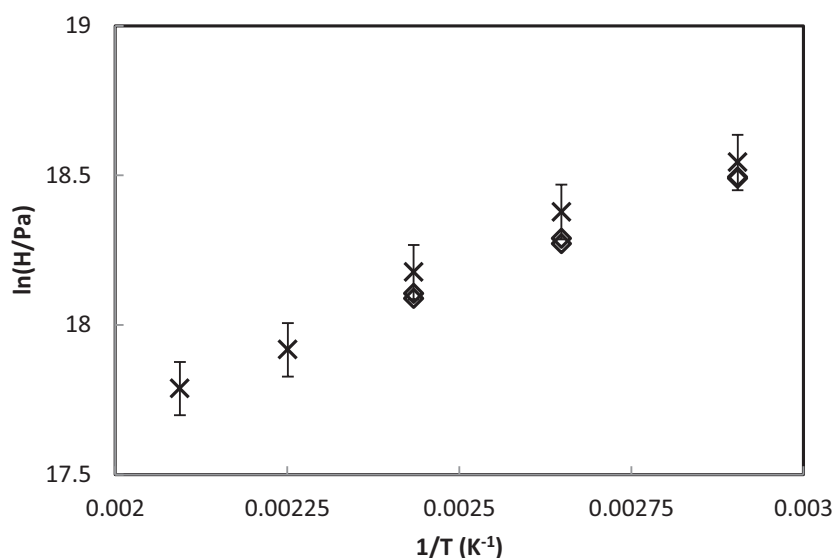


Figure II-10: Henry's constant of the hydrogen/n-hexane binary mixture: Widom test (x), Gao et al.¹¹⁶ (◇)

Calculations by the Widom test were conducted for 18 other H₂-oxygenated binary systems: alcohols, esters, ethers, aldehydes, ketones and acids (values of Henry's constants are presented in Table II-6 in Appendix II-B) at the exact temperatures where experimental data are available. In Figure II-11, we show the results obtained by the Widom test for the binary mixture hydrogen/acetone. The values of the Henry constants of this mixture are generally consistent with the experimental data from various sources. Table II-4 shows all the deviations and also biases between correlated values of Henry's constants and those obtained by Widom tests. Comparing the biases and absolute deviations (AAD), we can evaluate whether the calculation of Henry's constant from molecular simulation leads to a systematic underestimation or overestimation of experimental data.

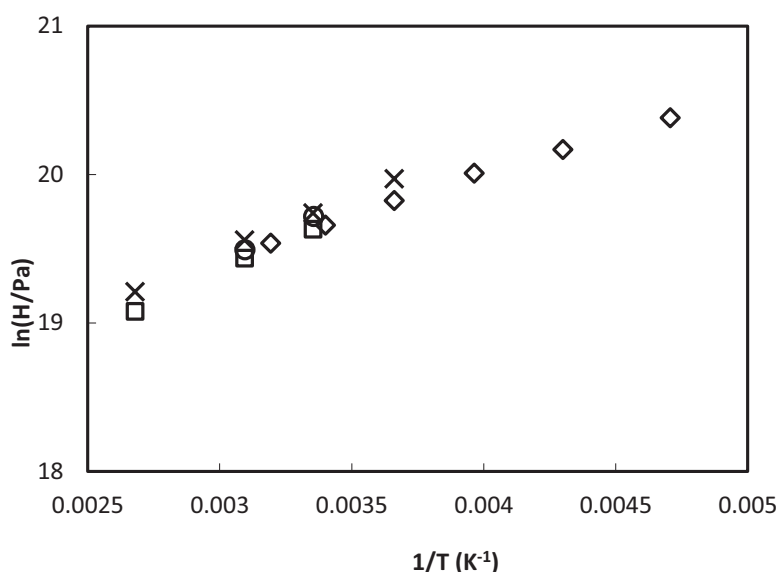


Figure II-11: Henry's constant of the hydrogen/acetone binary mixture. Experimental data are taken from Brunner, E. et al.¹⁴⁷ (□), Horiuti, J. et al.²²⁷ (○), Purwanto et al.¹³² (◇), Widom test (x)

In Table II-4, we see that almost all bias values are positive and equal in absolute value to AAD. This means that molecular simulation overestimates most of the experimental values (underestimates solubilities). The only exception is methyl acetate where the predicted Henry's constant is systematically smaller than the experimental one. These deviations could perhaps be reduced by investigating the possible quantum effects of hydrogen, as discussed by Beck et al.³¹⁰, and Wang et al.³¹¹, or by fitting an interaction parameter to correct for the dispersive forces inadequacies. Yet, it was not the scope of this work to improve the Monte Carlo approach, but rather we wanted to simply evaluate its use as a predictive tool. Considering an experimental uncertainty of 10%, we can consider that for some systems, the average deviations are acceptable. The exceptions are the first elements of a family which are often the most difficult to deal with using predictive methods, such as methanol, ethanol, acetic acid, dimethyl ether and small diols. Therefore, we avoid using molecular simulation results for the first elements of a family. For acids, we do not have enough data to compare with and additional experimental measurements are thus required.

Table II-4: Absolute Average Deviation (AAD %) between correlated values and calculated values by the Widom test of Henry's constants for the binary systems containing hydrogen and various solvents

Chemical family	Solvent used	N _{pt}	T _{min} – T _{max} (K)	AAD*	Bias**
n-alkanes	n-hexane	5	377.6 – 477.6	19%	19%
	n-octane	7	298.15 – 543.15	6%	6%
1-alcohols	Methanol	11	213.15 – 476.6	84%	58%
	Ethanol	9	213.15 – 475.8	33%	33%
	1-propanol	6	253.15 – 513.6	7%	5%
	1-butanol	10	233.15 – 533.15	22%	22%
Aldehydes	Propanal	6	293.2 – 393.2	26%	26%
	Butanal	6	293.15 – 393.15	45%	45%
Ketones	Acetone	4	273.15 – 373.15	6%	6%
Ethers	Di ethyl ether	4	233.15 – 294.15	3%	3%
	Di propyl ether	2	293.15 – 298.15	2%	2%
Esters	Methyl acetate	5	233.05 – 313.15	4%	-4%
	Ethyl acetate	5	273.65 – 312.95	3%	-1%
Diols	1,2-ethanediol	3	298.15 – 373.15	13%	12%
	1,3-propanediol	3	298.15 – 373.15	38%	38%
	1,4-butanediol	3	298.15 – 373.15	40%	40%
Acids	Acetic Acid	3	298.15 – 348.15	88%	80%

$$* AAD = \frac{1}{N_{pt}} \sum \left| \frac{H_i^{cal} - H_i^{exp}}{H_i^{exp}} \right| \times 100 (\%)$$

$$** Bias = \frac{1}{N_{pt}} \sum \left(\frac{H_i^{cal} - H_i^{exp}}{H_i^{exp}} \right) \times 100 (\%)$$

II.4.5 Completing the database using Monte Carlo molecular simulation results

In order to complete the experimental database, new Henry's constants were obtained using molecular simulation, as explained in the previous section. This was done only for chemical families where preliminary tests (cf. Table II-4) showed reasonable deviations (<10%) : linear alcohols, ketones, ethers and esters. We then extrapolated the calculations to higher temperatures, so as to cover a temperature range relevant to hydroprocessing units from 298.15 K to about 650 K (the maximum temperature limit depends on the critical temperature of the solvent). Table II-5 summarizes the hydrogen Henry's constant in different solvents. We observed that the average statistical uncertainty varies between 3% and 8% (smaller than the experimental uncertainty)

Table II-5: Henry's constant of hydrogen in organic solvent using molecular simulation

Chemical family	solvent used	Npts	Temperature (K)	H _i (MPa)	Statistical uncertainty (%)
1-alcohols	1-pentanol	7	298.15	361.85	8.4
			323.15	326.26	3.12
			373.15	246.78	5.28
			423.15	185.68	2.79
			473.15	133.53	2.88
			523.15	93.15	6.43
			573.15	50.71	13.77
	1-hexanol	7	298.15	327.26	6.23
			323.15	294.43	6.48
			373.15	229.15	3.27
			423.15	171.03	2.92

			473.15	127.12	3
			523.15	91.28	5.09
			573.15	60.02	10.55
	1-octanol	7	298.15	285.11	5.18
			323.15	256.42	5.28
			373.15	201.16	4.95
			423.15	148.37	3.45
			473.15	114.47	5.53
			523.15	84.31	4.58
			573.15	61.31	4.95
ketones	2-butanone	6	298.15	323.33	2.98
			323.15	270.05	3.89
			373.15	195.54	2.86
			423.15	141.66	2.64
			473.15	95.43	5.64
			523.15	60.07	3.6
	2-pentanone	6	298.15	293.63	3.75
			323.15	243.95	3.42
			373.15	184.21	3.47
			423.15	136.54	1.86
			473.15	97.74	4.43
			523.15	60.83	12.28
	2-hexanone	6	298.15	273.21	3.82
			323.15	229.37	2.68
			373.15	177.20	2.54
			423.15	132.41	2.65
			473.15	99.70	3.66
			523.15	46.28	10.82
	2-octanone	6	298.15	252.03	2.72

			323.15	210.03	4.48
			423.15	124.72	4.46
			473.15	94.58	4
			523.15	73.61	4.08
			573.15	51.94	5.83
esters	methyl propionate	6	298.15	264.85	5.18
			323.15	226.20	3.07
			373.15	165.60	2.65
			423.15	122.41	2.65
			473.15	83.78	4.34
			523.15	51.20	11
	ethyl propionate	6	298.15	248.44	3.83
			323.15	213.27	2.74
			373.15	158.14	2.81
			423.15	117.09	3.17
			473.15	85.88	3.39
			523.15	58.92	6.74
	methyl butanoate	6	298.15	243.01	3.55
			323.15	204.09	2.52
			373.15	157.74	2.82
			423.15	118.63	2.82
			473.15	86.85	5.97
			523.15	59.06	7.17
	ethyl butanoate	6	298.15	227.33	6.99
			323.15	193.67	4.44
			373.15	146.35	3.99
			423.15	114.82	3.11
			473.15	84.68	4.71
			523.15	60.94	5.7

ethers	methyl ethyl ether	7	233.15	252.21	-
			273.15	190.57	-
			288.15	171.94	-
			298.15	161.66	1.72
			323.15	135.80	1.9
			373.15	93.13	2.22
			423.15	50.57	11.03
	methyl propyl ether	7	233.15	249.94	-
			273.15	196.22	-
			298.15	165.00	1.84
			323.15	143.49	2.08
			373.15	103.48	1.41
			423.15	69.90	2.68
			473.15	10.27	33.98

As a conclusion for this section, we can state that because of low deviations between the Henry constants obtained by molecular simulation and the experimental ones, we can use the molecular simulation as an efficient method to produce pseudo-data of hydrogen solubility. Pseudo-data for systems of hydrogen with linear ketones, ethers and esters were generated with Widom's tests at different temperatures as shown in Figure II-12 to Figure II-15. Table II-3 shows the correlation parameters both excluding and including the molecular simulation results. It appears that the parameters and the deviations do not change much whenever the temperature range is the same as that of the literature data. However, when the temperature range is increased, the deviation increases only slightly for both correlations, indicating that the two parameter correlation is often quite sufficient.

These data also show that towards high temperatures, the slope of $d(\ln H)/d(1/T)$, or the enthalpy of solvation, increase significantly. These results allow us to confirm the trend of $\ln H$ at high temperature based on results of Naumova et al.²¹⁹ in case of hydrogen/1-butanol.

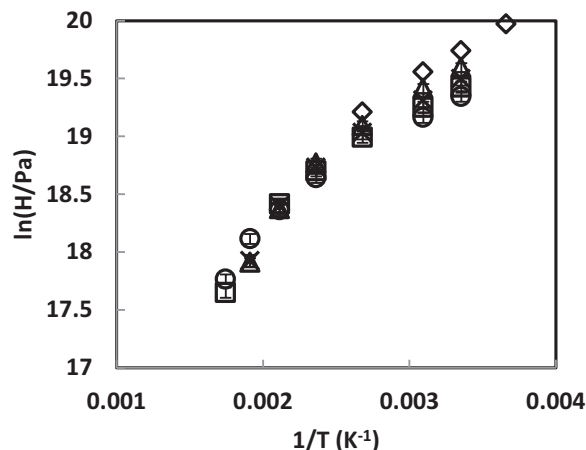
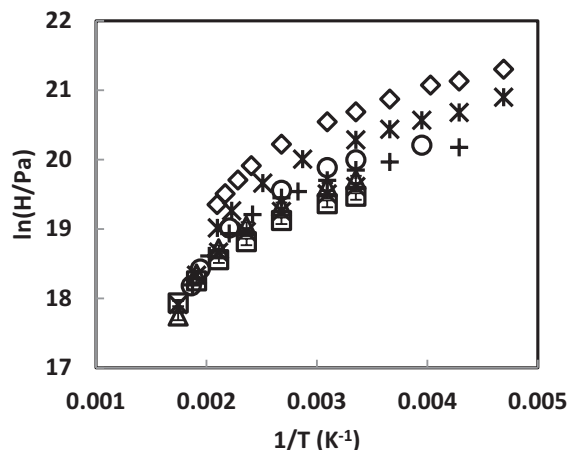


Figure II-12: Molecular Simulation Henry’s constant of binary systems hydrogen/1-alcohols: methanol (\diamond), ethanol (*), 1-propanol (\circ), 1-butanol (+), 1-pentanol (Δ), 1-hexanol (x), 1-octanol (\square)
Figure II-13: Molecular Simulation Henry’s constant of binary systems hydrogen/linear ketones: acetone (\diamond), 2-butanone (Δ), 2-pentanone (\square), 2-hexanone (\times), 2-octanone (\circ)

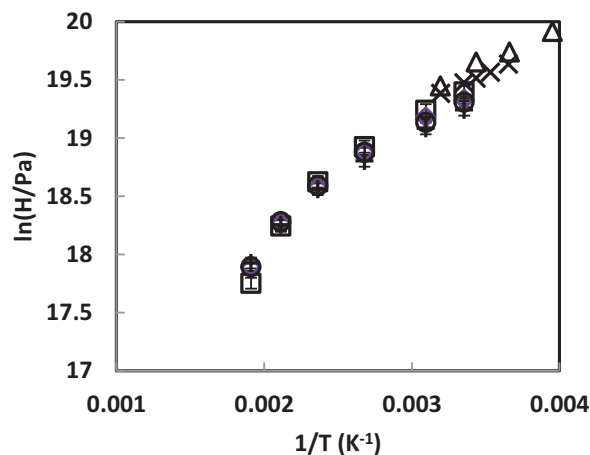
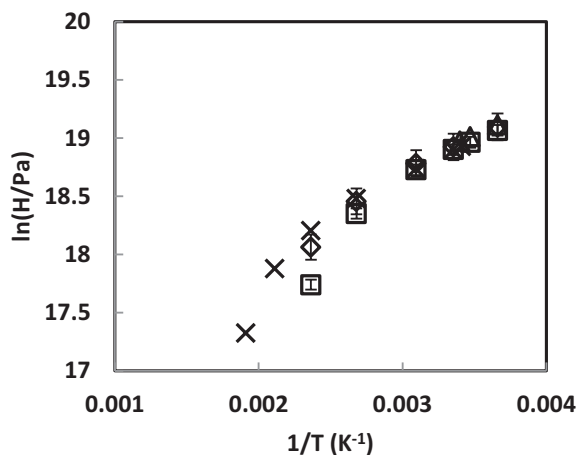


Figure II-14: Molecular Simulation Henry’s constant of binary systems hydrogen/ethers: diethyl ether (Δ), dipropyl ether (x), methyl ethyl ether (\square), methyl propyl ether (\diamond)
Figure II-15: Molecular Simulation Henry’s constant of binary systems hydrogen/esters: methyl acetate (Δ), ethyl acetate (x), methyl propionate (\square), ethyl propionate (\diamond), methyl butanoate (\circ), ethyl butanoate (+)

II.5 Final discussion : Comparison of hydrogen Henry's constant in different organic families

Using the developed correlations it is now possible to evaluate some trends. These are determined using the three-parameter correlation because of its higher accuracy. However, considered that in some cases the conditions plotted may be extrapolated, the results must still be taken with caution.

Effect of chain length

Figure II-16 shows the logarithm of Henry's constant as a function of the number of carbon and oxygen atoms for a number of chemical families. It clearly shows that the the Henry's constant is first of all a function of the chemical family, with a rather well established order which is: $H_{\text{diols}} > H_{\text{alcools}} > H_{\text{esters}} > H_{\text{aldehydes}} > H_{\text{ethers}} > H_{\text{alkanes}}$

The Figure II-16 also shows that molecular weight has generally a decreasing effect on the Henry constant. This is most visible for the first compounds of a chemical family: low carbon number means higher Henry constants. For increasing chain length, the Henry constant tends towards the behavior for n-alkanes. This is coherent with the behavior observed elsewhere: Hinkle et al.¹⁷³ show a mass-based Henry constant which they say will asymptote out for large carbon numbers, and Torres et al.⁴ also nicely show how the molar Henry constant of heavy compounds should decrease with molecular weight. The Figure II-16 shows that the opposite trend is in fact visible for small alkanes, when plotted at constant temperature. Yet, the trend is the same when plotted at fixed reduced temperature (cf. Figure II-17).

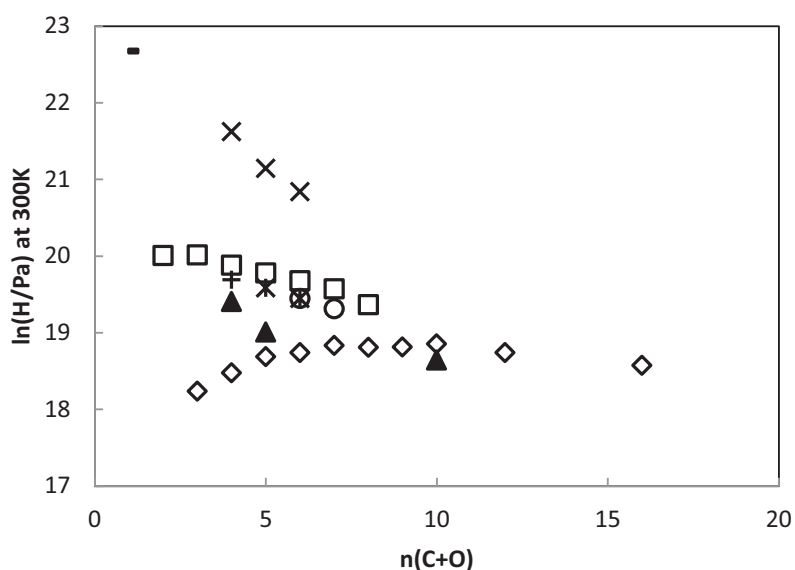


Figure II-16: Henry constant behavior as a function of chain length for the investigated families at fixed temperature ($T = 300\text{K}$): (-) water, (\times) diols, (\square) 1-alcohols, (\circ)esters, (+) ketones, (*) acetates, (\diamond) n-alkanes, (\blacktriangle) aldehydes

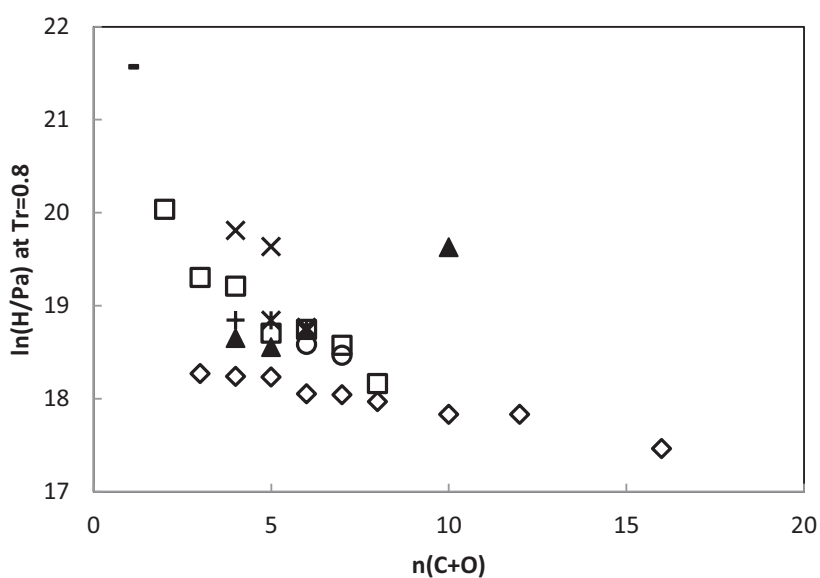


Figure II-17 : Henry constant behavior as a function of chain length for the investigated families at fixed reduced temperature ($T_r = 0.8$): (-) water, (\times) diols, (\square) 1-alcohols, (\circ)esters, (+) ketones, (*) acetates, (\diamond) n-alkanes, (\blacktriangle) aldehydes

II.6 Conclusions

The main target of this paper was to evaluate the VLE behavior of hydrogen in oxygenated solvents, with special emphasis on high temperature conditions. To this end, it was decided to focus our attention on the Henry constants. All the data found in the literature was converted into Henry's constant and was analyzed. A reliable database for Henry's constant of hydrogen in n-alkanes and oxygenated compounds using all the available experimental data in literature is constructed. The analysis involving experimental uncertainties (as reported by the authors) and correlation of the available data lead us to estimate an average uncertainty for Henry's constant between 5% and 10%. Using internal coherence analysis for each oxygen-bearing solvents, some inconsistent data have been removed. In addition, the observation of Henry's constant trend within each chemical family also helps eliminating some other data. A Henry constant correlation is also proposed. However, the data are very limited for certain chemical families (acids, linear ketones) and for high temperatures. In order to complete the database, molecular simulation was used as a tool to produce pseudo-experimental data of solubility of hydrogen. After validating the Widom insertion method, additional pseudo-data were produced for some systems such as: alcohols, linear ketones, ethers, esters with the statistical uncertainty of about 8%. Finally, the influence of molecular weight and temperature on Henry's constant is analyzed. An important effect of molecular weight is observed for the families whose experimental data are largely available. In terms of temperature, we found that the slope $d(\ln H)/d(1/T)$ is rather small at low temperature. However, when the temperature increases, this slope also increases.

In conclusion, this data analysis allowed us not only discarding inconsistent data but also understanding the effect of some factors such as temperature, molecular weight or chemical family on the hydrogen solubility.

Appendix II-A: Conversion into Henry's constant

Ostwald coefficient $L_{V,B}$

This is the volume of gas absorbed at equilibrium versus the volume of pure solvent $V_A^{l,*}$ at a specific temperature and total pressure:

$$L_{V,B}^0 = (V_B^g / V_A^{l,*})_{eq} \quad (\text{II. A. 1})$$

Where V_B^g is volume of gas.

According to IUPAC-NIST Solubility Data Series Guide¹⁶², Ostwald coefficient can be converted to Henry's law constant by calculating the molar fraction of hydrogen:

$$x_B = \frac{1}{1 + \frac{RT}{p^\theta V_{m,A}^{l,*} L_{V,B}}} \quad (\text{II. A. 2})$$

Where $V_{m,A}^{l,*}$: molar liquid volume of pure solvent A, $p^\theta = 101325 \text{ Pa}$, $R = 8.1314 \text{ J. mol}^{-1} \cdot \text{K}^{-1}$, T is specified temperature.

Bunsen coefficient α_B

This is the volume of gas V_B^g , that is absorbed by a volume of pure solvent $V_A^{l,*}$, is reduced to the standard condition ($T^\theta = 273.15\text{K}$ and $p^\theta = 101325 \text{ Pa}$)

$$\alpha_B = [V_B^g(T^\theta, p_B^\theta) / V_A^{l,*}]_{eq} \quad (\text{II. A. 3})$$

As Ostwald coefficient, Bunsen coefficient is converted to Henry's law constant:

$$x_B = \frac{1}{1 + \frac{RT^\theta}{p^\theta V_{m,A}^{l,*} \alpha_B}} \quad (\text{II. A. 4})$$

Kuenen coefficient S_B

This is the volume of gas V_B^g , that is absorbed by a mass of pure solvent $m_A^{l,*}$, is reduced to the standard condition ($T^\theta = 273.15K$ and $p^\theta = 101325 Pa$)

$$S_B = [V_B^g(T^\theta, p_B^\theta)/m_A^{l,*}]_{eq} = \frac{\alpha_B V_{m,A}^{l,*}}{M_A} \quad (\text{II. A. 5})$$

Where M_A is molecular weight of solvent (g/mol), $m_A^{l,*}$ is mass of pure solvent A.

Conversion between Henry's law constant and Kuenen coefficient is expressed using the molar fraction of solute:

$$x_B = \frac{1}{1 + \frac{RT^\theta}{p^\theta M_A S_B}} \quad (\text{II. A. 6})$$

Note : A is solvent (oxygenated compounds) and B is solute (hydrogen)

From the equations (II.A.2), (II.A.4), (II.A.6), we can have molar fraction of hydrogen in solvent and then we can calculate Henry constant by using equation (2.2) because all of solubility coefficients is determined at ambient conditions.

Appendix II-B: Molecular Simulation results

Table II-6 : Henry's constant of hydrogen in organic solvent and n-alkanes by using molecular simulation

Chemical family	solvent used	Ntp	Temperature (K)	H _i (MPa)
n-alkanes	n-hexane	5	377.6	95.77
			444.3	60.44
			344.3	113.00
			410.9	78.30
			477.6	53.10

	n-octane	7	298.15	153.06
			323.15	132.97
			373.15	104.32
			453.15	70.23
			483.15	58.92
			513.15	47.58
			543.15	34.68
1-alcohols	methanol	11	213.15	1773.49
			233.15	1498.17
			248.15	1412.06
			273.15	1156.02
			298.15	960.29
			323.15	830.25
			373.15	603.71
			415.2	441.92
			437.5	359.71
			460.7	294.99
			476.6	252.68
	ethanol	9	213.15	1182.70
			233.15	950.19
			253.15	851.50
			273.15	746.33
			298.15	640.15
			348.15	484.87
			398.15	344.81
			448.15	230.85
	1-propanol	6	475.8	180.54
253.15			594.71	
298.15			481.84	

			323.15	430.83
			373.15	309.82
			452.5	180.34
			513.6	100.11
			536.8	78.45
	1-butanol	10	233.15	576.95
			273.15	467.06
			298.15	414.51
			323.15	358.59
			353.15	305.01
			373.15	279.34
			413.15	219.00
			453.15	166.21
			493.15	120.63
			533.15	79.53
Aldehydes	propanal	6	293.2	356.34
			313.2	302.36
			333.2	263.34
			353.2	227.23
			373.2	198.47
			393.2	169.63
	butanal	11	293.15	318.40
			313.15	269.51
			333.15	243.70
			353.15	211.47
			373.15	189.01
			393.15	165.16
Ketones	acetone	4	273.15	470.88
			298.15	373.71

			323.15	311.50
			373.15	220.09
Ethers	dimethyl ether	4	288.15	191.18
			306.15	166.81
			316.15	153.54
			373	87.39
	diethyl ether	4	233.15	261.85
			273.15	199.91
			288.15	180.32
			294.15	173.72
	di propyl ether	2	293.15	165.86
			298.15	161.43
Esters	methyl acetate	5	233.05	524.79
			253.05	445.30
			273.15	373.66
			291	342.46
			313.15	278.66
	ethyl acetate	5	273.65	335.97
			283.15	313.71
			291	298.15
			298.15	286.35
			312.95	261.68
Diols	1,2-ethanediol	3	298.15	2439.35
			323.15	2612.93
			373.15	1762.90
	1,3-propanediol	3	298.15	2260.18
			323.15	1923.13
			373.15	1280.46
	1,4-butanediol	3	298.15	1716.57

			323.15	1459.88
			373.15	902.18
Carboxylic acid	acetic acid	3	298.15	1047.28
			323.15	899.42
			348.15	749.48

In Chapter II, the available experimental data of the solubility of hydrogen (i.e Henry's constant) in oxygen-bearing solvents in the literature have been investigated. Based on the internal and external data analysis, the inconsistent data have been removed from the database. This work allowed qualifying the experimental data for the prediction of solubility using GC-PPC-SAFT Equation of state. Modeling of these systems using GC-PPC-SAFT is presented in the two next chapter III and IV. Accounting for non-additive repulsion between segments (additive mixing rules on diameters is broken) is envisaged as a further improvement of our model. This is done in two steps. Chapter III is devoted to theoretical extension of square well chains equation of state to no-additive effect. In Chapter IV, GC-PPC-SAFT is then improved based on the development of Chapter III.

CHAPTER III

DEVELOPMENT OF A NON ADDITIVE HOMONUCLEAR SQUARE WELL CHAINS EQUATION OF STATE VALIDATED AGAINST MONTE CARLO SIMULATION

Thi-Kim-Hoang TRINH^{a,b}, Jean-Philippe PASSARELLO^b,

Jean-Charles DE HEMPTINNE^a, Rafael LUGO^a, Veronique LACHET^a

^a IFP Energies nouvelles, 1 et 4 avenue de Bois-Préau, 92852 Reuil-Malmaison, France

^b Laboratoire de Science des Procédés et des Matériaux (LSPM), Université Paris 13, CNRS,
99 avenue Jean-Baptiste Clément, 93430 Villetaneuse, France

Keyword: Square-well potential, non-additive parameter, Monte Carlo simulation, compressibility factor, inter – segment distribution function

Abstract

This work consists of the adaptation of a non-additive hard sphere theory inspired by Malakhov and Volkov, Polym. Sci. Ser. A. 2007;49(6):745-756 to a square-well chain. Using the thermodynamic perturbation theory, an additional term is proposed that describes the effect of perturbing the chain of square well spheres by a non-additive parameter. In order to validate this development, NPT Monte Carlo simulations of thermodynamic and structural properties of the non-additive square well (NASW) for a pure chain and a binary mixture of chains are done. Good agreements are observed between the compressibility factor originating from the theory and from the molecular simulations.

III.1 Introduction

Computation of realistic phase equilibria is of central importance in chemical engineering and more specifically for designing unit operations. In this domain, the equations of state play a

major role allowing to deal with a wide range of mixtures in a broad range of pressures and temperatures. A good equation of state is capable of calculating and in the best case of predicting phase equilibria. This is the reason why theoretically rooted equation of state (based on statistical mechanics) such as SAFT^{7,8} are more and more used in engineering problems.

Certain systems remain however difficult to model such as small molecule (e.g. gases) + solvent requiring non-zero binary parameters. From now on, the common practice is to use the so-called k_{ij} i.e. binary parameter acting on energy of the dispersion term : $\varepsilon_{ij} = \sqrt{\varepsilon_{ii} \cdot \varepsilon_{jj}}(1 - k_{ij})$. Far more rarely, the effect on phase equilibria computation of binary parameter l_{ij} on cross diameter i.e. $\sigma_{ij} = \frac{\sigma_{ii} + \sigma_{jj}}{2}(1 - l_{ij})$ was explored¹³⁵. Only limited number of Equations of state were developed to account for this possible non-additivity effect mainly for spherical³¹²⁻³¹⁹ or hard chain^{320,321} molecules. To the best of our knowledge no Equation of state was developed for non-additive attractive chain molecules.

Our general goal is to propose an adequate implementation of a non-additive diameter in an engineering but theoretically rooted EOS such as PC-SAFT. As a first step, in a procedure similar to that followed by Gross and Sadowski^{13,322}, we will first consider square well chain fluids as prototype fluids. The main goal of the work reported in this paper is to develop a non-additive Square Well Chain Equation of state that applies to small molecule + solvent systems. Extension to PC-SAFT will be presented in the next chapter.

This chapter is presented as follows. First, the general description of square well chains equation of state based on statistical mechanics is presented. Next, the development of a non-additive term for square well chains is shown with in particular the determination of the inter-segment distribution functions of square-well chains. Finally, the approach is validated against Monte Carlo molecular simulations for the pure chains and for the mixtures of square wells chains.

III.2 Development of non-additive Square Well Chain Equation of state

III.2.1 General expression of the equation of state

The interaction potential between segments i and j of two non-additive square-well homonuclear chain molecules is defined as:

$$\mathbf{u}_{ij}(\mathbf{r}) = \begin{cases} \infty & r < \sigma_{ij} \\ -\varepsilon_{ij} & \sigma_{ij} \leq r < \lambda\sigma_{ij} \\ \mathbf{0} & r \geq \lambda\sigma_{ij} \end{cases} \quad (3.1)$$

With

$$\sigma_{ij} = \frac{\sigma_i + \sigma_j}{2} (1 - l_{ij})$$

Notice that $l_{ii} = l_{jj} = 0$; non-additivity implies non-zero l_{ij} .

The equation of state derived from the above potential may be obtained by using perturbation techniques that start by subdividing the potential into a reference and a perturbation part:

$$\mathbf{u}_{ij}(\mathbf{r}) = \mathbf{u}_{ij}^{ref}(\mathbf{r}) + \mathbf{u}_{ij}^{pert}(\mathbf{r}) \quad (3.2)$$

In standard procedures, one would choose the reference part as repulsive. This would lead to deal with non-additive hard chains as reference fluid for which little is known; in particular analytical expression of inter-segment distribution functions are unknown and simulation data for these functions are not available whereas they are needed to compute the perturbation part.

So, rather than starting from the very beginning with the development of a new equation of state, we base our work on the proposal of Malakhov and Volkov³²³, who developed a model of non-additive chains of hard spheres using a specifically designed perturbation. Doing so, the reference term is chosen as the additive potential i.e. for which $l_{ij} = 0$. The reference potential is written:

$$u_{ij}^{pert}(\mathbf{r}) = \begin{cases} \infty & r < \sigma_{ij} \\ -\varepsilon_{ij} & \sigma_{ij} \leq r < \lambda\sigma_{ij} \\ \mathbf{0} & r \geq \lambda\sigma_{ij} \end{cases} \quad (3.3)$$

With

$$\sigma_{ij} = \frac{\sigma_i + \sigma_j}{2}$$

This is the potential of usual square-well chain (SWC) molecules for which equations of state are available.³²² This potential and its parameters are denoted with SWC superscript in the rest of the paper. Several authors have studied on the use of a square well reference that lead to the Square Well chains equation of state^{97,101,324,325}.

The perturbation part is simply defined as the difference between the non-additive and additive potentials and denoted NAS (Non – Additive Segments). In terms of Helmholtz free energy one obtains :

$$\frac{A}{NkT} = \frac{A^{SWC}}{NkT} + \frac{A^{NAS}}{NkT} \quad (3.4)$$

where N is the total number of molecules, k is the Boltzmann constant, and T is the absolute temperature. A^{SWC} denotes the system energy in additive interactions³²² i.e. ordinary square-well chain fluids (SWC).

The contribution A^{NAS} (NAS = Non – Additive Segments) is the perturbation term that acts as a correction to the additive behavior. In the same way as in the work of Malakhov and Volkov³²³, this term is evaluated here at the first order :

$$\frac{A^{NAS}}{NkT} = \frac{1}{2} \rho \sum_i \sum_j x_i m_i x_j m_j \int 4\pi r^2 dr g_{ij}^{SWC}(r) \beta u_{ij}^{NAS}(r) \quad (3.5)$$

Where $g_{ij}^{SWC}(r)$ represents the intersegment distribution function of a fluid of ordinary square-well chains. In equation (3.5) x_i , x_j are molar fractions of molecule i and j respectively;

m_i, m_j are the number of constitutive segments or the length chain of molecule i and j ; ρ is the total molecular density and $\beta = \frac{1}{kT}$.

III.2.2 Computation of the perturbed contribution of the Helmholtz free energy

Following again Malakhov and Volkov³²³, an explicit expression of A^{NAS} is obtained by making a limited development at first order of u_{ij}^{NAS} at the neighborhood of the additive potential (using the Taylor series).

$$u_{ij}^{NAS}(r) = \left(\frac{\partial u_{ij}^{NAS}(r)}{\partial \sigma_{ij}} \right)_{\sigma_{ij}=\sigma_{ij}^{SWC} \text{ or } l_{ij}=0} (\sigma_{ij} - \sigma_{ij}^{SWC}) + \dots \quad (3.6)$$

Where the diameter for the additive case is written : $\sigma_{ij}^{SWC} = \frac{\sigma_i + \sigma_j}{2}$.

In order to evaluate the derivative, we used the function $e^{-\beta u_{ij}(r)}$. One has :

$$\frac{d e^{-\beta u_{ij}(r)}}{d \sigma_{ij}} = -e^{-\beta u_{ij}(r)} \beta \frac{d u_{ij}(r)}{d \sigma_{ij}} \quad (3.7)$$

And recalling that $\sigma_{ij} = \sigma_{ij}^{SWC} (1 - l_{ij})$, we can deduce then :

$$\beta u_{ij}^{NAS}(r) = e^{\beta u_{ij}^{SWC}(r)} \left(\frac{d e^{-\beta u_{ij}(r)}}{d \sigma_{ij}} \right)_{l_{ij}=0} \sigma_{ij}^{SWC} l_{ij} \quad (3.8)$$

Taking advantage that $e^{-\beta u_{ij}(r)}$ can be expressed in terms of Heaviside step functions, we find:

$$e^{-\beta u_{ij}} = [H(\mathbf{r} - \sigma_{ij}) - H(\mathbf{r} - \lambda\sigma_{ij})]e^{\beta\epsilon_{ij}} + H(\mathbf{r} - \lambda\sigma_{ij}) \quad (3.9)$$

The derivative of which is written as:

$$\frac{de^{-\beta u_{ij}(\mathbf{r})}}{d\sigma_{ij}} = e^{\beta\epsilon_{ij}} \left(\frac{dH(\mathbf{r} - \sigma_{ij})}{d\sigma_{ij}} - \frac{dH(\mathbf{r} - \lambda\sigma_{ij})}{d\sigma_{ij}} \right) + \frac{dH(\mathbf{r} - \lambda\sigma_{ij})}{d\sigma_{ij}} \quad (3.10)$$

Which can be written in terms of Dirac functions :

$$\frac{de^{-\beta u_{ij}(\mathbf{r})}}{d\sigma_{ij}} = e^{\beta\epsilon_{ij}} \left(-\delta(\mathbf{r} - \sigma_{ij}) + \lambda\delta(\mathbf{r} - \lambda\sigma_{ij}) \right) - \lambda\delta(\mathbf{r} - \lambda\sigma_{ij}) \quad (3.11)$$

Therefore, we have:

$$\left(\frac{de^{-\beta u_{ij}^{SWC}(\mathbf{r})}}{d\sigma_{ij}} \right)_{l_{ij}=0} = e^{\beta\epsilon_{ij}} \left(-\delta(\mathbf{r} - \sigma_{ij}^{SWC}) + \lambda\delta(\mathbf{r} - \lambda\sigma_{ij}^{SWC}) \right) - \lambda\delta(\mathbf{r} - \lambda\sigma_{ij}^{SWC}) \quad (3.12)$$

Recall that we need to find the expression of free energy according to the equation (3.5)

Combining equations (3.5), (3.6) and (3.12) we get :

$$\begin{aligned} \frac{A^{NAS}}{NkT} = 2\pi\rho \sum_i \sum_j x_i x_j m_i m_j \int_0^\infty r^2 g_{ij}^{SWC}(r) \times \sigma_{ij}^{SWC} \times l_{ij} \times e^{\beta u_{ij}^{SWC}(r)} \\ \times \left(-e^{\beta\epsilon_{ij}} [\delta(\mathbf{r} - \sigma_{ij}^{SWC}) - \lambda\delta(\mathbf{r} - \lambda\sigma_{ij}^{SWC})] + \lambda\delta(\mathbf{r} - \lambda\sigma_{ij}^{SWC}) \right) dr \quad (3.13) \end{aligned}$$

This expression can be further simplified using standard arguments making use of cavity function⁶⁰ defined by $y_{ij}^{SWC}(r) = g_{ij}^{SWC}(r)e^{\beta u_{ij}^{SWC}(r)}$. This function is continuous at $r = \sigma_{ij}$:

$$\begin{aligned} \frac{A^{NAS}}{NkT} = & -2\pi\rho \sum_i \sum_j x_i x_j m_i m_j \times \sigma_{ij}^{SWC} \times l_{ij} \\ & \times \left(\sigma_{ij}^{SWC 2} y_{ij}^{SWC} (\sigma_{ij}^{SWC}) e^{\beta\epsilon_{ij}} - (\lambda\sigma_{ij}^{SWC})^2 y_{ij}^{SWC} (\lambda\sigma_{ij}^{SWC}) e^{\beta\epsilon_{ij}} \right. \\ & \left. + (\lambda\sigma_{ij}^{SWC})^2 \lambda y_{ij}^{SWC} (\lambda\sigma_{ij}^{SWC}) \right) \quad (3.14) \end{aligned}$$

Where the cavity functions are evaluated either at the upper side of the limit (indicated by "+"), or at the lower side of the limit (marked with "-") :

$$y_{ij}^{SWC}(\sigma_{ij}^{SWC}) = g_{ij}^{SWC}(\sigma_{ij}^{SWC+}) e^{-\beta\epsilon_{ij}} \quad (3.15)$$

$$y_{ij}^{SWC}(\lambda\sigma_{ij}^{SWC}) = g_{ij}^{SWC}(\lambda\sigma_{ij}^{SWC-}) e^{-\beta\epsilon_{ij}} \quad (3.16)$$

It leads to:

$$\begin{aligned} \frac{A^{NAS}}{NkT} = & -2\pi\rho \sum_i \sum_j x_i x_j m_i m_j \sigma_{ij}^{SWC 3} l_{ij} [g_{ij}^{SWC}(\sigma_{ij}^{SWC+}) - \lambda^3 g_{ij}^{SWC}(\lambda\sigma_{ij}^{SWC-}) \\ & + e^{-\beta\epsilon_{ij}} \lambda^3 g_{ij}^{SWC}(\lambda\sigma_{ij}^{SWC-})] \quad (3.17) \end{aligned}$$

This expression requires having average inter - segment distribution functions at contact $g_{ij}^{SWC}(r = \sigma_{ij}^{SWC+})$ and at limit $g_{ij}^{SWC}(r = \lambda.\sigma_{ij}^{SWC-})$ for a chain of spheres interacting via an additive square well potential. This is the subject of the next section.

III.2.3 Determination of inter segment distribution function $g_{ij}^{SWC}(r)$

We must now determine the inter-segment distribution function $g_{ij}^{SWC}(r)$. In this work, we used the suggestion of Paredes et al³²⁷ who proposed to link $g_{ij}^{SWC}(r)$ (between 2 segments of 2 different chains) to the radial distribution function of disconnected spheres (called $g_{S,S}$) and the inter-segment distribution function of dimers (called $g_{D,D}$). Expressions for this latter radial distribution exist in the literature as a function of $\eta = \rho v_m$, v_m being the molecular hard core volume and $T^* = kT/\varepsilon = 1/\beta\varepsilon$.

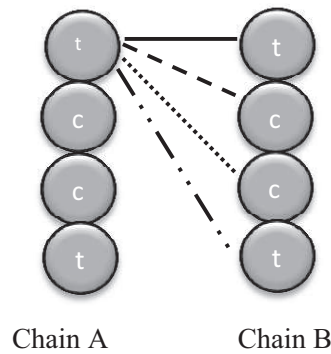


Figure III-1: Interactions between chain A and chain B

For two identical chains containing m segments, there are 4 interactions between terminal segments, $(m - 2)^2$ interactions between internal segments and $4(m - 2)$ interactions between a terminal segment and an internal segment. Therefore, we obtain the average inter-segment distribution function between 2 identical molecules as (cf. Figure III-1) :

$$g_{ij} = \frac{4g_{TT} + 4(m - 2)g_{IT} + (m - 2)^2g_{II}}{m^2} \quad (3.18)$$

Where g_{TT} is the radial distribution function between two terminal segments; g_{IT} is the radial distribution function between an internal segment and external terminal segment; g_{II} is the

radial distribution function between two internal segments and m is the chain length.

According to Paredes et al.³²⁷, the inter-segment functions are supposed to depend on accessible surfaces. In their work, the relations between the inter-segment distribution functions and $g_{D,D}$ and $g_{S,S}$ are written as:

$$g_{TT} = g_{D,D} \quad (3.19)$$

$$g_{IT} = \frac{3}{2}g_{DD} - \frac{1}{2}g_{SS} \quad (3.20)$$

$$g_{II} = 2g_{DD} - g_{SS} \quad (3.21)$$

These results are consistent with the study of Chiew et al.^{328,329} who worked on the site-site correlation function of 4-mer hard chain by using the Percus-Yevick approximation. It is also compatible with the Flory theory of Hall et al.³³⁰⁻³³² and it can be extended to the square well potential (with $\lambda = 1.5$).

For the general case, we must deal with molecules having different numbers of segments m_i and m_j . Computing the average inter-segment distribution function is performed by a weighted average of the number of interactions:

$$g_{ij} = \frac{4g_{T_iT_j} + 2(m_i - 2)g_{I_iT_j} + 2(m_j - 2)g_{I_jT_i} + (m_j - 2)(m_i - 2)g_{I_iI_j}}{m_i m_j} \quad (3.22)$$

Based on homonuclear chains relations, we make the following approximation :

$$g_{T_iT_j}(\eta) \approx g_{TT}(\eta) \quad (3.23)$$

$$g_{I_iI_j}(\eta) \approx g_{II}(\eta) \quad (3.24)$$

$$g_{T_i I_j}(\eta) \approx g_{T_j I_i}(\eta) \approx g_{IT} \quad (3.25)$$

In order to determine the inter-segment distribution function, it is necessary to have the inter-segment distribution function of square well spheres and dimers as a function of packing fraction and temperature. B. J. Zhang et al.³³³ fitted the values of $g_{S,S}$ (called g_{SWS}) and $g_{D,D}$ (called g_{SWD}) at contact for the chain molecule with a square well potential as simple functions of compactness η and temperature:

$$g_{SWS}(\sigma^+, \eta, \beta\varepsilon) = \sum_{p=0}^4 \sum_{q=1}^4 a_{pq}(\beta\varepsilon)^p \frac{\eta^{q-1}}{(1-\eta)^q} \quad (3.26)$$

$$g_{SWD}(\sigma^+, \eta, \beta\varepsilon) = \sum_{p=0}^4 \sum_{q=1}^4 b_{pq}(\beta\varepsilon)^p \frac{\eta^{q-1}}{(1-\eta)^q} \quad (3.27)$$

Where a_{pq} , b_{pq} are coefficients of these equations and are determined by regression of distribution function data at contact ($r = \sigma_{ij}^{ref}$) obtained by Monte Carlo simulation^{334,335} over the temperature–density range $0 \leq \beta\varepsilon \leq 0.7$ ($T^* > 1.42$) and $0 \leq \eta \leq 0.5$. Their values are listed in Table III-6 and Table III-7 in Appendix III-A. In this work, we shall use these functions, and evaluate them for mixtures at η and $\beta\varepsilon_{ij}$.

Note that in equation (3.17), we also need the distribution functions evaluated at $r = \lambda \cdot \sigma_{ij}^{SWC}$. As mentioned above, in this development we use the value of λ equal to 1.5 which is the most current width in square well potential where data are more abundant in the literature^{336–338}. Because the relations in equations (3.26) and (3.27) have given good results for the determination of $g_{S,S}$ and $g_{D,D}$ at contact, we assumed that these relations also allow to well represent the inter-segment distribution functions of spheres and dimers at $r = \lambda \cdot \sigma_{ij}^{SWC}$. Therefore, we repeat the B. J. Zhang et al.³³³'s work on determination of $g_{S,S}$ and $g_{D,D}$ at

$$r = \lambda. \sigma_{ij}^{SWC}.$$

Table III-1: Summary of conditions of Monte Carlo simulation for fitting and for the validation

	m	η	T*	Method	Authors
For fitting	1	$0.05 \leq \eta \leq 0.45$	1.5, 2, 3, 10	NVT	Largo et al. ³³⁹
	2	$0 \leq \eta \leq 0.4$	1.5, 2	BGY Equation	Lipson et al. ³³⁷
For validation	4	$0 \leq \eta \leq 0.35$	1.5	BGY Equation	Lipson et al. ³³⁸
	6, 8, 16	$0 \leq \eta \leq 0.3$	1.5	BGY Equation	Lipson et al. ³³⁶
	4	$0.05 \leq \eta \leq 0.45$	1.5	NVT	Tavares et al. ³³⁴
	8	$0.36 \leq \eta \leq 0.45$	1.5	NVT	Tavares et al. ³³⁴
	16	$0.36 \leq \eta \leq 0.45$	1.5	NVT	Tavares et al. ³³⁴
	4	$0 \leq \eta \leq 0.5$	1.5	NPT	This work

The values of a_{pq} and b_{pq} in Equation (3.26) and (3.27) at $r = \lambda. \sigma_{ij}^{SWC}$ are obtained by regressing the data from the study of Lipson et al.^{337,338} for $g_{SWD}(\lambda\sigma^+, \eta, \beta\varepsilon)$ ($m = 2$) and from the study of Largo et al.³³⁹ for $g_{SWS}(\lambda\sigma^+, \eta, \beta\varepsilon)$ ($m = 1$) with the conditions detailed in Table III-1. In fact, there are the different methods to obtain the inter-segment distribution function. In Table III-1, we can see three typical methods. The first method is the NVT that consists a Monte Carlo simulation where we impose the temperature, the volume and the number of particles of the system. The second method is the NPT that similar with the NVT method except we impose the pressure instead of the volume. The third method called BYG integral equation. This method has been solved for many short-ranged potentials such as hard sphere^{340,341}, square well³⁴² and Lennard-Jones^{343,344} fluids. See the original articles for more details.

The examples of this fitting are shown in Figure III-2. The values of these coefficients are listed in Table III-8 and Table III-9 in Appendix III-A. See the original article for more details.

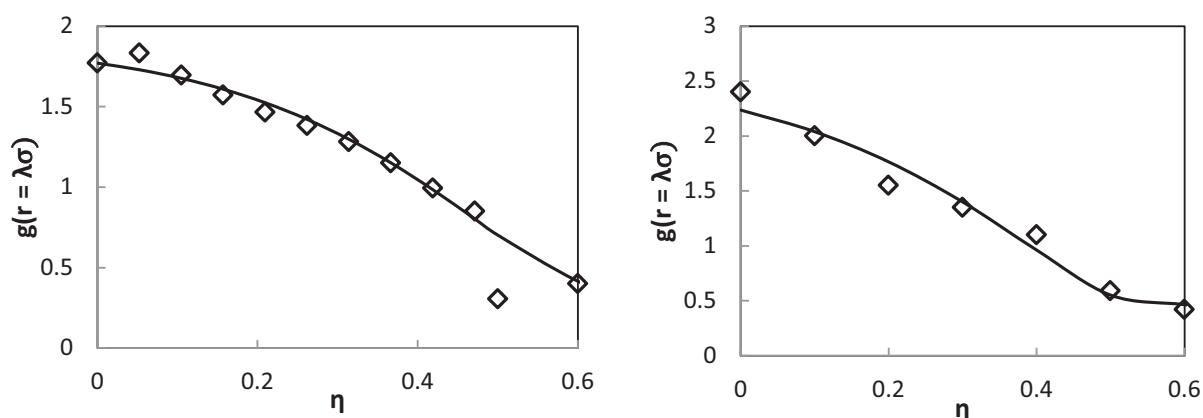


Figure III-2: Fitting inter-segment distribution functions of square well spheres (on the left) and square well dimers (on the right) at $\lambda = 1.5$ and $T^* = 1.5$. Full line are $g(r)$ calculated from the fitted polynomial functions and empty points are $g(r)$ originating from Lipson et al.^{337,338} and Largo et al.³³⁹

III.3 Monte Carlo simulation data

In this work, we used Monte Carlo simulation to validate the approach by comparing, for the both simulation and model the inter-segment distribution function for pure chains and the compressibility factor for mixtures of chains. The MC simulations were performed with a standard NPT algorithm using $N = 250$ particles at different reduced pressures ($P^* = P\sigma^3/\varepsilon_{ij}$) and reduced temperature ($T^* = kT/\varepsilon_{ij}$). The average properties are computed during a production run lasting 500 million Monte Carlo steps, one step corresponding to a single Monte Carlo move. Before each production run, a preliminary run of 50 million Monte Carlo steps is carried out to achieve equilibrium. The number of Monte Carlo steps may change depending on the convergence. In the case of square-well interactions, a spherical *cutoff* equal to half of the simulation box was used while classical tail corrections were employed³⁰⁹. For the intramolecular terms, the bonding is fixed with tangent spheres. There is no either bending or torsion between two segments. The different Monte Carlo moves and their corresponding attempt probabilities used during the simulations are molecular translation (20%), molecular rotation (20%), regrowth with configurational bias (59%) and volume change (1%). The amplitude of translations, rotations and volume changes was adjusted during the simulation to

achieve an acceptance ratio of 40% for these moves.

III.3.1 Pure chains of square wells

For each simulation, the radial distribution functions $g(r)$ for a pure square well chain are given directly. In NPT, in order to determine the $g(r)$, it is necessary to get the histogram that represents the average number of particles whose distance from a given particle lies in the interval $(r, r + dr)$. After, the radial distribution function is calculated by this expression:

$$g(r + 1/2dr) = \frac{h(r)}{\frac{N}{V} \times \frac{4}{3} \pi ((r + dr)^3 - r^3)} \quad (3.28)$$

Where $h(r)$ is the histogram; N is total number of particles in the system; V is the volume of simulation box.

The MC simulation conditions including the reduced temperature, the imposed pressure, the chain length, the diameter of segment are summarized in Table III-2.

Table III-2: Summary of different MC simulations performed on pure chains with $m = 4$.

Case	T*	P*/T*	P (Pa)	N	m	σ
SW1a	1.5	0.001	20700	250	4	1
SW1b		0.02	414000			
SW1c		0.03	621000			
SW1d		0.05	1035000			
SW1e		0.1	2070000			
SW1f		0.2	4140000			
SW1g		0.8	16560000			
SW1h		1	20700000			
SW1i		1.5	31050000			

The radial distribution functions of such chains are obtained and shown in Table III-3.

Table III-3: Molecular simulation results for pure chains of square well at contact and at $r = \lambda\sigma$ with $\lambda = 1.5$

			At $r = \sigma$	At $r = \lambda\sigma$ With $\lambda = 1.5$
	η	Uncertainty (%)	$g(r)$	$g(\lambda\sigma)$
SW1a	0.0022	0.19	3.4608	1.3647
SW1b	0.3460	0.58	1.6185	1.1912
SW1c	0.3462	0.79	1.5331	1.146
SW1d	0.3487	0.58	1.4383	1.1263
SW1e	0.3563	0.49	1.4307	1.0755
SW1f	0.3660	0.24	1.4704	1.0601
SW1g	0.3981	0.21	1.7218	1.0286
SW1h	0.4063	0.15	1.8049	3.4443
SW1i	0.4211	0.20	1.968	3.4976

III.3.2 Mixtures of chains of square wells

For mixtures of chains of square-well, the same approach using Monte Carlo simulation method was employed. In the simulation box, we defined a number of particles for each type of molecules. And the property that we consider is the compressibility factor. The compressibility is calculated from following equation:

$$Z = \frac{P}{\rho kT} \quad (3.29)$$

Where P , ρ , T , v is the pressure, the molecular density, the temperature and the molar volume of

system respectively, k is Boltzmann constant.

As mentioned above, a standard NPT algorithm is used for these calculations. It means that the pressure P , the number of particles N (for each type of molecules in the simulation box) and the temperature T of the system are imposed. The computation gives a density that yields directly the compressibility factor using Equation (3.29).

Otherwise, we also use some parameters such as the reduced temperature T^* ($T^* = k_B T / \varepsilon$ where ε is the dispersive energy), the reduced pressure P^* ($P^* = \sigma^3 P / \varepsilon$, where σ is the diameter of the particle, this property is reduced in the mixture of 2 different particles). In case of mixture of chains, each particle has the same dispersive energy ε_{ij} . We present usually the compressibility factor Z as a function of the compacity η with:

$$\eta = \frac{\pi}{6} \rho = \sum_i x_i m_i \sigma_i^3 \quad (3.30)$$

The density, and thus the molar volume are obtained directly from the statistical averages performed over the different Monte Carlo configurations. For example in the post-treatment, the molecular density is determined by:

$$\rho = \frac{N}{\langle V \rangle} \quad (3.31)$$

Where N is the number of particles in the box that is a fixed input in our case and $\langle V \rangle$ is the average molar volume. The MC simulation conditions for chain mixtures are summarized in Table III-4.

Non-zero values of the non-additive parameter l_{ij} are taken into account by the use of the modified Lorentz-Berthelot combining rule:

$$\sigma_{ij} = \frac{\sigma_i + \sigma_j}{2} (1 - l_{ij}) \quad (3.32)$$

In fact, in the MC simulation, we impose the diameter values σ_i, σ_j of each component. We choose a value of l_{ij} , so the cross diameter is calculated by using Equation (3.32) then imposed in MC simulation.

Table III-4: Summary of the different MC simulations performed on mixtures.

Case	T*	P*/T*	P	N ₁	m ₁	σ_2/σ_1	N ₂	m ₂
SW2a	1.5	0.02	414000	100	1	1.5	100	4
SW2b		0.05	1035000					
SW2c		0.1	2070000					
SW2d		0.2	4140000					
SW2e		0.5	10350000					
SW2f		0.8	16560000					
SW3a	1.5	0.02	414000	100	2	1.5	100	5
SW3b		0.05	1035000					
SW3c		0.1	2070000					
SW3d		0.2	4140000					
SW3e		0.5	10350000					
SW3f		0.8	16560000					
SW4a	1.5	0.02	414000	100	1	3	100	4
SW4b		0.05	1035000					
SW4c		0.1	2070000					
SW4d		0.2	4140000					
SW4e		0.5	10350000					
SW4f		0.8	16560000					
SW5a	1.5	0.02	414000	100	2	3	100	5
SW5b		0.05	1035000					
SW5c		0.1	2070000					

SW5d		0.2	4140000					
SW5e		0.5	10350000					
SW5f		0.8	16560000					
SW6a	30	0.02	8280000	100	1	1.5	100	4
SW6b		0.05	20700000					
SW6c		0.1	41400000					
SW6d		0.2	82800000					
SW6e		0.5	207000000					
SW6f		0.8	331200000					
SW7a	1.5	0.02	414000	50	1	1.5	150	4
SW7b		0.05	1035000					
SW7c		0.1	2070000					
SW7d		0.2	4140000					
SW7e		0.5	10350000					
SW7f		0.8	16560000					

In fact, here we only consider the positive values of l_{ij} . The geometric combining rule seems more adapted than the arithmetic one. Therefore it is rather expected to the values $l_{ij} > 0$. Note that we consider the results of compressibility factor Z of chain mixtures for the case of $l_{ij} = 0$ and $l_{ij} = 0.1$ (except in the case SW2 where we have also simulated the systems at an additional condition of $l_{ij} = 0.05$). The results of molecular simulations for these mixtures are presented in Table III-5.

Table III-5: Molecular simulation results for mixtures of square well chains with or without a non-additive parameter

	$l_{ij} = 0$			$l_{ij} = 0.05$			$l_{ij} = 0.1$		
	η	Z	Uncertainty (%)	η	Z	Uncertainty (%)	η	Z	Uncertainty (%)
SW2a	0.3303	0.2299	0.85	0.3433	0.2211	0.76	0.3511	0.2163	1.21
SW2b	0.3419	0.5551	0.61	0.3572	0.5314	0.65	0.3661	0.5184	0.70
SW2c	0.3606	1.0528	0.70	0.3706	1.0244	0.40	0.3819	0.994	0.40
SW2d	0.3826	1.9845	0.32	0.3925	1.9343	0.23	0.4023	1.887	0.35
SW2e	0.4149	4.5747	0.18						
SW2f	0.4366	6.9548	0.24	0.4476	6.784	0.25	0.4579	6.6316	0.38
SW3a	0.2747	0.3597	0.97				0.3472	0.2846	0.67
SW3b	0.3658	0.6754	0.68				0.3863	0.6395	0.84
SW3c	0.3760	1.3142	0.40				0.3994	1.2373	0.43
SW3d	0.3924	2.5182	0.44				0.4155	2.3787	0.67
SW3e	0.4219	5.856	0.41						
SW3f	0.4417	8.9496	0.28				0.4686	8.4356	0.37
SW4a	0.3872	1.4738	0.66				0.3887	1.4682	0.91
SW4b	0.4127	3.457	0.66				0.4196	3.4002	0.96
SW4c	0.4451	6.411	0.43				0.4483	6.365	0.50
SW4d	0.4807	11.873	0.73				0.4884	11.686	0.64
SW4e	0.5420	26.3225	0.21						

SW4f	0.5607	40.716	0.53				0.5633	40.528	0.35
SW5a	0.3976	1.8042	0.66				0.4053	1.7698	0.47
SW5b	0.4249	4.2205	0.80				0.4287	4.1835	0.59
SW5c	0.4468	8.0275	2.27				0.4575	7.839	0.23
SW5d	0.4868	14.734	0.32				0.4923	14.571	0.39
SW5e	0.5323	33.6925	0.83						
SW5f	0.5435	52.792	0.81				0.5510	52.072	0.45
SW6a	0.0561	1.3519	0.16				0.0572	1.3282	0.11
SW6b	0.1062	1.7879	0.24				0.1085	1.7495	0.30
SW6c	0.1569	2.42	0.27				0.1615	2.3500	0.27
SW6d	0.2169	3.5003	0.28				0.2238	3.3919	0.37
SW6e	0.3048	6.2265	0.38						
SW6f	0.3510	8.6524	0.42				0.3663	8.2896	0.22
SW7a	0.34412	0.3157	0.59				0.3535	0.3073	0.77
SW7b	0.3580	0.7587	0.65				0.3648	0.7445	0.42
SW7c	0.3698	1.4689	0.65				0.3793	1.4322	0.38
SW7d	0.3889	2.7934	0.48				0.3973	2.7346	0.33
SW7e	0.4222	6.4327	0.24						
SW7f	0.4432	9.8048	0.25				0.4515	9.6244	0.25

III.4 Validation of Square Wells Chains EoS against Monte Carlo simulation results

In this section, two properties are validated against Monte Carlo (MC) simulation. At first, the inter-segment distribution functions at contact and at $r = \lambda\sigma$ (with $\lambda = 1.5$) for the pure chains is presented. Comparisons with molecular simulation results available in the literature are also provided. At second, the compressibility factor for mixtures of square-well chains is validated by MC simulation.

III.4.1 Validation of inter-segment distribution function

In Figures III-3 and III-4, our approach to calculate the distribution functions for chains is compared to the simulation reported by Lipson et al.^{337,338} and Tavares et al.³³⁴ for $m = 4, 6, 8$ and 16. On the left of Figure III-3 and Figure III-4, the radial distribution function is evaluated at contact ($r = \sigma$) and at ($r = \lambda\sigma$) for different compacities for chain length $m=4$ and a reduced temperature of 1.5. Comparable figures for the other studied chain lengths ($m=6, 8, 16$) are provided in Appendix III-B. We see that the inter-segment distribution function, which is about 4 for ideal gas and rises slightly for longer chains, first decreases as the density increases, passes through a minimum and then increases at higher densities. Our model represents correctly the qualitative behavior obtained by molecular simulation.

We observe that, at medium and high density, a reasonable agreement is obtained between the relation proposed for the calculation of $g(\sigma)$ and $g(\lambda\sigma)$ and the values calculated by Lipson and al.³³⁶⁻³³⁸ and Tavares et al.³³⁴. At low densities the agreement is less good. However, the free energy A^{NAS} corresponding to the non-additive term in Equation (3.17) depends on the inter-segment distribution function $g(r)$ and on the density ρ or the reduced density ρ^* that is a function of compacity η ($\rho^* = \rho \sum_i x_i m_i \sigma_i^3 = \frac{6\eta}{\pi}$); it is the products of these two terms ($g(r)*\rho$) that must be modeled correctly. Such quantity is shown on the right part of Figure III-3 where a good agreement is found between the theory and the simulations whatever the compacity. In view of all the approximation made, the above results allow us validating the

expression of the site-site distribution function (3.22).

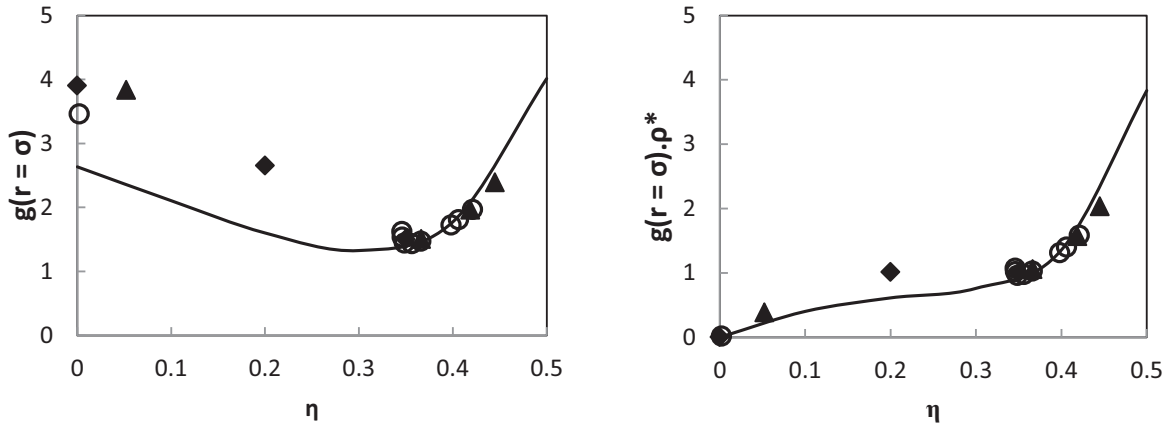


Figure III-3: Values of inter-segment distribution function at contact calculated in this work and taken from literature: (\blacklozenge) Lipson et al.^{337,338} and (\blacktriangle) Tavares et al.³³⁴ in case $m = 4$ at $T^* = 1.5$. In this work, simulation results (o), calculation by equation (3.22) (—)

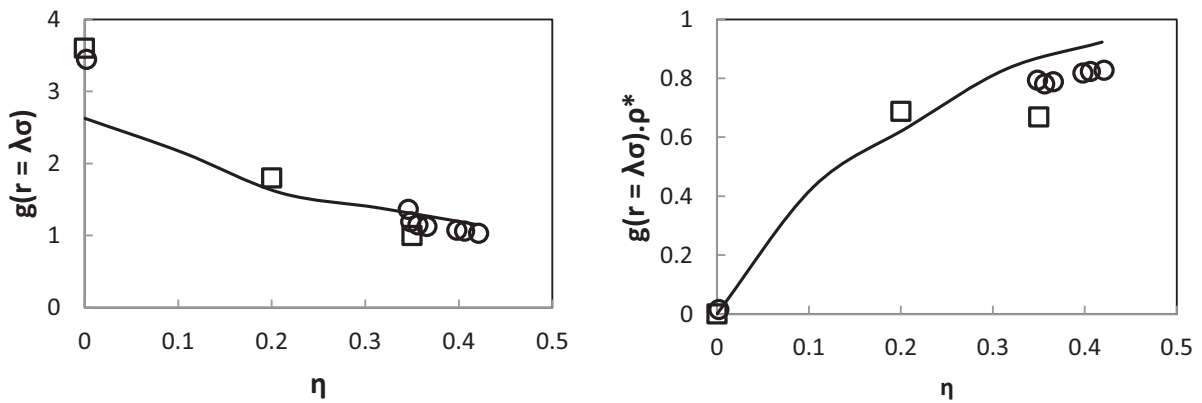


Figure III-4: Values of inter-segment distribution function at $r = \lambda\sigma$ (with $\lambda = 1.5$) calculated in this work and taken from literature: (\square) Lipson et al.^{337,338} in case $m = 4$ at $T^* = 1.5$; In this work, simulation results (o); calculation by equation (3.22) (—)

III.4.2 Validation of compressibility factor

After the validation of the inter-segment distribution functions for the pure square-well chains, we compare the compressibility factor Z of binary mixture of square well chains calculated from our EoS to the ones originating from our Monte Carlo simulations. In Figure III-5, we observe that the results of the compressibility factor Z calculated by the square well chains Equation of state are consistent with the Monte Carlo simulation results for the case SW2. In case SW4, at intermediate densities ($0.3 \leq \eta \leq 0.5$), despite some small deviations, the values of Z without l_{ij} originating from molecular simulations and those from square well chains EoS calculation seem consistent.

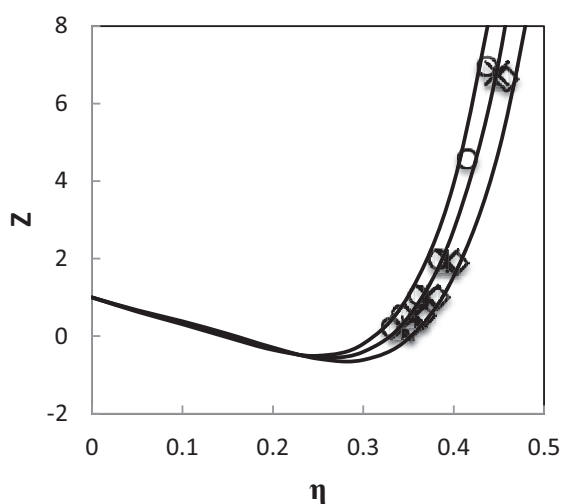


Figure III-5: Comparison of the compressibility factor Z calculated by square-well chains EoS and issued from molecular simulation for the case SW2. The symbols denote the Monte Carlo simulation data: Circles, $l_{ij} = 0$; asterisks, $l_{ij} = 0.05$; diamonds, $l_{ij} = 0.1$. The solid lines are the predictions of the equation of state of square well chains.

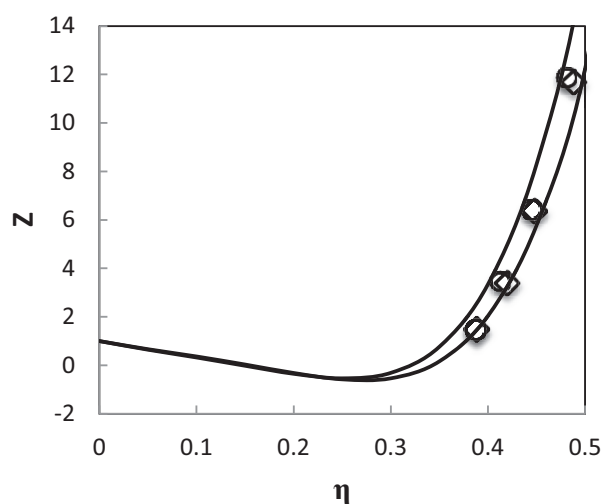


Figure III-6: Comparison of the compressibility factor Z calculated by square-well chains EoS and issued from molecular simulation for the case SW4. The symbols denote the Monte Carlo simulation data: Circles, $l_{ij} = 0$; diamonds, $l_{ij} = 0.1$. The solid lines are the predictions of the equation of state of square well chains.

In case of non-zero l_{ij} parameter and for conditions SW2, Figure III-5 shows that there is good agreement between the calculation by square well chains EoS and molecular simulations at

$l_{ij} = 0.05$. However, at $l_{ij} = 0.1$, the deviations become higher when the density of the system increases. The same observations are found in case SW4 (cf. Figure III-6). In the case SW6 (cf. Figure III-7), the reduced temperature has been considerably increased ($T^* = 30$), it means that the behavior of the chains is similar to that of a hard chain. We can see that the results from Monte Carlo simulations are consistent with those calculated by square-well chains EoS. Figure III-8 represents the values of Z for a non equimolar mixture. We observe that there are small deviations between the values originating from molecular simulation and those obtained by the EoS.

The deviations in each case above may be correlated with the observation made in Figure III-3 and Figure III-4. They show that the calculation of inter-segment distribution functions and the values originating from molecular simulation are very different at high density. It may be explained by the fitting of the radial distribution functions g_{DD} and g_{SS} . In fact, they are fitted at the densities between 0 and 0.4 then we have extrapolated them at high densities. In Equation (3.17), the inter-segment distribution function is one of the contributions of the free energy of non-additive term. Therefore, we believe that a way to improve the observed deviations on the compressibility factor would be to better correlate the inter-segment distribution functions (Equations 3.26 and 3.27) and add more the data of molecular simulation at high densities.

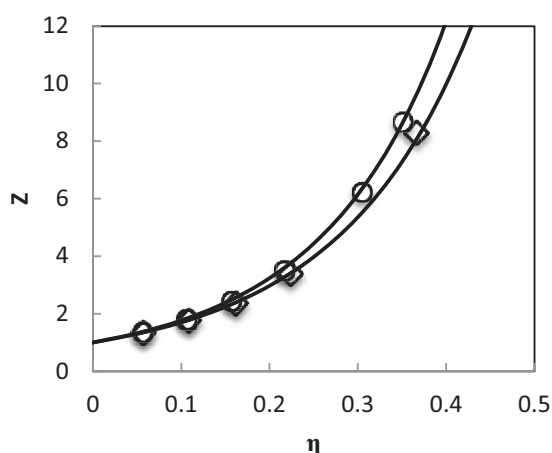


Figure III-7: Comparison of the compressibility factor Z calculated by square-well chains EoS and issued from molecular simulation for the case SW6. The symbols denote the Monte Carlo simulation data: Circles, $l_{ij} = 0$; diamonds, $l_{ij} = 0.1$. The solid lines are the predictions of the equation of state of square well chains.

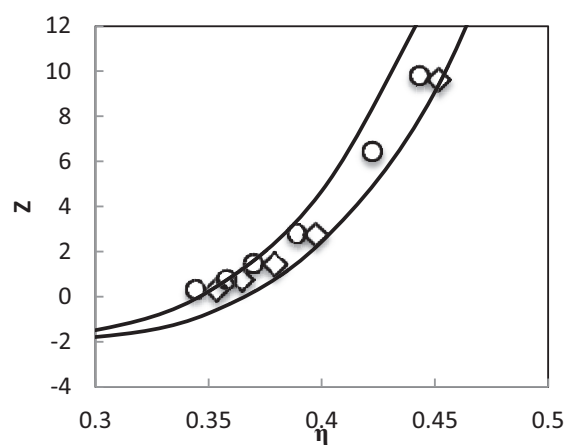


Figure III-8: Comparison of the compressibility factor Z calculated by square-well chains EoS and issued from molecular simulation for the case SW7. The symbols denote the Monte Carlo simulation data: Circles, $l_{ij} = 0$; diamonds, $l_{ij} = 0.1$. The solid lines are the predictions of the equation of state of square well chains.

These results prove that our model take into account slightly well the approximations made for this evaluation of $g(r)$.

III.5 Conclusions

The main target of this paper is to develop a physically-meaningful predictive approach for introducing a repulsive correction in an equation of state. This is done by using the perturbation theory, applied on a reference consisting of chains of square well molecules. The approach is validated against molecular simulation.

The correction works well at low density, but more substantial deviations at high density. Two possible paths are suggested for further improvement: Either the inter-segment distribution functions are refitted using new molecular simulation data at high density, or a re-mapping of the l_{ij} parameter is performed as suggested in the work of Parricaud³⁴⁵.

For the mixtures of square wells spheres, according to Paricaud³⁴⁵, a modification in the

non-additive parameter may be needed could allow better predictions. In his development for non-additive hard-sphere systems, the non-additive theoretical terms contained $\sigma_{ij}^2(\sigma_{ij}^{NAS} - \sigma_{ij})$ that was proposed to be replaced by $(\sigma_{ij}^{NAS 3} - \sigma_{ij}^3)$. This modification allow a correct calculation of the second virial coefficient but to the best of our knowledge the second virial coefficient of non-additive square well chain is unknown. This method cannot be extended here for chain molecules. However, we consider this as an empirical ‘re-scaling’ of l_{ij} , which may help improving the comparison with Monte Carlo simulation, this path may be further investigated in the future.

Appendix III-A: The values of a_{pq} and b_{pq} in equation (3.26) and (3.27) at contact and at $\lambda = 1.5$

Table III-6: Values of a_{pq} at contact

a_{pq}	q				
	p				
		1	2	3	4
0		1	1.5	0.5	0
1	0.796		-2.774	0.929	-0.441
2	1.211		-21.738	49.269	-21.245
3	-0.194		37.165	-100.66	50.837
4	0		-23.186	68.17	-37.694

Table III-7 : Values of b_{pq} at contact

b_{pq}	q				
	p				
		1	2	3	4
0	0.539		1.122	0.849	-0.28

1	0.362	0.695	-6.602	6.341
2	6.646	-39.522	71.354	-42.271
3	-14.254	76.477	-126.845	70.255
4	14.751	-65.946	92.625	-43.548

Table III-8 : Values of a_{pq} at $\lambda=1.5$

a_{pq}	q			
	p			
	1	2	3	4
0	0,39971235	-0,253303103	-0,90766587	0,36773252
1	2,23090715	-0,814209759	-1,5151413	1,85997259
2	1,23339104	-19,75524069	45,417694	-22,7662545
3	-1,26689783	38,72263605	-102,966537	50,5019509
4	-1,46680101	-21,99486901	68,2862575	-33,7783636

Table III-9 : Values of b_{pq} at $\lambda=1.5$

b_{pq}	q			
	p			
	1	2	3	4
0	0,99976794	-0,619769592	-0,11246443	-0,15939359
1	0,07548764	3,068742688	-9,23475302	9,21151101
2	6,12672467	-36,52181926	66,3940585	-43,9966187
3	-14,7504035	79,28258946	-130,880088	70,5244228
4	14,3442077	-63,52369801	90,7216739	-39,4943939

Appendix III-B: The inter-segment distribution functions of pure chains of square wells

The inter-segment distribution function evaluated in contact ($r = \sigma_{ij}$) depending on the density of the spheres for chain length $m=6, 8, 16$ and temperature (T):

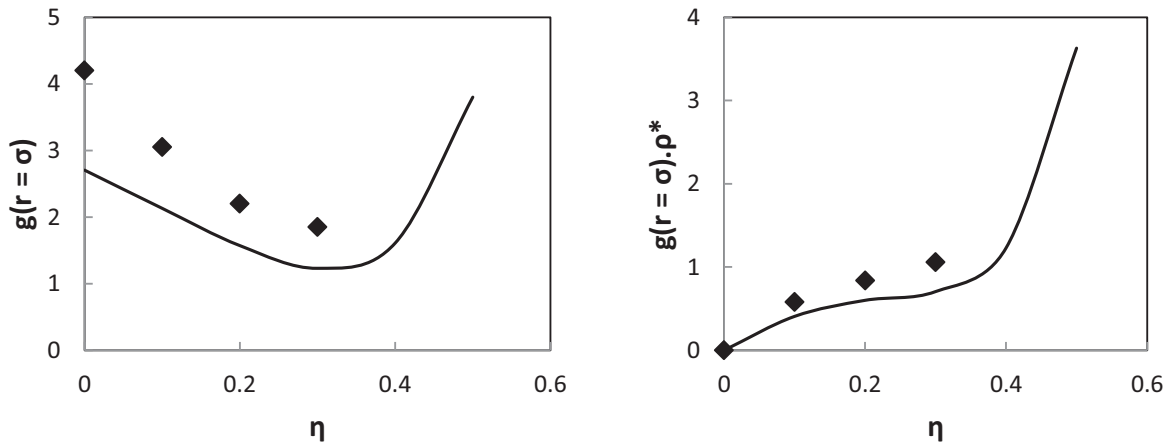


Figure III-9: Values of inter-segment distribution function at contact calculated and taken from literature in case $m=6$. Simulation data are taken from Lipson et al.^{337,338} (\blacklozenge); this study (—)

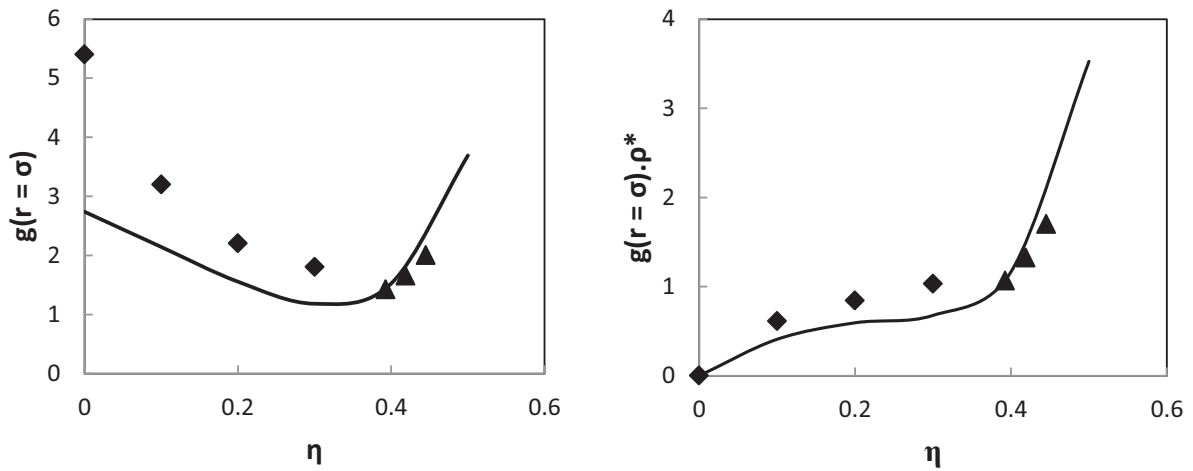


Figure III-10: Values of inter-segment distribution function at contact calculated and taken from literature in case $m=8$ at $T^*=1.5$. Simulation data are taken from Lipson et al.^{337,338} (◆) and Tavares et al.³³⁴ (▲); this study (—)

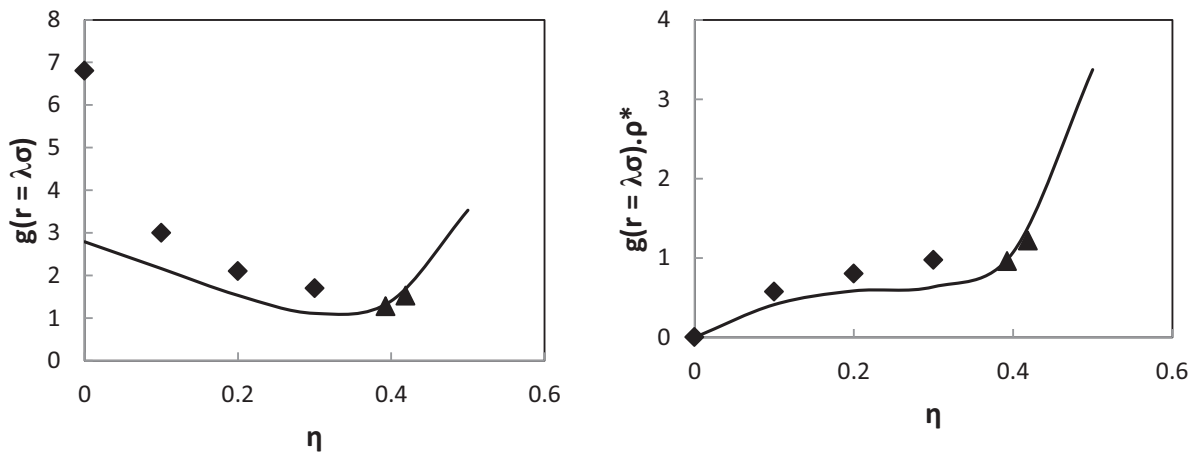


Figure III-11: Values of inter-segment distribution function at contact calculated and taken from literature in case $m=16$ at $T^*=1.5$. Simulation data are taken from Lipson et al.^{337,338} (◆) and Tavares et al.³³⁴ (▲); this study (—)

The radial distribution function evaluated in $r = \lambda \cdot \sigma_{ij}^{ref}$ depending on the density of the spheres for chain length $m=6, 8, 16$ and temperature (T):

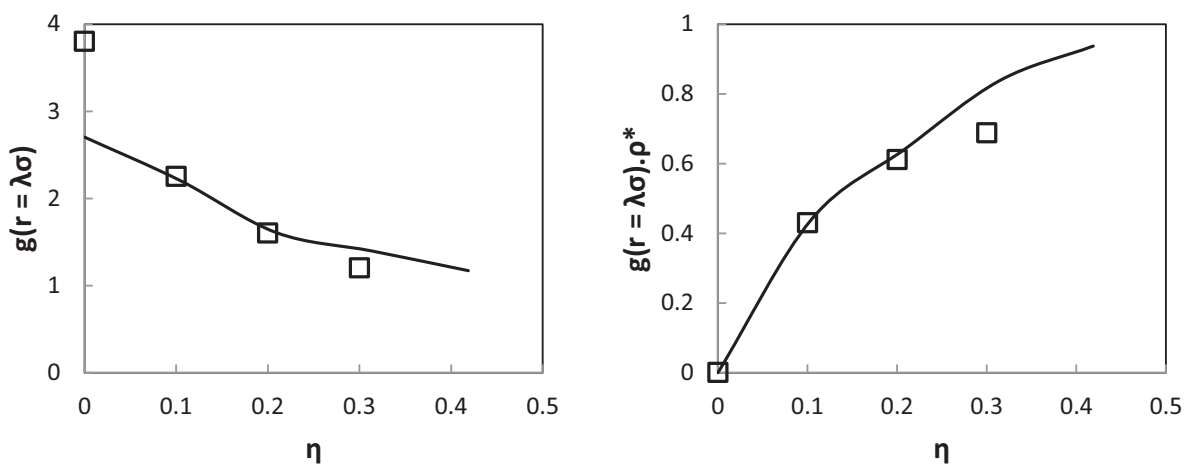


Figure III-12: Values of inter-segment distribution function at $\lambda=1.5$ calculated and taken from literature in case $m=6$ at $T^*=1.5$. Simulation data are taken from Lipson et al.^{337,338} (\square); this study (—)

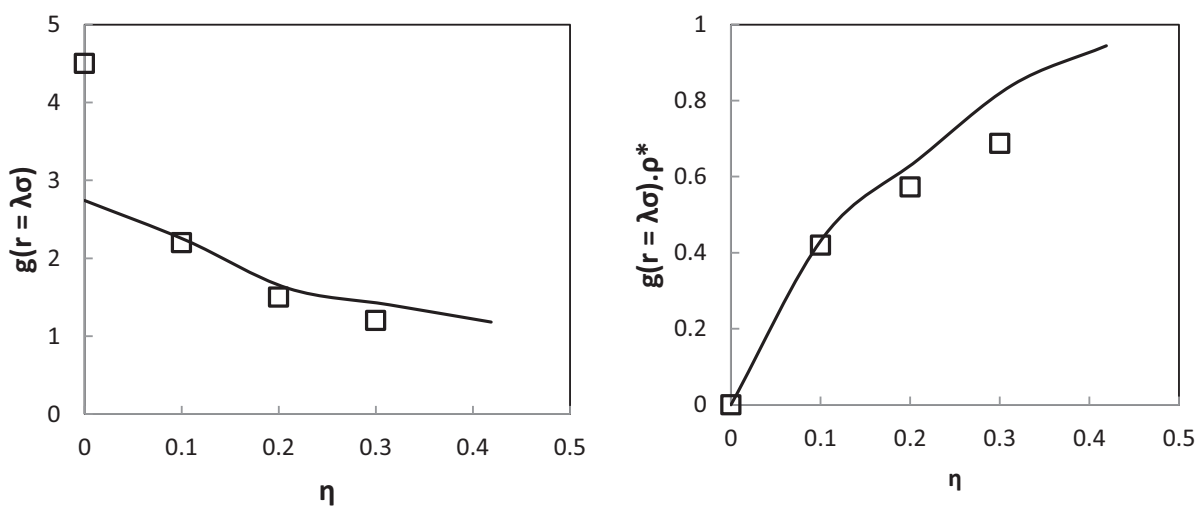


Figure III-13: Values of inter-segment distribution function at $\lambda=1.5$ calculated and taken from literature in case $m=8$ at $T^*=1.5$. Simulation data are taken from Lipson et al.^{337,338} (\square); this study (—)

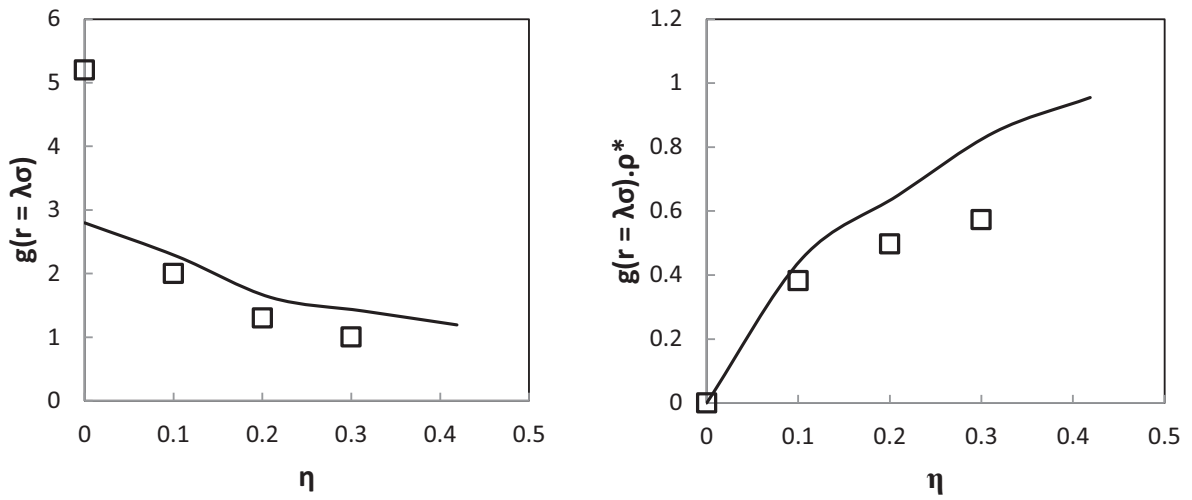


Figure III-14: Values of inter-segment distribution function at $\lambda=1.5$ calculated and taken from literature in case $m=16$ at $T^*=1.5$. Simulation data are taken from Lipson et al.^{337,338} (\square); this study (—)

In Chapter III, a free energy non-additive term of the Square Well Chains have been developed. This term introduces a new parameter l_{ij} which allows correcting the repulsive term in the Equation of state e.g. PC-SAFT. The development is validated by comparison with Monte Carlo simulations. In the next chapter, the development is used to allow GC-PPC-SAFT accounting for non-additive effects. This extension is applied to systems containing hydrogen and oxygenated compounds. A group contribution method to compute l_{ij} parameter is also proposed.

CHAPTER IV

USE OF A NON ADDITIVE GC-PPC-SAFT EQUATION OF STATE TO MODEL HYDROGEN SOLUBILITY IN OXYGENATED ORGANIC COMPOUNDS

*Thi-Kim-Hoang TRINH^{a,b}, Jean-Philippe PASSARELLO^b,
Jean-Charles DE HEMPTINNE^a, Rafael LUGO^a*

^a IFP Energies nouvelles, 1 et 4 avenue de Bois-Préau, 92852 Rueil-Malmaison, France

^b Laboratoire de Science des Procédés et des Matériaux (LSPM), Université Paris 13, CNRS,
99 avenue Jean-Baptiste Clément, 93430 Villetaneuse, France

Keyword : PC-SAFT, group contribution method, hydrogen, oxygenated compound, non-additive

Abstract

The equation of state based on the Group Contribution – Polar Perturbed Chain – Statistical Associating Fluid Theory (GC-PPC-SAFT), which is PC-SAFT combined with the group contribution proposed by Tamouza et al., *Fluid Phase Equilib.* 2004;222-223:67-76 and a polar term developed by Nguyen Huynh et al., *Fluid Phase Equilib.* 2008;264(1-2):62-75, is employed here to model the solubility of hydrogen in oxygenated compounds mixtures such as alcohols, ethers, diols, aldehydes. Our analysis shows that in such systems, the gas solubility may be driven by available volume effects. For this reason, a modified version of this equation of state taking into account non-additive segment diameters, is used in this work.

Systematic tests are performed on binary mixtures and a predictive scheme is proposed. A correlation based on the group contribution method is also suggested as a predictive way to determine the non-additive parameter (l_{ij}). Correlations and predictions are qualitatively and quantitatively satisfactory. The deviations are within the experimental uncertainty (~10%)

IV.1 Introduction

The presence of oxygenated compounds^{203,204} in biomass feeds (e.g. alcohols, aldehydes, acids, esters, ethers,...), makes that several major issues of biomass feeds must be overcome, such as a low LHV (lower heating value), high viscosity or chemical instability^{201,202}. A possible way of removing oxygen consists in using a hydrotreatment unit operating at high pressure and temperature²⁰⁵ in presence of hydrogen ($P = 7$ to 20 MPa, $T = 573.15$ K to 723.15 K). Describing the solubility of hydrogen in these oxygenated solvents is an important step in the design of the process. Several thermodynamic models which allow calculation of hydrogen/hydrocarbons phase equilibrium for conventional hydrotreating processes exist. Typical examples are the Grayson Streed method (GS)⁴, the cubic equations of state like Soave - Redlich - Kwong (SRK) and Peng Robinson (PR)¹¹⁷. The Predictive SRK (PSRK) Equation of state⁶⁴ may also be used, but the quality of the results vary considerably depending on the feed or temperature range. Some authors used the different version of the Statistical Associating Fluid Theory equation of state (SAFT EoS) to predict the solubility of hydrogen in hydrocarbons^{16,127}. However, because of the complexity of biomass feeds (the presence of water and a large variety of oxygenated compounds), there is no currently well-defined thermodynamic approach to predict the behavior of these systems.

In the last decade, our research group has developed a group contribution (GC) method¹⁴ combined with a version of the SAFT EoS to predict the fluid-phase equilibrium of systems of interest in the petroleum industry. Satisfactory results are obtained for phase equilibrium calculations of systems containing n-alkanes, n-alcohols, aromatic compounds and alkyl esters, including small molecules like CO_2 , NH_3 , CH_4 ^{136,346-349}. In this paper, the problem of the hydrogen solubility in oxygen-bearing solvents is addressed using a version of GC-SAFT called GC-PPC-SAFT. The calculation of hydrogen solubility (i.e. Henry's constant) using this model have given quite high deviations between the experimental data and the predicted values. Therefore, we have regressed binary interaction parameter k_{ij} on available data but the values obtained are negative i.e. not physically acceptable. Here another way is explored introducing a repulsive correction.

This chapter consists of three parts: first, the description of the model that we use to

predict the hydrogen solubility in oxygenated solvents. Second, the analysis of the use of predictive binary interaction parameter k_{ij} for the computation of these systems. The next section will explain the reason that led us to develop a non-additive term (with the non-additive parameter l_{ij}) in GC-PPC-SAFT and a brief explanation of the model development (for more details see Chapter III). Finally, the results of prediction and correlation of this new parameter are shown and discussed.

IV.2 GC-PPC-SAFT Equation of State

IV.2.1 Model description

The GC-PPC-SAFT model, namely Group Contribution – Polar Perturbed Chain – Statistical Associating Fluid Theory, is the combination of PPC-SAFT¹⁵ with the GC¹⁴ concept in order to determine the three parameters ε/k , σ and m . This equation is presented as a sum of Helmholtz energy terms at given temperature, volume and composition:

$$A^{res} = (mA^{hs} + A^{chain}) + A^{disp} + A^{assoc} + A^{multi-polar} \quad (4.1)$$

where the first terms (i.e. excluding $A^{multi-polar}$) is exactly the PC-SAFT EoS by Gross and Sadowski¹³. The reference term A^{hs} is based on the hard sphere theory of Boublik³⁵⁰ and Mansoori³⁵¹. It is written as:

$$\frac{A^{hs}}{NkT} = \frac{6}{\rho\pi} \left[\left(\frac{\zeta_2^3}{\zeta_3^2} - \zeta_0 \right) \ln(1 - \zeta_3) + \frac{3\zeta_1\zeta_2}{1 - \zeta_3} + \frac{\zeta_2^3}{\zeta_3(1 - \zeta_3)^2} \right] \quad (4.2)$$

Where :

$$\zeta_k = \frac{\pi}{6} N_{Av} \rho \left[\sum_{i=1}^n x_i m_i (d_{ii})^k \right] \quad (4.3)$$

Here $k = 1, 2, 3$. N_{Av} is Avogadro's number and d_{ii} represents the corresponding temperature dependent hard-sphere diameter, which is related to the parameter σ_{ii} using the equation of Chen and Kreglewski⁸⁰.

$$d_{ii} = \sigma_{ii} \left[1 - 0.12 \exp\left(-\frac{3\varepsilon_{ij}}{kT}\right) \right] \quad (4.4)$$

The term A^{chain} describes the formation of the molecular chain, developed with the assumption of infinite association strength. Following Chapman⁷, its expression is:

$$\frac{A^{\text{chain}}}{NkT} = - \sum_{i=1}^n x_i (m_i - 1) \ln(g_{ii}^{\text{seg}}(d_{ii})) \quad (4.5)$$

where $g_{ii}^{\text{seg}}(d)$ is the radial distribution function for additive hard spheres, evaluated at contact ; its expression is given according to Boublik³⁵⁰ et Mansoori³⁵¹.

The sum ($mA^{\text{hs}} + A^{\text{chain}}$) is the reference term of the PC-SAFT model. The London-type attractive interactions between segments (dispersive interactions) are taken into account through the second order perturbation theory of Barker and Henderson⁷ applied to chain molecules, and written as:

$$\frac{A^{\text{disp}}}{NkT} = \frac{A_1^{\text{disp}}}{NkT} + \frac{A_2^{\text{disp}}}{NkT} \quad (4.6)$$

These expressions, according to Gross et al¹³, require the mixture parameters $\overline{m^2 \varepsilon \sigma^3}$ and $\overline{m^2 \varepsilon^2 \sigma^3}$ calculated by the following rules :

$$\overline{m^2 \varepsilon \sigma^3} = \sum_i^n \sum_j^n x_i x_j m_i m_j \left(\frac{\varepsilon_{ij}}{kT} \right) \sigma_{ij}^3 \quad (4.7)$$

and

$$\overline{m^2 \varepsilon^2 \sigma^3} = \sum_i^n \sum_j^n x_i x_j m_i m_j \left(\frac{\varepsilon_{ij}}{kT} \right)^2 \sigma_{ij}^3 \quad (4.8)$$

These averages involve three parameters: the dispersion energy between two segments: ε_{ij}/k , the diameter of segment σ_{ij} and the chain length m_i . Here, ε_{ij} is defined as:

$$\varepsilon_{ij} = (1 - k_{ij}) \sqrt{\varepsilon_i \varepsilon_j} \quad (4.9)$$

In the original rules, the parameter k_{ij} is zero; this parameter allows to take into account the deviations to the Lorentz-Berthelot rule due to dispersive interactions between two molecules of different types.

However, to improve the predictive ability of the model, it was found necessary under certain conditions to use non-zero parameters k_{ij} . Nguyen Huynh et al.³⁴⁶ proposed to calculate the k_{ij} parameters by using a relation established by Hudson and McCoubrey¹⁹ based on the dispersive interaction theory of London et al.²⁷ and semi-empirically modified by introducing an adjustable parameter for each component. The expression is written as follows:

$$1 - k_{ij} = \frac{2\sqrt{J_i J_j}}{J_i + J_j} \quad (4.10)$$

where J_i and J_j are the pseudo-ionization energies of molecules i and j which are calculated by group contribution (Equation 4.18). These are adjustable semi empirical parameters. Note that this approach implies that the k_{ij} values are positive. This is important in view of the observation

made below regarding hydrogen solubility in oxygenated compounds (see the next section for more details).

For the cross diameters σ_{ij} , the combining rule is :

$$\sigma_{ij} = \frac{\sigma_i + \sigma_j}{2} \quad (4.11)$$

Spheres that obey the relation between diameters given above are called additive; there is also a modified version of this rule involving a binary parameter l_{ij} (in which case the spheres are called non-additive). Some authors (Nguyen T.B. et al.¹³⁵, Sadowski et al.^{29,30},...) used Equation (4.11) corrected with $(1 - l_{ij})$ with the purpose to adjust repulsive forces. However, it appears that in the original PC-SAFT this correction only affects the dispersion term and not the repulsive and chain term since $d_{ij} = (d_{ii} + d_{jj})/2$: it enters into Equation (4.6) in exactly the same way as the k_{ij} parameter. It is better to develop a term in the rigorous way that take into account the non-additive effect then propose an predictive approach.

In section 3, we will give brief explanations how our model was modified to take into account the non-additive interactions between chains in accordance with the thermodynamic perturbation theory.

The contribution A^{assoc} (associative term) takes into account the quasi-chemical interactions due to localized attractions, such as hydrogen bonds and charge transfer at short distance (donor-acceptor):

$$\frac{A^{assoc}}{NkT} = \sum_{i=1}^n x_i \left\{ \sum_{A_i} \left(\ln X^{A_i} - \frac{X^{A_i}}{2} \right) + \frac{1}{2} M_i \right\} \quad (4.12)$$

where M_i denotes the number of association sites on each molecule, X^{A_i} is the mole fraction of unbound site A, and the internal sum bears on all association sites located on the molecule j . The unbound fractions are given by the system of implicit equations considering all

sites A_i, B_i, C_i, \dots of all species $i = 1, 2, 3, \dots$

The value of X^{A_i} is computed using a balance on the sites and an equilibrium constant written as:

$$\Delta^{A_i B_j} = \kappa^{A_i B_j} g_{ij} \sigma^3 \exp\left(\frac{\varepsilon^{A_i B_j}}{kT} - 1\right) \quad (4.13)$$

Where two additional parameters are introduced: the energy of association between sites A and B on molecules i and j respectively $\varepsilon^{A_i B_j}$ and the volume of association $\kappa^{A_i B_j}$.

In Equation (4.13), g_{ij} is the radial distribution function at contact, taking into account the interactions between component i and component j , as expressed by Gross and Sadowski.¹³

Often, only self – associating molecules are considered in such a way that all sites are identical (except their charge). Hence, the association parameters are considered as pure component parameters. Huang and Radosz¹⁰⁷ have defined the well-known categories of 1A (for acids), 2B (for alcohols), 3B (for alcohols and water) or 4C (for water). In the context of group contribution, we now consider that the sites (and therefore its parameters) belong to the groups. Therefore, a group of molecule i can have an associative site that is independent from that of another group on the same molecule.

The term $A^{\text{multi-polar}}$ describes the polarity of segments (dipole moment μ and quadrupole moment Q) and was proposed by Nguyen-Huyh³⁴⁶ based on the theory of Gubbins and Twu²³ for spherical molecules and the segment approach of Jog and Chapman²⁴ for chain molecules. This term involves the polar moments (either dipole or quadrupole) and a new parameter which is the polar fraction x_p ²⁵. The general expression of this term is written as:

$$A^{\text{multi-polar}} = \frac{A_2}{1 - \frac{A_3}{A_2}} \quad (4.14)$$

Where A_2 and A_3 are respectively the perturbation terms of the second and the third order that

take into account the multi-polar interactions.

IV.2.2 Group contribution parameterization of the PPC-SAFT model

a. Average chain parameters

These three parameters can either be determined for each molecule or be calculated by group contribution. In order to improve the predictive ability of the model, we used a group contribution method. This is usually done by reducing the number of necessary parameters and by determining parameters that we can use for a greater number of molecules.

Any molecule in SAFT is characterized by at least three parameters (σ , ε and m). Tamouza et al.¹⁴ proposed a method for calculating the parameters of the molecule by using group parameters that are reused here. We have:

$$\varepsilon_{molecule} = \frac{(\sum_{i=1}^{n \text{ groups}} n_i)}{\sqrt{\prod_{i=1}^{n \text{ groups}} \varepsilon_i^{n_i}}} \quad (4.15)$$

$$\sigma_{molecule} = \frac{\sum_{i=1}^{n \text{ groups}} n_i \sigma_i}{\sum_{i=1}^{n \text{ groups}} n_i} \quad (4.16)$$

$$m_{molecule} = \sum_{i=1}^{n \text{ groups}} n_i R_i \quad (4.17)$$

Where ε_i , σ_i and R_i represent the contribution to the energy of dispersion, the diameter and the chain length of the functional group i in a component which is composed of n_{groups} different groups, n_i is the number of groups of type i in the molecule.

We also consider the pseudo-ionization energy J proposed by Nguyen Huynh et al.³⁴⁶, as

an additional group parameter. The molecular pseudo ionization energies J can be calculated by a group contribution method:

$$J = \sqrt{\prod_{i=1}^{n \text{ groups}} J_i^{n_i}} \quad (4.18)$$

b. Polar parameters

These parameters are involved in the polar term. The polar groups require two additional parameters: the dipole moment μ (or the quadrupole moment Q) and the dipolar fraction x_p^μ (or quadrupolar fraction x_p^Q). In fact, polar fractions x_p^μ and x_p^Q are inversely proportional to the chain length. Hence, the actual parameter used is rather the product ($x_p^\mu m$ or $x_p^Q m$) which represent the number of dipoles or quadrupoles in the molecule.

c. Association parameters : energy of association and volume of association

Despite the fact that the association parameters are often considered to be pure component parameters, they in fact represent interactions between two sites. For unlike sites, the following combining rules that are, at least partially, theoretically supported^{356,357}:

$$\varepsilon^{A_i B_j} = \frac{\varepsilon^{A_i} + \varepsilon^{B_j}}{2} (1 - w_{ij}) \quad (4.19)$$

$$\kappa^{A_i B_j} = \sqrt{\kappa^{A_i} \kappa^{B_j}} (1 - u_{ij}) \quad (4.20)$$

Where w_{ij} and u_{ij} are two additional parameters that allow us to adjust the energy of association

and the volume of association respectively. In this work, they are most often taken to be zero unless mentioned otherwise.

IV.3 Predictive use of GC-PPC-SAFT on hydrogen + oxygenated mixtures

In order to investigate the trends that may exist in the solubility behavior of hydrogen in various solvents, the use of Henry's constant appears to be a relevant descriptor, as already discussed in chapter II. In fact, Henry's law constant is widely used to describe the low solubility of light solutes (such as hydrogen) in a variety of solvents over a wide temperature range³³⁻³⁵. When Henry's constant of a solute increases with temperature, it corresponds to a decrease in the solubility. In our case, the solute is hydrogen and the solvents are the molecules listed in Table II-1 in Chapter II. The Henry's law constant of a solute in a solvent, H_i is defined by the expression:

$$H_i = \lim_{x_i \rightarrow 0} \left(\frac{f_i^L}{x_i} \right) \quad (4.21)$$

Where f_i^L is the fugacity of hydrogen (solute i) in the liquid phase, x_i is its mole fraction in the liquid phase.

The database used in this work has been analyzed in detail for its global coherence in Chapter II. Beside the vapor-liquid equilibrium data, we also have in our database the solubility coefficients such as Ostwald coefficient, Bunsen coefficient and Kuenen coefficient. They have been converted into Henry's constant using the definitions in the IUPAC³⁶ guide.

The original GC-PPC-SAFT model was first tested in pure prediction for the phase equilibrium calculation of H₂-oxygenated compounds considered in the database. The GC-PPC-SAFT parameters of hydrogen and oxygenated compounds were determined in previous studies^{2,4,31-34} and reused here (Table IV-3 in Appendix IV-A). The k_{ij} was predicted using Equation (4.10). As the pseudo-ionization parameters of some groups are not defined (aldehydes, ketones, esters,...), the k_{ij} between hydrogen and molecules from these families are set equal to

zero.

In terms of Henry's constants, a typical example is shown in Figure IV-1. We can see that GC-SAFT significantly overestimates the experimental Henry's constant (meaning it underestimates the solubility).

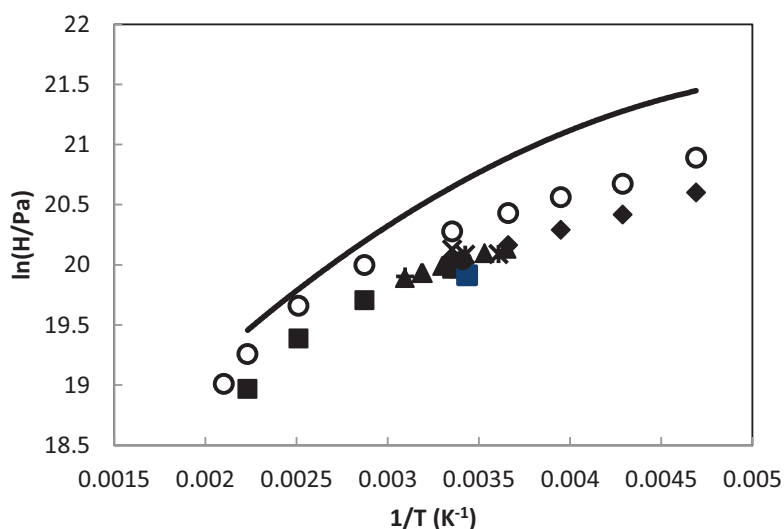


Figure IV-1: Diagram of $\ln H$ as a function of $1/T$ for the binary mixture hydrogen/ethanol. Experimental data are taken from Wainwright et al.¹⁴² (■), Brunner et al.¹⁴⁴ (■), Makranczy et al.²¹³ (×), Just et al.²¹⁴ (◇), Katayama et al.¹⁴¹ (◆), Purwanto et al.¹³² (+), Timofeev et al.²¹⁷ (*), Maxted et al.¹⁴⁵ (▲), Luhring et al.¹³⁰ (●), pseudo-data by molecular simulation (ref: Chapter 2) (○), predictive calculation by GC-PPC-SAFT with predictive k_{ij} (—)

The usual way of improving the results consists in adjusting the binary parameter (k_{ij}). When this is done, the results are dramatically improved (cf. Figure IV-2), many systems requiring a non-zero value k_{ij} .^{124,126,303}

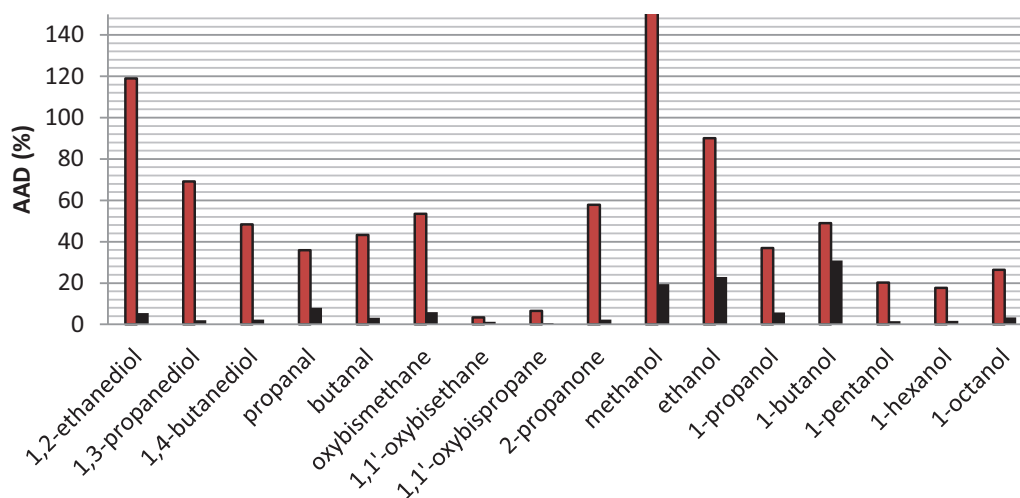


Figure IV-2: Deviations of Henry's constant of the binary mixtures H_2 -oxygenated components: without k_{ij} regression (■), with k_{ij} regression (■)

However, the adjusted k_{ij} are mostly negative as depicted on Figure IV-3. The numerical values are shown in Table IV-4 in Appendix IV-B. Yet, it has been shown that only positive k_{ij} values can be justified from a theoretical point of view (see NguyenHuynh et al.³⁴⁶). The original Lohrenz – Berthelot combining rule on dispersive energy $\varepsilon_{ij} = \sqrt{\varepsilon_i \varepsilon_j}$ should overestimate the true dispersive interactions according to Hudson and McCoubrey.³⁵² Here, the opposite is observed: the 'net attraction' between the oxygenated species and hydrogen seems to be underestimated by the Lohrenz-Berthelot rule. Generally, this means that the polarity or cross association has been neglected or under estimated. Yet, there is no evidence of such phenomenon with hydrogen.

One may wonder then if the hydrogen GC-PPC-SAFT parameterization should not be reconsidered. Several such parameters have been investigated by Kadri¹⁸ using hydrogen + n-alkane VLE, and the best parameters are found to be those of Le Thi et al.¹⁶ that are used here. It is not possible to determine hydrogen parameters on its vapor pressure and liquid molar volume, as is usually done for other components, because of its highly supercritical behavior, and because of its quantum behavior. This is why this set of parameters had to be determined on binary VLE.

The same overestimation of Henry's constants is also observed with the Monte Carlo

simulations (see Figure IV-1), yet to a smaller extent. These results suggest searching for other causes for the observed deviation between SAFT and experimental data.

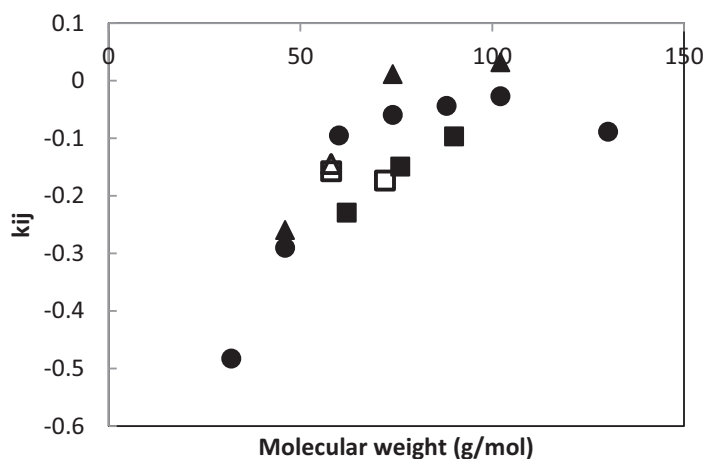


Figure IV-3: Values of k_{ij} parameter as a function of molecular weight of chemical families: H₂/diol (■), H₂/aldehyde (□), H₂/ether (▲), H₂/acetone (Δ), H₂/1-alcohols (●)

An alternative explanation for the observed k_{ij} is to assume that this behavior is not the result of a missing attractive contribution but to a decrease of the repulsion between hydrogen and oxygenated molecule.

Our analysis of this phenomenon starts with the work of Clever and al.³⁵⁸ who studied the solubility of noble gases such as neon, krypton and helium in hydrocarbon solvents. A linear behavior of the gas solubility as a function of the free volume was observed. Recall that this volume is computed according to $V_{free} = V_m - V_{vdW}$ i.e. the difference between the molar volume (macroscopic observed volume) and the volume of van der Waals at 298.15 K. Their study suggests that the gas fits into the spaces left by the solvent. The solubility seemed primarily governed by the probability of insertion of the gas molecule in the solvent. This behavior reflects the absence of high energy interaction (polar or association) between rare gases and solvent.

We made a similar plot regarding solubility of hydrogen in a large variety of solvents as follows. Remind that the relationship between concentration and Henry's constant is:

$$C = \frac{V_m P}{H} \approx \frac{const}{H} \quad (4.22)$$

Where V_m is the molar volume of solvent, P is the total pressure and C is the gas concentration in the liquid phase (mol/L).

Figure IV-4 shows the gas concentration (in mol/L) which is essentially the inverse of Henry's constant, as a function of the ratio of the free volume and molar liquid volume. In this work, the values of the molar volume and the volume of van der Waals at 298.15 K are taken from the DIPPR database³⁰⁷.

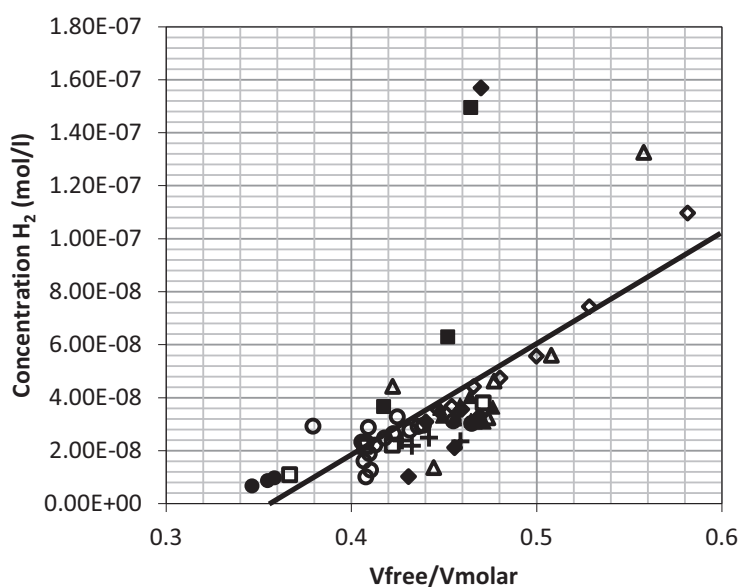


Figure IV-4: Hydrogen concentration in oxygen-bearing solvents as a function of the ratio of free volume and molar volume at 298.15 K: alcohols (o), alkanes (◇), esters (▲), ethers (Δ), ketones (□), diols (●), aldehydes (■), aromatics (+), heterocyclics (◆)

It is noted that in Figure IV-4, the hydrogen solubility in the solvent increases with the free volume. Despite the data dispersion, the hydrogen solubility seems strongly (mainly) dependent at a first good approximation on the free volume fraction and not on the chemical

nature of the solvent (within experimental dispersion). The free volume is conditioned by the repulsive interactions. In order to model the solubility of hydrogen in oxygenated environments, it is necessary to carefully consider these interactions and in particular combining rules on diameters.

Notice first that the additive combining rule (see Equation 4.11) is strictly observed in the case of hard spheres (or segments) but not necessarily when the segments interact via a soft potential. Several authors^{359,360} argued that a geometric mixing rule would be better justified from a theoretical point of view. This means that one should use a modified combining rule:

$$\sigma_{ij} = \frac{\sigma_i + \sigma_j}{2} (1 - l_{ij}) \quad (4.23)$$

With non-zero positive l_{ij} values.

In the work of Spackman³⁶¹ testing additivity of cross van der Waals atomic diameters, it was observed that non additivity is higher when hydrogen atoms (if compared to other atoms) are involved..

The observation of Spackman³⁶¹ maybe understood if one acknowledges that repulsion is driven by electron clouds overlap. In the case of H atom, since it has no kernel electrons, its electron cloud is highly deformable. In the case of H₂ molecule, it was even shown by Williams³⁶² that the repulsion centers in hydrogen was to be shifted from nuclei to bond center in order to fit well the repulsion energy between two hydrogen molecules. This foreshortening effect was supported by X-Ray and neutron diffraction.

Those phenomena are of importance since, as discussed by Williams and Craycroft³⁶², the periphery of most organic compounds is composed of hydrogen. This may be a cause for breaking the additive combining rule on diameter. The repulsion operated by H atom may depend:

- On the attached atom (C, O, ...) to H. The effect may be important if highly electronegative atoms are bonded to hydrogen. In particular, H acquires an electron deficit along the series H(C), H(N) and H(O). This deficit increases the deformation

of the cloud and reduces the repulsion in the same sequence.

- On the chemical environment via electrical field generated by polar molecules that can distort electron clouds (polarizability effect) especially when they are close.

The hydrogen molecule itself can be regarded as very specific. It is a small molecule that can fill the cavities in the liquid solvent more easily than the bigger chain molecules. In other words, it is expected that hydrogen can easily go very close to solvent molecules. As a consequence, in the solubility conditions, hydrogen is probably very sensitive to repulsive interactions, more than bigger chain molecules. All those elements put in the light the complexity of repulsive interactions in hydrogen containing systems.

From this discussion, it is suggested that hydrogen+solvent systems modeling may be driven by repulsion and that the use of non-additive diameters may help improving the predictive power for the solubility of hydrogen in various solvents and especially oxygenated solvents due to their high polarity.

IV.4 Extension of GC-PPC-SAFT to non-additive square wells chains

In a previous chapter, we proposed an equation of state of non-additive square-well chains developed on the basis of the work of Malakhov and Volkov³²³.

The segment i – segment j interaction potential u_{ij} is written as:

$$u_{ij}(r) = \begin{cases} \infty & r < \sigma_{ij} \\ -\varepsilon_{ij} & \sigma_{ij} \leq r < \lambda\sigma_{ij} \\ 0 & r \geq \lambda\sigma_{ij} \end{cases} \quad (4.24)$$

where r is the distance between two segments, σ_{ij} is the cross diameter and $\sigma_{ij} = \frac{\sigma_i + \sigma_j}{2}(1 - l_{ij})$, ε_{ij} denotes the depth of the potential well, and λ is the reduced well-width. Throughout this work a well-width of 1.5 is assumed.

Using a perturbation, the final equation of state consists of two terms, the additive square-well chain EoS (reference) and a correction accounting for the non-additivity (NA):

$$\frac{A}{NkT} = \frac{A^{SWC}}{NkT} + \frac{A^{NA}}{NkT} \quad (4.25)$$

where A is the Helmholtz energy, N is the total number of molecules, k is the Boltzmann's constant, and T is the absolute temperature. A^{SWC} denotes the additive square well chain Helmholtz energy. The contribution A^{NA} is evaluated here at first order and it contains the non additivity correction which is given by :

$$\frac{A^{NA}}{NkT} = -2\pi\rho \sum_i \sum_j x_i x_j m_i m_j \sigma_{ij}^3 l_{ij} [g_{ij}(\sigma_{ij}^+) - \lambda^3 g_{ij}(\lambda\sigma_{ij}^-) + e^{-\beta\epsilon_{ij}} \lambda^3 g_{ij}(\lambda\sigma_{ij}^-)] \quad (4.26)$$

In this expression, we can see the presence of non-additive parameter l_{ij} in the new contribution of GC-PPC-SAFT Equation of state. A non-zero l_{ij} allow adjusting the repulsive interaction between molecules. This expression requires having average inter - segment distribution functions at contact $g_{ij}(r = \sigma_{ij}^+)$ and at limit $g_{ij}(r = \lambda\sigma_{ij}^-)$ for a chain of spheres interacting via an additive square well potential. Notice that these functions depend on the chain lengths m_i and m_j have been mainly studied in the context of chains of hard spheres. The average inter-segment distribution function is obtained from:

$$g_{ij} = \frac{4g_{T_i T_j} + 2(m_i - 2)g_{I_i T_j} + 2(m_j - 2)g_{I_j T_i} + (m_j - 2)(m_i - 2)g_{I_i I_j}}{m_i m_j} \quad (4.27)$$

Where

$$g_{T_i T_j} = g_{DD} \quad (4.28)$$

$$g_{I_i T_j} = g_{I_j T_i} = \frac{3}{2}g_{DD} - \frac{1}{2}g_{SS} \quad (4.29)$$

$$g_{I_i I_j} = 2g_{DD} - g_{SS} \quad (4.30)$$

The dimer-dimer (g_{DD}) and segment-segment (g_{SS}) inter-segment distribution function can be fitted to following empirical expression according to B.J. Zhang et al.³³³:

$$g_{SS}(\sigma^+, \eta, \beta \epsilon) = \sum_{p=0}^4 \sum_{q=1}^4 a_{pq} (\beta \epsilon)^p \frac{\eta^{q-1}}{(1-\eta)^q} \quad (4.31)$$

$$g_{DD}(\sigma^+, \eta, \beta \epsilon) = \sum_{p=0}^4 \sum_{q=1}^4 b_{pq} (\beta \epsilon)^p \frac{\eta^{q-1}}{(1-\eta)^q} \quad (4.32)$$

Let us recall that the potential in PC-SAFT is not exactly square well but has a shoulder to take into account the 'soft' character of the repulsive interactions (see Figure IV-5)

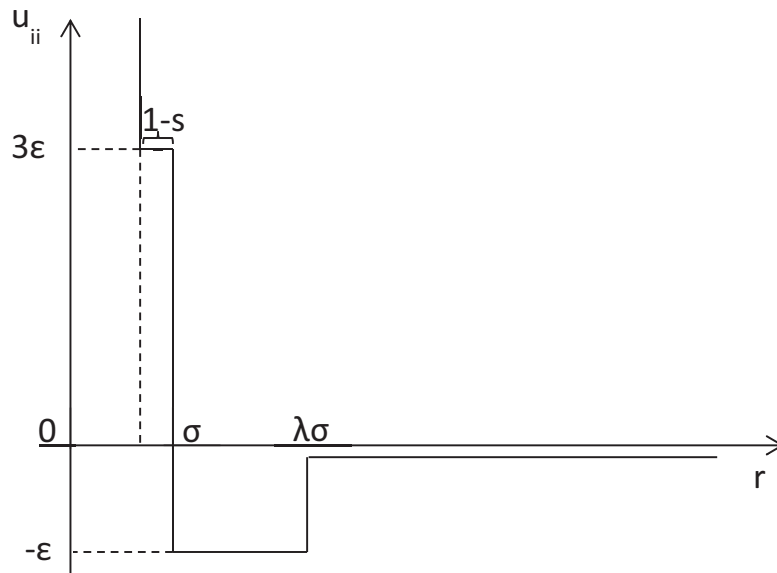


Figure IV-5: Potential modified in PC-SAFT Equation of state

$$u(r) = \begin{cases} \infty & r < (1-s)\sigma_{ij} \\ 3\varepsilon & (1-s)\sigma_{ij} < r < \sigma_{ij} \end{cases}$$

in addition to the 'square well' part

$$u(r) = \begin{cases} -\varepsilon & \sigma_{ij} < r < \lambda\sigma_{ij} \\ 0 & r > \lambda\sigma_{ij} \end{cases}$$

Strictly speaking, Equation (4.26) applies only for the square well chains ($s = 0$). For PC-SAFT, we could adopt the same methodology as in the previous chapter to the soft potential of PC-SAFT to obtain the analogous expression (4.26) applicable to the full PC-SAFT equation of state. The latter would be more complex involving two more distribution functions $g_{ij}(r = \sigma_{ij}^-)$ and $g_{ij}(r = (1-s)\sigma_{ij}^+)$. But to the best of our knowledge, the analytical expressions of these functions are unknown, and their values have not been estimated by simulation. However, these functions correspond to distances where the potential is 'repulsive'; we can therefore expect that their values are smaller than those of $g_{ij}(r = \sigma_{ij}^+)$ and $g_{ij}(r = \lambda\sigma_{ij}^-)$ involved in the Equation (4.26). For this reason, and in order to maintain our model as simple as possible, we have chosen to neglect the non-additive terms with $g_{ij}(r = \sigma_{ij}^-)$ and $g_{ij}(r = (1-s)\sigma_{ij}^-)$. This is equivalent to using the expression (4.26) to correct the PC-SAFT non-additive interactions (i.e. $A^{SWC} = A^{PC-SAFT}$). But in this case, the potential is a full potential with shoulder. In the same spirit as the perturbative treatment of the 'soft' potential which leads in particular to introduce a hard sphere diameter $d(T)$ that depends on temperature as in Equation (4.4), we make the following approximations for the distribution functions: $g_{ij}(r = \sigma_{ij}^+) \approx g_{ij}^{SW}(r = d_{ij}^+)$ and $g_{ij}(r = \sigma_{ij}^-) \approx g_{ij}^{SW}(r = d_{ij}^+)$.

SW refers to the square well potential and d_{ij} is the additive cross hard sphere diameter ($d_{ij} = \frac{d_{ii} + d_{jj}}{2}$). This means that, from the perspective of calculating distribution functions, the full potential is equivalent to a square well potential but parameterized by d_{ij} .

The final equations used and its derivatives are available in Appendix IV-C.

IV.5 Results of the prediction and correlation of hydrogen solubility in oxygenated solvents

The use of a predictive scheme for computing thermodynamic properties of systems containing gases and oxygenated compounds requires the simultaneous use of k_{ij} and l_{ij} parameters. The determination of the required parameters is done in two steps. First, the pseudo-ionization parameters of the oxygenated groups are determined, and second, the l_{ij} parameters are regressed.

IV.5.1 Determination the pseudo-ionization energy of oxygenated groups

The values of pseudo-ionization energy of hydroxyl group and ester group have already been determined by NguyenHuynh et al^{15,363}. For the correlation of k_{ij} of systems containing the other oxygenated groups such as ether, aldehyde or ketone, it is necessary to determine the pseudo-ionization energy of these groups. Considering the lack of data, we will consider that all oxygenated groups other than esters and alcohols have the same value of pseudo ionization energy.

To obtain these pseudo-ionization energy we need to model small gas + oxygenated compounds as in previous studies. In those earlier studies the small gas was CO_2 . Here only a few Henry's constant are available for CO_2 in oxygenated compounds systems as they are expected to need no l_{ij} . In order to verify this, a regression of parameter l_{ij} by GC-PPC-SAFT with a predictive k_{ij} was performed on the Henry constant of this gas with alcohols (for which a predictive k_{ij} can be computed, using the J_{OH} from previous work as shown in the parameter table of Appendix IV-A). In Figure IV-6, we observe that the numerical values l_{ij} of ethane/alcohols systems are approximately zero except in the case of methanol/ethane. This validates the assumption that the impact of non-additivity effect is negligible in the case of hydrocarbon gas in oxygenated solvents.

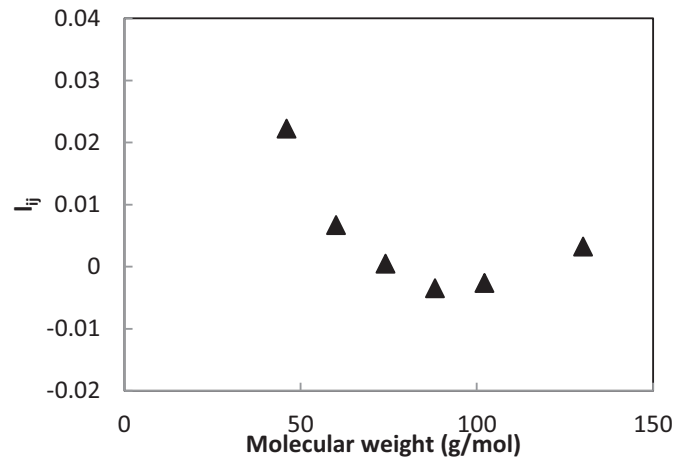


Figure IV-6 : Regressed and correlated values of non-additive parameter l_{ij} for binary mixtures of ethane/alcohols (▲)

In order to determine the pseudo-ionization energy of oxygenated groups, we followed a two-step procedure. First, k_{ij} values were adjusted by regressing the Henry constants of ethane in oxygenated component with the objective function :

$$F_{obj} = \frac{1}{N} \sum_{\text{propriété } X} \left(\frac{H^{cal} - H^{exp}}{H^{exp}} \right)^2 \quad (4.33)$$

For this work, we have collected all available Henry's constants in database. It contains these binary systems: C_2H_6 /propanal⁴⁹, C_2H_6 /diethyl ether⁵⁰, C_2H_6 /1,2-ethanediol⁵¹⁻⁵⁴, C_2H_6 /acetone^{50,55-57}, C_2H_6 /methyl acetate^{50,56}, C_2H_6 /ethyl acetate^{58,59}, C_2H_6 /pentyl acetate⁵⁹. All available data is described in of Table IV-5 and Table IV-6 of Appendix IV-B.

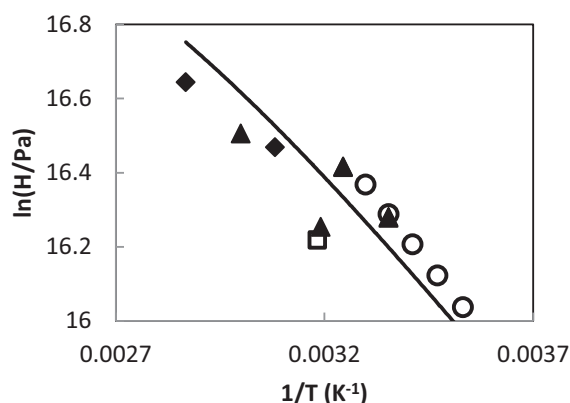


Figure IV-7 : Diagram of $\ln H$ as a function of $1/T$ for the binary mixture ethane/1-propanol. Experimental data are taken from Gjaldbaek et al.³⁶⁶ (\blacktriangle), Yaacobi et al.³⁷³ (o), Suzuki et al.³⁷⁴ (Δ), Kodama et al.³⁷⁵ (\square), Jimenez-Gallegis et al.³⁷⁶ (\blacklozenge), GC-PPC-SAFT (—)

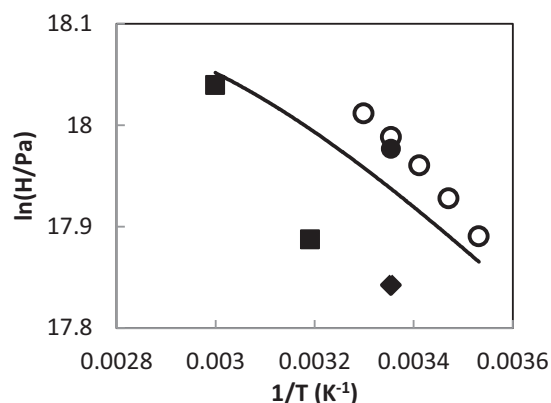


Figure IV-8: Diagram of $\ln H$ as a function of $1/T$ for the binary mixture methane/1-propanol. Experimental data are taken from Makranczy et al.²¹³ (\blacklozenge), Bo. S et al.¹⁵⁴ (\bullet), Yaacobi et al.³⁷³ (o), Suzuki et al.³⁷⁴ (\blacksquare), GC-PPC-SAFT (—)

In a second step, the values of J for the oxygenated groups are determined by fitting the regressed values of k_{ij} parameter for binary mixtures of ethane/oxygenated compound according to Equation (4.10) and (4.18).

Table IV-1: Pseudo-ionization Energies and Experimental Values of oxygenated solvents

Component	Pseudo-ionization energy (eV)	Experimental ionization energy ³⁷⁷ (eV)
Acetone	14.98	9.703 ± 0.006
Diethyl ether	10.56	9.51 ± 0.03
Propanal	9.74	9.96 ± 0.01

The value J of the oxygenated groups was acceptable because it appears that the values of pseudo-ionization energy of oxygen-bearing solvent calculated by the group contribution are close to the experimental ionization energy (see Table IV-1). The values of pseudo-ionization energy J of different oxygenated groups are given in Table IV-2.

Table IV-2: Values of pseudo-ionization energy of different oxygenated groups

Group	Pseudo-ionization energy (eV)
alkanol	28.008
ester	14
Other oxygenated groups	6.5

IV.5.2 Predictive method of non-additive parameter l_{ij}

In the proposed approach, k_{ij} is computed using the equation (4.10), while it is suggested to determine l_{ij} using a group contribution approach as proposed by Le et al¹⁶ which is the arithmetic average weighted by the number of segment – segment interactions between their molecules :

$$l_{ij} = \frac{1}{n_i^{group} n_j^{group}} \sum_i \sum_j n_i^{group k} n_j^{group l} l_{ij}^{kl} \quad (4.34)$$

Where $n_i^{group k}$, $n_j^{group l}$ is the number of group k in molecule i and group l in molecule j ; l_{ij}^{kl} is the non-additive parameter of group k in component i and group l of component j .

From earlier studies¹⁶, it appears that the impact of the non-additivity of the square wells on hydrogen/n-alkane systems is negligible (this means that $l_{ij} \text{ H}_2/\text{CH}_2$ and $l_{ij} \text{ H}_2/\text{CH}_3$ are zero), thus in the equation (4.34), we only need to determine the value of l_{ij} between H_2 and an oxygenated group. Using the available data of Henry's constant of hydrogen in different solvents (which are published in Table II-1 in Chapter II) in predictive GC-PPC-SAFT model, l_{ij} for H_2 /oxygenated groups is regressed and shown in Table IV-2.

Figure IV-9 compares the results for l_{ij} from Equation (4.34) with molecular (H_2 +solvent) values that have been regressed separately. It means that the points in Figure IV-9 are the molecule – molecule values of l_{ij} regressed on experimental data of mixtures containing hydrogen and the different alcohols. The black line in this figure represents the molecule –

molecule values of l_{ij} calculated by Equation (4.34) in which the l_{ij} group-group are regressed on the experimental data in the database. We can see that the longer the chains the lower the value of l_{ij} parameter. The Equation (4.34) fits this behavior.

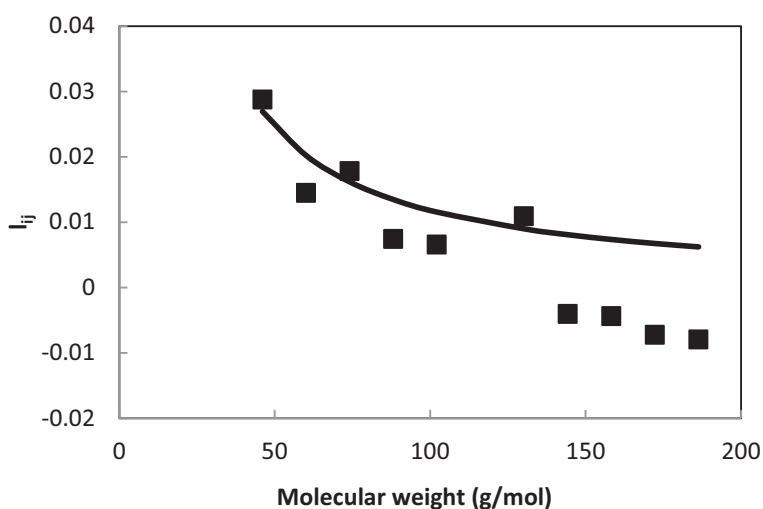


Figure IV-9 : Regressed and correlated values of non-additive parameter l_{ij} for binary mixture: H_2 /alcohol (■), l_{ij} correlated curve for H_2 /alcohol (—)

The value of l_{ij} for H_2 -O- was found to be very small (-0.007). Figure IV-10 shows that the impact of this value is not significant on the prediction of Henry's constant of hydrogen in diethyl ether. It means that the influence of non-additive effect is not considerable. Therefore, in this work we consider that l_{ij} H_2 -O- is equal zero. We can observe in Table IV-3, that the more polar and associative the solvent the higher the values of the non-additive parameter l_{ij} . For example, the polarity of OH and CHO group are high, therefore, the l_{ij} values between these groups and hydrogen are higher than that with the other oxygenated groups. This is in accordance with the discussion in section 3 of this chapter where it was stated that the polar molecules create an electric field that can distort the electron cloud of hydrogen molecule.

Table IV-3: Correlated values of l_{ij} H₂/oxygenated group by using equation (34)

	H ₂ /OH	H ₂ /CHO	H ₂ /COO	H ₂ /HCOO	H ₂ /-O-	H ₂ /CH ₂	H ₂ /CH ₃
l_{ij}	0.081	0.099	0.053	0.046	0	0	0

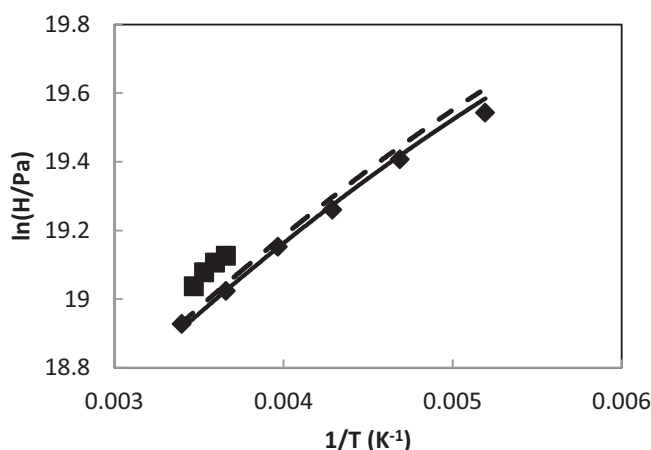


Figure IV-10: Diagram of $\ln H$ as a function of $1/T$ for the binary mixture hydrogen/diethyl ether. Experimental data are taken from Krichevskii et al.²⁰⁷ (\blacklozenge); Michels et al.²⁰⁹ (\blacksquare); predictive calculation by GC-PPC-SAFT with predictive k_{ij} and l_{ij} (—); GC-PPC-SAFT (only k_{ij}) (- -)

With this predictive method for non-additive parameter l_{ij} , we can obtain satisfactory results in calculation of Henry's constant at high temperatures. As observed in the four systems of hydrogen with 1-propanol, ethanol, methyl acetate and propanal in the figures below (Figure IV-11-14), we see that at low and average temperature, GC-PPC-SAFT allow predicting the Henry's constant with acceptable deviations. At high temperature, a good agreement between the calculation of GC-PPC-SAFT and the results obtained by molecular simulation is found.

We also compared the predictions using GC-PPC-SAFT with those by PSRK⁶⁴, an equation of state that is often used in engineering. We observe that PSRK predictions may sometimes be accurate, but sometimes over- or underestimate the data significantly. For example, we note that either PSRK cannot reproduce well the shape of Henry's constant (cf. Figure IV-13) or completely overestimates the Henry's constants (cf. Figure IV-14).

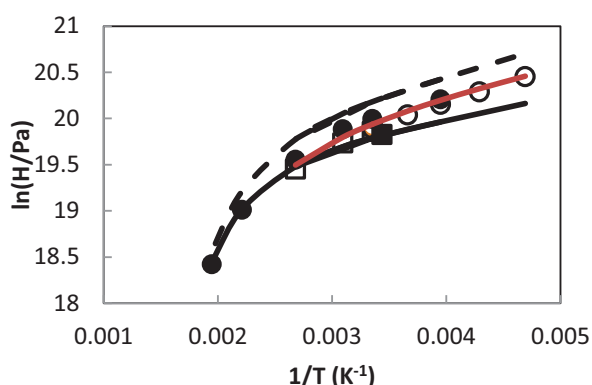


Figure IV-11: Diagram of $\ln H$ as a function of $1/T$ for the binary mixture hydrogen/1-propanol. Experimental data are taken from Makrancy et al.²¹³ (\circ), Katayama et al.¹⁴¹ (\odot), Wainwright et al.¹⁴² (\blacksquare), Brunner et al.²¹⁸ (\square); pseudo-data by molecular simulation (\bullet); predictive calculation by GC-PPC-SAFT with predictive k_{ij} and l_{ij} (—); GC-PPC-SAFT (only k_{ij}) (- - -); calculation by PSRK (—)

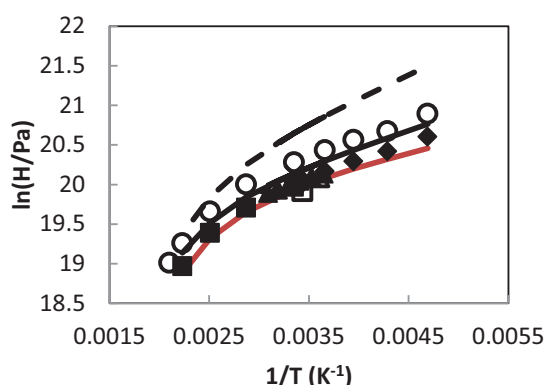


Figure IV-12: Diagram of $\ln H$ as a function of $1/T$ for the binary mixture hydrogen/ethanol. Experimental data are taken from Wainwright et al.¹⁴² (\blacksquare), Brunner et al.¹⁴⁴ (\square), Makrancy et al.²¹³ (\blacksquare), Just et al.²¹⁴ (\diamond), Katayama et al.¹⁴¹ (\blacklozenge), Purwanto et al.¹³² ($+$), Timofeev et al.²¹⁷ (Δ), Maxted et al.¹⁴⁵ (\blacktriangle), Luhning et al.¹³⁰ (\bullet), pseudo-data by molecular simulation (\circ), predictive calculation by GC-PPC-SAFT with predictive k_{ij} and l_{ij} (—); GC-PPC-SAFT (only k_{ij}) (- - -); calculation by PSRK (—)

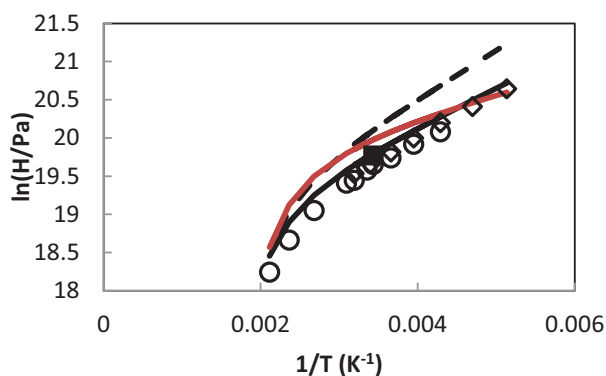


Figure IV-13: Diagram of $\ln H$ as a function of $1/T$ for the binary mixture hydrogen/methyl acetate. Experimental data are taken from Horiuti et al.²²⁷ (\diamond), Wainwright et al.¹⁴² (\blacksquare); pseudo-data by molecular simulation (\circ); predictive calculation by GC-PPC-SAFT (k_{ij} and l_{ij}) (—); GC-PPC-SAFT (only k_{ij}) (- - -); calculation by PSRK (—)

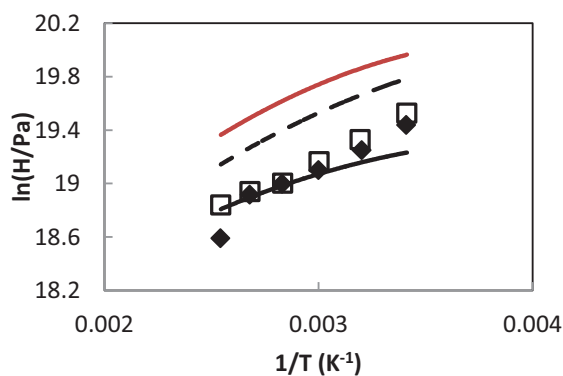


Figure IV-14: Diagram of $\ln H$ as a function of $1/T$ for the binary mixture hydrogen/propanal. Experimental data are taken from Vasileva et al.²²³ (\square , \blacklozenge); pseudo-data by molecular simulation (\circ); predictive calculation by GC-PPC-SAFT (k_{ij} and l_{ij}) (—); GC-PPC-SAFT (only k_{ij}) (- - -); calculation by PSRK (—)

Figure IV-15 shows the relative deviation between the experimental Henry constant of hydrogen in oxygenated solvents and those calculated by using GC-PPC-SAFT. We observed that with a predictive method (i.e. group contribution) for both parameters k_{ij} and l_{ij} , we improve the overall predictive results in comparison with only predictive k_{ij} . For some solvents, the deviation is increased but for these only one or two data points exist and the deviations remain reasonable (~20%) in view of estimated experimental uncertainty.

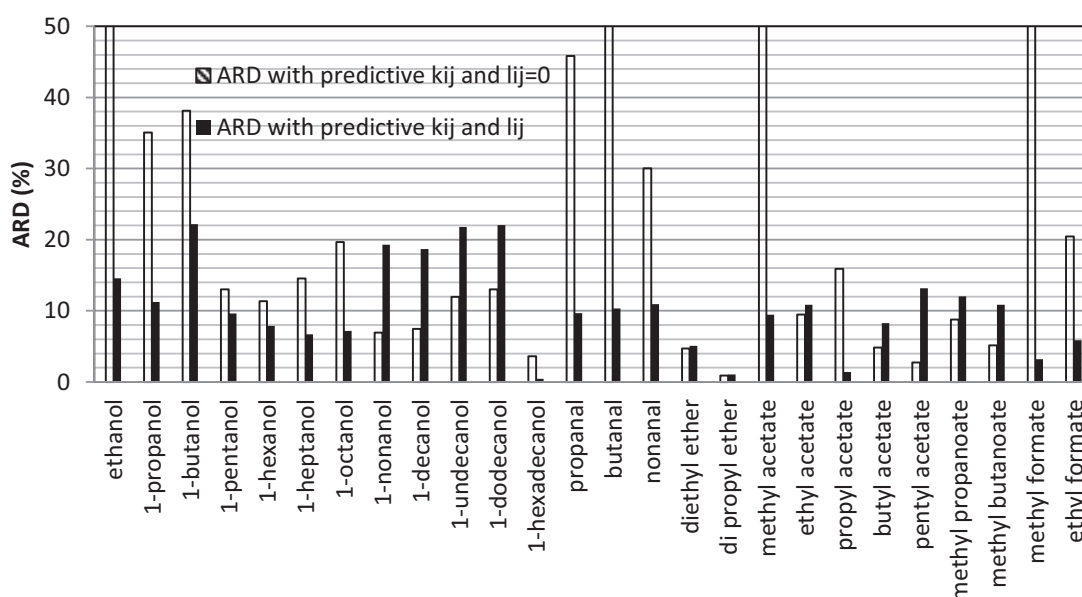


Figure IV-15: Relative deviation of Henry's constant of hydrogen in oxygenated solvents: using GC-PPC-SAFT with predictive k_{ij} ($l_{ij}=0$) and with both predictive k_{ij} , l_{ij}

As an example, Figure IV-16 and Figure IV-17 show the experimental data and the calculated values by GC-PPC-SAFT (with both parameters l_{ij} and k_{ij}) of Henry's constant for all oxygenated families investigated such as 1-alcohols, aldehydes, esters, ethers at 298.15K as a function of molecular weight. In comparison between these values, we observe that with the non-additive parameter, the GC-PPC-SAFT equation of state allows calculating the Henry constant of hydrogen in oxygen-bearing solvent with reasonable deviations.

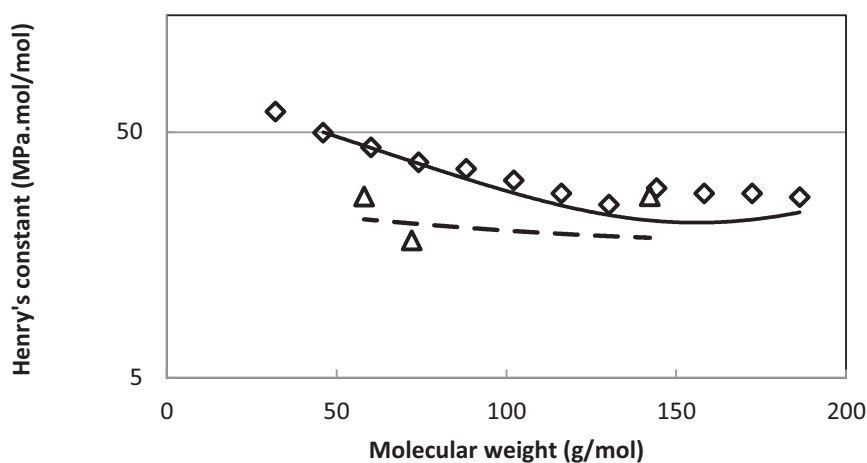


Figure IV-16: Experimental values and calculated values by GC-PPC-SAFT (with both k_{ij} and l_{ij}) of Henry's constant of hydrogen in oxygenated compounds and in n-alkanes depending to their molar weight at 298.15K. Experimental data : H₂/1-alcohol (◇), H₂/aldehyde (Δ); GC-PPC-SAFT: H₂/1-alcohol (—), H₂/aldehyde (---)

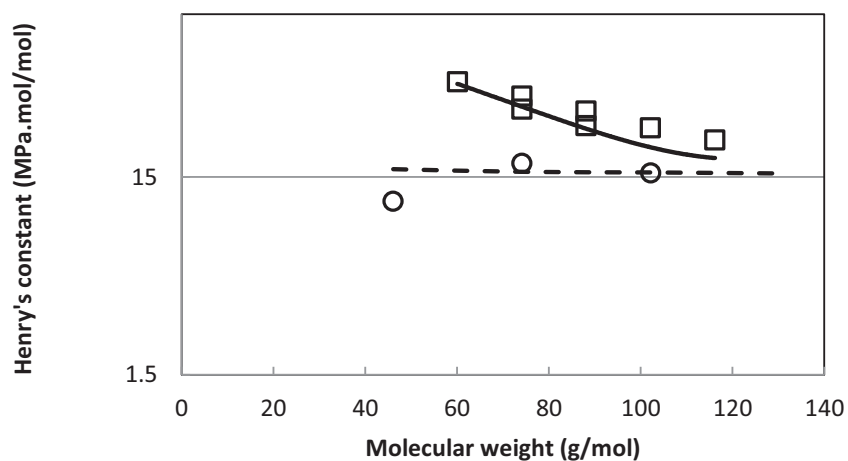


Figure IV-17: Experimental values and calculated values by GC-PPC-SAFT (with both k_{ij} and l_{ij}) of Henry's constant of hydrogen in oxygenated compounds and in n-alkanes depending to their molar weight at 298.15K. Experimental data : H₂/n-alkane (+), H₂/ester (□); H₂/ether (○); GC-PPC-SAFT H₂/ester (—), H₂/ether (---)

IV.6 Conclusions

The main target of this chapter is to develop a physically-meaningful predictive approach as an extension to the GC-PPC-SAFT Equation of State, for the systems of hydrogen with oxygenated molecules.

At first, we used the GC-PPC-SAFT with a predictive way for computing the hydrogen solubility in oxygenated solvents. However, very high deviations are observed with respect to experimental Henry's constant. The adjustment of k_{ij} parameter on these Henry constants leads to negative values that are not physically acceptable.

Observing the relationship between free volume and hydrogen solubility led us to develop a new parameter that is based on repulsive interactions. Based on theoretical development of the Chapter III, our equation of state was extended to systems with non-additive diameters.. A predictive scheme of the non-additive parameter using a group contribution is suggested and the values of this parameter depend on the polarity and association of the oxygen-bearing group. This new equation was tested with success to predict the solubility of hydrogen in oxygen-bearing components. The deviations between the experimental Henry's constants and those calculated by non-additive GC-PPC-SAFT are within the experimental uncertainty (~10%).

Appendix IV-A Parameters for the use of GC-PCC-SAFT

We have used the hydrogen parameters from the work of Tran .T. K.S et al³¹. For binary mixture containing small molecules such as methanol, acetone, ..., the pure component parameters are used. All these parameters are available in Table IV-4 . The parameters of the alkyl groups and oxygenated groups like OH, CHO, C = O, O-, ... were developed by Nguyen Huynh et al.¹⁵. In addition, we used the group parameters for diols as developed by Rozmus at al.³². In their study, an expression was proposed to calculate the cross self-association volume of OH group:

$$\kappa^{A\alpha B\beta} = \kappa_0^{A\alpha B\beta} + \kappa_1^{A\alpha B\beta} \left(1 - \frac{2}{n}\right) \quad (\text{IV. A. 1})$$

Where $\kappa_0^{A\alpha B\beta} = 0.00885$, $\kappa_1^{A\alpha B\beta} = 0.006374$, the original value of $\kappa^{A\alpha B\beta}$ of alkanol group and n is the distance (number of carbon) between two associative groups.

Table IV-4: Group contribution parameters for alkanes and oxygenated compounds for the use of GC-PPC-SAFT

	Group	ε/k (K)	σ (Å)	μ	x_p^u	Q	x_p^o	$\varepsilon^{A\alpha B\beta}/k$ (K)	$\kappa^{A\alpha B\beta}$	J (eV)	R**	Reference
alkanes	CH3	189.9628	3.4872	0	0	0	0	0	0	22.755	0.7866	Mourah et al. ³⁷⁸
	CH2	261.0866	3.9308	0	0	0	0	0	0	6.254	0.3821	Mourah et al. ³⁷⁸
alkanol	OH	307.5094	2.8138	1.7	0.5	0	0	2143.3	0.0088	28.008	0.8318	NguyenHuynh et al. ³⁴⁸
diol	OH diol	307.5094	2.8138	1.7	0.5	0	0	2143.3	(*)	28.008	-	Rozmus et al. ¹⁷¹
aldehyde	CHO	397.6683	3.8538	3.1614	0.6	0	0	2143.3	0.0088	-	0.7180	NguyenHuynh ¹⁵
ketone	C=O	480.7307	3.7495	2.7	0.57	0	0	2143.3	0.0088	-	R ₂ =0.5154 R ₃ =0.4539	NguyenHuynh ¹⁵
ether	-O-	280.9593	3.5764	1.2	1.2	0	0	2143.3	0.0088	-	0.5465	NguyenHuynh ¹⁵
ester	COO	362.8198	3.3447	2.0177	1.15	0	0	2143.3	0.0088	-	R ₂ =0.8273 R ₃ =0.8116	NguyenHuynh ¹⁵
formate	HCOO	289.5501	3.3765	1.9	1.2041	0	0	2143.2976	0.008847	-	1.1360849	NguyenHuynh ¹⁵
H ₂ [#]		26.627	2.906	0	0	0	0	0	0	15	1.112	NguyenHuynh et al. ¹⁷
Methanol [#]		166.8	2.6321	1.7	0.35	0	0	2069.09	0.2373	15.55	2.8271	NguyenHuynh et al. ¹⁷
Ethanol [#]		191.6306	2.9178	1.7	0.2	0	0	2125.522	0.094	12.76415	3.072205	NguyenHuynh et al. ¹⁷
Acetone [#]		258.8688	3.5747	2.72	0.57	0	0	2143.3	0.0088	-	2.0886	NguyenHuynh et al. ¹⁷
Methane [#]		147.4177	3.6582	0	0	0	0	0	0	12.61	1.033354	NguyenHuynh ¹⁵
Ethane [#]		189	3.5098	0	0	0	0	0	0	11.52	1.6364	NguyenHuynh ¹⁵
CO [#]		95.25	3.3979	2	0.45	2	0.45	0	0	18	1.17	NguyenHuynh ¹⁵

H ₂ S [#]		225.05	3.4161	0	0	0	0	449.71	0.0947	10.45	1.3018	NguyenHuynh ¹⁵
NH ₃ [#]		204.6311	3.2386	1.469	1.3976	0	0	646.3276	0.00597	0	1.1158	Grandjean et al. ³⁴⁹

*: value of $\kappa^{A\alpha B\beta}$ depends on the number of carbon in a diol and is calculated by the equation (IV.A.1)

** : for some groups the R parameter depends on its position within the molecule (indicated here as R₂ and R₃). For details see the original articles^{171,363}.

#: some small molecules are considered as consisting of a single group

Appendix IV-B Experimental data in the literature

Table IV-5 : Experimental Henry's constant of ethane in oxygenated solvent

Solvent used	Temperature (K)	Henry's constant (MPa)	
propanal	293.2	7.78	
	313.2	9.66	
	333.2	12.15	
	353.2	13.62	
	373.2	16.3	
	393.2	18.29	
acetone	298.15	12.05	
	298.15	10.28	
	313.15	12.46	
	308.15	11.85	
	303.15	11.15	
	298.15	10.51	
	293.15	9.91	
	288.15	9.35	
	283.15	8.76	
Diethyl ether	278.15	8.23	
	273.15	7.68	
	298.15	3.37	
	1,2-ethanediol	283.2	196.4
		293.2	230.1
303.2		270.3	
298.15		172.3	

	323.15	218.2
	348.15	261.7
	373.15	281
	398.15	296.1
	298.16	189.83
	298.16	188.25
	298.16	189.04
	308.14	207.19
	308.14	207.62
	298.15	62.82
Methyl acetate	298.15	13.33
	313.15	11.4
	308.15	10.77
	303.15	10.2
	298.15	9.67
	293.15	9.11
	288.15	8.6
	283.15	8.07
	278.15	7.58
	273.15	7.12
Ethyl acetate	298.15	5.12
	295.15	8.21
	303.15	8.4
	313.15	8.72
Pentyl acetate	295.15	4.71

	303.15	5.06
	323.15	6.16

Table IV-6: Experimental Henry's constant of methane in oxygenated solvent

Solvent used	Temperature (K)	Henry's constant (MPa)
Dimethyl ether	282.9	21.83
	313.3	21.85
	343.3	24.43
	283.2	21.7
Diethyl ether	284.3	19.18
	313.3	22.48
	342.5	23.97
	293.15	21.87
	273.15	19.6
	252.55	16.95
	231.85	13.84
	211.55	10.92
	196.45	8.57
	192.75	8.07
	273.15	21.26
	283.15	22.51
n-propyl ether	293.15	83.94
	298.15	77.56
1,2-ethanediol	298.15	644.2

	323.15	672.7
	348.15	680.2
	373.15	670.6
	398.15	630.3
	283.2	687.3
	293.2	698.7
	303.2	725.1
	323.15	720.4
	373.15	700.9
	398.15	621.8
	303.15	694.7
	323.15	660
	373.15	526.8
	398.15	471.5
	423.15	419.2
	298.15	587.7
	303.15	968.6
	323.15	818.4
	373.15	567.3
	398.15	481.4
	423.15	415.8
	298.15	656.3
	323.15	665.1

	348.15	682.3
	373.15	675.5
	398.15	636.9
1,4-butanediol	303.15	599
	323.15	561.2
	373.15	497.7
	398.15	433.5
	423.15	376
	303.15	691.3
	323.15	639.7
	373.15	534.2
	398.15	491.8
	423.15	460.4
acetone	183.15	14.3
	213.15	18.43
	233.15	21.85
	253.15	22.91
	273.15	26.15
	293.15	26.88
	291.15	52.49
	291.15	52.4
	298.15	54.44
	298.15	54.83
	310.15	55.24
	310.15	55.44
	298.15	82.12

	293.15	73.98
	298.15	66.42
	283.15	62.09
	278.15	57.69
	313.15	56.62
	293.15	54.03
	273.15	51.2
	251.35	46.38
	232.15	41.15
	212.55	34.78
	196.55	28.91
Acetic acid	298.15	169.3
	323.15	176.8
	348.15	193.5
Ethyl acetate	303.52	38.61
	333.14	40.62
	363.18	41.7
Methyl acetate	313.15	53.42
	293.15	51.07
	273.15	48.59
	252.75	45.13
	231.55	40.75
	212.55	35.62
	196.55	30.67
Ethyl formate	303.48	48.57
	333.15	50.47
	363.18	50.95

Appendix IV-C: Derivatives of the free energy of non-additive term

The PPC-SAFT equation is expressed from the reduced residual free energy $F = \frac{A^{res}(T,V,N)}{RT}$ with temperature variables, volume and number of moles of each component³⁷⁹. The thermodynamic properties are then calculated according to the formula proposed by Michelsen³⁸⁰:

- Relation between the pressure and the free energy :

$$P = -RT \left. \frac{\partial F}{\partial V} \right]_{T,N} + \frac{NRT}{V} \quad (IV.C.1)$$

$$\frac{\partial P}{\partial V} = -RT \left. \frac{\partial^2 F}{\partial V^2} \right]_{T,N} - \frac{NRT}{V^2} \quad (IV.C.2)$$

- Relation between the fugacity coefficient and the free energy :

$$\ln(\varphi_i) = \left(\frac{\partial F}{\partial N_i} \right)_{T,V,N_j} - \ln \left(\frac{PV}{NRT} \right) \quad (IV.C.3)$$

$$\frac{\partial \ln(\varphi_i)}{\partial N_j} = \left. \frac{\partial^2 F}{\partial N_i \partial N_j} \right]_{T,V,N_{k \neq i,j}} + \frac{1}{N} \quad (IV.C.4)$$

- Relation between residual entropy and the free energy :

$$\frac{S^{res}(T,V,N)}{R} = -T \left. \frac{\partial F}{\partial T} \right]_{V,N} - F \quad (IV.C.5)$$

- Relation between residual enthalpy and the free energy :

$$H^{res}(T, P, N) = A^{res}(T, V, N) + TS^{res}(T, V, N) + PV - NRT \quad (IV. C. 6)$$

In the new version of PC-SAFT equation of state, we adjust a term into the sum which is presented in Equation (1):

$$A^{res} = (mA^{hs} + A^{chain}) + A^{disp} + A^{assoc} + A^{multi-polaire} + A^{NAHS} \quad (IV. C. 7)$$

Where the last term A^{NAHS} originates from the equation (7) that is written here, but with the variables n_i (number of mole of component i), V (total volume) and T (temperature):

$$\begin{aligned} \frac{A^{pert}}{NkT} = & -2\pi\rho \\ & \times \sum_i \sum_j x_i x_j m_i m_j \sigma_{ij}^{ref 3} l_{ij} \left[g_{ij}^{ref}(\sigma_{ij}^{ref+}) - \lambda^3 g_{ij}^{ref}(\lambda\sigma_{ij}^{ref-}) \right. \\ & \left. + e^{-\beta\varepsilon_{ij}} \lambda^3 g_{ij}^{ref}(\lambda\sigma_{ij}^{ref-}) \right] \quad (IV. C. 8) \end{aligned}$$

Where $\rho = \frac{N}{V} = \frac{\sum n_l \times N_{Av}}{V}$

N is total number of molecules in the investigated system

V is total volume

We have $x_i = \frac{n_i}{\sum n_l}$ and $x_j = \frac{n_j}{\sum n_l}$ with n_l is the number of moles of component l in the mixture.

We rewrite:

$$\frac{A^{pert}}{NkT} = F^* = -2\pi \frac{\sum n_l \times N_{Av}}{V} \times \sum_i \sum_j \frac{m_i n_i m_j n_j}{(\sum n_l)^2} \times d_{ij}^3 l_{ij} g_{ij} \quad (IV. C. 9)$$

Where $g_{ij} = g_{ij}^{ref} (\sigma_{ij}^{ref+}) - \lambda^3 g_{ij}^{ref} (\lambda \sigma_{ij}^{ref-}) + e^{-\beta \epsilon_{ij}} \lambda^3 g_{ij}^{ref} (\lambda \sigma_{ij}^{ref-})$ (IV.C.10)

Where $d_{ij} = \sigma_{ij}^{ref}$ (note that in the PC-SAFT, d_{ij} is the temperature – dependent diameter.

Equation (IV.C.8) becomes:

$$\frac{A^{pert}}{NkT} = -2\pi \frac{N_{Av}}{V} \times \sum_i \sum_j \frac{m_i n_i m_j n_j}{\sum n_l} \times d_{ij}^3 l_{ij} g_{ij} \quad (IV.C.11)$$

In order to calculate the thermodynamic properties, we need to determine $F = \frac{A}{RT}$. We have here

$F^* = \frac{A}{NkT}$ with $N = \sum n_l \times N_{Av}$. Indeed,

$$\frac{A}{RT} = \frac{A}{N_{Av} kT} = \frac{A}{\sum n_l \times N_{Av} kT} \times \sum n_l = \frac{A}{NkT} \times \sum n_l \quad (IV.C.12)$$

Therefore:

$$\frac{A}{RT} = 2\pi \frac{N_{Av}}{V} \times \sum_i \sum_j \frac{m_i n_i m_j n_j}{\sum n_l} \times d_{ij}^3 l_{ij} g_{ij} \times \sum n_l \quad (IV.C.13)$$

$$F = \frac{A}{RT} = 2\pi \frac{N_{Av}}{V} \times \sum_i \sum_j m_i n_i m_j n_j \times d_{ij}^3 l_{ij} g_{ij} \quad (IV.C.14)$$

To obtain the derivatives of F, firstly we need to derive the inter-segment distribution function g_{ij} .

- First derivative of $g(r)$ as a function of (V)

$$\frac{\partial g_{ij}}{\partial V} = \frac{\partial g_{ij}}{\partial \eta} \times \frac{\partial \eta}{\partial V} \quad (IV.C.15)$$

Where

$$\frac{\partial g_{ij}}{\partial \eta} = \sum_{p=0}^4 \sum_{q=1}^4 a_{pq} (\beta \varepsilon_{ij})^p \frac{\eta^{q-2}}{(1-\eta)^{q+1}} (\eta + q - 1) \quad (IV.C.16)$$

$$\frac{\partial \eta}{\partial V} = -\frac{\pi}{6} \times N_{Av} \times \frac{N}{V^2} \sum_{i=1}^n x_i m_i d_{ii}^3 \quad (IV.C.17)$$

➤ Second derivative of g(r) as a function of V

$$\begin{aligned} \frac{\partial^2 g_{ij}}{\partial V^2} &= \frac{\partial \left(\frac{\partial g_{ij}}{\partial V} \right)}{\partial V} = \frac{\partial \left(\frac{\partial g_{ij}}{\partial \eta} \times \frac{\partial \eta}{\partial V} \right)}{\partial V} = \frac{\partial^2 g_{ij}}{\partial \eta \partial V} \times \frac{\partial \eta}{\partial V} + \frac{\partial g_{ij}}{\partial \eta} \times \frac{\partial^2 \eta}{\partial V^2} \\ &= \frac{\partial \left(\frac{\partial g_{ij}}{\partial \eta} \right)}{\partial \eta} \times \frac{\partial \eta}{\partial V} \times \frac{\partial \eta}{\partial V} + \frac{\partial g_{ij}}{\partial \eta} \times \frac{\partial^2 \eta}{\partial V^2} \\ &= \frac{\partial^2 g_{ij}}{\partial \eta^2} \times \left(\frac{\partial \eta}{\partial V} \right)^2 + \frac{\partial g_{ij}}{\partial \eta} \times \frac{\partial^2 \eta}{\partial V^2} \quad (IV.C.18) \end{aligned}$$

Where

$$\frac{\partial^2 g_{ij}}{\partial \eta^2} = \sum_{p=0}^4 \sum_{q=1}^4 a_{pq} \left(\frac{\varepsilon}{kT} \right)^p \frac{\eta^{q-2}}{(1-\eta)^{q+1}} \left[\frac{1}{\eta} [(\eta + q - 1)(q - 2) + \eta] + \frac{1}{1-\eta} (\eta + q - 1)(q + 1) \right] \quad (IV.C.19)$$

➤ First derivative of g(r) as a function of T

$$\frac{\partial g_{ij}}{\partial T} = \frac{\partial g_{ij}}{\partial \eta} \times \frac{\partial \eta}{\partial T} + \left(\frac{\partial g_{ij}}{\partial T} \right)_{\eta=const} \quad (IV.C.20)$$

With

$$\left(\frac{\partial g_{ij}}{\partial T}\right)_{\eta=const} = \sum_{p=0}^4 \sum_{q=1}^4 a_{pq} (\beta \varepsilon_{ij})^p \times \left(-\frac{p}{T}\right) \times \frac{\eta^{q-1}}{(1-\eta)^q} \quad (IV.C.21)$$

➤ Second derivative of g(r) as a function of T

$$\begin{aligned} \frac{\partial^2 g_{ij}}{\partial T^2} = & \frac{\partial^2 g_{ij}}{\partial \eta^2} \times \frac{\partial \eta}{\partial T} \times \frac{\partial \eta}{\partial T} + \left(\frac{\partial \left(\frac{\partial g_{ij}}{\partial \eta}\right)}{\partial T}\right)_{\eta=const} \times \frac{\partial \eta}{\partial T} + \left(\frac{\partial^2 g_{ij}}{\partial T^2}\right)_{\eta=const} + \frac{\partial g_{ij}}{\partial \eta} \\ & \times \frac{\partial^2 \eta}{\partial T^2} \quad (IV.C.22) \end{aligned}$$

Where

$$\left(\frac{\partial^2 g_{ij}}{\partial T^2}\right)_{\eta=const} = \sum_{p=0}^4 \sum_{q=1}^4 a_{pq} (\beta \varepsilon_{ij})^p \times \frac{p(p+1)}{T^2} \times \frac{\eta^{q-1}}{(1-\eta)^q} \quad (IV.C.23)$$

$$\left(\frac{\partial \left(\frac{\partial g_{ij}}{\partial \eta}\right)}{\partial T}\right)_{\eta=const} = - \sum_{i=0}^4 \sum_{j=1}^4 \frac{p}{T} a_{pq} (\beta \varepsilon_{ij})^p \frac{\eta^{q-2}}{(1-\eta)^{q+1}} (\eta + q - 1) \quad (IV.C.24)$$

➤ First derivative of g(r) as a function of n_i

$$\frac{\partial g_{ij}}{\partial n_i} = \frac{\partial g_{ij}}{\partial \eta} \times \frac{\partial \eta}{\partial n_i} \quad (IV.C.25)$$

➤ Second derivate of g(r) in function of n_i and n_j :

$$\frac{\partial^2 g_{ij}}{\partial n_i \partial n_j} = \frac{\partial^2 g_{ij}}{\partial \eta^2} \times \frac{\partial \eta}{\partial n_j} \times \frac{\partial \eta}{\partial n_i} + \frac{\partial g_{ij}}{\partial \eta} \times \frac{\partial^2 \eta}{\partial n_i \partial n_j} \quad (IV.C.26)$$

- Second derivative of $g(r)$ as function of V and n_i

$$\frac{\partial^2 g_{ij}}{\partial V \partial n_i} = \frac{\partial \left(\frac{\partial g}{\partial \eta} \right)}{\partial \eta} \times \frac{\partial \eta}{\partial n_i} \times \frac{\partial \eta}{\partial V} + \frac{\partial g}{\partial \eta} \times \frac{\partial^2 \eta}{\partial V \partial n_i} = \frac{\partial^2 g}{\partial \eta^2} \times \frac{\partial \eta}{\partial n_i} \times \frac{\partial \eta}{\partial V} + \frac{\partial g}{\partial \eta} \times \frac{\partial^2 \eta}{\partial V \partial n_i} \quad (IV.C.27)$$

- Second derivative of $g(r)$ as a function of T and n_i

$$\begin{aligned} \frac{\partial^2 g_{ij}}{\partial T \partial n_i} &= \frac{\partial \left(\frac{\partial g_{ij}}{\partial \eta} \right)}{\partial \eta} \times \frac{\partial \eta}{\partial n_i} \times \frac{\partial \eta}{\partial T} + \frac{\partial g_{ij}}{\partial \eta} \times \frac{\partial^2 \eta}{\partial T \partial n_i} + \frac{\partial \left(\frac{\partial g_{ij}}{\partial T} \right)_{\eta=const}}{\partial \eta} \times \frac{\partial \eta}{\partial n_i} \\ &= \frac{\partial^2 g_{ij}}{\partial \eta^2} \times \frac{\partial \eta}{\partial n_i} \times \frac{\partial \eta}{\partial T} + \frac{\partial g_{ij}}{\partial \eta} \times \frac{\partial^2 \eta}{\partial T \partial n_i} + \frac{\partial \left(\frac{\partial g_{ij}}{\partial T} \right)_{\eta=const}}{\partial \eta} \times \frac{\partial \eta}{\partial n_i} \quad (IV.C.28) \end{aligned}$$

- Second derivative of $g(r)$ as a function of T and V

$$\frac{\partial^2 g_{ij}}{\partial T \partial V} = \frac{\partial^2 g_{ij}}{\partial \eta^2} \times \frac{\partial \eta}{\partial V} \times \frac{\partial \eta}{\partial T} + \frac{\partial g_{ij}}{\partial \eta} \times \frac{\partial^2 \eta}{\partial T \partial V} + \frac{\partial \left(\frac{\partial g_{ij}}{\partial T} \right)_{\eta=const}}{\partial \eta} \times \frac{\partial \eta}{\partial V} \quad (IV.C.29)$$

After obtaining the derives of g_{ij} , we continue derivative for the radial distribution function for chains

- First derivative of g_{ij}^{ref} as a function of V

$$\frac{\partial g_{ij}^{ref}}{\partial V} = \frac{4 \frac{\partial g_{D,D}}{\partial V} + (m_i + m_j - 4) \left(3 \frac{\partial g_{D,D}}{\partial V} - \frac{\partial g_{S,S}}{\partial V} \right) + (m_j - 2)(m_i - 2) \left(2 \frac{\partial g_{D,D}}{\partial V} - \frac{\partial g_{S,S}}{\partial V} \right)}{m_i m_j} \quad (IV. C. 30)$$

➤ Second derivative of g_{ij}^{ref} as a function of V

$$\frac{\partial^2 g_{ij}^{ref}}{\partial V^2} = \frac{4 \frac{\partial^2 g_{D,D}}{\partial V^2} + (m_i + m_j - 4) \left(3 \frac{\partial^2 g_{D,D}}{\partial V^2} - \frac{\partial^2 g_{S,S}}{\partial V^2} \right) + (m_j - 2)(m_i - 2) \left(2 \frac{\partial^2 g_{D,D}}{\partial V^2} - \frac{\partial^2 g_{S,S}}{\partial V^2} \right)}{m_i m_j} \quad (IV. C. 31)$$

➤ First derivative of g_{ij}^{ref} as a function of T

$$\frac{\partial g_{ij}^{ref}}{\partial T} = \frac{4 \frac{\partial g_{D,D}}{\partial T} + (m_i + m_j - 4) \left(3 \frac{\partial g_{D,D}}{\partial T} - \frac{\partial g_{S,S}}{\partial T} \right) + (m_j - 2)(m_i - 2) \left(2 \frac{\partial g_{D,D}}{\partial T} - \frac{\partial g_{S,S}}{\partial T} \right)}{m_i m_j} \quad (IV. C. 32)$$

➤ Second derivative of g_{ij}^{ref} as a function of T

$$\frac{\partial^2 g_{ij}^{ref}}{\partial T^2} = \frac{4 \frac{\partial^2 g_{D,D}}{\partial T^2} + (m_i + m_j - 4) \left(3 \frac{\partial^2 g_{D,D}}{\partial T^2} - \frac{\partial^2 g_{S,S}}{\partial T^2} \right) + (m_j - 2)(m_i - 2) \left(2 \frac{\partial^2 g_{D,D}}{\partial T^2} - \frac{\partial^2 g_{S,S}}{\partial T^2} \right)}{m_i m_j} \quad (IV. C. 33)$$

- First derivative of g_{ij}^{ref} as a function of n_i

$$\frac{\partial g_{ij}^{ref}}{\partial n_i} = \frac{4 \frac{\partial g_{D,D}}{\partial n_i} + (m_i + m_j - 4) \left(3 \frac{\partial g_{D,D}}{\partial n_i} - \frac{\partial g_{S,S}}{\partial n_i} \right) + (m_j - 2)(m_i - 2) \left(2 \frac{\partial g_{D,D}}{\partial n_i} - \frac{\partial g_{S,S}}{\partial n_i} \right)}{m_i m_j} \quad (IV.C.34)$$

- Second derivative of g_{ij}^{ref} as a function of n_i and n_j

$$\frac{\partial^2 g_{ij}^{ref}}{\partial n_i \partial n_j} = \frac{4 \frac{\partial^2 g_{D,D}}{\partial n_i \partial n_j} + (m_i + m_j - 4) \left(3 \frac{\partial^2 g_{D,D}}{\partial n_i \partial n_j} - \frac{\partial^2 g_{S,S}}{\partial n_i \partial n_j} \right) + (m_j - 2)(m_i - 2) \left(2 \frac{\partial^2 g_{D,D}}{\partial n_i \partial n_j} - \frac{\partial^2 g_{S,S}}{\partial n_i \partial n_j} \right)}{m_i m_j} \quad (IV.C.35)$$

- Second derivative of g_{ij}^{ref} as a function of V and n_i

$$\frac{\partial^2 g_{ij}^{ref}}{\partial V \partial n_i} = \frac{4 \frac{\partial^2 g_{D,D}}{\partial V \partial n_i} + (m_i + m_j - 4) \left(3 \frac{\partial^2 g_{D,D}}{\partial V \partial n_i} - \frac{\partial^2 g_{S,S}}{\partial V \partial n_i} \right) + (m_j - 2)(m_i - 2) \left(2 \frac{\partial^2 g_{D,D}}{\partial V \partial n_i} - \frac{\partial^2 g_{S,S}}{\partial V \partial n_i} \right)}{m_i m_j} \quad (IV.C.36)$$

- Second derivative of g_{ij}^{ref} as a function of T and n_i

$$\frac{\partial^2 g_{ij}^{ref}}{\partial T \partial n_i} = \frac{4 \frac{\partial^2 g_{D,D}}{\partial T \partial n_i} + (m_i + m_j - 4) \left(3 \frac{\partial^2 g_{D,D}}{\partial T \partial n_i} - \frac{\partial^2 g_{S,S}}{\partial T \partial n_i} \right) + (m_j - 2)(m_i - 2) \left(2 \frac{\partial^2 g_{D,D}}{\partial T \partial n_i} - \frac{\partial^2 g_{S,S}}{\partial T \partial n_i} \right)}{m_i m_j} \quad (IV.C.37)$$

➤ Second derivative of g_{ij}^{ref} as a function of T and V

$$\frac{\partial^2 g_{ij}^{ref}}{\partial T \partial V} = \frac{4 \frac{\partial^2 g_{D,D}}{\partial T \partial V} + (m_i + m_j - 4) \left(3 \frac{\partial^2 g_{D,D}}{\partial T \partial V} - \frac{\partial^2 g_{S,S}}{\partial T \partial V} \right) + (m_j - 2)(m_i - 2) \left(2 \frac{\partial^2 g_{D,D}}{\partial T \partial V} - \frac{\partial^2 g_{S,S}}{\partial T \partial V} \right)}{m_i m_j} \quad (IV.C.38)$$

Now we have the derivatives of F :

➤ First derivative of F as a function of V

$$\frac{\partial F}{\partial V} = 2\pi \times N_{Av} \times \left(\frac{N}{V} \times \text{doubleSommedv} - \frac{N}{V^2} \times \text{doubleSomme0} \right) \quad (IV.C.39)$$

With

$$\text{doubleSomme0} = - \sum_i \sum_j m_i n_i m_j n_j \times d_{ij}^3 l_{ij} g_{ij} \quad (IV.C.40)$$

$$\text{doubleSommedv} = - \sum_i \sum_j m_i n_i m_j n_j \times d_{ij}^3 l_{ij} \frac{\partial g_{ij}}{\partial V} \quad (IV.C.41)$$

- Second derivative of F as a function of V

$$\begin{aligned} \frac{\partial^2 F}{\partial V^2} = & 2\pi N_{Av} \\ & \times \left(\frac{2}{V^3} \text{doubleSomme0} - \frac{2}{V^2} \text{doubleSommedv} + \frac{1}{V} \right. \\ & \left. \times \sum_i \sum_j m_i n_i m_j n_j \times d_{ij}^3 l_{ij} \frac{\partial^2 g_{ij}}{\partial V^2} \right) \quad (IV.C.42) \end{aligned}$$

- First derivative of F as a function of T

$$\frac{\partial F}{\partial T} = -2\pi \frac{N_{Av}}{V} \times \sum_i \sum_j m_i n_i m_j n_j l_{ij} \left(d_{ij}^3 \frac{\partial g_{ij}}{\partial T} + 3d_{ij}^2 \frac{\partial d_{ij}}{\partial T} g_{ij} \right) \quad (IV.C.43)$$

Where

$$\frac{\partial g_{ij}}{\partial T} = - \sum_i \sum_j m_i n_i m_j n_j \times 3d_{ij}^2 \frac{\partial d_{ij}}{\partial T} l_{ij} g_{ij} - \sum_i \sum_j m_i n_i m_j n_j \times d_{ij}^3 l_{ij} \frac{\partial g_{ij}}{\partial T} \quad (IV.C.44)$$

- Second derivative of F as a function of T

$$\begin{aligned} \frac{\partial^2 F}{\partial T^2} &= \frac{\partial \left(\frac{\partial F}{\partial T} \right)}{\partial T} \\ &= -2\pi \frac{N_{Av}}{V} \sum_i \sum_j m_i n_i m_j n_j l_{ij} \left(3d_{ij}^2 \frac{\partial d_{ij}}{\partial T} \frac{\partial g_{ij}}{\partial T} + d_{ij}^3 \frac{\partial^2 g_{ij}}{\partial T^2} + 6d_{ij} \left(\frac{\partial d_{ij}}{\partial T} \right)^2 g_{ij} \right. \\ &\quad \left. + 3d_{ij}^2 \frac{\partial^2 d_{ij}}{\partial T^2} g_{ij} + 3d_{ij}^2 \frac{\partial d_{ij}}{\partial T} \frac{\partial g_{ij}}{\partial T} \right) \quad (IV.C.45) \end{aligned}$$

➤ First derivative of F as a function of n_i :

$$\frac{\partial F}{\partial n_l} = -2\pi \times \frac{N_{Av}}{V} \times \frac{\partial}{\partial n_l} \left(\sum_i \sum_j m_i n_i m_j n_j l_{ij} d_{ij}^3 g_{ij} \right) \quad (IV.C.46)$$

Where

$$\begin{aligned} &\frac{\partial}{\partial n_l} \left(\sum_i \sum_j m_i n_i m_j n_j l_{ij} d_{ij}^3 g_{ij} \right) \\ &= \sum_i \sum_j m_i n_i m_j n_j l_{ij} d_{ij}^3 \frac{\partial g_{ij}}{\partial n_l} + \sum_i m_i n_i m_l l_{il} d_{il}^3 g_{il} + \sum_j m_l m_j n_j l_{lj} d_{lj}^3 g_{lj} \\ &= \sum_i \sum_j m_i n_i m_j n_j l_{ij} d_{ij}^3 \frac{\partial g_{ij}}{\partial n_l} + 2 \times \sum_i m_i n_i m_l l_{il} d_{il}^3 g_{il} \quad (IV.C.47) \end{aligned}$$

➤ Second derivative of F as a function of n_i and n_j

$$\frac{\partial^2 F}{\partial n_l \partial n_k} = -2\pi \times \frac{N_{Av}}{V} \times \frac{\partial^2}{\partial n_l \partial n_k} \left(\sum_i \sum_j m_i n_i m_j n_j l_{ij} d_{ij}^3 g_{ij} \right) \quad (IV.C.48)$$

Where

$$\begin{aligned} & \frac{\partial^2}{\partial n_l \partial n_k} \left(\sum_i \sum_j m_i n_i m_j n_j l_{ij} d_{ij}^3 g_{ij} \right) \\ &= 2 \times l_{ij} d_{ij}^3 \times \left(\sum_{i,j=k} m_i n_i m_k \frac{\partial g_{il}}{\partial n_k} + \sum_{j,i=k} m_i n_i m_l \frac{\partial g_{kl}}{\partial n_l} \right) + 2 \times l_{ij} d_{ij}^3 m_k m_l g_{kl} \\ &+ \sum_i \sum_j m_i n_i m_j n_j l_{ij} d_{ij}^3 \frac{\partial^2 g_{ij}}{\partial n_l \partial n_k} \quad (IV. C. 49) \end{aligned}$$

➤ Second derivative of F as a function of V and n_i

$$\begin{aligned} \frac{\partial^2 F}{\partial V \partial n_l} &= 2\pi N_{Av} \left(\frac{\partial}{\partial n_l} \left(-\frac{N}{V} \times \sum_i \sum_j m_i n_i m_j n_j \times d_{ij}^3 l_{ij} \frac{\partial g_{ij}}{\partial V} \right) \right. \\ &\quad \left. + \frac{\partial}{\partial n_l} \left(-\frac{N}{V^2} \times \sum_i \sum_j m_i n_i m_j n_j \times d_{ij}^3 l_{ij} g_{ij} \right) \right) \quad (IV. C. 50) \end{aligned}$$

Where

$$\begin{aligned} & \frac{\partial}{\partial n_l} \left(-\frac{N}{V} \sum_i \sum_j m_i n_i m_j n_j \times d_{ij}^3 l_{ij} \frac{\partial g_{ij}}{\partial V} \right) \\ &= -\frac{N}{V} \sum_i \sum_j m_i n_i m_j n_j l_{ij} d_{ij}^3 \frac{\partial^2 g_{ij}}{\partial V \partial n_l} - \frac{2N}{V} \sum_i m_i n_i m_l l_{ij} d_{ij}^3 \frac{\partial g_{ij}}{\partial V} \\ &\quad - \frac{1}{N} \sum_i \sum_j m_i n_i m_j n_j \times d_{ij}^3 l_{ij} \frac{\partial g_{ij}}{\partial V} \quad (IV. C. 51) \end{aligned}$$

And

$$\begin{aligned} \frac{\partial}{\partial n_l} \left(-\frac{N}{V^2} \sum_i \sum_j m_i n_i m_j n_j \times d_{ij}^3 l_{ij} g_{ij} \right) \\ = -\frac{N}{V^2} \sum_i \sum_j m_i n_i m_j n_j l_{ij} d_{ij}^3 \frac{\partial g_{ij}}{\partial n_l} - \frac{2N}{V^2} \sum_i m_i n_i m_l l_{ij} d_{ij}^3 g_{il} \\ - \frac{1}{V^2} \sum_i \sum_j m_i n_i m_j n_j \times d_{ij}^3 l_{ij} g_{ij} \quad (IV. C. 52) \end{aligned}$$

➤ Second derivative of F as a function of T and n_i

$$\begin{aligned} \frac{\partial^2 F}{\partial T \partial n_l} = -2\pi \frac{N_{Av}}{V} \left[\frac{\partial}{\partial n_l} \left(\sum_i \sum_j m_i n_i m_j n_j l_{ij} d_{ij}^3 \frac{\partial g_{ij}}{\partial T} \right) \right. \\ \left. + 3 \frac{\partial}{\partial n_l} \left(\sum_i \sum_j m_i n_i m_j n_j l_{ij} d_{ij}^2 \frac{\partial d_{ij}}{\partial T} g_{ij} \right) \right] \quad (IV. C. 53) \end{aligned}$$

With

$$\begin{aligned} \frac{\partial}{\partial n_l} \left(\sum_i \sum_j m_i n_i m_j n_j l_{ij} d_{ij}^3 \frac{\partial g_{ij}}{\partial T} \right) \\ = \sum_i \sum_j m_i n_i m_j n_j l_{ij} d_{ij}^3 \frac{\partial^2 g_{ij}}{\partial T \partial n_l} + 2 \times \sum_i m_i n_i m_l l_{ij} d_{ij}^3 \frac{\partial g_{ij}}{\partial T} \quad (IV. C. 54) \end{aligned}$$

And

$$\begin{aligned} \frac{\partial}{\partial n_l} \left(\sum_i \sum_j m_i n_i m_j n_j l_{ij} d_{ij}^2 \frac{\partial d_{ij}}{\partial T} g_{ij} \right) \\ = \sum_i \sum_j m_i n_i m_j n_j l_{ij} d_{ij}^2 \frac{\partial d_{ij}}{\partial T} \frac{\partial g_{ij}}{\partial n_l} + 2 \\ \times \sum_i m_i n_i m_l l_{ij} d_{ij}^2 \frac{\partial d_{ij}}{\partial T} g_{ij} \quad (IV. C. 55) \end{aligned}$$

➤ Second derivative of F as a function of T and V

$$\frac{\partial^2 F}{\partial T \partial V} = -2\pi \times \left[\frac{\partial}{\partial V} \left(\frac{N_{Av}}{V} \sum_i \sum_j m_i n_i m_j n_j l_{ij} d_{ij}^3 \frac{\partial g_{ij}}{\partial T} \right) + 3 \frac{\partial}{\partial V} \left(\frac{N_{Av}}{V} \sum_i \sum_j m_i n_i m_j n_j l_{ij} d_{ij}^2 \frac{\partial d_{ij}}{\partial T} g_{ij} \right) \right] \quad (IV. C. 56)$$

Where

$$\begin{aligned} & \frac{\partial}{\partial V} \left(\frac{N_{Av}}{V} \sum_i \sum_j m_i n_i m_j n_j l_{ij} d_{ij}^3 \frac{\partial g_{ij}}{\partial T} \right) \\ &= -\frac{N_{Av}}{V^2} \sum_i \sum_j m_i n_i m_j n_j l_{ij} d_{ij}^3 \frac{\partial g_{ij}}{\partial T} \\ &+ \frac{N_{Av}}{V} \sum_i \sum_j m_i n_i m_j n_j l_{ij} d_{ij}^3 \frac{\partial^2 g_{ij}}{\partial T \partial V} \quad (IV. C. 57) \end{aligned}$$

And

$$\begin{aligned} & \frac{\partial}{\partial V} \left(\frac{N_{Av}}{V} \sum_i \sum_j m_i n_i m_j n_j l_{ij} d_{ij}^2 \frac{\partial d_{ij}}{\partial T} g_{ij} \right) \\ &= -\frac{N_{Av}}{V^2} \sum_i \sum_j m_i n_i m_j n_j l_{ij} d_{ij}^2 \frac{\partial d_{ij}}{\partial T} g_{ij} \\ &+ \frac{N_{Av}}{V} \sum_i \sum_j m_i n_i m_j n_j l_{ij} d_{ij}^2 \frac{\partial d_{ij}}{\partial T} \frac{\partial g_{ij}}{\partial V} \quad (IV. C. 58) \end{aligned}$$

CHAPTER V

SOLUBILITY OF THE OTHER GASES IN OXYGENATED SOLVENTS

In the previous chapter, the prediction and correlation of Henry's constant of hydrogen in various solvents, using the GC-PPC-SAFT equation of state with the non-additive parameter have been discussed. As mentioned in the introduction, in this thesis, we have worked mainly on the solubility of hydrogen in oxygen-bearing compounds (hydrogen is the reactive gas). But in order to predict completely the vapor-liquid equilibria involved in the hydrotreatment process, we must also take into account the sub-product gases like hydrogen sulfide, carbon monoxide and ammonia. Water is also an important product, but considering its complexity it will not be discussed here. In this chapter, we use the same methodology as before (data analysis, evaluation with GC-PPC-SAFT) to examine other light molecules. The prediction and also the correction of Henry's constant and phase equilibrium using GC-PPC-SAFT Equation of state will be discussed.

V.1 Introduction

Pyrolysis oils are very complex mixtures that contain a wide variety of chemical compounds such as typically oxygenated aromatics. Also, as shown in Table V-1, small quantities of nitrogen and sulfur may be found.

Table V-1: Example of chemical/atomic composition of pyrolysis liquids derived from biomass and fuel oils.³⁸¹

Analysis	Pyrolysis oil	Fuel oil
C, dry (wt%)	56	85
H, dry (wt%)	6	11.1
O, dry (wt%)	38	1
Water (wt%)	20-30	0.025

Solids (wt%)	0.01-0.1	0
Ash (wt%)	0.01-0.2	0.01
Nitrogen (wt%)	0-0.4	0
Sulfur (wt%)	0-0.05	0.2

Hydrotreatment process, indeed, leads also to sub-product like hydrogen sulfide, ammonia and carbon monoxide. Knowledge of the solubility of those gases in apolar as well as polar solvents is useful for the design of bio-oil hydroprocessing units and is the subject of the present work. Some pure component properties of these gases are summarized in Table V-2.

Table V-2: Pure component properties of carbon monoxide from DIPPR¹⁶⁵

Property	CO	H ₂ S	NH ₃
Molecular Weight (kg/kmol)	28.0101	34.08088	17.03052
Critical Temperature (K)	132.92	373.53	405.65
Critical Pressure (Pa)	3.499E+06	8962910	1.128E+07
Critical Volume (m ³ /kmol)	0.0944	0.0985	0.07247
Dipole moment (Debye)	0.112125	0.968354	1.46902
Acentric Factor	0.0481621	0.0941677	0.252608
Characteristics	colorless odorless very toxic	colorless odor of rotten egg toxic corrosive	colorless pungent gas

Applications	polycarbonate, polyurethane, metal carbonyls and oxy- alcohol manufacture	sodium sulfide and thiophenes manufacture	fertilizer nitric acid manufacture refrigerating fluid
--------------	------------------------------------------------------------------------------------	-------------------------------------------------	-----------------------------------------------------------------

In the same spirit as in Chapter II where the solubility of hydrogen was investigated, we used here Henry's constant as a reference property for phase equilibrium. This property is very useful for analyzing data consistency but is not sufficient to describe the solubility here since in process conditions H_2S , NH_3 and CO are not always infinitely diluted. Complete phase diagrams have thus to be taken into account.

In this chapter, we repeat the steps of data analysis for systems containing gases like carbon monoxide, ammonia and hydrogen sulfide. After that, the GC-PPC-SAFT equation of state is used for either predicting or when needed, correlating the solubility of these gases in oxygenated solvents.

V.2 General strategy for modeling solubility of CO , H_2S and NH_3 in polar solvents

V.2.1 Representation of pure components with PPC-SAFT

The carbon monoxide is considered as a polar molecule with a very low dipolar moment and a relatively high quadrupolar moment. According to the study of NguyenHuynh et al.¹⁵, the pseudo-ionization energy of carbon monoxide is determined from the regression of k_{ij} on the experimental data for the binary mixture CO /propane. The values of these parameters are provided in Table V-3. In fact, according to Gross et al.¹³, because of a small value of dipole moment ($\sim 0.11D$), carbon monoxide may be considered as a non-associating component. Therefore, all calculations below are entirely predictive (k_{ij} is calculated from the pseudo-ionization energy by equation (4.10) in Chapter IV).

Table V-3: Pure component parameters of carbon monoxide, hydrogen sulfide and ammonia using in GC-PPC-SAFT EoS

	ε/k (K)	σ (Å)	μ	$x_p^{\mu m}$	Q	x_p^Q	$\varepsilon^{A\alpha B\beta}/k$ (K)	$\kappa^{A\alpha B\beta}$	J (eV)	R**	Reference
CO	95.25	3.398	2	0.45	2	0.45	0	0	18	1.17	NguyenHuynh ¹⁵
H ₂ S	225.05	3.416	0	0	0	0	449.71	0.0947	10.45	1.3018	NguyenHuynh ¹⁵
NH ₃	204.6311	3.239	1.469	1.3976	0	0	646.3276	0.00597	0	1.1158	Grandjean et al. ³⁴⁹

The hydrogen sulfide is considered to be an associative molecule (type 3B with 2 positive sites) with a small dipolar moment (0.97D). As argued by Tamouza³⁸², such a small value for a dipole has no considerable impact on the phase equilibrium; the dipole was thus neglected by Nguyen Huynh¹⁵. All parameters of hydrogen sulfide used for predictions by GC-PPC-SAFT are provided in Table V-3. The parameters of this gas are determined by regressing the pure component data available in DIPPR³⁰⁷ (i.e. pressure of saturation, the enthalpy of vaporization, the density) and verified on H₂S/propane mixtures¹⁷ (available data originating from DETHERM³⁸³).

The parameters of ammonia have been determined by Grandjean et al.³⁴⁹ and are given in Table V-3. Ammonia is described as a molecule with 4 associative sites: one negative site on the nitrogen atom; 3 other sites are identically positive on each hydrogen atom. In the same way as the other gases we mentioned above, the PPC-SAFT parameters of ammonia are determined by regressing the pure component data issued from DIPPR³⁰⁷ and then verified on the VLE and LLE of NH₃/propane.

V.2.2 Mixtures

To model mixtures, the PPC-SAFT Equation of state uses four types of binary interaction parameters. First of all, we have the binary interaction parameter k_{ij} on the cross dispersive

energy ε_{ij} of the system:

$$\varepsilon_{ij} = (1 - k_{ij})\sqrt{\varepsilon_i\varepsilon_j} \quad (5.1)$$

The predictive scheme to compute this parameter has been proposed by NguyenHuynh et al.³⁴⁶. The predictive k_{ij} is calculated by the pseudo-ionization energy J (adjustable parameter) of each component of the investigated system:

$$1 - k_{ij} = \frac{2\sqrt{J_i J_j}}{(J_i + J_j)} \quad (5.2)$$

The second interaction parameter, that has been investigated in this thesis, is the non-additive parameter l_{ij} . This parameter modulates the repulsive term in the extension of GC-PPC-SAFT to non-additive systems through cross diameters:

$$\sigma_{ij} = \frac{\sigma_i + \sigma_j}{2} (1 - l_{ij}) \quad (5.3)$$

In the previous chapter, it was argued that non-zero l_{ij} may be linked to electron clouds deformation which can be applied to the hydrogen atom whose electron cloud is highly deformable (no kernel electron). This deformation is expected to be lower in the case of O, N and S atoms. Use of non-zero l_{ij} seems only necessary when species of small size, with high hydrogen content (such as H_2 , CH_4) and in highly polar solvent are involved.

For these reasons, it is expected that CO containing mixtures will not require use of l_{ij} . Regarding H_2S and NH_3 , use of non-zero l_{ij} is a priori more questionable. However, these two species associate via hydrogen bond with solvent (oxygenated species). Association effect is generally strong and is expected to be more important than non-additivity effect (non-zero l_{ij}). Probably, those systems can be treated by setting $l_{ij} = 0$.

However the two cross-association parameter on the energy of association (w_{ij}) and the volume of association (u_{ij}) may play an important role. Recall that those parameters are defined by:

$$\varepsilon^{A_i B_j} = \frac{\varepsilon^{A_i} + \varepsilon^{B_j}}{2} (1 - w_{ij}) \quad (5.4)$$

$$\kappa^{A_i B_j} = \sqrt{\kappa^{A_i} \kappa^{B_j}} (1 - u_{ij}) \quad (5.5)$$

The use of these parameters has been investigated in this work. Let us also stress that because associating interactions occur among sites, these sites may be related to molecules or to groups. Whenever possible, in order to comply with the group contribution approach, the sites are associated to groups (in particular OH), meaning that these parameters are molecule – group interaction parameters.

V.3 Solubility of carbon monoxide (CO) in oxygenates

V.3.1 Database and consistency tests

Table V-4 summarizes the data that we have extracted from the literature sources that we have found in DETHERM. We consider here all types of solubility data of carbon monoxide in oxygenated solvents with the widest ranges of temperature and pressure.

Table V-4: Database of binary mixtures of carbon monoxide in organic components

Solvent	Temperature range (K)	Pressure range (MPa)	$N_{\text{total pts}}$ / $N_{\text{accepted pts}}$	Type of data (with reference)
methanol	243.15 – 498.75	0 – 100.7	42	PTx ^{143,208,384–386} , H ^{152,386} , L ^{213,214,387,388} , H* ^{130,153}
ethanol	275.15 – 448.0	0.1 – 6.64	32	PTx ³⁸⁵ , L ^{213,214,387,388} , α ³⁸⁹ , H* ^{153,390}

1-propanol	293.15 – 323.15	0.1 – 4.0	15/13	PTx ³⁸⁵ , L ^{213,388} , α ³⁸⁸ Removed : PTx³⁸⁵
1-butanol	293.15 – 553.15	0 – 30.4	21/19	PTx ^{385,391} , L ^{213,388} Removed : PTx³⁸⁵
1-pentanol	293.15 – 298.15	0.1	3	L ^{213,214}
1-hexanol	298.15	0.1	1	L ²¹³
1-heptanol	298.15	0.1	1	L ²¹³
1-octanol	282.94 – 298.15	0.1	5	L ²¹³ , α ¹⁶¹
1-nonanol	298.15	0.1	1	L ²¹³
1-decanol	298.15 – 553.20	0.1 – 30.0	12	PTx ³⁹² , L ²¹³ , α ³⁸⁸
1-undecanol	298.15	0.1	1	L ²¹³
1-dodecanol	298.15	0.1	1	L ²¹³
1-hexadecanol	498	0.1	1	H ¹¹⁹
Acetone	193.35 – 298.15	0.1	19	L ^{214,227,387} , α ²¹⁴
Nonanal	313.15 - 373	0.9 – 1.0	5	PTx ¹²⁸ , H* ²²⁵
Acetic acid	293.15 – 448.0	0.1 – 6.6	10	PTx ¹³¹ , L ^{214,387} , H* ¹⁵³
Propanoic acid	298.0 – 553.2	0 – 30.4	18	PTx ³⁹³ , H ³⁹³ , H* ¹⁵³
Dimethyl ether	288.15 – 316.15	0.4 – 7.7	3	PTx ¹³⁴
Diethyl ether	194.35 – 293.15	0.1	8	L ^{227,228}
Methyl acetate	194.35 – 313.25	0.1	7	L ²²⁷
Ethyl acetate	293.15 – 333.20	0.1 – 12.01	5/3	PTx ³⁹⁴ , L ²¹⁴ Removed : PTx³⁹⁴
Propyl acetate	298.15	0.1	2	L ³⁹⁵
Pentyl acetate	293.15 – 298.15	0.1	2	L ²¹⁴

Note: Npt: number of data points

PTx : Equilibrium phase binary H₂/oxygen-bearing compounds

H: Henry's law constant (Pa.mol/mol)

L: Ostwald coefficient, α : Bunsen and S: Kuenen coefficient; H*: Henry's constant with different units like Pa.m³/mol or Pa.m³/kg

As mentioned above, in order to investigate the gas solubility, Henry's constant appears to be a relevant descriptor. All the data described in Table V-4 have therefore been converted into Henry's constants. In addition to the vapor-liquid equilibrium data, we also have in our database solubility coefficients such as Ostwald coefficient, Bunsen coefficient and Kuenen coefficient. They have been converted into Henry's constant using the definitions provided in the IUPAC¹⁶² guide.

Internal consistency

In this table, we find that data are mostly available for binary systems of CO and alcohols from methanol to n-hexadecanol. We have more experimental data for short alcohols while for longer alcohols except 1-decanol, the only data source is Ostwald coefficients from Makranczy et al.²¹³. Among other solvents, there is only one ketone (e.g. acetone), one aldehyde (e.g. nonanal), 2 carboxylic acid, 2 ethers and 4 esters. As observed, the ranges of temperature and pressure are not as large as expected. And because in some cases there is only a single data source, it is very difficult to evaluate the consistency of these experimental data. In Figure V-1 and Figure V-2, we observe that there are different data sources that were converted into Henry's constant. They seem consistent with each other even if the data scatter is significant.

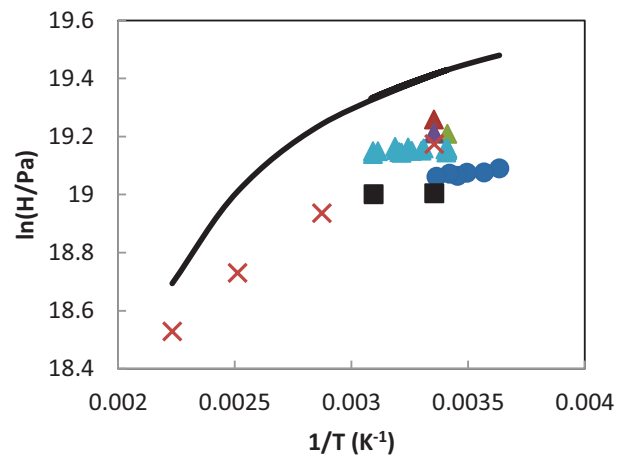
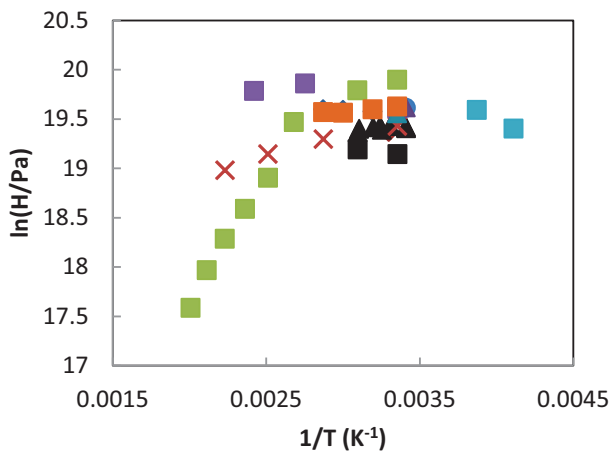


Figure V-1: Henry's constant of carbon monoxide in methanol. Experimental data are taken from Li et al.³⁸⁶ (◆), Liu et al.¹⁵² (◇), Makranczy et al.²¹³ (▲), Just et al.²¹⁴ (▲), Skirrow et al.³⁸⁷ (▲), Gjaldbaek et al.³⁸⁸ (▲, ●), Dake et al.¹⁵³ (x), Brunner et al.¹⁴³ (■), Krichevskii et al.²⁰⁸ (■), Huamin et al.³⁸⁴ (■), Tonner et al.³⁸⁵ (■)

Figure V-2: Henry's constant of carbon monoxide in ethanol. Experimental data are taken from Bunsen et al.³⁸⁹ (●), Makranczy et al.²¹³ (▲), Just et al.²¹⁴ (▲), Skirrow et al.³⁸⁷ (▲), Gjaldbaek et al.³⁸⁸ (▲), Dake et al.¹⁵³ (x), Tonner et al.³⁸⁵ (■); Calculation by GC-PPC-SAFT (—)

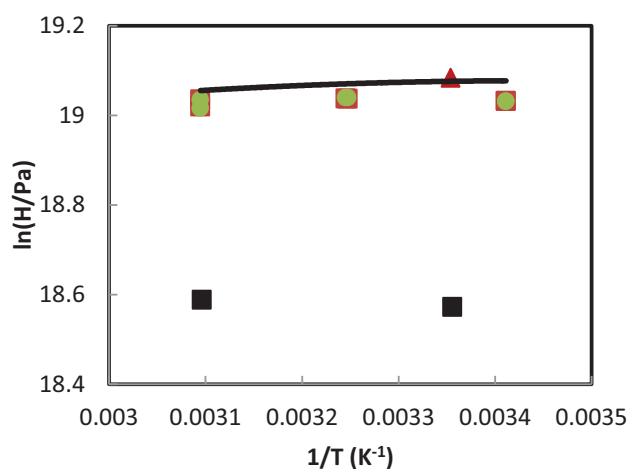


Figure V-3: Henry's constant of carbon monoxide in 1-propanol. Experimental data are taken from Makranczy et al.²¹³ (\blacktriangle), Gjaldbaek et al.³⁸⁸ (\blacksquare , \bullet), Tonner et al.³⁸⁵ (\blacksquare); Calculation by GC-PPC-SAFT (—)

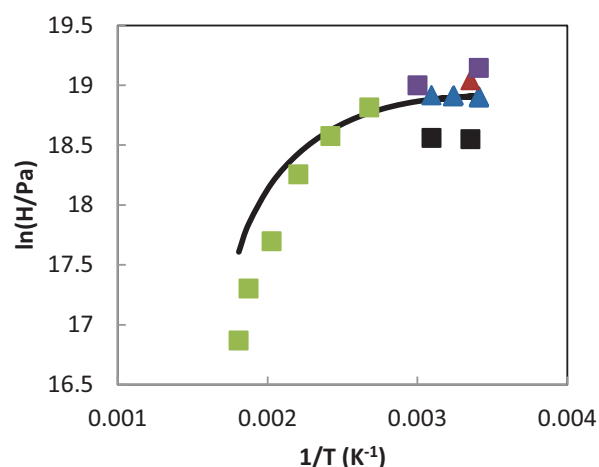


Figure V-4: Henry's constant of carbon monoxide in 1-butanol. Experimental data are taken from Makranczy et al.²¹³ (\blacktriangle), Gjaldbaek et al.³⁸⁸ (\blacksquare , \bullet), Tonner et al.³⁸⁵ (\blacksquare), Vasileva et al.³⁹¹ (\blacksquare , \blacksquare); Calculation by GC-PPC-SAFT (—)

Regarding 1-propanol (cf. Figure V-3), we noticed a clear discrepancy between the Henry constant and the PTx data of Toner et al.³⁸⁵. In Figure V-4, we observe that the values of $\ln H$ of Tonner et al.³⁸⁵ do not fit well with those of Makranczy et al.²¹³, Gjaldbaek et al.³⁸⁸ and Vasileva et al.³⁹¹. We decided in this case to keep the values of these three authors and eliminate those of Toner et al.³⁸⁵.

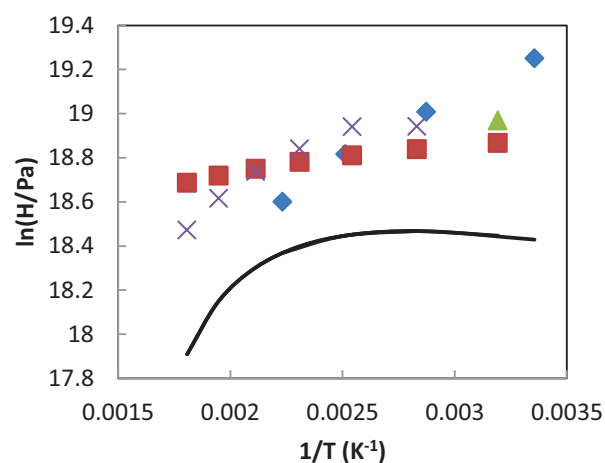
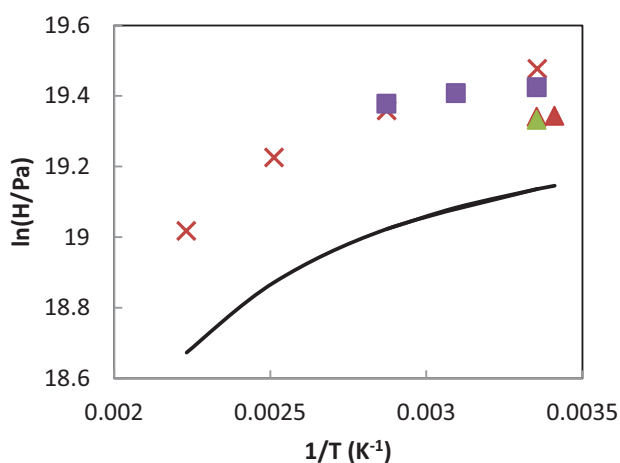


Figure V-5: Henry's constant of carbon monoxide in acetic acid. Experimental data are taken from Just et al.²¹⁴ (▲), Skirrow et al.³⁸⁷ (▲), Dake et al.¹⁵³ (x), Jonasson et al.¹³¹ (■); Calculation by GC-PPC-SAFT (—)

Figure V-6: Henry's constant of carbon monoxide in propanoic acid. Experimental data are taken from Vasileva et al.³⁹³ (◆, ■, ■), Dake et al.¹⁵³ (x); Calculation by GC-PPC-SAFT (—)

In Figure V-5, we see significant differences between the experimental data from two authors (Just et al.²¹⁴, Skirrow et al.³⁸⁷) and the others (Dake et al.¹⁵³, Jonasson et al.¹³¹). However, we find that this difference is acceptable considering the data scatter because we estimate that the experimental uncertainty is about 10%. Therefore, we decide to use all these data for the prediction of the solubility of carbon monoxide. The same observation is made for data in Figure V-6. In general, the Henry constant of carbon monoxide in an oxygenated solvent decreases with temperature. In the case of CO/methanol, we observe that there is a peak of Henry's constants at about 300 K. It means that at temperatures below 300 K, the Henry constant of CO increases with temperature. This phenomenon is also observed in the case of hydrogen in water.

External consistency

From the database of the binary systems containing carbon monoxide, we see that the experimental Henry's constant are most numerous at 298.15 K. Therefore in Figure V-7, we gathered all available Henry's constants of carbon monoxide in oxygenated solvents at 298.15 K

and plotted them as a function of molecular weight of the solvent. We find that they decrease with the molecular weight of the solvent. In addition, the order of magnitude of the solubility of this gas in a chemical family is similar to that observed for the hydrogen solubility but always smaller (it means that hydrogen is less soluble than carbon monoxide).

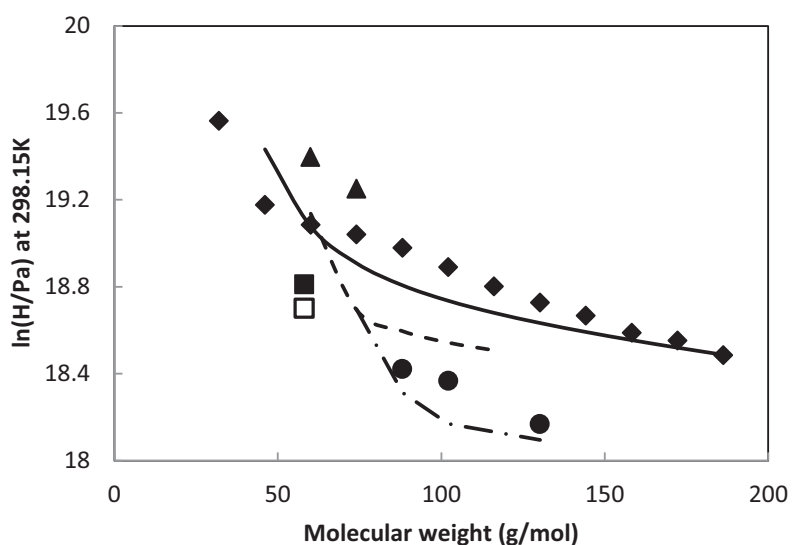


Figure V-7: Henry's constant of carbon monoxide in oxygenated solvent (in order of a chemical family) as a function of molecular weight at 298.15K. CO/alcohol (◆), CO/acetone (■), CO/carboxylic acid (▲), CO/ester (●). Calculation by GC-PPC-SAFT: (—) CO/alcohol, (□) CO/acetone, (•••) CO/carboxylic acid, (— · —) CO/ester.

Figure V-8 teaches us that the Henry constant values of CO in ethyl acetate issued from the paper of Zhu et al³⁹⁴ is higher than those of CO in methyl acetate. Therefore, the values of this author are eliminated from our database.

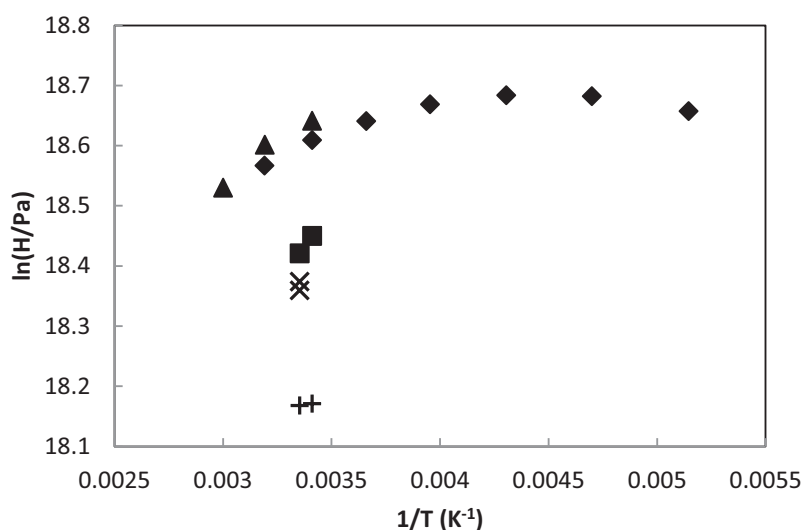


Figure V-8: Henry's constant of carbon monoxide in methyl acetate (Horiuti et al.²²⁷, ◆), ethyl acetate (Just et al.²¹⁴ ■, Zhu et al.³⁹⁴ ▲), propyl acetate (Gjaldbaek et al.³⁹⁵, ×) and pentyl acetate (Just et al.²¹⁴, ++)

V.3.2 Prediction of phase equilibrium and the solubility of carbon monoxide in oxygenated solvent

In Figure V-3 and Figure V-4, we find that the calculation by predictive GC-PPC-SAFT is very good on Henry's constants. The deviations are close or below 10% except in the case of CO/ethanol, we have about 30% of deviation. The bubble pressure predictions show deviations close to 20% which can be considered satisfactory. The non-additive parameter l_{ij} may be useful to improve the calculations. Unfortunately, this parameter only help reduce the deviation of Henry's constants (~5%) and bubble pressure (~16%) for the system CO/ethanol. For the other mixtures, l_{ij} does not improve the results. In the case of CO/1-propanol the prediction of Henry's constant using GC-PPC-SAFT performs the good agreement with experimental data. As evaluated above, the VLE data of this mixture have been removed from our database. In Figure V-5 and Figure V-6, we find that there are deviations between the experimental data and the predictive calculation by GC-PPC-SAFT for CO/acetic acid and CO/propanoic acid.

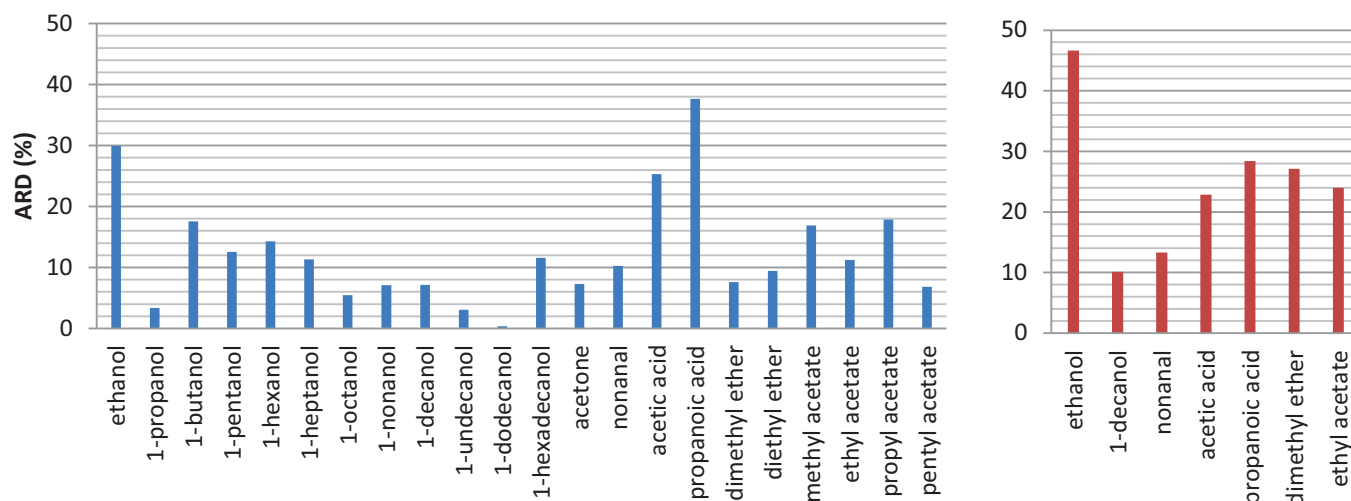


Figure V-9: Average Relative Deviation of Henry's constant (■) and bubble pressure (■) of carbon monoxide in oxygenated solvent

As observed in Figure V-9, the deviations of Henry's constants for some solvents can reach 30% but remains of the order of 10-15% which may still be considered reasonable considering the purely predictive character of the model.

V.4 Solubility of hydrogen sulfide (H₂S) in oxygenates

Hydrogen sulfide is another important gas in the hydrotreatment process of bio-oil. In fact, in bio-oil, there is a small quantity of sulfur (< 0.05%wt³⁸¹). After the hydrodeoxygenation of bio-oil, hydrogen sulfide is generated beside the other sub-products.

V.4.1 Database and consistency analysis

The solubility of this gas in oxygenated solvents is reported in many articles. All the available data that we found in the literature are listed in Table V-5.

Table V-5: Database of binary mixtures of hydrogen sulfide in organic components

Solvent	Temperature range (K)	Pressure range (MPa)	Npt	Type of data (with reference)
methanol	194.65 – 448.15	0 – 11.2	39	PT _x ^{155,156,206,396} , α ³⁹⁷ , S ³⁹⁸ , H ^{156,398,399}
ethanol	265.15 – 295.15	0.1	11	α ³⁸⁹ , H* ⁴⁰⁰
1-butanol	263.15 – 333.15	0.1	3	PT _x ⁴⁰¹
1-octanol	265.15 - 293.15	0.1	5	H* ⁴⁰⁰
1,2-ethanediol	263.15 – 398.15	0.1 – 6.75	15	PT _x ⁴⁰² , α ⁴⁰³ , H ^{151,399} , H* ⁴⁰⁰
Dioctyl ether	265.15 - 293.15	0.1	5	H* ⁴⁰⁰
Acetone	263.15 – 298.15	0.1	2	PT _x ⁴⁰¹
Acetic acetic	263.15 – 333.15	0.1	3	PT _x ⁴⁰¹
Hexanoic acid	265.15 - 293.15	0.1	5	H* ⁴⁰⁰

As in the case of hydrogen and carbon monoxide, the Henry constant is the main property used to consider the gas solubility in oxygenated solvents. Therefore, the conversion of other solubility coefficients into Henry's constant is necessary and presented in Appendix II-A of Chapter II.

Internal consistency

Because of the lack of experimental data for the binary mixture of hydrogen sulfide in oxygenated solvent, we used a maximum number of available data that we found in the literature. However, it is always necessary to check their consistency. In the three figures below, the available data of Henry's constant of H₂S in methanol, ethanol and 1,2-ethanediol respectively are consistent with each other. It is found that Henry's constants of hydrogen sulfide increase with temperature. The solubility decreases when temperature increases. The experimental uncertainty is estimated between 10% and 20% due to the delicate measurement of

hydrogen sulfide.

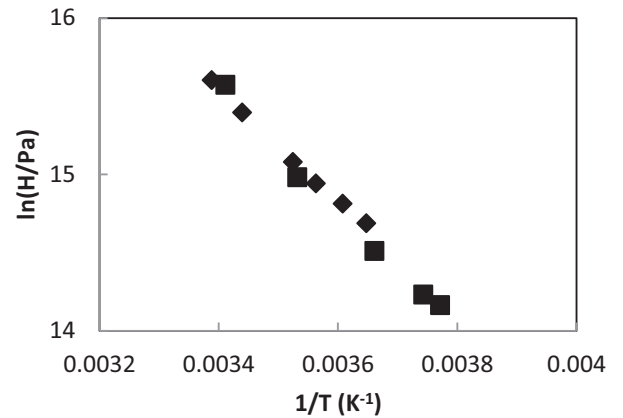
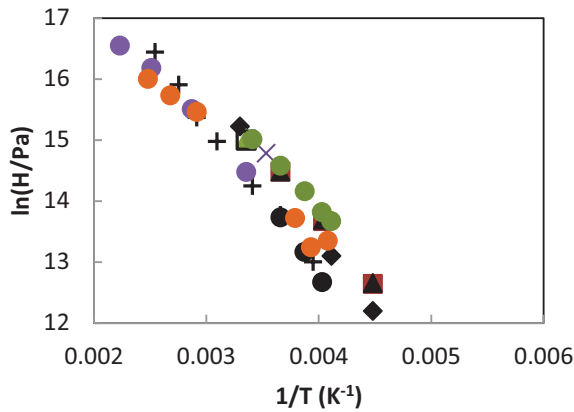


Figure V-10: Henry's constant of hydrogen sulfide in methanol. Experimental data are taken from Fischer et al.¹⁵⁶ (\blacktriangle , \square), Zel'venskii et al.³⁹⁸ (\blacktriangle , \blacksquare), Schalk et al.³⁹⁹ (\times), Yorizane et al.²⁰⁶ (\bullet), Bezdel et al.³⁹⁷ (\blacklozenge), Leu et al.¹⁵⁵ ($+$), Preuss et al.³⁹⁶ (\bullet), Data issued by IFPEN (\bullet , \bullet)

Figure V-11: Henry's constant of hydrogen sulfide in ethanol. Experimental data are taken from Bunsen et al.³⁸⁹ (\blacklozenge), Gerrard et al.⁴⁰⁰ (\blacksquare)

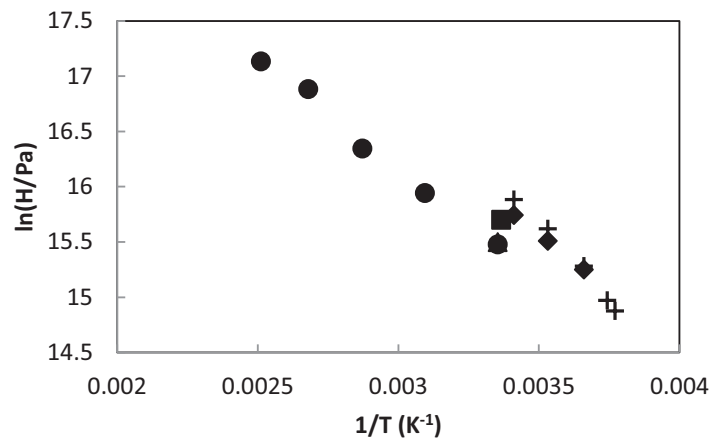


Figure V-12: Henry's constant of hydrogen sulfide in 1,2-ethanediol. Experimental data are taken from Byeseda et al.⁴⁰³ (\blacksquare), Lenoir et al.¹⁵¹ (\blacktriangle), Schalk et al.³⁹⁹ (\blacklozenge), Jou et al.⁴⁰² (\bullet), Gerrard et al.⁴⁰⁰ ($+$)

External consistency

Even though we do not have a large database of Henry's constant of H_2S , we still observe in Figure V-13 that this property tends to decrease with molecular weight. In the same way as observed with hydrogen, here we see that the Henry constant for diols is highest and that of 1-octyl ether is lowest. The order of Henry's constants mentioned in Chapter II is respected in this case. In comparison with the Henry constants of carbon monoxide in oxygenated solvents (cf. Figure V-7), we note that Henry's constants of hydrogen sulfide are smaller than those of carbon monoxide. It means that H_2S is more soluble than CO. This may be explained by the existence of hydrogen bond between H_2S and the oxygen-bearing components.

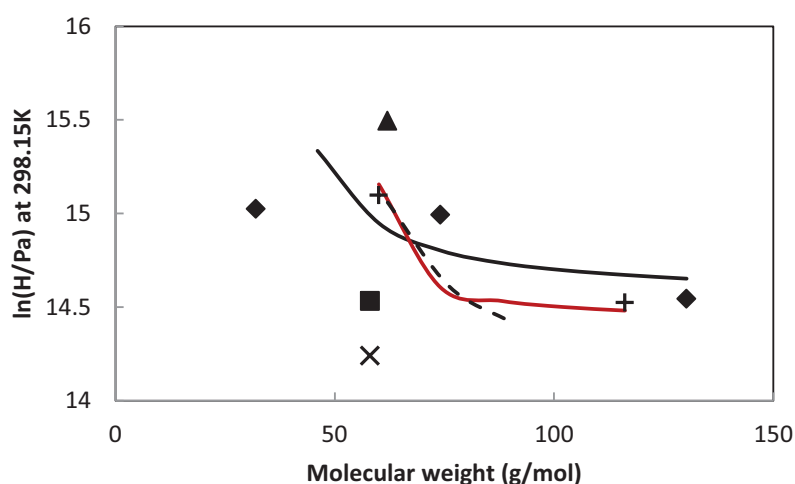


Figure V-13: Henry's constant of carbon monoxide in oxygenated solvent (in order of a chemical family) as a function of molecular weight at 298.15K. H_2S /alcohol (◆), H_2S /acetone (■), H_2S /carboxylic acid (+), H_2S /dioctyl ether (*), H_2S /1,2-ethanediol (▲). Calculation by GC-PPC-SAFT: (—) H_2S /alcohol, (---) H_2S /diol, (—) H_2S /diol, (×) H_2S /acetone

V.4.2 Prediction of phase equilibrium and the solubility of hydrogen sulfide in oxygenated solvents

Figure V-14 and Figure V-15 show the behavior of GC-PPC-SAFT when reproducing

Henry's constant of H₂S in ethanol and 1-octanol respectively both in a predictive and in a correlative way. The predictive way means that a predictive k_{ij} already exists in the calculation using GC-PPC-SAFT and the other binary parameters are equal to zero. As mentioned above, the hydrogen sulfide is an associative molecule type 3B with 2 positive sites. Otherwise, it appears that the cross-association between the oxygenated group and the H₂S must be regressed in order to obtain a reasonable result. This is achieved by tuning the cross-association parameter w_{ij} that is a correction term on the cross-association (Equation 5.4).

We adjust the interaction parameter w_{ij} on available experimental data of Henry's constant and the vapor-liquid equilibrium of the mixture (see Table V-8).

The values of this interaction parameter of H₂S with a number of oxygenated group are presented in Table V-6. Sometimes, the values of w_{ij} are specific to some oxygenated compounds such as acetic acid and acetone. The higher the polarity and association of the solvent component the higher value of w_{ij} (meaning a lower value of the interaction energy). This comes from the association which is taken into account in the polar term in PC-SAFT and there is a problem with the decoupling between the polarity and association.

Table V-6: Values of cross-association parameter w_{ij} for hydrogen sulfide used in GC-PPC-SAFT

	H ₂ S/OH alcohol	H ₂ S/OH diol	H ₂ S/COOH	H ₂ S/acetic acid	H ₂ S/acetone
w_{ij}	0.379	0.256	0.0604	0.0641	0.186
ε_{ij}^{ass} without w_{ij}	1296.50				
ε_{ij}^{ass} with w_{ij}	805.13	964.60	1218.20	1213.40	1055.35

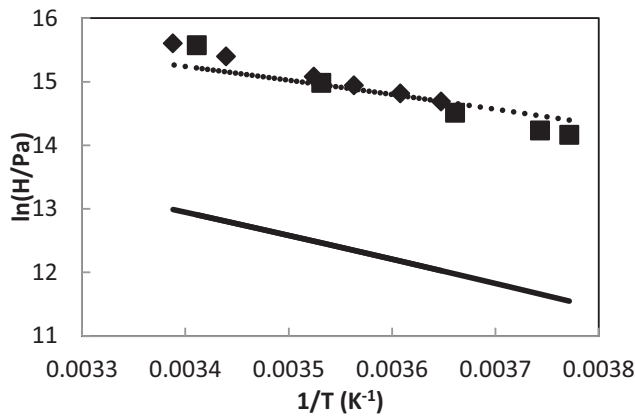


Figure V-14: GC-PPC-SAFT predictions of Henry's constant of hydrogen sulfide in ethanol. Experimental data are taken from Bunsen et al.³⁸⁹ (♦), Gerrard et al.⁴⁰⁰ (■); GC-PPC-SAFT (with predictive k_{ij}) (—), GC-PPC-SAFT (with regressed w_{ij}) (...)

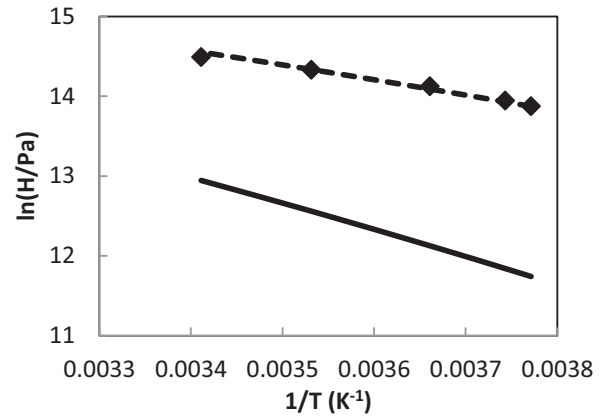


Figure V-15: GC-PPC-SAFT predictions of Henry's constant of hydrogen sulfide in 1-octanol. Experimental data are taken from Gerrard et al.⁴⁰⁰ (♦); GC-PPC-SAFT (with predictive k_{ij}) (—), GC-PPC-SAFT (with regressed w_{ij}) (...)

In Figure V-16 and Figure V-17, with adjusted w_{ij} , good computations are observed not only for the Henry constants of hydrogen sulfide in 1,2-ethanediol but also the vapour-liquid equilibrium of this mixture.

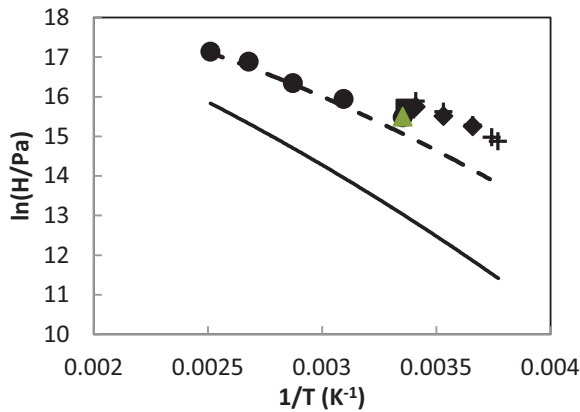


Figure V-16: GC-PPC-SAFT predictions of Henry's constant of hydrogen sulfide in 1,2-ethanediol. Experimental data are taken from Byeseda et al.⁴⁰³ (■), Lenoir et al.¹⁵¹ (▲), Schalk et al.⁴⁰² (♦), Jou et al.⁴⁰² (●), Gerrard et al.⁴⁰⁰ (+); GC-PPC-SAFT (with predictive k_{ij}) (—), GC-PPC-SAFT (with regressed w_{ij}) (...)

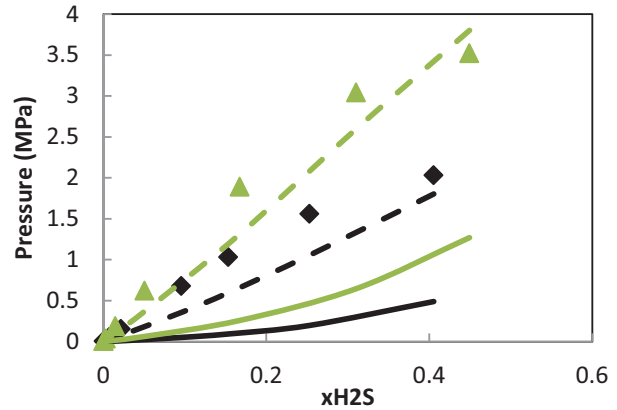


Figure V-17: GC-PPC-SAFT predictions of PTx of mixture $H_2S/1,2$ -ethanediol at 298.15 K (♦) and 323.15K (▲). Experimental data are taken from Jou et al.⁴⁰². GC-PPC-SAFT (with predictive k_{ij}) (—), GC-PPC-SAFT (with regressed w_{ij}) (...)

As observed in in Figure V-18 and Figure V-19, by using GC-PPC-SAFT with a regressed cross-association parameter, we can obtain good results in prediction of the solubility of H₂S and also the VLE of H₂S/oxygenated solvent mixtures. These deviations are acceptable because they are within the experimental uncertainty (vary from 10% to 20%) except to H₂S/1,2 ethanediol.

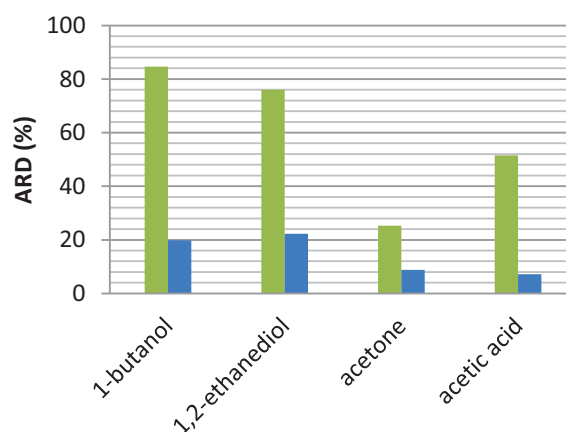
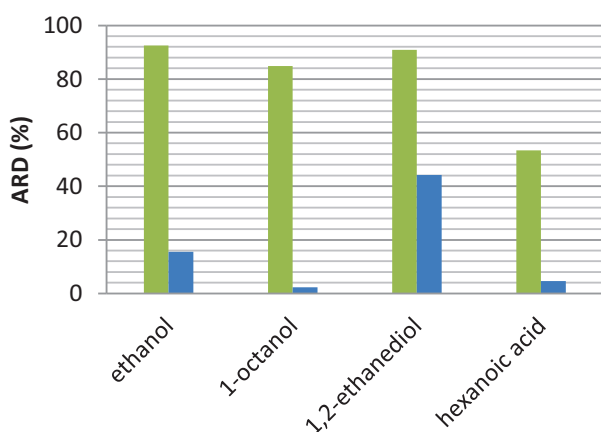


Figure V-18: Average Relative Deviation of Henry's constant of hydrogen sulfide: predictive GC-PPC-SAFT (■), GC-PPC-SAFT with w_{ij} regression (■)
Figure V-19: Average Relative Deviation of bubble pressure of hydrogen sulfide: predictive GC-PPC-SAFT (■), GC-PPC-SAFT with w_{ij} regression (■)

V.5 Solubility of ammonia (NH₃) in oxygenates

Ammonia is an important component originating from the reaction of denitrification during the hydrotreatment process of biomass charges. In pyrolysis oil (after the liquefaction), the content of nitrogen varies between 0 and 0.4%wt.³⁸¹ As carbon monoxide and hydrogen sulfide, ammonia is one of the gaseous products after the hydrotreating process of biomass feeds.

V.5.1 Database and consistency analysis

In Table V-7, the available data of the solubility and the VLE of ammonia in oxygenated solvents is summarized with references.

Table V-7: Database of binary mixtures of ammonia in organic components

Solvent	Temperature range (K)	Pressure range (MPa)	Npt	Type of data (with reference)
methanol	253.15 – 512.47	0 – 12.22	39	PTx ^{157,158,404–408} , H* ^{409,410}
ethanol	273.15 – 328.15	0 – 0.7	23	PTx ^{159,160,404} , α ⁴¹¹ , H* ^{409,410}
1-propanol	273.15 – 308.15	0.1	18	α ⁴¹¹ , H* ^{409,410}
1-butanol	263.15 – 333.15	0.1	4	PTx ⁴⁰¹ , H* ⁴⁰⁹
2-propanol	273.15 – 308.15	0.1	7	H* ^{409,410}
Dimethyl ether	253.15 – 333.15	0.1 – 2.73	5	PTx ⁴¹²
Diethyl ether	273.15 – 288.15	0.1	3	L ²²⁸
Acetone	263.15 – 298.15	0.1	3	PTx ⁴⁰¹ , H* ⁴⁰⁹
1,2-ethanediol	263.15 – 338.10	0.1	16	PTx ^{401,413}

The conversion of different solubility coefficients are detailed in previous sections. Here we followed the same methodology. In 3 figures below, we have the diagrams of $\ln H$ as a function of $1/T$ of ammonia in methanol, ethanol and 1-propanol respectively. As in the case of hydrogen sulfide, we observe here that Henry's constants of ammonia in oxygenated solvents increase with temperature meaning that ammonia is less soluble at low temperature. We also observe that there are some inconsistencies between the available data. In the case of $\text{NH}_3/\text{methanol}$ (cf. Figure V-20), the experimental data taken from Hatem et al.⁴¹⁰, Schaefer et al.¹⁵⁸ are far from the other data. In the same way, in Figure V-21, we can distinguish two distinct groups of data. The experimental data in the same group are consistent to each other. On the other hand, the inconsistency is observed between two groups. It is difficult here to determine which data are correct therefore we decide keeping them all in the database.

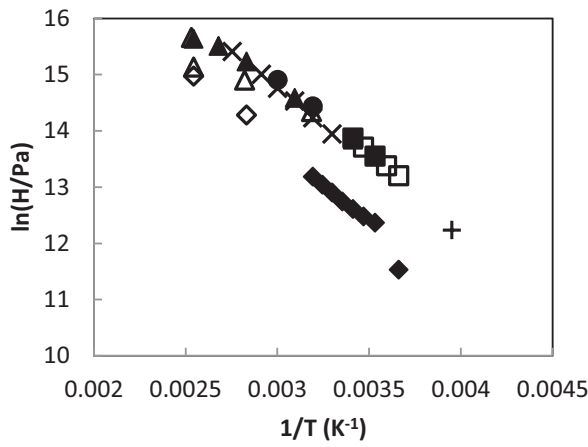


Figure V-20: Henry's constant of ammonia in methanol. Experimental data are taken from Hatem et al.⁴¹⁰ (◆), Kudo et al.⁴⁰⁴ (□), Xu et al.⁴⁰⁵ (×), Doering et al.⁴⁰⁷ (+), Inomata et al.¹⁵⁷ (●), Preuss et al.⁴⁰⁶ (▲), Feng et al.⁴⁰⁸ (■), Schaefer et al.¹⁵⁸ (◇, Δ)

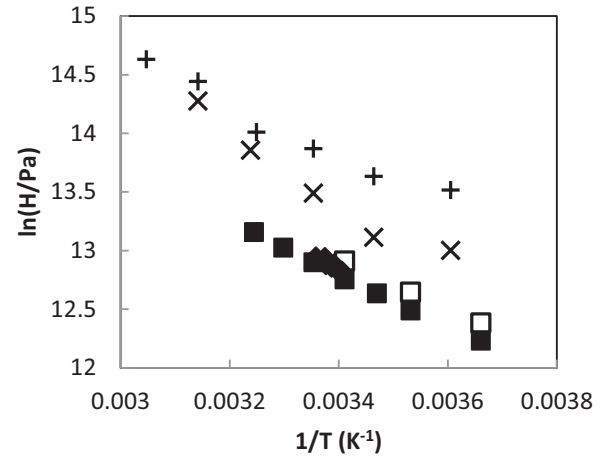


Figure V-21: Henry's constant of ammonia in ethanol. Experimental data are taken from Pagliani et al.⁴¹¹ (◆), Hatem et al.⁴¹⁰ (■), Kudo et al.⁴⁰⁴ (□), Zeng et al.¹⁶⁰ (×), Huang et al.¹⁵⁹ (+)

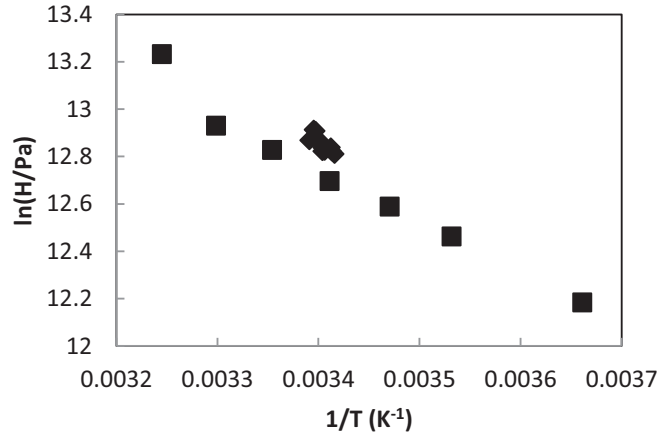


Figure V-22: Henry's constant of ammonia in 1-propanol. Experimental data are taken from Pagliani et al.⁴¹¹ (◆), Hatem et al.⁴¹⁰ (■)

V.5.2 Prediction and correlation of phase equilibrium and the solubility of ammonia in oxygenated solvents

As discussed above, ammonia is a component that has 4 associative sites. Therefore, in the calculations of Henry's constant by GC-PPC-SAFT, the cross association correction parameter w_{ij} is used. The experimental data of Henry constants and also the vapor pressure are used in the regression. The adjusted values of w_{ij} may be found in Table V-8. The values of association energy without w_{ij} are the same for the oxygenated groups and acetone (because the parameters of acetone are determined by group contribution method). In the case of ethanol, the value of ε_{ij}^{ass} without w_{ij} is a little bit different because we use the pure component parameters for ethanol (instead of its group contribution description).

Table V-8: Values of cross-association parameter w_{ij} for ammonia used in GC-PPC-SAFT

	NH ₃ /ethanol	NH ₃ /OH (1-alcohol)	NH ₃ /OH (diol)	NH ₃ /OH (2-alcohol)	NH ₃ /acetone	NH ₃ /-O-
w_{ij}	-0.309	-0.058	-0.0063	-0.0504	0.2775	0.6403
ε_{ij}^{ass} without w_{ij}	1385.92	1394.81				
ε_{ij}^{ass} with w_{ij}	1813.71	1475.28	1403.59	1465.14	1007.72	501.75

When regressing the correction parameter on available data of Henry's constant and vapor-liquid equilibrium (VLE) (see Table V-8), we obtain good computations (cf. Figure V-23-Figure V-26 in case of ammonia/ethanol). At temperature of 328.15 K, the prediction is maybe less accurate than the cases at 307.75 K (cf. Figure V-25) or at 277.35 K (cf. Figure V-24), but it remains acceptable. In addition, we see that without w_{ij} , the predictions by GC-PPC-SAFT underestimate the pressures. The adjusted w_{ij} allows reproducing very well the shape of phase equilibrium curve.

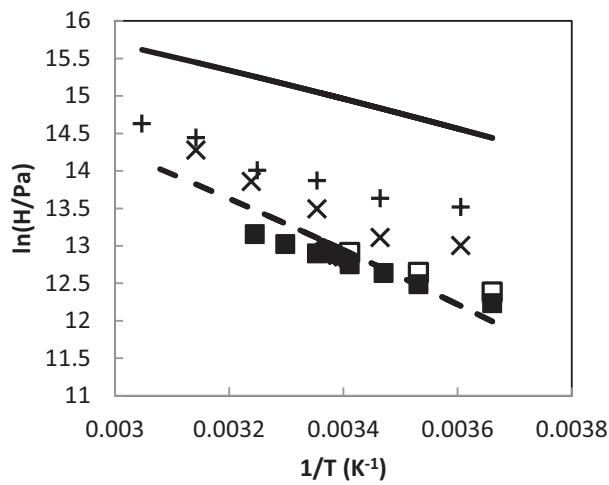


Figure V-23: GC-PPC-SAFT prediction of Henry's constant of ammonia in ethanol. Experimental data are taken from Pagliani et al.⁴¹¹ (\blacklozenge), Hatem et al.⁴¹⁰ (\blacksquare), Kudo et al.⁴⁰⁴ (\square), Zeng et al.¹⁶⁰ (\times), Huang et al.¹⁵⁹ ($+$); GC-PPC-SAFT (with predictive k_{ij}) (—), GC-PPC-SAFT (with regressed w_{ij}) (---)

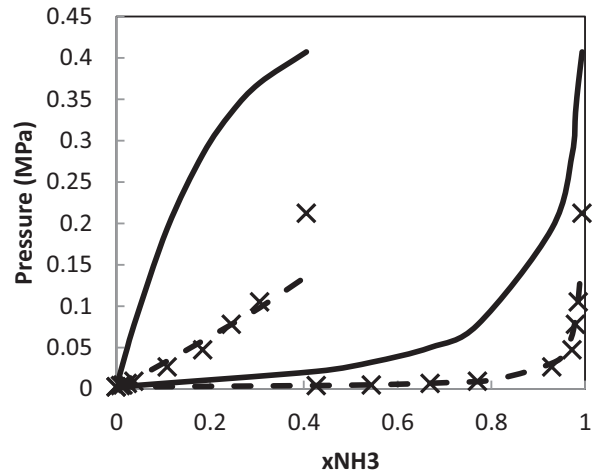


Figure V-24: GC-PPC-SAFT predictions of PT_x of mixture ammonia/ethanol at 277.35K. Experimental data are taken from Zeng et al.¹⁶⁰ (\times); GC-PPC-SAFT (with predictive k_{ij}) (—), GC-PPC-SAFT (with regressed w_{ij}) (---)

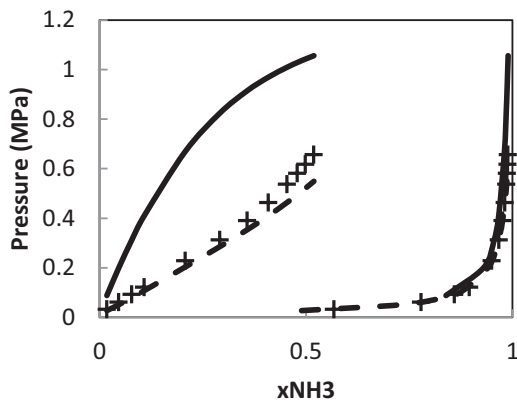


Figure V-25: GC-PPC-SAFT predictions of PT_x of mixture ammonia/ethanol at 307.75K. Experimental data are taken from Huang et al.¹⁵⁹ ($+$); GC-PPC-SAFT (with predictive k_{ij}) (—), GC-PPC-SAFT (with regressed w_{ij}) (---)

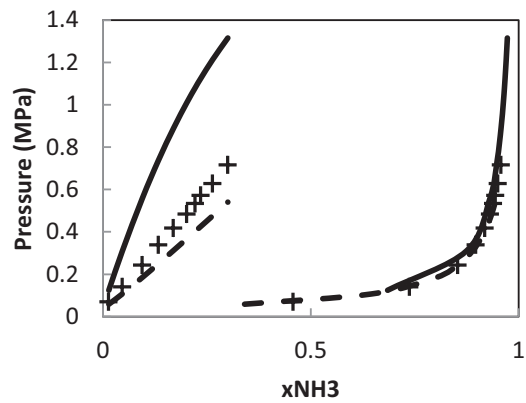


Figure V-26: GC-PPC-SAFT predictions of PT_x of mixture ammonia/ethanol at 328.15K. Experimental data are taken from Huang et al.¹⁵⁹ ($+$); GC-PPC-SAFT (with predictive k_{ij}) (—), GC-PPC-SAFT (with regressed w_{ij}) (---)

We observe in Figure V-27 that using the cross-association correction parameters allows reducing the deviations between the calculated Henry's constants and the experimental ones. However the slope of $\ln H$ versus $1/T$ is not very well captured by our model (with or without k_{ij}). We can see the same problems in Figure V-28.

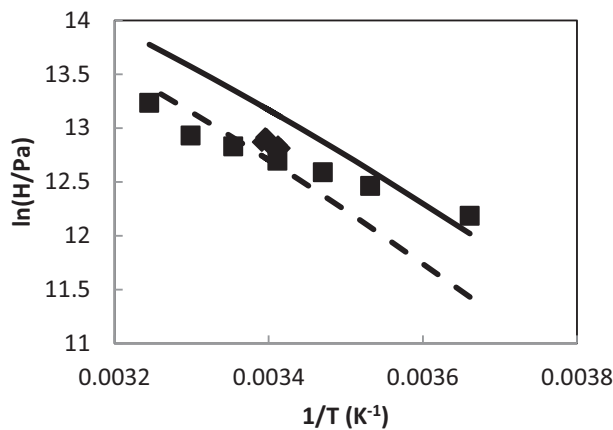


Figure V-27: GC-PPC-SAFT predictions of Henry's constant of ammonia in 1-propanol. Experimental data are taken from Pagliani et al.⁴¹¹ (◆), Hatem et al.⁴¹⁰ (■); GC-PPC-SAFT (with predictive k_{ij}) (—), GC-PPC-SAFT (with regressed w_{ij}) (...)

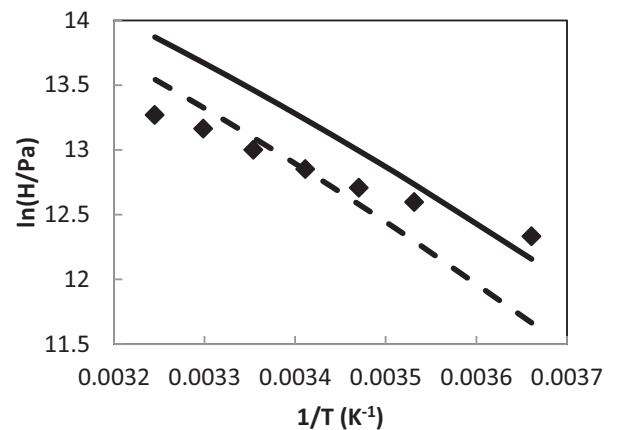


Figure V-28: GC-PPC-SAFT predictions of Henry's constant of ammonia in 2-propanol. Experimental data are taken from Hatem et al.⁴¹⁰ et Kuznetsov et al.⁴⁰⁹ (◆); GC-PPC-SAFT (with predictive k_{ij}) (—), GC-PPC-SAFT (with regressed w_{ij}) (...)

The results of GC-PPC-SAFT predictions for the vapor-liquid equilibrium of binary mixtures of ammonia and dimethyl ether are shown in Figure V-29, Figure V-30 and Figure V-31 at different temperatures (253.15 K, 273.15 K and 313.15 K respectively). Using the “predictive” cross association parameters ($\epsilon_{ij}^{ass} = \frac{\epsilon_i^{ass} + \epsilon_j^{ass}}{2}$, $\kappa_{ij}^{ass} = \sqrt{\kappa_i^{ass} \kappa_j^{ass}}$), a negative azeotrope is observed indicating strong cross association, too strong here if we look at the data. We observed that with a regressed w_{ij} , we can obtain a good shape of the VLE curves with an azeotrope even though the deviations between the predicted values and experimental ones are slightly high.

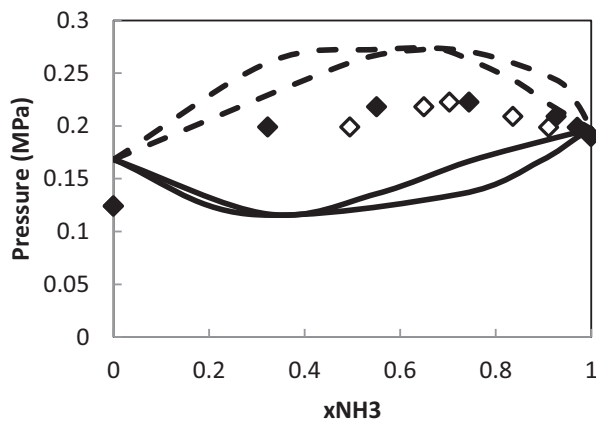


Figure V-29: GC-PPC-SAFT predictions of PT_{xy} of mixture ammonia/dimethyl ether at 253.15K. Experimental data are taken from Lippold et al.⁴¹²; bubble points (\blacklozenge) and dew points (\lozenge); GC-PPC-SAFT (with predictive k_{ij}) (—), GC-PPC-SAFT (with regressed w_{ij}) (...)

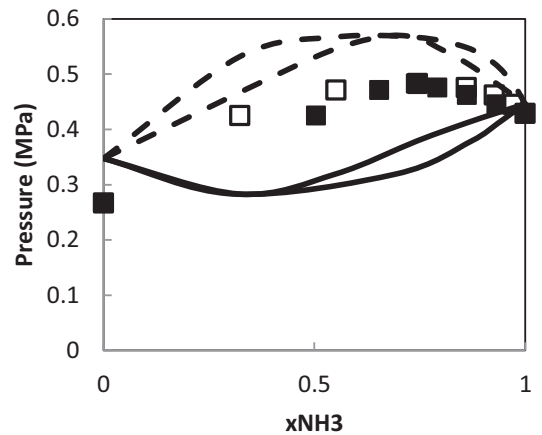


Figure V-30: GC-PPC-SAFT predictions of PT_{xy} of mixture ammonia/dimethyl ether at 273.15K. Experimental data are taken from Lippold et al.⁴¹²; bubble points (\blacksquare) and dew points (\square); GC-PPC-SAFT (with predictive k_{ij}) (—), GC-PPC-SAFT (with regressed w_{ij}) (...)

In the case of ammonia/diethyl ether, the only experimental data we have is Henry's constant converted from Ostwald coefficients of Christoff et al.²²⁸ (cf. Figure V-32). Adjusting w_{ij} allows improving the prediction results of GC-PPC-SAFT for Henry's constant.

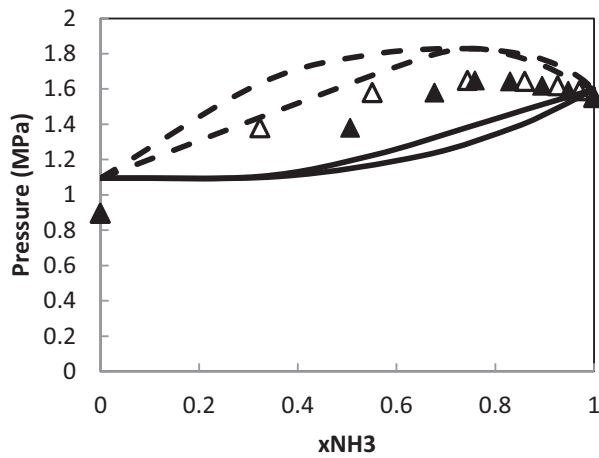


Figure V-31: GC-PPC-SAFT predictions of PT_{xy} of mixture ammonia/dimethyl ether at 313.15 K. Experimental data are taken from Lippold et al.⁴¹² (▲); GC-PPC-SAFT (with predictive k_{ij}) (—), GC-PPC-SAFT (with regressed w_{ij}) (...)

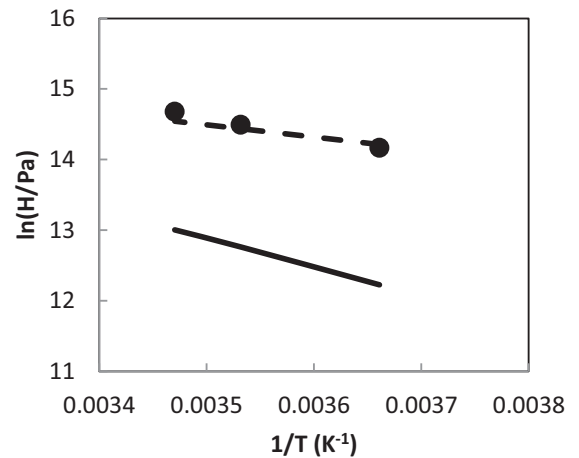


Figure V-32: GC-PPC-SAFT predictions of Henry's constant of ammonia in diethyl ether. Experimental data are taken from Christoff et al.²²⁸ (●); GC-PPC-SAFT (with predictive k_{ij}) (—), GC-PPC-SAFT (with regressed w_{ij}) (...)

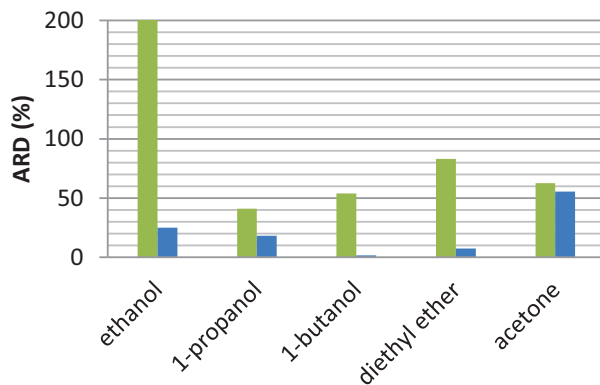


Figure V-33: Average Relative Deviation of Henry's constant of ammonia: predictive GC-PPC-SAFT (■), GC-PPC-SAFT with w_{ij} regression (■)

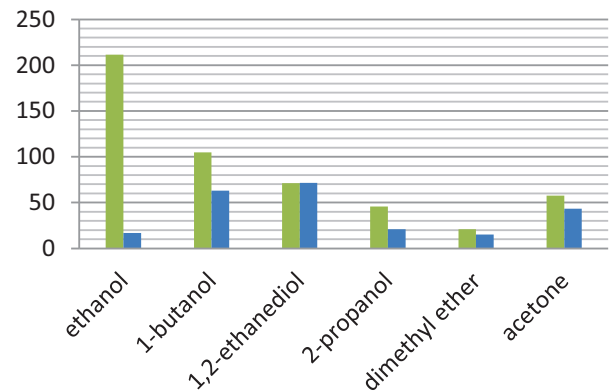


Figure V-34: Average Relative Deviation of bubble pressure of ammonia mixtures: predictive GC-PPC-SAFT (■), GC-PPC-SAFT with w_{ij} regression (■)

In Figure V-33 and Figure V-34, we see that the deviations between the predicted values and experimental ones significantly decrease by using a w_{ij} regression. In some cases, this is not actually efficient for example for acetone or 1,2-ethanediol. In addition, in Table V-8 we find

that the value of w_{ij} in the case of 1,2-ethanediol is not very significant, therefore we decide not using this parameter for this system.

In conclusion, for the binary systems of ammonia and oxygenated solvents, the use of cross-association parameter w_{ij} is really needed for the predictions of GC-PPC-SAFT for the vapor-liquid equilibrium in general. The adjusted w_{ij} also allow take into account the presence of azeotrope of the mixtures.

V.6 Conclusion

The objective of this chapter is to evaluate the VLE behavior of hydrogen in oxygenated solvents. As in Chapter II, for these small gases, we consider Henry's constant as the main property to evaluate the solubility of gases in oxygenated compounds. All the data found in the literature was converted into Henry's constant and was analyzed. Because of the lack of experimental data, we also used the vapor-liquid equilibrium for some systems. After an internal coherence analysis, we can remove some inconsistent data in the literature. As in the case of hydrogen, this data analysis allowed us to evaluate the experimental data, an important step for predicting of gas solubility by using GC-PPC-SAFT equation of state. As observed, the Henry constants of these gases decrease with the molecular weight of solvent and seem to be dependent on the polarity and the association of oxygenated solvents. The trend of this property as a function of molecular weight of solvent seems the same with that of mixtures containing hydrogen. We have an identical observation in the case of hydrogen sulfide. Table V-11 summarizes the important points concerning the data analysis and the prediction using GC-PPC-SAFT Equation of state in this chapter.

Table V-11: Summary of data consistency and the prediction by GC-PPC-SAFT for systems containing hydrotreating gases

Gas	Consistency/trends	GC-PPC-SAFT
CO	<ul style="list-style-type: none"> - Removed data PTx of Toner et al.³⁸⁵ for CO/1-propanol and CO/1-butanol - Henry's constants reduce with temperature - lnH decrease with molecular weight of solvents 	Predictive from pseudo-ionization energy J Déviation: <ul style="list-style-type: none"> - Henry's constant : ~30% - Bubble pressure : ~20%
H ₂ S	<ul style="list-style-type: none"> - Good consistency between different data sources - Lack of experimental data to analyze the coherence. - Henry's constants increase with temperature - lnH decrease with molecular weight of solvents 	Including w_{ij} Déviation: <ul style="list-style-type: none"> - Henry's constant : ~20% - Bubble pressure : ~20%
NH ₃	<ul style="list-style-type: none"> - Henry's constants increase with temperature - lnH decrease with molecular weight of solvents 	Including w_{ij} Déviation: <ul style="list-style-type: none"> - Henry's constant : ~20% - Bubble pressure : ~20%

We can also easily observe in Figure V-35 that ammonia is the most soluble gas in oxygen-bearing solvents and the solubility of this gas seems to decrease with the molecular weight of the solvent. The inverse trend is found in mixtures of carbon monoxide and hydrogen sulfide in oxygenated compounds.

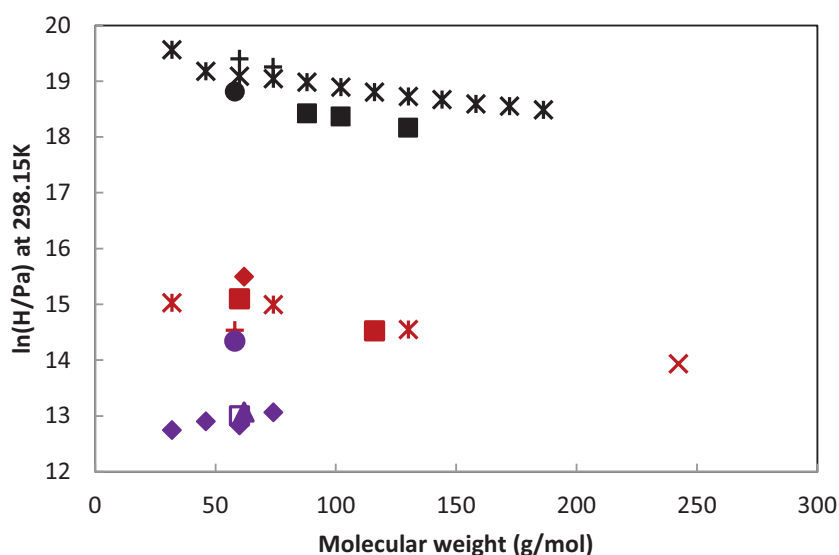


Figure V-1: Henry's constant of carbon monoxide in oxygenated solvent (in order of a chemical family) as a function of molecular weight at 298.15 K. (*) CO/alcohols, (+) CO/carboxylic acid, (●) CO/acetone, (■) CO/esters, (◆) H₂S/diol, (+) H₂S/acetone, (*) H₂S/alcohols, (■) H₂S/carboxylic acid, (x) H₂S/ether, (●) NH₃/acetone, (◆) NH₃/1-alcohols, (□) NH₃/2-alcohol, (▲) NH₃/diol

The predictions of the solubility of hydrotreating gases using GC-PPC-SAFT provide good results in general but for some particular solvent such as ethanol, acetic acid,... a special treatment is required. For example, in GC-PPC-SAFT we usually use the specific parameters for the small molecules. We find that this solution improves a little bit the results of prediction but the deviations are still high (>20%) but acceptable due to the experimental uncertainty (vary from 10% to 20%). In this case, additional measurement may help reducing the experimental uncertainties and as a consequence improve the regression.

GENERAL CONCLUSIONS

This thesis is about the thermodynamic modeling of phase equilibrium of mixtures containing hydrogen or other light components such as hydrogen sulfide, carbon monoxide and ammonia in oxygenated compounds for biomass processing applications. This work is mainly related to the hydrotreating process of bio-oils from biomass, an important intermediate product for second-generation biofuel production. The objective of this work is to develop a predictive equation of state for the phase equilibria involved in bio-oil hydrotreatment.

First, a brief summary of the thermodynamic framework (e.g. phase equilibrium, Henry's constant) and the state of the art of models that could be used for the prediction of gas solubility is given. The description of molecular simulation has been also provided, this technique being considered in this work as a validation method and as a tool to extrapolate data at high temperature.

A database of validated experimental data of hydrogen solubility has been constructed. As we consider that the solubility of a solute in organic solvents is at infinite dilution, all the available data in the literature have been converted into Henry's constant. We estimated that the experimental uncertainty is about 10%. The consistency of data i.e Henry's constant of hydrogen in organic compounds has been analyzed. A correlation as function of the temperature has been proposed for each binary system (H_2 + solvent). After analyzing the data consistency, the trend of Henry's constant of hydrogen is studied. Indeed, Henry's constants of hydrogen decrease with the temperature of the system and the molecular weight of solvents. This database is considered as the data reference and has been presented in Chapter II of this manuscript. The same methodology has been applied for the other hydrotreating gases such as carbon monoxide, hydrogen sulfide and ammonia (see Chapter V). For some mixtures, there are a lack of data and we have proposed to use the Monte Carlo simulation with Widom insertion test to produce the pseudo-experimental data of Henry's constant of hydrogen.

In this work, we have chosen GC-PPC-SAFT to model the gas solubility and phase equilibrium in the hydrotreatment process. It appeared that the differences between experimental data and predictions are quite significant, especially for short polar and associative compounds. An improvement is then proposed through the use of a binary interaction parameter of the

attractive term. In general, the regression for mixtures of hydrogen with solvents provides negative values of this binary parameter, which excludes the use of the predictive rule introduced by Nguyen Huynh et al³⁴⁶. Based on the link between repulsive interactions and the free volume effect, the GC-PPC-SAFT model was improved by adding a contribution for taking into account non-additive cross diameters which leads to the introduction of a new binary interaction parameter l_{ij} . We firstly developed this new term for the Square Well Chains Equation of state. Monte Carlo simulations are also used as a validation method for the development of non-additive term of Square Well Chains Equation of state that is presented in Chapter III.

The extension of GC-PPC-SAFT by integrating the non-additive contribution into the model is necessary to model the hydrogen solubility in oxygenated compounds. We have described all the important derivatives in order to calculate the thermodynamic properties with the non-additive contribution and then integrate them into the GC-PPC-SAFT framework. This new parameter has been tested on Henry's constants of hydrogen. A predictive method for this parameter based on a group contribution method has then been proposed. Thus, a completely predictive model is proposed providing satisfactory results with deviations that are within the experimental uncertainty (~10%). We observed that the new model follows the same trend at high temperature as that which was observed with molecular simulation and validated on some high temperature data. It is therefore possible to state that the model allows describing correctly the hydrogen solubility in hydrotreatment conditions, with an uncertainty of 10%.

The GC-PPC-SAFT Equation of state has been used on binary systems containing CO, NH₃ and H₂S, which are reaction products of the hydrotreatment. Water will be investigated in a separate study. For binary systems of CO+oxygenated solvents the predictive calculations yield deviations of about 20%. In the case of NH₃ and H₂S, which are associative compounds, the use of a cross-association parameter w_{ij} allows reducing the deviation between experimental data and calculated values. The acceptable deviations are obtained within the experimental uncertainty (~20%).

We have thus succeeded to develop a predictive thermodynamic model that provides satisfactory results in term of prediction of gas solubility of hydrotreatment gases in organic solvents especially hydrogen.

PERSPECTIVES

This investigation has led to good results in term of hydrotreatment gas solubility prediction in oxygen-bearing solvents, some improvement can be made to this work. This development of GC-PPC-SAFT equation of state with the new predictive parameter could be applied to industrial systems but at first we need to acquire the new experimental data especially for the ternary and multi-component systems.

In future studies, in order to improve the prediction of the gas solubility in general and the hydrogen solubility in particular, some additional investigations may be conducted. As discussed in Chapter III, high deviations are found between the calculated values of the inter-segment distribution function and the ones issued from Monte Carlo simulations. After some evaluations and discussion, we assume that the problem comes from the lack of the molecular simulation data. Acquisition of such data would allow us to enlarge the fitting zone and consequently to reduce the deviations of the model. It would be better to have the spectrometric data of these functions. A research in the literature may be necessary to find this kind of property.

The model should be extended to the water + hydrogen system, but an improved parameterization of water is probably needed to this end. Another project will investigate this. Finally, in this thesis, we have developed the non-additive parameter in GC-PPC-SAFT equation of state and applied it mainly for the systems containing hydrogen. It is supposed that this parameter could be used for the other systems containing small molecules and featuring liquid – liquid equilibria, such as methanol + hydrocarbons.

PUBLICATION LIST

Posters

“Hydrogen solubility in oxygenated compounds using the GC-PPC-SAFT Equation of state” – Trinh T.K.H., de Hemptinne J-C., Lugo R., Passarello J-P. SFGP Congress 2013 – Lyon, France.

“The GC-PPC-SAFT Equation of state (EoS) with a non-additive segment diameter” – Trinh T.K.H., Passarello J-P., de Hemptinne J-C., Lugo R. 27th European Symposium on Applied Thermodynamics (ESAT) Conference 2014 – Eindhoven, Netherland.

“Prédiction des équilibres de phases associés à l’hydrotraitement de la biomasse par GC-PPC-SAFT” – Journée Doctorale de l’Ecole Doctorale Institut Galilée 2014 – Paris, France

Oral Communication

“A non-additive hard sphere version of PPC-SAFT for hydrogen containing systems” – Trinh T.K.H., Passarello J-P., de Hemptinne J-C., Lugo R. 28th European Symposium on Applied Thermodynamics (ESAT) Conference 2015 – Athens, Greece.

Articles

“Hydrogen solubility in hydrocarbon and oxygenated compounds” – Trinh T.K.H., de Hemptinne J-C., Lugo R., Ferrando N., Passarello J-P. – Journal of Chemical Engineering Data, 2015 : Submitted

“Modélisation de la solubilité de l’hydrogène dans les composés oxygénés avec l’équation d’état (EoS) GC-PPC-SAFT” – Trinh T.K.H., de Hemptinne J-C., Lugo R., Passarello J-P. – Récents Progrès en Génie des Procédés, Numéro 14, 2013 : Accepted

REFERENCES

1. Wertz J. "Le Bioraffinage Ou Valorisation Optimale de La Biomasse Pétrole Brut Biomasse". ValBiom, France, 2010.
2. Pinto MS. "Global biofuels outlook 2010-2020". In: *World Biofuels Markets.*; 2011.
3. Olarte M. V., Zacher A. H., Elliott D. C., Santosa, D. M., Neuenschwander, G. G., Hart, T. R., Rotness, L. J. "Bio- oil Upgrading and Stabilization at PNNL". In: *Harvesting Clean Energy Conference 2011*. Boise, Idaho; 2011.
4. Torres R., Hemptinne J-C. de, Machin I. "Improving the modeling of Hydrogen solubility in heavy oil cuts using an augmented Grayson Streed (AGS) Approach". *Oil&Gas Sci Technol*. 2013;68(2):217-233.
5. Redlich O., Kwong J.N.S. "On the Thermodynamics of Solutions. V. An Equation of State. Fugacities of Gaseous Solutions". *Chem Rev*. 1949;44(1):233-244.
6. Peng D., Robinson D.B. "A New Two-Constant Equation of State". *Ind Eng Chem Fundam*. 1976;15(1):59-64.
7. Chapman W.G., Gubbins K.E., Jackson G., Radosz M. "SAFT: Equation-ofstate solution model for associating fluids". *Fluid Phase Equilib*. 1989;52(0):31-38.
8. Chapman W.G., Gubbins K.E., Jackson G., Radosd M. "New Reference Equation of State for Associating Liquids". *Ind Eng Chem Res*. 1990;29:1709-1721.
9. Wertheim M.S. "Fluids with highly directional attractive forces. I. Statistical thermodynamics". *J Stat Phys*. 1984;35(1-2):19-34.
10. Wertheim M.S. "Fluids with highly directional attractive forces. III. Multiple attraction sites". *J Stat Phys*. 1986;42(3-4):459-476.
11. Wertheim M.S. "Fluids with highly directional attractive forces. II. Thermodynamic perturbation theory and integral equations". *J Stat Phys*. 1984;35(1-2):35-47.
12. Jog P.K., Chapman W.G. "Application of Wertheim ' s thermodynamic perturbation theory to dipolar hard sphere chains". *Mol Phys*. 1999;97(3):307-319.
13. Gross J., Sadowski G. "Perturbed-Chain SAFT: An Equation of State Based on a Perturbation Theory for Chain Molecules". *Ind Eng Chem Res*. 2001;40(4):1244-1260.
14. Tamouza S., Passarello J-P., Tobaly P., de Hemptinne J-C. "Group contribution method with SAFT EOS applied to vapor liquid equilibria of various hydrocarbon series". *Fluid*

- Phase Equilib.* 2004;222-223:67-76.
15. Nguyen-huynh D. "Modélisation thermodynamique de mélanges symétriques et asymétriques de composés polaires et/ou aromatiques par GC-SAFT". Université Paris Nord, 2008.
 16. Thi C. Le, Tamouza S., Passarello J-P., Tobaly P., de Hemptinne J-C. "Modeling Phase Equilibrium of H₂ + n-Alkane and CO₂ + n-Alkane Binary Mixtures Using a Group Contribution Statistical Association Fluid Theory Equation of State (GC-SAFT-EOS) with a k_{ij} group contribution method". *Ind Eng Chem Res.* 2006;45:6803-6810.
 17. Nguyen-huynh D., Tran T.K.S., Tamouza S., Passarello J-P., Tobaly P. "Modeling Phase Equilibria of Asymmetric Mixtures Using a Group-Contribution SAFT (GC-SAFT) with a k_{ij} correlation method based on London's theory. 1. Application to binary mixture containing aromatic hydrocarbons, n-alkanes, CO₂, N₂ and H₂S". *Ind Eng Chem Res.* 2008;47(22):8859-8868.
 18. Kadri M. "Etude Des Équilibres de Phase H₂ + Oxygénés À L'aide de L'Équation D'état GC-PPC-SAFT". Internship Report, Université Paris Nord; 2010.
 19. de Hemptinne J-C., Ledannois J-M., Mouglin P., Barreau A. "Select Thermodynamic Models for Process Simulation". Technip Editions. Paris, France; 2012.
 20. Fogg P.G.T., Gerrard W. "Solubility of Gases in Liquids". John Wiley & Sons Ltd., Chichester, New York, 1990.
 21. Young C.L. "Solubility Data Series Volumes 5/6, Hydrogen and Deuterium". Pergamon, Oxford; 1981.
 22. Cook M.W., Hanson D.N., Alder B.J. "Solubility of Hydrogen and Deuterium in Nonpolar Solvents". *J Chem Phys.* 1957;26(4):748.
 23. Benson B.B., Daniel Krause J. "Empirical laws for dilute aqueous solutions of nonpolar gases". *J Chem Phys.* 1976;64(2):689.
 24. Prausnitz J.M., Lichtenthaler R.N., de Azevedo E.G. "Molecular Thermodynamics of Fluid-Phase Equilibria". Prentice-Hall Editions, California, US; 1998.
 25. Yen L.C., Mcketta J.J. "Thermodynamic Correlation of Nonpolar Gas Solubilities in Polar, Nonassociated Liquids". *AIChE J.* 1951;8(4):501-507.
 26. Wilhelm E., Battino R. "Thermodynamic Functions of the Solubilities of Gases in Liquids at 25°C". *Chem Rev.* 1973;73(1):1-9.

27. Fernández-Prini R., Alvarez J.L., Harvey A.H. "Henry's constants and vapor-liquid distribution constants for gaseous solutes in H₂O and D₂O at high temperatures". *J Phys Chem Ref Data*. 2003;32(2):903-916.
28. Japas M.L., Sengers J.M.H.L. "Gas solubility and Henry's law near the solvent's critical point". *AIChE J*. 1989;35(5):705-713.
29. Abrams D.S., Prausnitz J.M. "Statistical thermodynamics of liquid mixtures: A new expression for the excess Gibbs energy of partly or completely miscible systems". *AIChE J*. 1975;21(1):116-128.
30. Renon H., Prausnitz J.M. "Local composition in thermodynamic excess functions for liquid mixtures". *AIChE J*. 1968;14:135-144.
31. Haghazarloo H., Lotfollahi M.N., Mahmoudi J, Asl A.H. "Liquid-liquid equilibria for ternary systems of (ethylene glycol+toluene+heptane) at temperatures (303.15, 308.15, and 313.15 K) and atmospheric pressure: Experimental results and correlation with UNIQUAC and NRTL models". *J Chem Thermodyn*. 2013;60:126-131.
32. Santori G., Franciolini M., Di Nicola G., Polonara F., Brandani S., Stryjek R. "An algorithm for the regression of the UNIQUAC interaction parameters in liquid-liquid equilibrium for single- and multi-temperature experimental data". *Fluid Phase Equilib*. 2014;374:79-85.
33. Nagata I., Meyer T., Gmehling J. "Correlation of binary liquid-liquid equilibrium data over a wide temperature range using UNIQUAC and extended UNIQUAC models". *Fluid Phase Equilib*. 1991;65:19-39.
34. Hooper H.H., Michel S., Prausnitz J.M. "Correlation of liquid-liquid equilibria for some water-organic liquid systems in the region 20-250°C". *Ind Eng Chem Res*. 1988;27(11):2182-2187.
35. Ferreira L.S., Trierweiler J.O. "Modeling and simulation of the polymeric nanocapsule formation process". *Adv Control pf Chem Process*. 2007;7(1):405-410.
36. Asher W.E., Pankow J.F. "Vapor pressure prediction for alkenoic and aromatic organic compounds by a UNIFAC-based group contribution method". *Atmos Environ*. 2006;40(19):3588-3600.
37. Wittig R., Lohmann J., Gmehling J. "Vapor-Liquid equilibria by UNIFAC group contribution. 6. Revision and Extension". *Ind Eng Chem Res*. 2003;42:183-188.
38. Corella J., Aznar MP., Delgado J., Aldea E. "Steam gasification of cellulosic wastes in a

- fluidized bed with downstream vessels". *Ind Eng Chem Res.* 1991;30(10):2252-2262.
39. Klamt A., Eckert F., Hornig M. "COSMO-RS: A novel view to physiological solvation and partition questions". *J Comput Aided Mol Des.* 2001;15(4):355-365.
 40. Klamt A., Eckert F. "COSMO-RS: a novel and efficient method for the a priori prediction of thermophysical data of liquids". *Fluid Phase Equilib.* 2000;172(1):43-72.
 41. Klamt A., Jonas V., Bürger T., Lohrenz J.C.W. "Refinement and Parametrization of COSMO-RS". *J Phys Chem A.* 1998;102(26):5074-5085.
 42. Klamt A. "Conductor-like Screening Model for Real Solvents: A New Approach to the Quantitative Calculation of Solvation Phenomena". *J Phys Chem.* 1995;99(7):2224-2235.
 43. Klamt A. "COSMO-RS: From Quantum Chemistry to Fluid Phase Thermodynamics and Drug Design". Elsevier Editions, Amsterdam, 2005.
 44. Klamt A., Eckert F., Arlt W. "COSMO-RS: An Alternative to Simulation for Calculating Thermodynamic Properties of Liquid Mixtures". *Annu Rev Chem Biomolec Eng.* 2010;1:101-122.
 45. Diedenhofen M., Klamt A. "COSMO-RS as a tool for property prediction of IL mixtures- A review". *Fluid Phase Equilib.* 2010;294(1-2):31-38.
 46. Grayson H.G., Streed C.W. "Vapor-Liquid Equilibria for High Temperature, High Pressure Hydrogen-Hydrocarbon Systems". In: *6th World Petroleum Congress.* Frankfurt am Main, Germany; 1963:169-181.
 47. Scatchard G. "Equilibria in Non-electrolyte Solutions in Relation to the Vapor Pressures and Densities of the Components". *Chem Rev.* 1931;8(2):321-333.
 48. Walas S.M. "Phase Equilibria in Chemical Engineering". Butterworth-Heinemann Editions, Massachusetts; 1985.
 49. Nguyen T.B. "Représentation des charges oxygénées associées à la valorisation de la biomasse: définition de descripteurs". Université Pierre Marie Curie, 2013.
 50. Waals J.D. Van Der, Rowlinson J.S. "On the Continuity of the Gaseous and Liquid States". North-Holland Editions, Amsterdam; 1988.
 51. Chávez L.M., Alonso F., Ancheyta J. "Vapor-liquid equilibrium of hydrogen-hydrocarbon systems and its effects on hydroprocessing reactors". *Fuel.* 2014;138:156-175.
 52. Qian J.W., Jaubert J.N., Privat R. "Phase equilibria in hydrogen-containing binary systems

- modeled with the Peng-Robinson equation of state and temperature-dependent binary interaction parameters calculated through a group-contribution method". *J Supercrit Fluids*. 2013;75:58-71.
53. Laugier S., Richon D., Renon H. "Representation of hydrogen-hydrocarbon vapour-liquid equilibria and saturated densities at high pressures and temperatures". *Chem Eng Sci*. 1986;41(9):2407-2417.
 54. Vidal J. "Mixing rules and excess properties in cubic equations of state". *Chem Eng Sci*. 1977;33(6):787-791.
 55. Huron M.J., Vidal J. "New mixing rules in simple equations of state for representing vapour-liquid equilibria of strongly non-ideal mixtures". *Fluid Phase Equilib*. 1979;3:255-271.
 56. Ioannidis S., Knox D.E. "Vapor-liquid equilibria predictions at high-pressures with the Huron-Vidal mixing rule". *Fluid Phase Equilib*. 2001;187-188:1-14.
 57. Michelsen M.L. "A method for incorporating excess Gibbs energy models in equations of state". *Fluid Phase Equilib*. 1990;60(1-2):47-58.
 58. Dahl S. "High Pressure VLE with a UNIFAC - based EOS". *AIChE J*. 1990;36(12):1829-1836.
 59. Wong D.S.H., Orbey H., Sandler S.I. "Equation of state mixing rule for nonideal mixtures using available activity coefficient model parameters and that allows extrapolation over large ranges of temperature and pressure". *Ind Eng Chem Res*. 1992;31(8):2033-2039.
 60. Voros N.G., Tassios D.P. "Vapor-liquid equilibria in nonpolar/weakly polar systems with different types of mixing rules". *Fluid Phase Equilib*. 1993;91(1):1-29.
 61. Coutsikos P., Kalospiros N.S., Tassios D.P. "Capabilities and limitations of the Wong-Sandler mixing rules". *Fluid Phase Equilib*. 1995;108(1-2):59-78.
 62. Skjold-Jorgensen S., Kolbe B., Gmehling J., Rasmussen P. "Vapor-Liquid Equilibria by UNIFAC Group Contribution. Revision and Extension". *Ind Eng Chem Process Des Dev*. 1979;18(4):714-722.
 63. Soave G. "Equilibrium Constants from a Modified Redlich - Kwong Equation of State". *Chem Eng Sci*. 1972;27(6):1197-1203.
 64. Su C.S. "Improvement of predictive Soave-Redlich-Kwong (PSRK) equation of state for representing volumetric properties of carbon dioxide-expanded organic solvents". *Chem*

- Eng Res Des.* 2014;92(11):2749-2757.
65. Schmid B., Gmehling J. "Revised parameters and typical results of the VTPR group contribution equation of state". *Fluid Phase Equilib.* 2012;317:110-126.
 66. Schmid B., Schedemann A., Gmehling J. "Extension of the VTPR Group Contribution Equation of State: Group Interaction Parameters for Additional 192 Group Combinations and Typical Results". *Ind Eng Chem Res.* 2014;53(3):3393-3405.
 67. Kumar S.K., Suter U.W., Reid R.C. "A statistical mechanics based lattice model equation of state". *Ind Eng Chem Res.* 1987;26(12):2532-2542.
 68. Sanchez I.C., Lacombe R.H. "Statistical thermodynamics of polymer solutions". *Macromolecules.* 1978;11(6):1145-1156.
 69. Panayiotou C., Vera J.H. "An Improved Lattice-Fluid Equation of State for Pure Component Polymeric Fluids". *Polym Eng Sci.* 1982;22(6):345-348.
 70. Panayiotou C., Vera J.H. "Statistical Thermodynamics of r-Mer Fluids and their mixtures". *Polym J.* 1982;14(9):681-694.
 71. Panayiotou C., Tsivintzelis I., Economou I.G. "Nonrandom hydrogen-bonding model of fluids and their mixtures. 2. Multicomponent mixtures". *Ind Eng Chem Res.* 2007;46(8):2628-2636.
 72. Panayiotou C., Tsivintzelis I., Economou I.G. "Nonrandom hydrogen-bonding model of fluids and their mixtures. 1. Pure Fluids". *Ind Eng Chem Res.* 2007;46(8):2628-2636.
 73. Grenner A., Tsivintzelis I., Economou I.G., Panayiotou C., "Kontogeorgis G.M. Evaluation of the Nonrandom Hydrogen Bonding (NRHB) Theory and the Simplified Perturbed-Chain - Statistical Associating Fluid Theory (sPC-SAFT). 1. Vapor - Liquid Equilibria". *Ind Eng Chem Res.* 2008;47:5636-5650.
 74. Tsivintzelis I., Economou I.G., Kontogeorgis G.M. "Modeling the phase behavior in mixtures of pharmaceuticals with liquid or supercritical solvents". *J Phys Chem B.* 2009;113(18):6446-6458.
 75. Tsivintzelis I., Economou I.G., Kontogeorgis G.M. "Modeling and simulation of the polymeric nanocapsule formation process". *AIChE J.* 2009;7:405-410.
 76. Tsivintzelis I., Grenner A., Economou I.G., Kontogeorgis G.M. "Equilibria and Prediction of Monomer Fraction in Hydrogen Bonding Systems". *Ind Eng Chem Res.* 2008;47:5651-5659.

77. McQuarrie D.A. "Statistical Mechanics". University Science Books Editions, California, US; 2000.
78. Lan S.S., Mansoori G.A. "Perturbation equation of state of pure fluids". *Int J Eng Sci.* 1976;14(3):307-317.
79. Chien C.H., Greenkorn R.A., Chao K.C. "Chain-of-Rotators Equation of State". *AIChE J.* 1983;29(4):560-571.
80. Chen S.S., Kreglewski A. "Applications of the Augmented van der Waals Theory of Fluids.: I. Pure Fluids". *Berichte der Bunsengesellschaft für Phys Chemie.* 1977;81(10):1048-1052.
81. Ikonomou D., Donohue M.D. "Thermodynamics of Hydrogen-Bonded Molecules : The Associated Perturbed Anisotropic Chain Theory". *AIChE J.* 1986;32(10):1716-1725.
82. George I., Donohue M.D. "Extension of the associated perturbed anisotropic chain theory to mixtures with more than one associating component". *Fluid Phase Equilib.* 1988;39(2):129-159.
83. Economou I.G., Tsonopoulos C. "Associating models and mixing rules in equations of state for water/hydrocarbon mixtures". *Chem Eng Sci.* 1997;52(4):511-525.
84. Vimalcttand P., Ikonomou G.D., Donohue M.D. "Correlation of equation of state parameters for the associated perturbed anisotropic chain theory". *Fluid Phase Equilib.* 1988;43(2-3):121-135.
85. Prigogine I. "The Molecular Theory of Solutions". North-Holland Editions, Amsterdam; 1957.
86. Boublik T., Nezbeda I. "Equation of state for hard dumbbells". *Chem Phys Lett.* 1977;46(2):315-316.
87. Alder B.J., Young D.A., Mark M. A. "Studies in Molecular Dynamics. X. Corrections to the Augmented van der Waals Theory for the Square Well Fluid". *J Chem Phys.* 1972;56(6):3013-3029.
88. Boublik T. "Statistical thermodynamics of convex molecule fluids". *Mol Phys.* 1974;27(5):1415-1427.
89. Twu H., Gubbins K.E. "Thermodynamics of polyatomic fluid mixtures-I: Theory". *Chem Eng Sci.* 1977;33:863-878.
90. Anderko A. "Extension of the AEOS model to systems containing any number of

- associating and inert components". *Fluid Phase Equilib.* 1989;50(1-2):21-52.
91. Anderko A. "A simple equation of state incorporating association". *Fluid Phase Equilib.* 1989;45(1):39-67.
 92. Heidemann R. A., Prausnitz J.M. "A van der Waals-type equation of state for fluids with associating molecules". *Proc Natl Acad Sci U S A.* 1976;73(6):1773-1776.
 93. Wertheim M.S. "Fluids of dimerizing hard spheres, and fluid mixtures of hard spheres and dispheres". *J Chem Phys.* 1986;85(5):2929-2936.
 94. Wei Y.S., Sadus R.J. "Equations of state for the calculation of fluid-phase equilibria". *AIChE J.* 2000;46(1):169-196.
 95. Colina C.M. "Thermodynamics and phase equilibria of carbon dioxide/polymer systems". North Carolina State University, 2004.
 96. Chapman W.G., Jackson G., Gubbins K.E. "Phase equilibria of associating fluids: Chain molecules with multiple bonding sites". *Mol Phys.* 1988;65(5):1057-1079.
 97. Banaszak M., Chiew Y.C., Radosz M. "Thermodynamic perturbation theory: Sticky chains and square-well chains". *Phys Rev E.* 1993;48(5):3760.
 98. Kraska T., Gubbins K.E. "Phase equilibria calculations with a modified SAFT equation of state. 2. Binary mixtures of n-alkanes, 1-alkanols, and water". *Ind Eng Chem Res.* 1996;35(2):4738-4746.
 99. Kraska T, Gubbins KE. Phase Equilibria Calculations with a Modified SAFT Equation of State. 1. Pure Alkanes, Alkanols, and Water. *Ind Eng Chem Res.* 1996;35(12):4727-4737.
 100. Blas F.J., Vega L.F. "Prediction of Binary and Ternary Diagrams Using the Statistical Associating Fluid Theory (SAFT) Equation of State". *Ind Eng Chem Res.* 1998;37(2):660-674.
 101. Gil-Villegas A., Galindo A., Whitehead P.J., Mills S.J., Jackson G., Burgess A.N. "Statistical associating fluid theory for chain molecules with attractive potentials of variable range". *J Chem Phys.* 1997;106(10):4168.
 102. Dominik A., Jain S., Chapman W.G. "New Equation of State for Polymer Solutions Based on the Statistical Associating Fluid Theory (SAFT)- Dimer Equation for Hard-Chain Molecules". *Ind Eng Chem Res.* 2007;46(17):5766-5774.
 103. Lymeriadis A., Adjiman C.S., Galindo A., Jackson G. "A group contribution method for associating chain molecules based on the statistical associating fluid theory (SAFT-

- gamma)". *J Chem Phys.* 2007;127(23):234903.
104. Lymeriadis A., Adjiman C.S., Jackson G., Galindo A. "A generalisation of the SAFT-gamma group contribution method for groups comprising multiple spherical segments". *Fluid Phase Equilib.* 2008;274(1-2):85-104.
 105. Tumakaka F., Gross J., Sadowski G. "Thermodynamic modeling of complex systems using PC-SAFT". *Fluid Phase Equilib.* 2005;228-229:89-98.
 106. Gross J., Vrabec J. "An equation-of-state contribution for polar components: Dipolar molecules". *AIChE J.* 2006;52(3):1194-1204.
 107. Huang S.H., Radosz M. "Equation of state for small, large, polydisperse and associating molecules". *Ind Eng Chem Res.* 1990;29(11):2284-2294.
 108. Oliveira M.B., Varanda FR, Marrucho IM, Queimada a. J, Coutinho J a. P. Prediction of Water Solubility in Biodiesel with the CPA Equation of State". *Ind Eng Chem Res.* 2008;47(12):4278-4285.
 109. Oliveira M.B., Pratas M.J., Marrucho I.M., Queimada A.J., Coutinho J.A.P. "Description of the Mutual Solubilities of Fatty Acids and Water With the CPA EoS". *AIChE J.* 2009;55(6):1604-1613.
 110. Oliveira M.B., Teles A.R.R., Queimada A.J., Coutinho J.A.P. "Phase equilibria of glycerol containing systems and their description with the Cubic-Plus-Association (CPA) Equation of State". *Fluid Phase Equilib.* 2009;280(1-2):22-29.
 111. Gros H.P., Bottini S., Brignole E.A. "Group contribution equation of state for associating mixtures". *Fluid Phase Equilib.* 1996;116(1 -2 pt 1):537-544.
 112. Skjold-Jørgensen S. "Gas solubility calculations. II. Application of a new group-contribution equation of state". *Fluid Phase Equilib.* 1984;16(3):317-351.
 113. Skjold-jørgensen S. "Group contribution equation of state (GC-EOS): A predictive method for phase equilibrium computations over wide ranges of temperature and pressures up to 30 MPa". *Ind Eng Chem Res.* 1988;27(1):110-118.
 114. Pereda S., Awan J.A., Mohammadi A.H., Valtz, A., Coquelet, C., Brignole, E.A., Richon, D. "Solubility of hydrocarbons in water: Experimental measurements and modeling using a group contribution with association equation of state (GCA-EoS)". *Fluid Phase Equilib.* 2009;275(1):52-59.
 115. Soria T.M., Sánchez F.A., Pereda S., Bottini S.B. "Modeling alcohol+water+hydrocarbon mixtures with the group contribution with association equation of state GCA-EoS". *Fluid*

- Phase Equilib.* 2010;296(2):116-124.
116. Gao W., Robinson R.L., Gasem K.A.M. "Solubilities of Hydrogen in Hexane and of Carbon Monoxide in Cyclohexane at Temperatures from 344.3 to 410.9 K and Pressures to 15 MPa". *J Chem Eng Data.* 2001;46:609-612.
 117. Ferrando N., Ungerer P. "Hydrogen/hydrocarbon phase equilibrium modelling with a cubic equation of state and a Monte Carlo method". *Fluid Phase Equilib.* 2007;254(1-2):211-223.
 118. Moysan J.M., Huron M.J., Paradowski H., Vidal J. "Prediction of the solubility of hydrogen in hydrocarbon solvents through cubic equations of state". *Chem Eng Sci.* 1983;38(7):1085-1092.
 119. Breman B.B., Beenackers A.A.C.M., Rietjens E.W.J., Stege R.J.H. "Gas-Liquid Solubilities of Carbon Monoxide, Carbon Dioxide, Hydrogen, Water, 1-Alcohols (n=1,2,3,4,5,6), and n-Paraffins (n=2,3,4,5,6) in Hexadecane, Octacosane, 1-Hexadecanol, Phenanthrene, and Tetraethylene Glycol at Pressures up to 5.5 MPa and Temperatures from 293 to 553 K". *J Chem Eng Data.* 1994;39(5):647-666.
 120. Park J., Robinson R.L., Gasem K.A.M. "Solubilities of Hydrogen in Heavy Normal Paraffins at Temperatures from 323.2 to 423.2 K and Pressures to 17.4 MPa". *J Chem Eng Data.* 1995;40:241-244.
 121. Gao W., Robinson R.L., Gasem K.A.M. "High-Pressure Solubilities of Hydrogen, Nitrogen, and Carbon Monoxide in Dodecane from 344 to 410 K at Pressures to 13.2 MPa". *J Chem Eng Data.* 1999;44:130-132.
 122. Huang S.H., Lin H-M., Tsai F-N., Chao K-C. "Solubility of Synthesis Gases in Heavy n - Paraffins and Fischer-Tropsch Wax". *Ind Eng Chem Res.* 1988;27:162-169.
 123. Twu C.H., Coon J.E., Harvey A.H., Cunningham J.R. "An Approach for the Application of a Cubic Equation of State to Hydrogen - Hydrocarbon Systems". *Ind Eng Chem Res.* 1996;35(5):905-910.
 124. Valderrama J., Cisternas L., Vergara M., Bosse M. "Binary interaction parameters in cubic equations of state for hydrogen-hydrocarbon mixtures". *Chem Eng Sci.* 1990;45:49-54.
 125. Huang H., Sandler S.I., Orbey H. "Vapor-liquid equilibria of some hydrogen + hydrocarbon systems with the Wong-Sandler mixing rule". *Fluid Phase Equilib.* 1994;96:143-153.
 126. Moysan J.M., Paradowski H., Vidal J. "Predictions of phase behavior of gas-containing

- systems with cubic equation of state". *Chem Eng Sci.* 1986;41(8):2069-2074.
127. Florusse L.J., Peters C.J., Pàmies J.C., Vega L.F., Meijer H. "Solubility of Hydrogen in Heavy n-Alkanes: Experiments and SAFT Modeling". *AIChE J.* 2003;49(12):3260-3269.
 128. Xie Z., Snavely W.K., Scurto A.M., Subramaniam B. "Solubilities of CO and H₂ in Neat and CO₂ -Expanded Hydroformylation Reaction Mixtures Containing 1-Octene and Nonanal up to 353 . 15 K and 9 MPa". *J Chem Eng Data.* 2009;54:1633-1642.
 129. Pereira C.G., Grandjean L., Betoulle S., Ferrando, N., Féjean, C., Lugo, R., de Hemptinne, J.C., Mougin, P. "Phase equilibria of systems containing aromatic oxygenated compounds with CH₄, CO₂, H₂, H₂S, CO and NH₃: Experimental data and predictions". *Fluid Phase Equilib.* 2014;382:219-234.
 130. Luehring P., Schumpe A. "Gas Solubilities (H₂, He , N₂, CO, O₂, Ar, CO₂,) in Organic Liquids at 293.2K". *J Chem Eng Data.* 1989;34:250-252.
 131. Jonasson A., Persson O., Rasmussen P., Soave G.S. "Vapor–liquid equilibria of systems containing acetic acid and gaseous components. Measurements and calculations by a cubic equation of state". *Fluid Phase Equilib.* 1998;152:67-94.
 132. Purwanto., Deshpande R.M., Chaudhari R. V., Delmas H. "Solubility of Hydrogen, Carbon Monoxide, and 1-Octene in Various Solvents and Solvent Mixtures". *J Chem Eng Data.* 1996;41(6):1414-1417.
 133. D'Angelo J.V.H., Francesconi A.Z. "Gas-Liquid Solubility of Hydrogen in n-Alcohols (n=1,2,3,4) at Pressures from 3.6 MPa to 10 MPa and Temperatures from 298.15 K to 525.15 K". *J Chem Eng Data.* 2001;46:671-674.
 134. Jonasson A., Persson O., Rasmussen P. "High-pressure Solubility of Hydrogen in Dimethyl Ether". *J Chem Eng Data.* 1996;40:1209-1210.
 135. Nguyen T-B, de Hemptinne J-C, Creton B, Kontogeorgis GM. Improving GC-PPC-SAFT equation of state for LLE of hydrocarbons and oxygenated compounds with water. *Fluid Phase Equilib.* 2014;372:113-125.
 136. Nguyen T-B., de Hemptinne J-C., Creton B., Kontogeorgis G.M. "GC-PPC-SAFT Equation of State for VLE and LLE of Hydrocarbons and Oxygenated Compounds. Sensitivity Analysis". *Ind Eng Chem Res.* 2013;52(21):7014-7029.
 137. Dohrn R., Peper S., Fonseca J.M.S. "High-pressure fluid-phase equilibria: Experimental methods and systems investigated (2000-2004)". *Fluid Phase Equilib.* 2010;288(1-2):1-54.

138. Fonseca J.M.S., Dohrn R., Peper S. "High-pressure fluid-phase equilibria: Experimental methods and systems investigated (2005-2008)". *Fluid Phase Equilib.* 2011;300(1-2):1-69.
139. Descamps C., Coquelet C., Bouallou C., Richon D. "Solubility of hydrogen in methanol at temperatures from 248.41 to 308.20K". *Thermochim Acta.* 2005;430(1-2):1-7.
140. Bezanehtak K., Combes G.B., Dehghani F., Foster N.R., Wales N.S. "Vapor - Liquid Equilibrium for Binary Systems of Carbon Dioxide + Methanol , Hydrogen + Methanol , and Hydrogen + Carbon Dioxide at High Pressures". *J Chem Eng Data.* 2002;60(32):161-168.
141. Katayama T., Nitta T. "Solubilities of Hydrogen and Nitrogen in Alcohols and n-Hexane". *J Chem Eng Data.* 1976;21(2):194-196.
142. Wainwright M.S., Ahn T., Trimm D.L., Cant N.W. "Solubility of Hydrogen in Alcohols and Esters". *J Chem Eng Data.* 1987;24(19):22-24.
143. Brunner E., Hultenschmidt W., Schlichtharle G. "Fluid mixtures at high pressures IV . Isothermal phase equilibria in binary mixtures consisting of (methanol + hydrogen or nitrogen or methane or carbon monoxide or carbon dioxide)". *J Chem Thermodyn.* 1987;19:273-291.
144. Brunner E., Hultenschmidt W. "Fluid mixtures at high pressures: VIII. Isothermal phase equilibria in the binary mixtures : (ethanol + hydrogen or methane or ethane)". *J Chem Thermodyn.* 1990;22(4):73-84.
145. Maxted E.B., Moon C.H. "The temperature coefficient of the solubility of hydrogen in organic solvents". *Trans Faraday Soc.* 1936;32:769-775.
146. Brunner E. "Fluid mixtures at high pressures III. Isothermal phase equilibria of (ethene + methanol)". *J Chem Thermodyn.* 1985;17:985-994.
147. Brunner E. "Solubility of Hydrogen in 10 Organic Solvents at 298.15, 323.15, and 373.15 K". *J Chem Eng Data.* 1985;30(3):269-273.
148. Brunner E. "Solubility of hydrogen in diols and their ethers". *J Chem Thermodyn.* 1980;12:993-1002.
149. Kim K.J., Way T.R., Feldman K.T. "Solubility of Hydrogen in Octane , 1-Octanol , and Squalane". *J Chem Eng Data.* 1997;42:214-215.
150. Xiuyang Lu, Zhaoli Wu YH. "Solubilities of Nz , Hz, Ar in 1-octanol at high pressure".

- Fluid Phase Equilib.* 1994;92:139-148.
151. Lenoir J., Renault P., Renon H. "Gas Chromatographic Determination of Henry's Constants of 12 Gases in 19 Solvents". *J Chem Eng Data*. 1971;16(3):340-342.
 152. Liu Q., Takemura F., Yabe A. "Solubility and Diffusivity of Carbon Monoxide in Liquid Methanol". *J Chem Eng Data*. 1996;41(3):589-592.
 153. Dake S.B., Chaudhari R.V. "Solubility of CO in Aqueous Mixtures of Methanol, Acetic Acid, Ethanol, and Propionic Acid". *J Chem Eng Data*. 1985;30(4):400-403.
 154. Bo S., Battino R., Wilhelm E. "Solubility of Gases in Liquids. 19. Solubility of He, Ne, Ar, Kr, Xe, N₂, O₂, CH₄, CF₄, and SF₆ in Normal 1-Alkanols n-C_nH_{2n+1}OH (1 ≤ n ≤ 11) at 298.15 K". *J Chem Eng Data*. 1993;38(4):611-616.
 155. Leu A-D., Carroll J.J., Robinson D.B. "The equilibrium phase properties of the methanol-hydrogen sulfide binary system". *Fluid Phase Equilib.* 1992;72:163-172.
 156. Fischer K., Chen J., Petri M., Gmehling J. "Solubility of H₂S and CO₂ in N-Octyl-2-pyrrolidone and of H₂S in Methanol and Benzene". *AIChE J.* 2002;48(4):887-893.
 157. Inomata H., Ikawa N., Arai K., Salto S. "Vapor-Liquid Equilibria for the Ammonia-Methanol-Water". *J Chem Eng Data*. 1988;33:26-29.
 158. Schäfer D., Xia J., Vogt M., Kamps Á.P.S., Maurer G. "Experimental investigation of the solubility of ammonia in methanol". *J Chem Eng Data*. 2007;52(5):1653-1659.
 159. Zeng Z., Chen J., Xue W., Huang L. "Measurement and Correlation of the Solubility of Ammonia in Ethanol between 277.35K and 318.25K". *Ind Eng Chem Res.* 2011;50(6):3592-3597.
 160. Huang L.J., Xue W.L., Zeng Z.X. "The Solubility of ammonia in ethanol between 277.35K and 328.15K". *Fluid Phase Equilib.* 2011;303(1):80-84.
 161. Wilcock R.J., Battino R., Danforth W.F., Wilhelm E. "Solubilities of gases in liquids II. The solubilities of He, Ne, Ar, Kr, O₂, N₂, CO, CO₂, CH₄, CF₄, and SF₆ in n-octane 1-octanol, n-decane, and 1-decanol". *J Chem Thermodyn.* 1978;10(9):817-822.
 162. Gamsjäger H., Lorimer J.W., Salomon M., Shaw D.G., Tomkins R.P.T. "The IUPAC-NIST Solubility Data Series: A Guide to Preparation and Use of Compilations and Evaluations". *J Phys Chem Ref Data*. 2010;39(2):023101.
 163. Eslamimanesh A., Mohammadi A.H., Richon D. "Thermodynamic consistency test for experimental solubility data in carbon dioxide/methane + water system inside and outside

- gas hydrate formation region". *J Chem Eng Data*. 2011;56(4):1573-1586.
164. Trejos V.M., López J.A., Cardona C.A. "Thermodynamic consistency of experimental VLE data for asymmetric binary mixtures at high pressures". *Fluid Phase Equilib*. 2010;293(1):1-10.
 165. Rowley R.L., Wilding W.V., Congote A., Giles N.F. "The use of database influence factors to maintain currency in an evaluated chemical database". *Int J Thermophys*. 2010;31(4-5):860-874.
 166. Diky V., Muzny C.D., Lemmon E.W., Chirico R.D., Frenkel M. "ThermoData Engine (TDE): Software implementation of the dynamic data evaluation concept. 2. Equations of state on demand and dynamic updates over the web". *J Chem Inf Model*. 2007;47(4):1713-1725.
 167. Frenkel M., Chirico R.D., Diky V., Yan X., Dong Q., Muzny C.D. "ThermoData Engine (TDE) software implementation of the dynamic data evaluation concept". *J Chem Inf Model*. 2005;45:816-838.
 168. Mathias P.M., Watanasiri S. "Some Patterns of Fluid Phase Behavior". *J Chem Eng Data*. 2011;56(4):1658-1665.
 169. Wilsak R., Thodos G. "Critical assessment of four vapor pressure functions over the complete vapor-liquid coexistence region". *Ind Eng Chem Fundam*. 1984;23(1):75-82. [http](http://).
 170. Othmer D.F. "Correlating Vapor Pressure and Latent Heat Data: A New Plot". *Ind Eng Chem*. 1940;32(6):841.
 171. Rozmus J., de Hemptinne J-C., Ferrando N., Mougín P. "Long chain multifunctional molecules with GC-PPC-SAFT: Limits of data and model". *Fluid Phase Equilib*. 2012;329:78-85.
 172. Ungerer P., Tavitian B., Boutin A. "Applications of Molecular Simulation in the Oil and Gas Industry". Technip Editions. Paris, France; 2005.
 173. Hinkle K.R., Mathias P.M., Murad S. "Evaluation and extrapolation of the solubility of H₂ and CO in n-alkanes and n-alcohols using molecular simulation". *Fluid Phase Equilib*. 2014;384:43-49.
 174. Ungerer P. "From Organic Geochemistry to Statistical Thermodynamics: the Development of Simulation Methods for the Petroleum Industry". *Oil Gas Sci Technol*. 2003;58(2):271-297.

175. Bourasseau E., Ungerer P., Boutin A. "Prediction of Equilibrium Properties of Cyclic Alkanes by Monte Carlo Simulations New Anisotropic United Atoms Intermolecular Potentials New Transfer Bias Method". *J Phys Chem*. 2002;106:5483-5491.
176. Kranias S., Pattou D., Lévy B., Boutin A. "An optimized potential for phase equilibria calculation for ketone and aldehyde molecular fluids". *Phys Chem Chem Phys*. 2003;5(19):4175.
177. Boutard Y., Ungerer P., Teuler J.M., Ahunbay, M.G., Sabater, S.F., Pérez-Pellitero, J., Mackie, A.D., Bourasseau, E. "Extension of the anisotropic united atoms intermolecular potential to amines, amides and alkanols". *Fluid Phase Equilib*. 2005;236(1-2):25-41.
178. Ferrando N., Lachet V., Teuler J-M., Boutin A. "Transferable force field for alcohols and polyalcohols". *J Phys Chem B*. 2009;113(17):5985-5995.
179. Ungerer P., Lachet V., Tavitian B. "Applications of Molecular Simulation in Oil and Gas Production and Processing". *Oil Gas Sci Technol - Rev l'IFP*. 2006;61(3):387-403.
180. Hirschfelder J.O., Curtiss C.F., Bird R.B. "The Molecular Theory of Gases and Liquids". University of Wisconsin; 1954.
181. Rzepka M., Lamp P., de la Casa-Lillo M.A. "Physisorption of Hydrogen on Microporous Carbon and Carbon Nanotubes". *J Phys Chem B*. 2000;102:10894-10898.
182. Yin Y.F., Mays T., McEnaney B. "Molecular Simulations of Hydrogen Storage in Carbon Nanotube Arrays". *Langmuir*. 2000;16(26):10521-10527.
183. Zhang X., Cao D., Chen J. "Hydrogen Adsorption Storage on Single-Walled Carbon Nanotube Arrays by a Combination of Classical Potential and Density Functional Theory". *J Phys Chem B*. 2003;107(21):4942-4950.
184. Potoff J.J., Panagiotopoulos A.Z. "Critical point and phase behavior of the pure fluid and a Lennard-Jones mixture". *J Chem Phys*. 1998;109(24):10914.
185. Cracknell R.F. "Molecular simulation of hydrogen adsorption in graphitic nanofibres". *Phys Chem Chem Phys*. 2001;3:2091-2097.
186. Darkrim F., Vermesse J., Malbrunot P., Levesque D. "Monte Carlo simulations of nitrogen and hydrogen physisorption at high pressures and room temperature. Comparison with experiments". *J Chem Phys*. 1999;110(8):4020.
187. Cornell W.D., Cieplak P., Bayly C.I., Gould I.R., Merz K.M., Ferguson D.M., Spellmeyer, D.C., Fox T., Caldwell J.W., Kollman P.A. "A Second Generation Force Field for the Simulation of Proteins, Nucleic Acids, and Organic Molecules". *J Am Chem Soc*.

- 1995;117(6):5179-5197.
188. Jorgensen W.L., Maxwell D.S., Tirado-Rives J. "Development and Testing of the OPLS All-Atom Force Field on Conformational Energetics and Properties of Organic Liquids". *J Am Chem Soc.* 1996;118(15):11225-11236.
189. Mackerell A.D., Wirkiewicz-Kuczera J., Karplus M. "An All-Atom Empirical Energy Function for the Simulation of Nucleic Acids". *J Am Chem Soc.* 1995;117(6):11946-11975.
190. Sun H. "COMPASS: An ab Initio Force-Field Optimized for Condensed-Phase Applications s Overview with Details on Alkane and Benzene Compounds". *J Phys Chem B.* 1998;102:7338-7364.
191. Martin M.G., Siepmann J.I. "Transferable Potentials for Phase Equilibria. 1. United-Atom Description of n-Alkanes". *J Phys Chem B.* 1998;5647(97):2569-2577.
192. Jorgensen W.L., Madura J.D., Swenson C.J. "Optimized Intermolecular Potential Functions for Liquid Hydrocarbons". *J Am Chem Soc.* 1984;106(20):6638-6646.
193. Toxvaerd S. "Molecular dynamics calculation of the equation of state of alkanes". *J Chem Phys.* 1990;93(6):4290.
194. Toxvaerd S. "Equation of state of alkanes II". *J Chem Phys.* 1997;107(13):5197.
195. Ungerer P., Beauvais C., Delhommelle J., Boutin A., Rousseau B., Fuchs A.H. "Optimization of the anisotropic united atoms intermolecular potential for n-alkanes". *J Chem Phys.* 2000;112(12):5499.
196. Ferrando N., Lachet V., Boutin A. "Transferable force field for carboxylate esters: application to fatty acid methylic ester phase equilibria prediction". *J Phys Chem B.* 2012;116(10):3239-3248.
197. Ferrando N., Lachet V., Pérez-Pellitero J., Mackie A.D., Malfreyt P., Boutin A. "A transferable force field to predict phase equilibria and surface tension of ethers and glycol ethers". *J Phys Chem B.* 2011;115(36):10654-10664.
198. Ferrando N., Gedik I., Lachet V., Pigeon L., Lugo R. "Prediction of phase equilibrium and hydration free energy of carboxylic acids by Monte Carlo simulations". *J Phys Chem B.* 2013;117(23):7123-7132.
199. Ferrando N., Boutin A., Lachet V. "Monte Carlo Simulations of Mixtures Involving Ketones and Aldehydes by a Direct Bubble Pressure Calculation". *J Phys Chem.*

- 2010;114:8680-8688.
200. Ferrando N., de Hemptinne J-C., Mougin P., Passarello J-P. "Prediction of the PC-SAFT associating parameters by molecular simulation". *J Phys Chem B*. 2012;116(1):367-377.
 201. Asphaug S. "Catalytic Hydrodeoxygenation of Bio-oils with Supported MoP-Catalysts". Thesis, Norwegian University of Science and Technology, 2013.
 202. Parapati D.R., Guda V.K., Penmetsa V.K., Steele P.H., Tanneru S.K. "Single Stage Hydroprocessing of Pyrolysis Oil in a Continuous Packed-Bed Reactor". *Environ Prog Sustain Energy*. 2014;33(3):726-731.
 203. Agblevor F.A., Mante O., McClung R., Oyama S.T. "Co-processing of standard gas oil and biocrude oil to hydrocarbon fuels". *Biomass and Bioenergy*. 2012;45:130-137.
 204. Venderbosch R.H., Ardiyanti A.R., Wildschut J., Oasmaa A., Heeres H.J. "Stabilization of biomass-derived pyrolysis oils". *J Chem Technol Biotechnol*. 2010;85(5):674-686.
 205. Furimsky E. "Review: Catalytic hydrodeoxygenation". *Appl Catal A Gen*. 2000;199(2):147-190.
 206. Yorizane M., Sadamoto S., Masuoka H., Eto Y. "Gas solubilities in methanol at high pressures". *Kogyo Kagaku Zasshi*. 1969;72:2174-2177.
 207. Krichevskii I.R., Efremova G.D. "Phase and volume relations in liquid-gas systems at high pressures. III". *Zh Fiz Khim*. 1951;25:577-583.
 208. Krichevskii I.R., Zhavoronkov N.M., Tsiklis D.S. "Solubility of hydrogen, carbon oxide and their mixtures in methanol under pressure". *Zh Fiz Khim*. 1937;9:317-328.
 209. Michels A., de Graaff W., van der Somme J. "Gas-Liquid Phase Equilibrium in the System Methanol - Hydrogen". *Appl Sci Res*. 1953;4(5):105-108.
 210. Choudhary V.R., Sane M.G., Vadgaonkar H.G. "Solubility of Hydrogen in methanol Containing Reaction Species for Hydrogenation of o-Nitrophenol". *J Chem Eng Data*. 1986;31(3):294-296.
 211. Horstmann S., Grybat A., Ihmels C.E., Gmehling J. "LTP-Research Groups Unpublished Phase Equilibrium Data". ; 2010.
 212. Shenderei E.R., Zel'venskii Y.A.D., Ivanovskii F.P. "Solubility of Hydrogen, Nitrogen and Methane in Methanol under Pressure at low Temperatures". *Gazov Promst*. 1961;6(3):42-45.

213. Makranczy J., Ruzs L., Balog-Megyery K. "Solubility of gases in normal alcohols". *Hung J Ind Chem*. 1979;7:41-46.
214. Just G. "Solubility of Gases in Organic Solvents". *Z Phys Chem Stoechiom Verwandtschaftsl*. 1901;37:342-367.
215. Ipatiev W.W., Drushina-Artemovich, S.I., Tichomirov W.I. "Solubility of Hydrogen in Water under Pressure". *Ber Dtsch Chem Ges B*. 1932;65:568-571.
216. Radhakrishnan K., Ramachandran P.A., Chaudhari R.V. "Solubility of Hydrogen in Methanol, Nitrobenzene, and Their Mixtures. Experimental Data and Correlation". *J Chem Eng Data*. 1983;28(1):1-4.
217. Timofeev V. "The Absorption of Hydrogen and Oxygen in Water and Alcohol". *Z Phys Chem Stoechiom Verwandtschaftsl*. 1890;6:141-152.
218. Brunner E. "Solubility of Hydrogen in Alcohols". *Phys Chem*. 1979;83(7):715-721.
219. Naumova A.A., Tyvina T.N., Kulik V.K. "Liquid-gas equilibrium in the system n-butanol - hydrogen". *J Appl Chem USSR*. 1981;54(3):422-424.
220. Tyvina T.N., Valuev K.I., Vasil'eva I.I., Sokolov B.I., Kharchenko A.I. "Gas-liquid equilibrium in systems formed by hydrogen with butanols". *J Appl Chem USSR*. 1977;50(11):2446-2449.
221. Ijams C.C. "Studies on the Solubility of Gases in Non-Aqueous Solvents". California University; 1941.
222. Preuss H., Roscher T. "Solubility of Hydrogen in 1-Tetradecanol". FIZ Report; 1978.
223. Vasileva I.I., Naumova A.A., Polyakov A.A., Tyvina T.N., Fokina V.V. "Composition and molar volume of hydrogen, nitrogen and methane solutions in propionic aldehyde". *Zh Prikl Khim*. 1987;60(2):408-410.
224. Aronovich R.A., Vasil'eva I.I., Loktev S.M, Naumova, A.A., Polyakov, A.A., Slivinskii, E. V., Tyvina, T. N. "Solubility and volume behavior of solutions of hydrogen and carbon monoxide in 2-methylbutanal". *Theor Exp Chem*. 1991;27(2):218-220.
225. Jauregui-Haza U.J., Pardillo-Fontdevila E.J., Wilhelm M., Delmas H. "Solubility of hydrogen and carbon monoxide in water and some organic solvents". *Lat Am Appl Res*. 2004;34:71-74.
226. Richter D. "Phase behavior and viscosity of systems comprising triglycerides, hydrogen, carbon dioxide, propane and dimethyl ether". Thesis, Universitaet Erlangen - Nuernberg,

- 2000.
227. Horiuti J. "On the Solubility of Gas and Coefficient of Dilatation by Absorption". *Sci Pap Inst Phys Chem Res Jpn.* 1931;17(341):125-256.
228. Christoff A. "The Dependence of the Absorption from the Surface Tension". *Z Phys Chem Stoechiom Verwandtschaftsl.* 1912;79:456-460.
229. Guerry D. Thesis Calculation of Results; 1944.
230. Gallardo M.A., Lopez M.C., Urieta J.S., Gutierrez C. "Solubility of 15 non-polar gases (He, Ne, Ar, Kr, Xe, H₂, D₂, N₂, O₂, CH₄, C₂H₄, C₂H₆, CF₄, SF₆ and CO₂) in cycloheptanone". *Fluid Phase Equilib.* 1990;58(1-2):159-172.
231. Herskowitz M., Wlsnlak J., Skladman L. "Hydrogen Solubility in Organic Liquids". *J Chem Eng Data.* 1983;28(2):164-166.
232. Tyvina T.N., Fokina V.V., Polyakov A.A. "Phase and volume relationships in the systems carbon monoxide - cyclohexanone and hydrogen - cyclohexanone". *J Appl Chem USSR.* 1985;58(2):393-396.
233. Trust D.B. "The Heterogeneous Phase Behavior of the Hydrogen - Propane, Carbon Monoxide - Propane and Hydrogen - Carbon Monoxide - Propane Systems". Thesis, University of Kansas, Lawrence, Kansas, 1968.
234. Trust D.B., Kurata F. "Vapor-Liquid Phase Behavior of the Hydrogen - Propane and Hydrogen - Carbon Monoxide - Propane Systems". *AIChE J.* 1971;17(1):86-91.
235. Williams R.B., Katz D.L. "Vapor Liquid Equilibria in Binary Systems. Hydrogen with Ethylene, Ethane, Propylene, and propane". *Ind Eng Chem.* 1954;46(12):2512-2520.
236. Bol'shakov P.E., Linshits L.R. "Phase equilibria in liquid-gas systems at high pressures". *Tr Gos Nauchno Issled Proektn Inst Azotn Promst Prod Org Sin.* 1954;3:18-27.
237. Toplieu K.T., Burriss W.L., Hsu N.T., Rearick H.H., Sage B.H. "Phase Behavior of the Hydrogen- Propane System". *Ind Eng Chem.* 1953;45(1):210-213.
238. Klink A.E., Chen H.Y., Amick E.H. "The Vapor-Liquid Equilibrium of the Hydrogen - n-Butane System at Elevated Pressures". *AIChE J.* 1975;21:1142-1148.
239. Nelson E.E., Bonnele W.S. "Solubility of Hydrogen in n-butane". *Ind Eng Chem.* 1943;35(2):204-206.
240. Augood D.R. "The Separation of HD and H₂ by Absorptive Fractionation". *Trans Inst*

- Chem Eng.* 1957;35:394-408.
241. Aroyanl H.J., Katz D.L. "Low Temperature Vapor-Liquid Equilibria". *Ind Eng Chem.* 1951;43(1):185-189.
242. Freitag P., Robinson B. "Equilibrium Phase Properties of the Hydrogen - Methane - Carbon Dioxide, Hydrogen - Carbon Dioxide - n-Pentane and Hydrogen - n-Pentane Systems". *Fluid Phase Equilib.* 1986;31(2):183-201.
243. Connolly J.F., Kandalic G.A. "Gas Solubilities, Vapor-Liquid Equilibria, and Partial Molal Volumes in Some Hydrogen-Hydrocarbon Systems". *J Chem Eng Data.* 1986;31(4):396-406.
244. Makranczy J., Megyery-Balog K., Ruesz L., Patyi L. "Solubility of gases in normal-alkanes". *Hung J Ind Chem.* 1976;4(2):269-280.
245. Nichols W.B., Reamer H.H., Sage B.H. "Volumetric and Phase Behavior in the Hydrogen - n-Hexane System". *AIChE J.* 1957;3(2):262-267.
246. Waters J.A., Mortimer G.A., Clements H.E. "Solubility of some light hydrocarbons and hydrogen in some organic solvents". *J Chem Eng Data.* 1970;15(1):174-176.
247. Zernov V.S., Kogan V.B., Egudina O.G., Kobayakov V.M., Babayants T.V., Kalichava L.I. "Phase Equilibria and Volume Ratios in the Systems Heptane - Ethylene". *J Appl Chem USSR.* 1990;63(7):1469-1472.
248. Peter S., Reinhartz K. "The phase equilibrium in the systems H₂ - n-heptane, H₂ - methylcyclohexane and H₂ - 2,2,4-trimethylpentane at higher pressures and temperatures". *Z Phys Chem NF.* 1960;24:103-118.
249. Peramanu S., Pruden B.P. "Solubility Study for the Purification of Hydrogen from High Pressure Hydrocracker Off-gas by an Absorption-Stripping Process". *Can J Chem Eng.* 1997;75:535-543.
250. Ene R., Bica I., Sandulescu D. "Determination of hydrogen solubility in liquid hydrocarbons at atmospheric pressure". *Rev Roum Chim.* 1982;27(5):609-613.
251. Yen L.C, McKetta J.J. "Solubility of Nitrous Oxide in Some Nonpolar Solvents". *J Chem Eng Data.* 1957;288(1):288-289.
252. Lachowicz S.K., Newitt D.M., Weale K.E. "The solubility of hydrogen and deuterium in n-heptane and n-octane at high pressures". *Trans Faraday Soc.* 1955;51:1198-1205.
253. Connolly J.F. "Vapor-Liquid Equilibrium Ratios for Four Binary Systems". *Proc Amer*

- Pet Inst Sec 3*. 1965;45:62-67.
254. Connolly J.F., Kandalic G.A. "Thermodynamic properties of solutions of hydrogen in n-octane". *J Chem Thermodyn*. 1989;21(8):851-858.
255. Thomsen E.S., Gjaldbaek J.C. "The Solubility of Hydrogen, Nitrogen, Oxygen and Ethane in Normal Hydrocarbons". *Acta Chem Scand 1947-1973*. 1963;17(1):127-133.
256. Sebastian H.M., Sfmnick J.J., Lin H-M., Chao K-C. "Gas-Liquid Equilibrium in the Hydrogen + n-Decane System at Elevated Temperatures and Pressures". *J Chem Eng Data*. 1980;25(1):68-70.
257. Sokolov V.I., Polyakov A.A. "Solubility of hydrogen in n-decane, n-tetradecane, 1-hexene, 1-pentene, 4-octene, isopropylbenzene, 1-methylnaphthalene, and decalin". *J Appl Chem USSR*. 1977;50(6):1347-1349.
258. Schofield B.A., Ring, Z.E., Missen R.W. "Solubility of Hydrogen in a White Oil". *Can J Chem Eng*. 1992;70:822-824.
259. Dohrn R., Brunner G. "Phase equilibria in ternary and quaternary systems of hydrogen, water and hydrocarbons at elevated temperatures and pressures". *Fluid Phase Equilib*. 1986;29:535-544.
260. Prausnitz J.M., Cukor P.M. "Solubilities of Gases in Liquids at Elevated Temperatures. Henry's Constants for Hydrogen, Methane, and Ethane in Hexadecane, Bicyclohexyl, and Diphenylmethane". *J Phys Chem*. 1972;76(4):598-601.
261. Graaf H., Smit J., Stamhuis J., Beenackers A.C.M. "Gas-Liquid Solubilities of the Methanol Synthesis Components in Various Solvents". *J Chem Eng Data*. 1992;37:146-158.
262. Fahim M.A., Elkilani A.S. "Prediction of the Solubility of Hydrogen in Naphtha Reformate Using the Modified UNIFAC Group Contribution Method". *Ind Eng Chem Res*. 1991;30:255-259.
263. Matsumoto D.K., Satterfield C.N. "Solubility of Hydrogen and Carbon Monoxide in Selected Nonaqueous Liquids". *Ind Eng Chem Process Des Dev*. 1985;24(4):1297-1300.
264. Miller S.A, Ekstrom A., Foster N.R. "Solubility and Mass-Transfer Coefficients for Hydrogen and Carbon Monoxide in n-Octacosane". *J Chem Eng Data*. 1990;35(3):125-127.
265. Ugrozov V.V. "Equilibrium Compositions of Vapor-Gas Mixtures over Solutions". *Russ J*

- Phys Chem.* 1996;70(7):1240-1241.
266. Ipat'ev V.V., Teodorovich V.P. "Solubility of hydrogen in water under pressure at high temperatures". *Zh Obs Khim.* 1934;4:395-399.
267. Maslennikova V.Y., Goryunova N.P., Subbotina L.A., Tsiklis D.S. "The Solubility of Water in Compressed Hydrogen". *Russ J Phys Chem.* 1976;50(2):240-243.
268. Gillespie P.C., Wilson G.M. "Vapor-Liquid Equilibrium Data on Water-Substitute Gas Components: N₂ - H₂O, H₂ - H₂O, CO - H₂O, H₂ - CO - H₂O, and H₂S - H₂O". GPA Report. Tulsa, Okla; 1980.
269. Wiebe R., Gaddy V.L. "The Solubility of Hydrogen in Water at 0, 50, 75 and 100 °C from 25 to 1000 Atmospheres". *J Am Chem Soc.* 1934;56:76-79.
270. Kling G., Maurer G. "The solubility of hydrogen in water and in 2-aminoethanol at temperatures between 323 K and 423 K and pressures up to 16 MPa". *J Chem Thermodyn.* 1991;23:531-541.
271. Piontek H.D. "Determining the composition of the liquid phases of the system H₂ - H₂O - tetralin at pressures between 50 and 300 bar and temperatures between 50 and 150 °C". Thesis, Universität Dortmund, 1986.
272. DeVaney W., Berryman J.M., Kao P.L., Eakin B. "High Temperature VLE Measurements for Substitute Gas Components", GPA Research Report.; 1978.
273. Winkler L.W. "Regularity in the Absorption of Gases in Liquids (Second Communication)". *Z Phys Chem Stoechiom Verwandtschaftsl.* 1906;55:344-354.
274. Winkler L.W. "The solubility of gases in water (first treatise)". *Ber Dtsch Chem Ges.* 1891;24:89-101.
275. Huefner G. "Study of the Absorption of Nitrogen and Hydrogen in Aqueous Solutions". *Z Phys Chem Stoechiom Verwandtschaftsl.* 1907;57:611-625.
276. De Wet W.J. "Determination of gas solubilities in water and some organic liquids". *J S Afr Chem Inst.* 1964;17:9-13.
277. Gniewosz S., Walfisz A. "The Absorption of Gases by Petroleum". *Z Phys Chem Stoechiom Verwandtschaftsl.* 1887;1:70-72.
278. Choudary V.R., Parande M.G., Brahme P.H. "Simple Apparatus for Measuring Solubility of Gases at High Pressures". *Ind Eng Chem Fundam.* 1982;21(4):472-474.

279. Longo L.D., Delivora-Papadopoulos M., Power G.G., Hill E.P., Forster R.E. "Diffusion equilibration of inert gases between maternal and fetal placental capillaries". *Am J Physiol.* 1970;219(3):561-569.
280. Power G.G., Stegall H. "Solubility of gases in human red blood cell ghosts". *J Appl Physiol.* 1970;29(2):145-149.
281. Mueller C. "The Absorption of Oxygen, Nitrogen and Hydrogen in Aqueous Solution of Non-Electrolytes". *Z Phys Chem Stoechiom Verwandtschaftsl.* 1912;81:483-503.
282. Gordon L.I., Cohen Y., Standley D.R. "The solubility of molecular hydrogen in seawater". *Deep Res.* 1977;24:937-941.
283. Amlie R.F., Ruetschi P. "Solubility of Hydrogen in Potassium Hydroxide and Sulfuric Acid . Salting-out and Hydration". *J Phys Chem.* 1966;622(6):718-723.
284. Crozier T.E., Yamamoto S. "Solubility of Hydrogen in Water , Seawater , and NaCl Solutions". *J Chem Eng Data.* 1974;19(3):242-244.
285. Bunsen R. "On the Law of Absorption of Gases". *Philos Mag J Sci.* 1855;9:116-130.
286. Milligan L.H. "The Solubility of Gasoline (Hexane and Heptane) in Water at 25 °C". *J Phys Chem.* 1925;28:494-497.
287. Gerecke J., Bittrich H.J. "The solubilities of H₂, CO₂ and NH₃ in an aqueous electrolyte solution". *Wiss Z Tech Hochsch Chem Leuna-mersebg.* 1971;13(2):115-122.
288. Gerecke J. "A contribution to the gas solubility in electrolyte solutions examined using the example of the solubility of H₂, CO₂ and NH₃ in water and in aqueous salt solutions". Thesis, TH Carl Schorlemmer, Leuna-Merseburg, 1969.
289. Geffcken G. "Contribution on the Knowledge of the Interference of Solubility". *Z Phys Chem Stoechiom Verwandtschaftsl.* 1904;49:257-302.
290. Findlay A., Shen B. "The influence of colloids and fine suspensions on the solubility of gases in water. Part II. Solubility of carbon dioxide and of hydrogen". *J Chem Soc, Trans.* 1912;101:1459-1468.
291. Lubarsch O. "The Absorption of Gases in Mixtures of Alcohol and Water". *Ann Phys Leipzig.* 1889;273(7):524-525.
292. Drucker K., Moles E. "Gas Solubility in Aqueous Solutions of Glycerol and Isobutyric Acid". *Z Phys Chem Stoechiom Verwandtschaftsl.* 1910;75:405-436.

293. Battino R., Wilhelm. E. "IUPAC Solubility Data Series". Pergamon, Oxford; 1981.
294. Morris D.R., Yang L., Giraudeau F., Steward F.R. "Henry's law constant for hydrogen in natural water and deuterium in heavy water". *Phys Chem Chem Phys*. 2001;3:1043-1046.
295. Stephen E.F., Hatfield N.S., People R.S., Pray H.A. "Battelle Memorial Report, BMI-1067". Columbus, US; 1956.
296. Alvarez J., Fernández-Prini R. "A semiempirical procedure to describe the thermodynamics of dissolution of non-polar gases in water". *Fluid Phase Equilib*. 1991;66(3):309-326.
297. Jung J. "Solubility of carbon Monoxide and Hydrogen in Water between 0 and 300 °C". 1962.
298. Pray H.A., Schweickert C.E., Minnich B.H. "Solubility of Hydrogen , Oxygen , Nitrogen , and Helium in Water". *Ind Eng Chem*. 1950;44(5):1146-1151.
299. Ahrens M., Heusler K.E. "Solubilities of Some Gases in Liquid Ammonia". *Z Phys Chem*. 1981;125:127-128.
300. Morrison T.J., Billett F. "The Salting-Out of Non-Electrolytes. Part II. The Effect of Variation in Non-Electrolytes". *J Chem Soc*. 1952:3819-3822.
301. Leskin V.V., Tudorovskaya G.L., Larionov V.A., Safonova N.A., Sedacheva N.P. "Solubility of hydrogen in the water - N-methylpyrrolidone solutions". *Depos Doc Oniitekhim*. 1984:1-9.
302. Tsonopoulos C., Wilson G.M. "High-temperature mutual solubilities of hydrocarbons and water. Part I: Benzene, cyclohexane and n-hexane". *AIChE J*. 1983;29(6):990-999.
303. Harvey A.H. "Semiempirical correlation for Henry's constants over large temperature ranges". *AIChE J*. 1996;42(5):1491-1494.
304. Robinson D.B., Peng D.Y. "The Characterization of the Heptanes and Heavier Fractions for the GPA Peng-Robinson Programs, Research Report RR-28, Project 756", booklet Only Sold by Gas Processors Association.; 1978.
305. Carroll J.J. "Henry's law revisited". *Chem Eng Prog*. 1999;1:49-56.
306. Harvey A.H. "Applications of Near-Critical Dilute-Solution Thermodynamics". *Ind Eng Chem Res*. 1998;37(3):3080-3088.
307. The DIPPR Information and Data Evaluation Manager for the Design Institute for

- Physical Properties, version 7.0.0, Database Date: 2012.
308. Abascal J.L.F., Vega C. "A general purpose model for the condensed phases of water: TIP4P/2005". *J Chem Phys.* 2005;123(23):234505.
 309. Allen M.P., Tildesley D.J. "Computer Simulation of Liquids". University Oxford; 1987.
 310. Beck T.L. "Quantum path integral extension of Widom's test particle method for chemical potentials with application to isotope effects on hydrogen solubilities in model solids". *J Chem Phys.* 1992;96(9):7175.
 311. Wang Q. "Thermodynamic properties and phase equilibrium of fluid hydrogen from path integral simulations". *Mol Phys.* 1996;89(4):1105-1119.
 312. Adams D.J., McDonald I.R. "Fluids of hard spheres with nonadditive diameters". *J Chem Phys.* 1975;63(5):1900.
 313. Dickinson E. "On the thermodynamics of polydisperse systems of non-additive hard particles". *Chem Phys Lett.* 1976;66(3):1-5.
 314. Gazzillo D. "Fluid-fluid phase separation of nonadditive hard-sphere mixtures as predicted by integral-equation theories". *J Chem Phys.* 1991;95(6):4565.
 315. Jagannathan K., Reddy G., Yethiraj A. "Integral equation theory for symmetric nonadditive hard sphere mixtures". *J Phys Chem B.* 2005;109(14):6764-6768.
 316. Rovere M., Pastore G. "Fluid-fluid phase separation in binary mixtures of asymmetric non-additive hard spheres". *J Phys Condens Matter.* 1994;6(23A):A163-A166.
 317. Saija F, Giaquinta P V. Entropy and Fluid - Fluid Separation in Nonadditive Hard-Sphere Mixtures: The Asymmetric Case. *J Phys Chem B.* 1998;106:2035-2040.
 318. Santos A., López De Haro M., Yuste S.B. "Equation of state of nonadditive d-dimensional hard-sphere mixtures". *J Chem Phys.* 2005;122(2).
 319. Hammawa H., Hamad E.Z. "A simple model for size non-additive mixtures". *J Chem Soc, Faraday Trans.,* 1996;92(24):4943-4949.
 320. Abu-Sharkh B.F., Hamad E.Z. "Simulation and Model Development for the Equation of State of Self-Assembling Nonadditive Hard Chains". *Macromolecules.* 2000;33(4):1345-1350.
 321. Abu-Sharkh B.F., Hamad E.Z. "Investigation of the Microstructure of Micelles Formed by Hard-Sphere Chains Interacting via Size Nonadditivity by Discontinuous Molecular

- Dynamics Simulation". *Langmuir*. 2004;20(1):254-259.
322. Gross J., Sadowski G. "Application of perturbation theory to a hard-chain reference fluid: an equation of state for square-well chains". *Fluid Phase Equilib*. 2000;168:183-199.
323. Malakhov A.O., Volkov V.V. "Phase behavior of polymer mixtures with nonadditive hard-sphere potential". *Polym Sci Ser A*. 2007;49(6):745-756.
324. Adidharma H., Radosz M. "Prototype of an Engineering Equation of State for Heterosegmented". *Ind Eng Chem Res*. 1998;37(11):4453-4462.
325. Tavares F.W., Chang J., Sandler S.I. "A completely analytic equation of state for the square-well chain fluid of variable well width". *Fluid Phase Equilib*. 1997;140:129-143.
326. Hansen J.P., McDonald I.R. "Theory of Simple Liquids; 3rd Edition". Academic Press Editions, London, England; 2005.
327. Lyra Paredes M.L., dos Reis R.A., Tavares F.W. "Inner segment radial distribution functions at contact point for chain-like molecules". *J Mol Liq*. 2009;147(3):198-210.
328. Chiew Y.C. "Percus-Yevick integral-equation theory for athermal hard-sphere chains, Part I: Equations of state". *Mol Phys*. 1990;70(1):129-143.
329. Chiew Y.C. "Percus-Yevick integral equation theory for athermal hard-sphere chains". *Mol Phys*. 1991;73(2):359-373.
330. Yethiraj A., Hall C.K., Honnell K.G. "Site-site correlations in short chain fluids". *J Chem Phys*. 1990;93(6):4453.
331. Honnell K.G., Hall C.K. "A new equation of state for athermal chains". *J Chem Phys*. 1989;90(3):1841.
332. Dickman R., Hall C.K. "Equation of state for chain molecules: Continuous-space analog of Flory theory". *J Chem Phys*. 1986;85(7):4108.
333. Zhang B., Liang S., Lu Y. "Calculating thermodynamic properties from perturbation theory II . An analytic representation for the square-well chain fluid". *Fluid Phase Equilib*. 2001;180:183-194.
334. Tavares F.W., Chang J., Sandler S.I. "Equation of state for the square-well chain fluid based on the dimer version of Wertheim's perturbation theory". *Mol Phys*. 1995;86(6):1451-1471.
335. Chang J., Sandler S.I. "The correlation functions of hard-sphere chain fluids: Comparison

- of the Wertheim integral equation theory with the Monte Carlo simulation". *J Chem Phys.* 1995;102(1):437.
336. Porter J.A., Fridrikh S.V., Lipson J.E.G. "Square-well chain fluids: The thermodynamic properties of hexamers, octamers, and hexadecamers". *J Chem Phys.* 2003;119(7):3883.
337. Taylor M.P., Luettmmer-Strathmann J., Lipson J.E.G. "Structure and phase behavior of square-well dimer fluids". *J Chem Phys.* 2001;114(13):5654.
338. Fridrikh S.V., Lipson J.E.G. "Square-well fluids: The statistical and thermodynamic properties of short chains". *J Chem Phys.* 2002;116(19):8483.
339. Largo J., Solana J.R., Yuste S.B., Santos A. "Pair correlation function of short-ranged square-well fluids". *J Chem Phys.* 2005;122(8):84510.
340. Kirkwood J.G., Maun E.K., Alder B.J. "Radial distribution functions and the equation of state of a fluid composed of rigid spherical molecules". *J Chem Phys.* 1950;18(8):1040-1047.
341. Co K.U., Kozak J.J., Luks K.D. "Solutions of the Yvon–Born–Green equation for the square-well fluid at very high densities". *J Chem Phys.* 1976;65(6):2327.
342. Lincoln W.W., Kozak J.J., Luks K.D. "Properties of solutions to the Yvon–Born–Green equation for the square-well fluid". *J Chem Phys.* 1975;62(6):2171.
343. Kirkwood J.G., Lewinson V.A., Alder B.J. "Radial distribution functions and the equation of state of fluids composed of molecules interacting according to the Lennard-Jones potential". *J Chem Phys.* 1952;20(6):929-938.
344. Broyle A.A. "Radial Distribution Functions from the Born-Green Integral Equation". *JChemPhys.* 1960;33(2):456-458.
345. Paricaud P. "Phase equilibria in polydisperse nonadditive hard-sphere systems". *Phys Rev E - Stat Nonlinear, Soft Matter Phys.* 2008;78(2):1-12.
346. Nguyen-huynh D., Passarello J., Tobaly P. "Modeling Phase Equilibria of Asymmetric Mixtures Using a Group-Contribution SAFT (GC-SAFT) with a kij correlation method based on London's theory. 1. Application to CO₂+ n-alkane, methane + n-alkane and ethane + n-alkane systems". *Ind Eng Chem Res.* 2008;47:8847-8858.
347. NguyenHuynh D., Passarello J-P., Tobaly P., de Hemptinne J-C. "Application of GC-SAFT EOS to polar systems using a segment approach". *Fluid Phase Equilib.* 2008;264(1-2):62-75.

348. NguyenHuynh D., Passarello J-P., de Hemptinne J-C., Volle F., Tobaly P. "Simultaneous modeling of VLE, LLE and VLLE of CO₂ and 1, 2, 3 and 4 alkanol containing mixtures using GC-PPC-SAFT EOS". *J Supercrit Fluids*. 2014;95:146-157.
349. Grandjean L., de Hemptinne J-C., Lugo R. "Application of GC-PPC-SAFT EoS to ammonia and its mixtures". *Fluid Phase Equilib*. 2014;367:159-172.
350. Boublik T. "Hard-Sphere Equation of State". *J Chem Phys*. 1970;53(1):471.
351. Mansoori G.A., Carnahan N.F., Starling K.E., Leland Jr. T.W. "Equilibrium Thermodynamic Properties of the Mixture of Hard Spheres". *J Chem Phys*. 1971;54(4):1523.
352. Mccoubrey J.C., Hudson G.H. "Intermolecular forces between unlike molecules: a more complete form of the combining rules". *Trans Faraday Soc*. 1960;56(2):761-766.
353. London F. "The general theory of molecular forces". *Trans Faraday Soc*. 1936;8:8-26.
354. Held C., Prinz A., Wallmeyer V., Sadowski G. "Measuring and modeling alcohol/salt systems". *Chem Eng Sci*. 2012;68(1):328-339.
355. Nann A., Held C., Sadowski G. "Liquid–Liquid Equilibria of 1-Butanol/Water/IL Systems". *Ind Eng Chem Res*. 2013;52(51):18472-18481.
356. Wolbach J.P., Sandler S.I. "Using Molecular Orbital Calculations To Describe the Phase Behavior of Cross-associating Mixtures". *Ind Eng Chem Res*. 1998;37(8):2917-2928.
357. Wolbach J.P., Sandler S.I. "The use of molecular orbital calculations to describe the phase behavior of hydrogen-bonding mixtures". *Int J Thermophys*. 1997;18(4):1001-1016.
358. Cleve H.L., Battino R., Saylor J.H., Gross D.P.M. "The solubility of Helium, Neon, Argon and Krypton in some hydrocarbon solvents". *J Phys Chem*. 1957;61(8):1078-1082.
359. Schnabel T., Vrabc J., Hasse H. "Unlike Lennard–Jones parameters for vapor–liquid equilibria". *J Mol Liq*. 2007;135(1-3):170-178.
360. Harvey A.H., Prausnitz J.M. "The nonadditive hard sphere mixtures as a reference system in equation of state calculations". *Fluid Phase Equilib*. 1989;48:197-208.
361. Spackman M.A. "Atom–atom potentials via electron gas theory". *J Chem Phys*. 1986;85(11):6579.
362. Williams D.E., Craycroft D.J. "Nonbonded H-H Repulsion Energy from ab Initio SCF Calculations of Methane, Water and Methanol dimers". *J Phys Chem*. 1987;91(6):6365-

- 6373.
363. Nguyen-huynh D., de Hemptinne J-C., Lugo R., Passarello J-P., Tobaly P. "Modeling Liquid À Liquid and Liquid À Vapor Equilibria of Binary Systems Containing Water with an Alkane , an Aromatic Hydrocarbon , an Alcohol or a Gas (Methane , Ethane , CO₂ or H₂S), Using Group Contribution Polar Perturbed-Chain Statistical Associating Fluid Theory". *Ind Eng Chem Res.* 2011;50:7467-7483.
364. Polyakov A.A., Tyvina T.N., Fokina V.V., Naumova A.A. "Compositions and Molar Volumes of Solutions of Ethylene, Ethane and Carbon Dioxide in Propionaldehyde". *J Appl Chem USSR.* 1986;59(6):1261-1263.
365. Ohgaki K., Sano F., Katayama T. "Isothermal Vapor-Liquid Equilibrium Data for Binary Systems Containing Ethane at High Pressures". *J Chem Eng Data.* 1976;21(1):55-58.
366. Gjaldbaek J.C., Niemann H. "The solubility of Nitrogen, Argon and Ethane in Alcohols and water". *Acta Chem Scand.* 1958;12(5):1015-1023.
367. Jou F-Y., Schmidt K.A.G., Mather A.E. "Vapor-liquid equilibrium in the system ethane+ethylene glycol". *Fluid Phase Equilib.* 2006;240(2):220-223.
368. Wang L-K., Chen G-J., Han G-H., Guo X-Q., Guo T-M. "Experimental study on the solubility of natural gas components in water with or without hydrate inhibitor". *Fluid Phase Equilib.* 2003;207(1-2):143-154.
369. Zeck S., Knapp H. "Solubilities of Ethylene , Ethane , and Carbon Dioxide in Mixed Solvents Consisting of Methanol , Acetone , and Water". *Int J Thermophys.* 1985;6(6):643-656.
370. Mu T., Zhang X., Han B., Li, H., Liu, J., Wu, W., Chen, J., Du, J. "Effect of phase behavior on the constant volume heat capacity of ethane + ethanol and ethane + acetone mixed fluids near the critical region and the intermolecular interaction". *Fluid Phase Equilib.* 2003;214(1):53-65.
371. Kordikowski A., Schenk A.P., Van Nielen R.M., Peters C.J. "Volume Expansions and Vapor-Liquid Equilibria of Binary Mixtures of a Variety of Polar Solvents and Certain Near-Critical Solvents". *J Supercrit Fluids.* 1995;8(3):205-216.
372. McDaniel A.S. "Absorption of hydrocarbon gases by non-aqueous liquids". *J Phys Chem.* 1911;15(6):587-610.
373. Yaacobi M., Ben-Naim A. "Solvophobic Interaction". *J Phys Chem.* 1972;78(2):175-178.
374. Suzuki K., Sue H., Ito M., Smith, R.L., Inomata, H., Arai, K., Saito, S. "Isothermal

- Vapor-Liquid Equilibrium Data for Binary Systems at High Pressures: Carbon Dioxide-Methanol, Carbon Dioxide-Ethanol, Carbon Dioxide-1-Propanol, Methane-Ethanol, Methane-1-Propanol, Ethane-Ethanol, and Ethane-1-Propanol Systems". *J Chem Eng Data*. 1990;35(8):63-66.
375. Kodama D., Tanaka H., Kato M. "High Pressure Phase Equilibrium for Ethane + 1-Propanol at 314.15 K". *J Chem Eng Data*. 2001;46(5):1280-1282.
376. Jimenez-Gallegos R., Galicia-Luna L.A., Bouchot C., Camacho-Camacho L.E., Elizalde-Solis O. "Experimental Determination and Correlation of Phase Equilibria for the Ethane + 1-Propanol and Propane + 1-Propanol Systems". *J Chem Eng Data*. 2006;51(5):1629-1633.
377. Lide D.R. "CRC Handbook of Chemistry and Physics". CRC Press. New York, USA; 2005.
378. Mourah M., NguyenHuynh D., Passarello J-P., de Hemptinne J-C., Tobaly P. "Modelling LLE and VLE of methanol+n-alkane series using GC-PC-SAFT with a group contribution k_{ij} ". *Fluid Phase Equilib*. 2010;298(1):154-168.
379. Buret G., de Hemptinne J-C. "Equation D'état SAFT: Amélioration Des Performance". IFP Energies Nouvelles report; 2009.
380. Michelsen M.L., Mollerup J. "Thermodynamic Models: Fundamentals and Computational Aspects". Tie-Line Publications, 2004.
381. Zacher A.H., Olarte M.V., Santosa D.M. "A review and perspective of recent bio-oil hydrotreating research". *Green Chem*. 2014;16(2):491.
382. Tamouza S. "Utilisation Prédictive de l'Equation d'état SAFT". Université Paris Nord, 2004.
383. DETHERM. Thermophysical properties of pure substances and mixtures. 2011.
384. Huamin S. "Solubility of Carbon Monoxide in Methanol and Carbon Dioxide under High Pressure". *Huaxue Gongcheng*. 1991;19(6):61-69.
385. Tonner S.P., Wainwright M.S., Trimm D.L., Cant N.W. "Solubility of carbon monoxide in alcohols". *J Chem Eng Data*. 1983;28(1):59-61.
386. Li N., Ma P., Xia S. "Determination of Solubility of Carbon Monoxide in Methanol - Dimethyl Carbonate under High Pressure". *Shiyou Huagong*. 2005;34(1):60-64.
387. Skirrow F.W. "The Solubility of Carbon Dioxide in binary Organic Mixtures". *Z Phys*

- Chem Stoechiom Verwandtschaftsl.* 1902;41:139-160.
388. Gjaldbaek J.C. "The Solubility of Carbon Monoxide in some Lower Monovalent Alcohols". *Mat meddelelser.* 1948;24(13):1-17.
389. Bunsen R. "Gasometric Methods. IV. Absorption Phenomena of Gases". *Gasometrische Methoden, Braunschweig.* 1877.
390. Khan M.M.T., Hallgudl S.B., Shukla S. "Solubility of Carbon Monoxide in Water-n - Butylamine , Ethanol-Cyclohexane and Water-Dimethylformamide Mixtures". *J Chem Eng Data.* 1989;34(3):353-355.
391. Vasil'eva I.I., Tyvina T.N., Kharchenko A.A. "Liquid-Gas Equilibrium in the System n-Butyl Alcohol - Carbon Monoxide". *J Appl Chem USSR.* 1982;55(12):2438-2438.
392. Tyvina T.N., Fokina V., Naumova A.A., Polyakov A.A. "Phase and volume relations in carbon monoxide - isodecanol and carbon monoxide - isononene systems". *Zh Prikl Khim.* 1984;57(9):2101-2104.
393. Vasileva I.I., Naumova A.A., Polyakov A.A., Tyvina T.N., Fokina V.V. "Liquid-Gas Phase Equilibria and Volumes of the Liquid Phase in a Propionic Acid - Carbon Monoxide System". *J Appl Chem USSR.* 1988;61:2165-2167.
394. Zhu R., Zhou J., Liu S., Ji J., Tian Y. "Vapor-liquid equilibrium data for the binary systems in the process of synthesizing diethyl carbonate". *Fluid Phase Equilib.* 2010;291(1):1-7.
395. Gjaldbaek J.C., Andersen E.K. "The Solubility of Carbon Dioxide, Oxygen, Carbon Monoxide and Nitrogen in Polar Solvents". *Acta Chem Scand.* 1954;8(8):1398-1413.
396. Preuss H., Moerke K. "Determination of the Vapor(gas)-Liquid Equilibrium in the System Hydrogen Sulfide - Methanol".; 1990.
397. Bezdel L.S., Teodorovich V.P. "Solubility of CO₂, H₂S, CH₄, and C₂H₆ in methanol at low temperatures". *Gazov Promst.* 1958;8:38-43.
398. Zel'venskii Y.A.D., Strunina A.V. "The Solubility of H₂S in Methanol at low Temperatures". *Gazov Promst.* 1960;1:42.
399. Schalk W. Diplomarbeit.Thesis, University Wien, 1973.
400. Gerrard W. "Solubility of hydrogen sulphide, dimethyl ether, methyl chloride and sulphur dioxide in liquids. The prediction of solubility of all gases". *J Appl Chem Biotechnol.*

- 1972;22(5):623-650.
401. Short I., Sahgal A., Hayduk W. "Solubility of ammonia and hydrogen sulfide in several polar solvents". *J Chem Eng Data*. 1983;28(1):63-66.
402. Jou F-Y., Deshmukh R.D., Otto F.D., Mather A.E. "Vapor-Liquid Equilibria of H₂S and CO₂ and Ethylene Glycol At Elevated Pressures". *Chem Eng Commun*. 1990;87(1):223-231.
403. Byeseda J.J., Deetz J.A., Manning W.P. "The Optisol (TM) Gas Sweetening Solvent". *Proc Gas Cond Conf*. 1985:1-15.
404. Kudo S., Toriumi T. "Total Pressure for Binary Systems of Liquid Ammonia - Alcohols. (1): Liquid NH₃ - CH₃OH Systems, Liquid NH₃ - C₂H₅OH Systems". *Tohoku Daigaku Hisui Yoeki Kagaku Kenkyusho Hokoku*. 1959;8:27-33.
405. Xu X., An L., Zheng G., Bai G. "Measurement of Vapor - Liquid Equilibrium Data for Products in Methanol Amination". *Gaoxiao Huaxue Gongcheng Xuebao*. 1995;9(2):97-105.
406. Preuss H. "Determination of the Vapor-Liquid Equilibrium in the System Ammonia - Methanol."; 1988.
407. Doering K.E. "Vapor Pressures of Mixtures Ammonia - Methyl Alcohol". report; 1963.
408. Feng Y., Xie R., Wu Z., Marsh K.N. "Vapor - Liquid Equilibria for Ammonia + Methanol". *J Chem Eng Data*. 1999;44(3):401-404.
409. Kuznetsov A.I., Panchenkov G.M., Gogoleva T.V. "The Solubility of Ammonia in Alcohols, Ketones, and Amines". *Russ J Phys Chem*. 1968;42(4):510-511.
410. Hatem M.S. "Contribution to the study of some physico-chemical systems alcohol - ammonia and alcohol - cyclic amines". *Bull Soc Chim Fr*. 1949;16(5):337-340.
411. Pagliani S., Emo A. "Absorption of ammonia gas in the alcohols". *Atti R Accad Sci Torino*. 1982;18:67-73.
412. Lippold H., Heide R. "Dimethyl Ether as a Component of Refrigerants". *Luft-Kaeltetech*. 1997;5(5):202-205.
413. Pan L., Yang Y.T., Zhou H., Chen Y.D., Zhang S. "Solubility of Ammonia in Mixed Solvent of Methanol and Ethylene Glycol". *Huaxue Gongcheng*. 2010;38(9):48-53.

RESUME

The main objective of this thesis is to develop a predictive tool to compute the vapor-liquid equilibria (VLE) associated with hydrotreating operation from biomass for process simulation. The construction of a reliable database of hydrogen and the other hydrotreating gases solubilities have been done. The model used based on the Group Contribution – Polar Perturbed Chain – Statistical Associating Fluid Theory (GC-PPC-SAFT), which is PC-SAFT combined with the group contribution proposed by Tamouza and a polar term developed by Nguyen Huynh. The systematic tests have been performed for mixtures of alcohols, aldehydes, esters, ethers, ketones, ... A new non-additive contribution has also been proposed based on the reflections on the repulsive interactions and the free volume effect. The model development are validated by Monte Carlo simulations. This non-additive term has been integrated in GC-PPC-SAFT Equation of state and tested for systems containing hydrogen. Group contribution method has been extended to its parameter. Average deviations on Henry's constant are within the experimental uncertainty (~10%). We also have performed the prediction of the other gases i.e. CO, H₂S, NH₃ solubility using GC-PPC-SAFT. A cross associative parameter has been used for systems containing H₂S and NH₃. The results are quite acceptable and within the experimental uncertainty (~20%).

Keyword: GC-PPC-SAFT, hydrogen, oxygenated compound, predictive, non-additive

RESUME

L'objectif de cette thèse est de développer un outil prédictif pour calculer les équilibres vapeur-liquide (VLE) associé à l'opération d'hydrotraitement à partir de biomasse pour la simulation de processus. La construction d'une base de données de solubilité fiables d'hydrogène et d'autres gaz d'hydrotraitement ont été réalisées. Le modèle utilisé a pour base l'équation Groupe Contribution- Polar Perturbed Chain - statistique Associer Fluid Theory (GC-PPC-SAFT), qui est version de PC-SAFT combiné avec la contribution de groupes proposé par Tamouza et un terme polaire développé par Nguyen Huynh. Des tests systématiques ont été effectués pour différents mélanges gaz + d'alcools, aldéhydes, esters, éthers, cétones, ... Une nouvelle contribution non-additif a été proposé sur la base des réflexions sur les interactions répulsives et l'effet de volume libre. Le modèle a été validé notamment par des simulations Monte Carlo. Ce terme non additif a été intégré dans GC-PPC-SAFT et testé pour les systèmes contenant de l'hydrogène. La méthode de contribution de groupes a été étendue au paramètre de ce nouveau terme. Des écarts moyens sur la constante de Henry sont en accord avec l'incertitude expérimentale (~ 10%). Nous avons également examiné la prédiction d' autres gaz i.e. CO, H₂S, NH₃ en utilisant GC-PPC-SAFT. Un paramètre associatif transversale a été utilisé pour des systèmes contenant H₂S et NH₃. Les résultats sont tout à fait acceptable et cohérent avec l'incertitude expérimentale (~20%).

Mots-clés: GC-PPC-SAFT, hydrogène, composé oxygéné, prédictive, non-additive